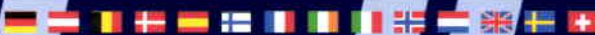


 esa


bulletin

number 102 - may 2000



European Space Agency
Agence spatiale européenne



european space agency

The European Space Agency was formed out of, and took over the rights and obligations of, the two earlier European Space Organisations: the European Space Research Organisation (ESRO) and the European Organisation for the Development and Construction of Space Vehicle Launchers (ELDO). The Member States are Austria, Belgium, Denmark, Finland, France, Germany, Ireland, Italy, Netherlands, Norway, Spain, Sweden, Switzerland and the United Kingdom. Canada is a Cooperating State.

In the words of the Convention: The purpose of the Agency shall be to provide for and to promote, for exclusively peaceful purposes, co-operation among European States in space research and technology and their space applications, with a view to their being used for scientific purposes and for operational space applications systems.

- (a) by elaborating and implementing a long-term European space policy, by recommending space objectives to the Member States, and by concerting the policies of the Member States with respect to other national and international organisations and institutions;
- (b) by elaborating and implementing activities and programmes in the space field;
- (c) by co-ordinating the European space programme and national programmes, and by integrating the latter progressively and as completely as possible into the European space programme, in particular as regards the development of applications satellites;
- (d) by elaborating and implementing the industrial policy appropriate to its programme and by recommending a coherent industrial policy to the Member States.

The Agency is directed by a Council composed of representatives of Member States. The Director General is the chief executive of the Agency and its legal representative.

The ESA HEADQUARTERS are in Paris.

The major establishments of ESA are:

THE EUROPEAN SPACE RESEARCH AND TECHNOLOGY CENTRE (ESTEC), Noordwijk, Netherlands.

THE EUROPEAN SPACE OPERATIONS CENTRE (ESOC), Darmstadt, Germany

ESRIN, Frascati, Italy.

Chairman of the Council: A. Bensoussan

Director General: A. Rodotà.

agence spatiale européenne

L'Agence Spatiale Européenne est issue des deux Organisations spatiales européennes qui l'ont précédée — l'Organisation européenne de recherches spatiales (CERS) et l'Organisation européenne pour la mise au point et la construction de lanceurs d'engins spatiaux (CECLES) — dont elle a repris les droits et obligations. Les Etats membres en sont: l'Allemagne, l'Autriche, la Belgique, le Danemark, l'Espagne, la Finlande, la France, l'Irlande, l'Italie, la Norvège, les Pays-Bas, le Royaume-Uni, la Suède et la Suisse. Le Canada bénéficie d'un statut d'Etat coopérant.

Selon les termes de la Convention: l'Agence a pour mission d'assurer et de développer, à des fins exclusivement pacifiques, la coopération entre Etats européens dans les domaines de la recherche et de la technologie spatiales et de leurs applications spatiales, en vue de leur utilisation à des fins scientifiques et pour des systèmes spatiaux opérationnels d'applications:

- (a) en élaborant et en mettant en oeuvre une politique spatiale européenne à long terme, en recommandant aux Etats membres des objectifs en matière spatiale et en concertant les politiques des Etats membres à l'égard d'autres organisations et institutions nationales et internationales;
- (b) en élaborant et en mettant en oeuvre des activités et des programmes dans le domaine spatial;
- (c) en coordonnant le programme spatial européen et les programmes nationaux, et en intégrant ces derniers progressivement et aussi complètement que possible dans le programme spatial européen, notamment en ce qui concerne le développement de satellites d'applications;
- (d) en élaborant et en mettant en oeuvre la politique industrielle appropriée à son programme et en recommandant aux Etats membres une politique industrielle cohérente.

L'Agence est dirigée par un Conseil, composé de représentants des Etats membres. Le Directeur général est le fonctionnaire exécutif supérieur de l'Agence et la représente dans tous ses actes.

Le SIEGE de l'Agence est à Paris.

Les principaux Etablissements de l'Agence sont:

LE CENTRE EUROPEEN DE RECHERCHE ET DE TECHNOLOGIE SPATIALES (ESTEC), Noordwijk, Pays-Bas.

LE CENTRE EUROPEEN D'OPERATIONS SPATIALES (ESOC), Darmstadt, Allemagne.

ESRIN, Frascati, Italie

Président du Conseil: A. Bensoussan

Directeur général: A. Rodotà.

bulletin

contents/sommaire

number 102 - may 2000



Cover: The Envisat spacecraft (see page 91)

Editorial/Circulation Office

ESA Publications Division
ESTEC, PO Box 299, Noordwijk
2200 AG The Netherlands
Tel.: (31) 71.5653400

Editors

Bruce Battrick
Dorothea Danesy

Layout

Carel Haakman

Graphics

Willem Versteeg

Montage

Paul Berkhout
Isabel Kenny

Advertising

Brigitte Kaldeich

The ESA Bulletin is published by the European Space Agency. Individual articles may be reprinted provided the credit line reads 'Reprinted from ESA Bulletin', plus date of issue. Signed articles reprinted must bear the author's name. Advertisements are accepted in good faith; the Agency accepts no responsibility for their content or claims.

Copyright © 2000 European Space Agency
Printed in the Netherlands ISSN 0376-4265

European Space Agency
Agence spatiale européenne

Metop: The Space Segment for Eumetsat's Polar System

P.G. Edwards & D. Pawlak

7

ASCAT — Metop's Advanced Scatterometer

R.V. Gelsthorpe, E. Schied & J.J.W. Wilson

19

GOME-2 — Metop's Second-Generation Sensor for Operational Ozone Monitoring

J. Callies et al.

28

GRAS — Metop's GPS-Based Atmospheric Sounder

M. Loiselet et al.

38

The Cluster-II Mission — Rising from the Ashes

The Cluster-II Project Team

47

Cluster-II: Scientific Objectives and Data Dissemination

C. Ph. Escoubet

54

Cluster-II: Evolution of the Operations Concept

M. Warhaut, S. Matussi & P. Ferri

61

Four Years of SOHO Discoveries — Some Highlights

B. Fleck et al.

69

The Second Report by ESA's Long-Term Space Policy Committee (LSPC)

G. Naja

87

ASAR — Envisat's Advanced Synthetic Aperture Radar

Y.-L. Desnos et al.

91

Earth-Observation Applications of Navigation Satellites

P. Silvestrin

101

The European Multi-User Facilities for the Columbus Laboratory

G. Reibaldi et al.

107

Vulcain-2 Cryogenic Engine Passes First Test with New Nozzle Extension

D. Coulon

123

Distributed Interactive Simulation for Space Projects

L. Argüello & J. Miró

125

INTELMOD

A. Donati & E. Romani

131

The Tether System Experiment

J. Gavira Izquierdo, H. Rozemeijer & S. Müncheberg

139

Intra-European Coordination in the UN Committee on Peaceful Uses of Outer Space

K. Bergquist

144

Programmes under Development and Operations

147

In Brief

156

Publications

171

Space Radiation Alarm

"CEASE"

COMPACT ENVIRONMENTAL ANOMALY SENSOR



FEATURES:

- Compact: 10 x 10 x 8.1 cm³, 1 kg
- Low Power: 1.5 W
- Flexible I/O: Supports 1553B and RS422
- Full GSE and operational software
- On-board determination of hazardous conditions

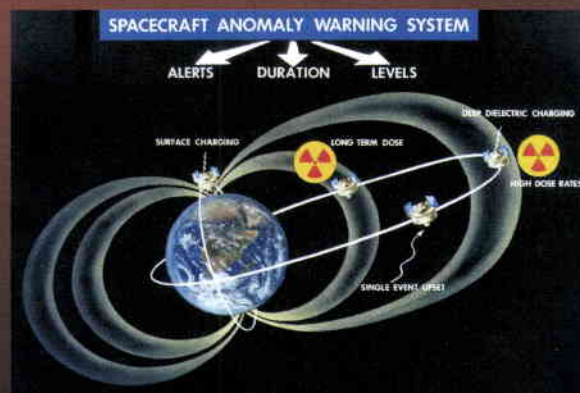
CEASE is a compact, radiation hard, low power, space "weather" hazard sensor developed to monitor the local radiation environment and to provide autonomous real-time warnings of:

- Total Radiation Dose
- Radiation Dose Rate
- Surface Charging
- Deep Dielectric Charging
- Single Event Effects
- Solar Cell Damage.

CEASE detailed radiation data is used to pinpoint causes of spacecraft anomalies, and to forecast hazardous conditions before they affect the mission. The spacecraft, in turn, can re-prioritize its operations, inhibit any anomaly sensitive tasks such as attitude control adjustments, or initiate other prudent actions as indicated by the **CEASE** warning flags. Device degradation mechanisms and radiation tolerance of components can also be monitored. The US Department of Defense has selected **CEASE** for several missions, including:

- **TSX-5**
- **STRV-1C**
- **SBIRS LADS**

and the **DSP** operational spacecraft.

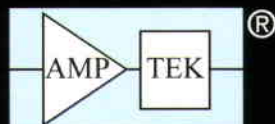


Amptek has a long and distinguished track record in the manufacture of space instrumentation. Mission examples include: DMSP, TIROS, CRRES, NEAR and APEX.

Current off-the-shelf Amptek sensors measure spacecraft charging, thermal and suprathreshold, and high energy particles. In addition, Amptek provided the X-ray Detector on the Mars PATHFINDER Mission.



High reliability components from Amptek have been the number one choice of many missions, including: GALILEO, CASSINI, GIOTTO, AXAF, SUISEI, CLUSTER, SOLAR, GEOTAIL, SOHO, INTEGRAL, WIND and AMPTE.



AMPTEK INC.

6 DE ANGELO DRIVE, BEDFORD, MA 01730-2204 U.S.A.

Tel: +1 (781) 275-2242 Fax: +1 (781) 275-3470 email: sales@amptek.com <http://www.amptek.com>

Alcatel Espacio

Your Best Spanish Space Supplier

Main Products

▼ Digital Electronic Equipment

- On-Board Data Handling
- Digital Payload Engineering
- Antenna Pointing Systems



▼ Radiofrequency Equipment

- S-Band TTC Digital Transponders and Transceivers
- S-Band TTC Spread Spectrum Transponders
- S-Band TTC High Power Amplifiers
- L-Band Transmitters
- BPSK/QPSK Modulators
- Filters, Diplexers, Multiplexers, etc.



▼ Systems Engineering

- On-Board Processing (OBP)/Multimedia
- Satellites Telecommunication Systems Studies
- Specific Checkout Equipment (SCOE)
- Power Benches



RF Active and Passive, On-Board Data Handling Equipment and Subsystems is our main line of business. We are specialised in the development and manufacture of a few equipment, through partnership with the main space prime contractors.

Our track record includes participation in more than 45 programs satellites.

Alcatel Espacio is a Spanish subsidiary company of Alcatel Space Industries



ARCHITECTS OF AN INTERNET WORLD

Alcatel Espacio, S.A. C/ Einstein, 7. 28760 Tres Cantos (PTM) • Madrid - Spain. Tel. 34 91 807 79 00 - Fax 34 91 807 79 99

www.alcatel.es/espacio/index_i.htm

**XIXth CONGRESS OF THE INTERNATIONAL SOCIETY
FOR PHOTOGRAMMETRY AND REMOTE SENSING (ISPRS)**

GEOINFORMATION FOR ALL

Amsterdam, The Netherlands

16-23 July 2000

MEET IN AMSTERDAM



For registration, call for papers and information about the exhibits, contact:

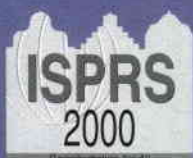
Secretariat: ISPRS Organizing Committee

Attn Ms Saskia Tempelman, c/o ITC

P.O. Box 6, 7500 AA ENSCHEDE, The Netherlands

Telephone: +31-53-4874358, Fax: +31-53-4874335

E-mail: ISPRS@ITC.NL, WWW: <http://www.itc.nl/~isprs>



Change supplier...



remain with us.



Officine Galileo
B.U. Spazio

Marketing Communications:
Via Montefeltro, 8
20156 MILANO, Italy
Phone: ++39.0230242.362
Fax: ++39.0230242.052
e-mail: mkt.space@officine-galileo.finmeccanica.it



Alenia

DIFESA
A FINMECCANICA COMPANY

We are providing the spacecraft's "heart" for several European space missions. Our new PCDE, modular electrical power system for telecommunications, scientific and remote sensing spacecraft's buses bring you into the new millennium with high performance, low cost solutions to your needs.

*OLD FRIENDS, NEW ORGANIZATION,
TO SERVE YOU BETTER.*

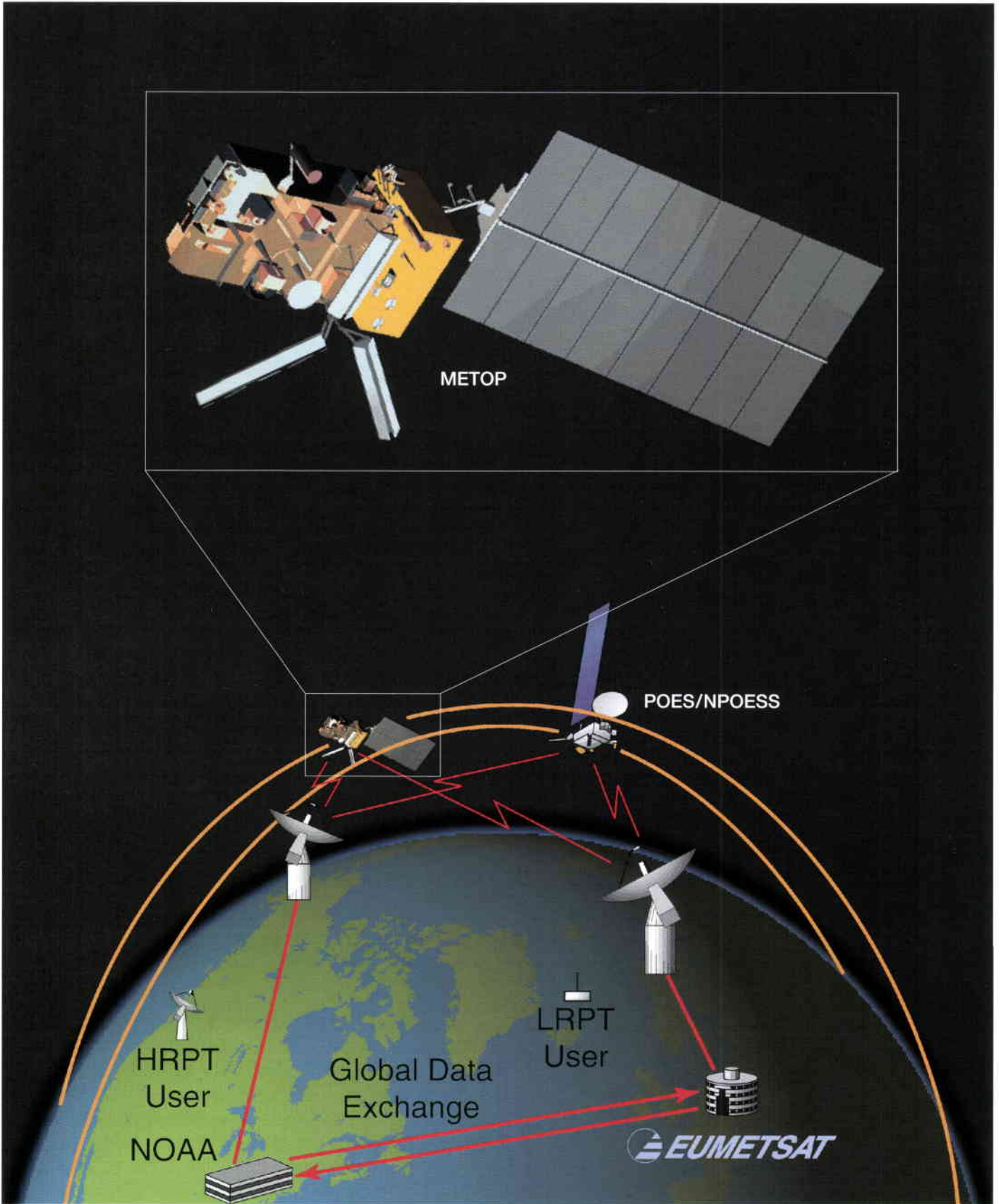


Figure 1. Principle of the Joint Polar System operations

Metop: The Space Segment for Eumetsat's Polar System

P.G. Edwards

Earth Observation Projects Department, ESA Directorate of Application Programmes, ESTEC, Noordwijk, The Netherlands

D. Pawlak

Matra Marconi Space*, Toulouse, France

Introduction

Over the years, the need for high-resolution data sets for a wide range of atmospheric parameters, with global coverage, has become more pressing with the increasing sophistication of the numerical weather-prediction models. The instrumentation initially embarked on the Tiros satellites has evolved and now spans the electromagnetic spectrum from microwaves through the infrared to the visible, thereby enabling height profiles of many parameters to be determined. After decades of such evolution, the new generation of polar-orbiting meteorological satellites under development on both sides of the Atlantic – Metop in Europe and the National Polar Orbiting Environmental Satellite System (NPOESS) in the USA – will carry considerably larger and more capable sets of instrumentation.

Metop-1 will be Europe's first polar-orbiting satellite dedicated to operational meteorology. As such, it marks the start of our contribution to balance a long-standing service provided by the United States from its Tiros, now POES (Polar Orbiting Environmental Satellite), Programme.

The first Tiros satellite was launched 40 years ago and in the intervening period the US has provided the data from this evolving series of satellites free of charge to the worldwide meteorological community. As early as 1967, Europe looked towards balancing this effort, but initially selected a geostationary satellite mission as the higher priority. This led to the development of the Meteosat series of satellites, the first of which was launched in 1977.

The US is currently operating polar-orbiting meteorological satellites in four Sun-synchronous orbital planes, for two services: an early morning and afternoon pair of military satellites (DMSP) and a mid-morning and afternoon civil pair operated by NOAA. There have been many earlier proposals to merge these services and this convergence is now underway in conjunction with an agreement

with Europe, represented by Eumetsat, to participate. The resulting Joint Polar System (JPS) will maintain three orbital planes, in the early morning, mid-morning and afternoon. The Eumetsat Polar System, of which Metop is the space segment, will provide the mid-morning service (at a mean local solar time of 09:30), whilst the US NPOESS satellites will provide the other two services.

There will be a transitional phase (termed the Interim JPS, or IJPS) during which the older generation of instruments will continue to fly as the newer instruments are introduced. Thus Metop-1, -2 and -3 will embark both the older instruments, provided by NOAA, as well as more advanced, European, ones. The principle of the joint systems is shown in Figure 1.

The Metop satellites were originally part of a much larger satellite concept, called POEM, which was to have been the successor to ERS-1 and -2, based on the Columbus Polar Platform. This very large satellite would have carried the payloads of both Envisat and Metop and was imagined to be re-serviceable in-orbit. At the ESA Ministerial Council in Granada (E) in 1992, this idea was abandoned and Envisat and Metop were born. Metop is a joint undertaking by ESA and Eumetsat and forms part of the Eumetsat Polar System (EPS). In addition to the space segment (i.e. Metop), the latter comprises the ground segment, the launch and various infrastructure elements. The EPS is at present planned to provide an operational service for a period of 14 years, which requires the provision of three Metop satellites, each with a nominal lifetime of 5 years – an overlap period is assumed between them for commissioning (Fig. 2).

The EPS, and Metop in particular, have a number of objectives. This system is the European contribution to the improved polar-

* Now Astrium SAS.

orbiting meteorological satellite service being offered to the world's meteorological organisations. It also has to satisfy some specific needs of the European and US meteorological services; in Europe there is an increasing trend towards commercialisation of earth-observation, and hence meteorological, data, while in the US there are concerns over the direct broadcasting of data from US-provided instruments at times of national crisis.

The notable improvements in the service required of Metop are:

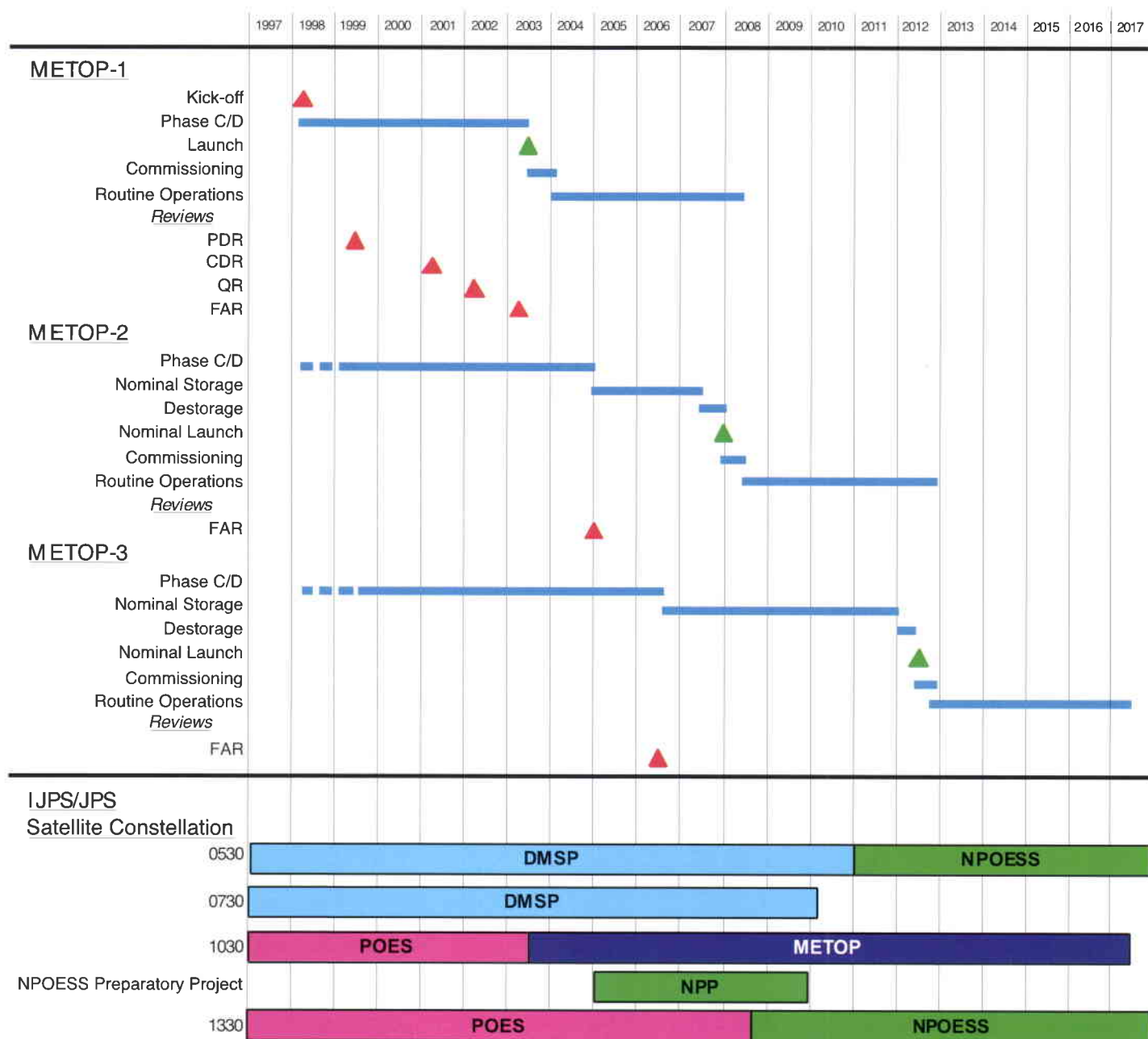
- Provision of new instrumentation (ASCAT, IASI, GOME-2 and GRAS) compared to the current generation of NOAA satellites.
- Provision of a low-data-rate digital direct broadcast service at VHF to replace the

analogue APT (Automatic Picture Transmission) system, employing data-compression to ensure high-quality images.

- Continuous on-board recording of the global data set to be dumped every orbit at a high-latitude ground station, with a ground segment sized to provide the global processed data within 2.25 h of the measurements being made.
- High pointing and orbital stability to ensure that data may be geo-located without reference to ground-control points in imagery.
- A selective encryption system to ensure the commercial and data-denial needs of Eumetsat and the US Government, respectively.

The satellite's main performance figures are provided in Table 1.

Figure 2. Timing of the joint meteorological systems operations



The payload composition of the first three Metop satellites may be divided into categories. In the first group are instruments providing the transition from the current NOAA satellites:

- *Advanced Very High Resolution Radiometer (AVHRR)*, an optical/infrared imager with a spatial resolution of about 1 km over a very wide swath of some 2000 km.
- *High-resolution Infra-Red Sounder (HIRS)*, a spectrometer with a relatively coarse spatial resolution and a mechanical scan over a wide swath, from which height profiles of atmospheric pressure and temperature may be derived – this instrument will not be embarked on Metop-3, its measurement functions being taken over by IASI, described below.
- *Advanced Microwave Sounding Unit A (AMSU-A)*, a mechanically scanned multi-channel microwave radiometer for the determination of pressure and temperature profiles.
- *Microwave Humidity Sounder (MHS)*, a new instrument, which will fly on the last of the NOAA satellites, which exactly replaces the AMSU-B currently provided by the UK Meteorological Office to NOAA.
- *Space Environment Monitor (SEM)*, which measures the charged-particle radiation environment in the vicinity of the satellite.
- *Data Collection System (DCS/Argos)*, a radio receiving and storage system, which receives brief telemetry signals from a large global network of remote stations, most of them unmanned and mobile. As well as providing these messages to a central processing and distribution site, this new version of the system may also send messages to the remote terminals.
- *Search and Rescue (S&R)*, a similar system which immediately rebroadcasts signals received from emergency transmitters typically carried on vessels and aircraft, enabling rescue services over a wide geographical area to locate the transmitter.

Table 1. Metop main features and performances

| Area | Performance |
|----------------------|---|
| Spacecraft orbit: | <ul style="list-style-type: none"> - Sun-synchronous near-circular orbit, altitude at ascending node: 796 to 844 km - Repeat cycle : 5 days (71 orbits) - Local solar time : 09h30 (descending node) |
| Launch mass: | 4174.8 kg |
| On-board propellant: | 315.7 kg of hydrazine, stored in 4 tanks (including residual) |
| Spacecraft attitude: | <ul style="list-style-type: none"> - Three-axis stabilised through reaction wheels - Orbit manoeuvres through hydrazine propulsion system - Pointing knowledge : 0.07° (X-axis), 0.10° (Y-axis), 0.17° (Z-axis) |
| Data handling: | <ul style="list-style-type: none"> - Instrument science data acquired as CCSDS packets - Science data formatting and multiplexing, encryption for selected instruments - Instrument and housekeeping data storage in a solid-state recorder (24 Gbit) |
| Communications: | <ul style="list-style-type: none"> - Omnidirectional S-band coverage (uplink 2 kbps, downlink 4.096 kbps) - Instrument global data stream downlinked via X band (70 Mbps data rate) - Real-time broadcasting of instrument data with HRPT: 3.5 Mbps via L-band for all instruments, and LRPT: 72 kbps via VHF for selected instruments |
| On-board power: | <ul style="list-style-type: none"> - 2210 W from solar panel, average power over one orbit (EOL) - Five 40 Ah batteries - 22 - 37.5 V unregulated, and 50 V regulated power lines for SVM/PLM units - 22 - 37 V unregulated power lines for European instruments - 28 V regulated power lines for NOAA instruments |
| Mission lifetime: | 5 years |
| Launcher: | Ariane-5, or Atlas IIAS |
| Operations: | <ul style="list-style-type: none"> - Spacecraft controlled by Eumetsat (Kiruna ground station) - Instrument X-band data down-linked nominally over 2 ground stations - Recorded data down-linked not later than one orbit after recording - Spacecraft autonomy required for 36 h without ground contact |

The second group are from the new generation, and offer improved sensing capabilities:

- *Infrared Atmospheric Sounding Interferometer (IASI)*, is an important new development, which will provide a significant improvement in the resolution of vertical temperature and humidity profiles in the atmosphere.
- *Advanced Scatterometer (ASCAT)*, developed within the framework of the Metop-1 contract, which uses multiple radar beams to measure the small-scale roughness of the ocean surface from three directions, over a wide swath on each side of the satellite, enabling the speed and direction of the wind to be determined.
- *Global Ozone Measurement Experiment 2*

(*GOME-2*), a successor to the ERS-2 GOME-1 with a number of improvements, is a high-resolution visible/ultraviolet spectrometer, which provides measurements over a wide swath and wide spectral range such that ozone profiles and total column amounts of many other trace gases may be determined.

- *GNSS Receiver for Atmospheric Sounding (GRAS)*, also developed within the framework of the MetOp-1 contract, is a geodetic-quality GPS receiver equipped with three antennas such that it is able to measure the signals from GPS satellites in occultation by the Earth's atmosphere, enabling temperature and pressure profiles to be determined.

The main performance parameters of these instruments are summarised in Table 2.

Table 2. Instrument performances

| Instrument | Main Characteristics | Main Data Products | Heritage | Notes |
|------------|---|--|-------------------------------|-------------------------------|
| AVHRR | Six-channel Vis/IR imager (0.6 - 12µm), swath 2000 km, 1 x 1km resolution | Wide-swath vertical sounding plus imagery | TIROS/POES | |
| HIRS | 20-channel Optical/IR filter-wheel radiometer; swath 2000 km; IFOV 17.4 km (nadir) | temperature profile, humidity profile generated by Tiros Operational Vertical Sounder (TOVS/ATOVS) | TIROS/POES | Disembarked for METOP-3 |
| AMSU-A1/A2 | Step-scan 15 channel total power MW radiometers for 50 GHz oxygen absorption line; swath 2000 km; IFOV 30 km (nadir) | combining data from HIRS, AMSU A1/A2 and MHS, supported by AVHRR Secondary Products: sea-surface temperature, cloud fraction/cloud top height, aerosol, precipitable water, surface emission, total ozone, sea-ice extent | TIROS/POES | |
| MHS | Five-channel quasi-optical heterodyne radiometer, 190 GHz for water-vapour absorption line plus 89 GHz for surface emissivity. Swath 2000 km, IFOV 30 km (nadir) | | TIROS/POES | As AMSU-B |
| IASI | Fourier-transform spectrometer, 4 IFOV's of 20 km at nadir in a square 50 x 50 km. Step-scanned across track (30 steps), synchronised to AMSU-A. Integrated (Near-IR) imager for cloud discrimination. Calibration: blackbody plus two deep-space views | Water-vapour sounding; NO ₂ and CO ₂ ; temperature sounding; surface and cloud properties. Swath width: 2000 km Performance: spectral range: 3.62-15.5 µm in 3 bands; resolution 0.35 cm ⁻¹ ; radiometric accuracy 0.25 - 0.58 K | New development | Replaces and supplements HIRS |
| ASCAT | C-band radar scatterometer, with three dual-swath antennas (fore/mid/aft). Measurement of radar backscatter at three different azimuth angles; fit to a model function to extract wind speed and direction. Incidence angle range: 25° - 65° | Surface-wind vectors over oceans; additional products (e.g. sea-ice cover; snow cover; vegetation density). Swath width: 2 x 500 km; Quasi-global coverage: 2.5 d. Wind velocity: ± 2ms ⁻¹ or 10%; Wind direction: ± 20° | ERS-1/-2 AMI-Scatterometer | |
| GOME-2 | Scanning spectrometer with spectral coverage: 250-790 nm at resolution 0.2-0.4 nm. Double monochromator design: first stage: quartz prism with physical separation of four channels; second stage: blazed gratings in each channel. Detector: 1024 pixel random-access silicon-diode arrays; | Ozone (total column and profiles, stratosphere and troposphere); NO ₂ BrO OClO ClO; Albedo and aerosol: cloud fraction, cloud-top altitude, cloud phase. Swath width: 960 or 1920 km, resolution 80 x 40 or 160 x 40 km | ERS-2 GOME-1 | |
| GRAS | GPS satellite receiver measuring changes during occultation (rising or setting); computation of bending angle and TEC; retrieval of refractive index vs altitude profile; fitting data to stratospheric model for temperature profile. Bending angle measurement accuracy better than 1 µrad. | Up to 500 occultations/day, with quasi-uniform geographical distribution Vertical temperature sounding of ±1 K, with vertical resolution of 150 m in the troposphere (5 - 30 km) and 1.5 km in the stratosphere | GPS/MET | |

Aspects of cooperation

The EPS and the Metop Programme are intensively collaborative in that five major agencies are extensively involved:

- Eumetsat: System authority, develops Ground Segment and MHS, co-funds Metop and IASI, procures launcher, operates system.
- ESA: Co-funds and develops Metop, ASCAT, GOME-2 and GRAS.

- NOAA: Funds US instruments for Metop; System authority for POES as part of IJPS.
- NASA: Develops/procures AVHRR, HIRS, AMSU and SEM for Metop.
- CNES: Co-funds and develops IASI; Funds and develops DCS, SARP.

A special relationship has been developed between ESA and Eumetsat, governed by a

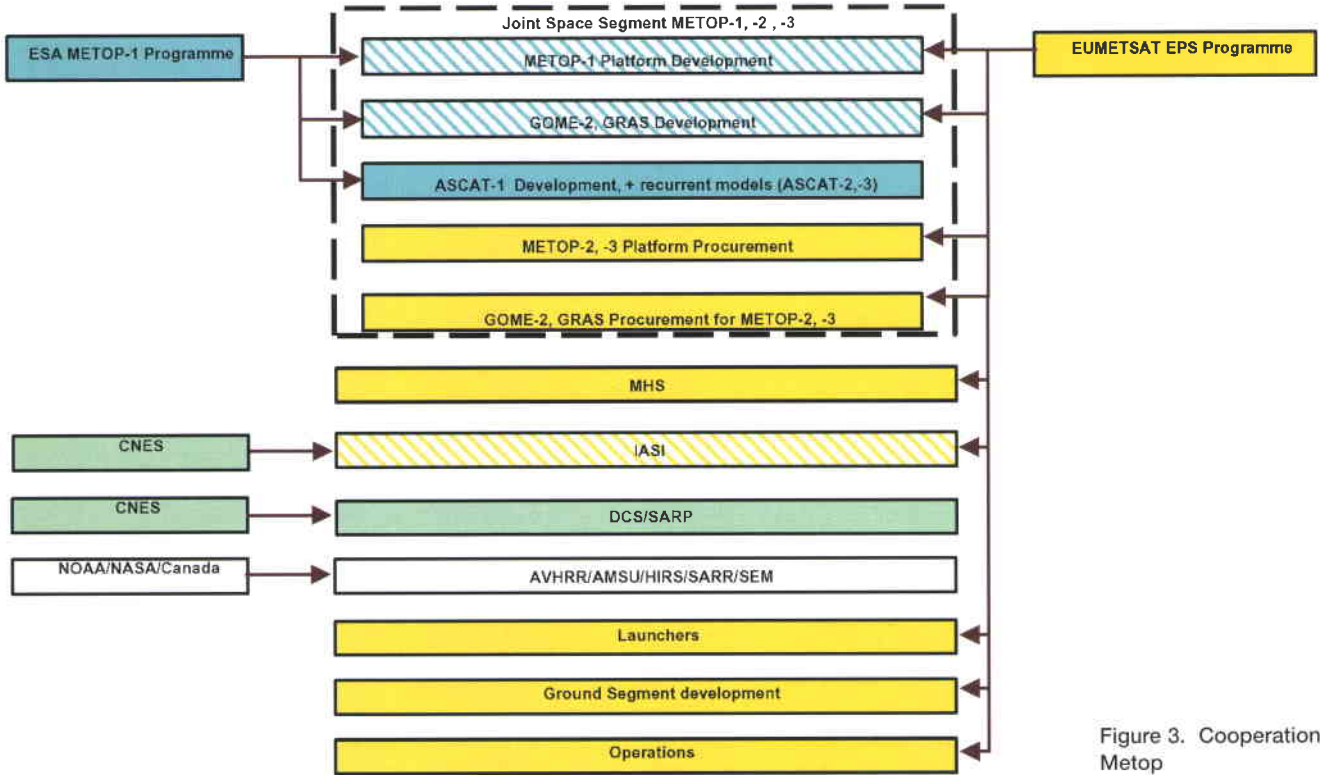


Figure 3. Cooperation on Metop

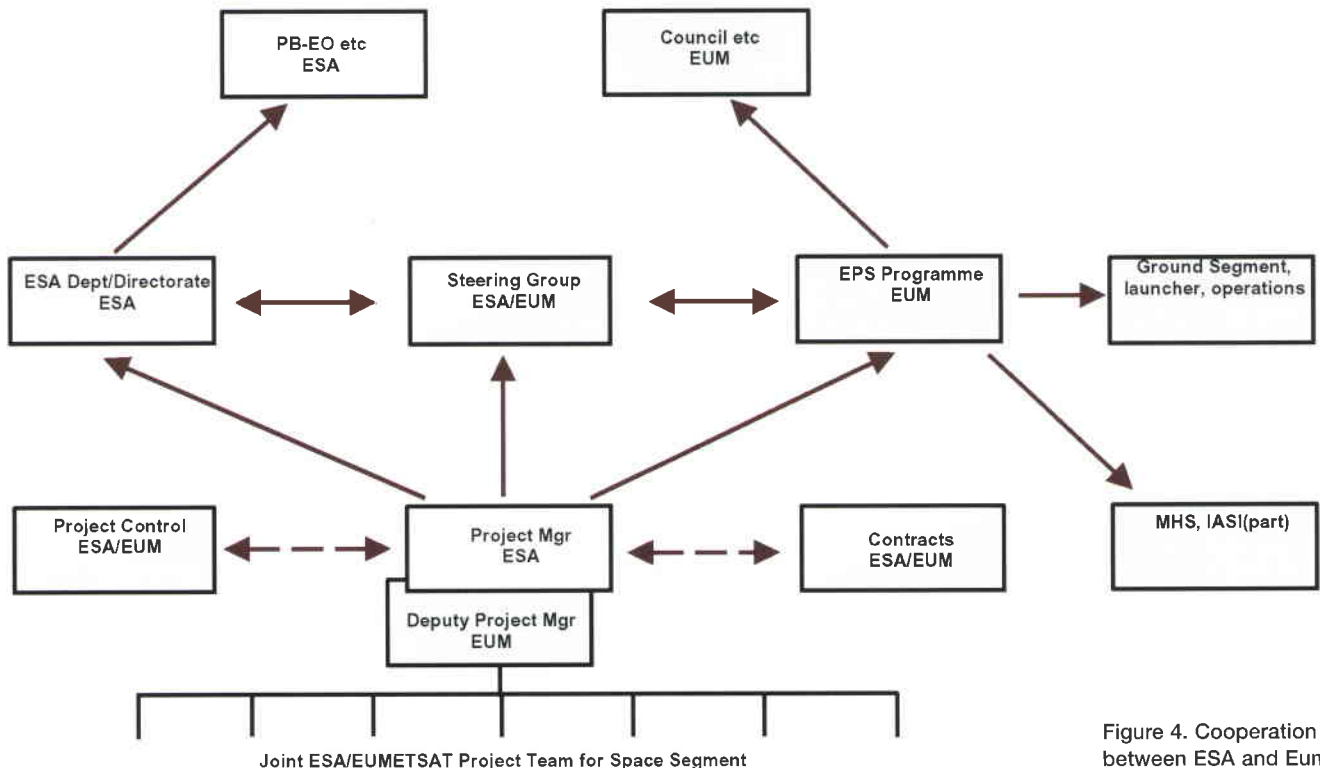


Figure 4. Cooperation between ESA and Eumetsat

legal act, the Cooperation Agreement, signed in December 1999. In this cooperation, a co-funding arrangement is established for the Metop industrial contracts, which is managed by a joint project team called the 'Single Space Segment Team (or SSST)', comprised of staff from both organisations and located at ESTEC. The team has an ESA project manager assisted by a Eumetsat deputy. The respective responsibilities are shown in Figures 3 and 4.

Industrial architecture

The Prime Contractor for Metop is Matra Marconi Space France (MMS-F). The contract includes the three Metop spacecraft and the ASCAT and GRAS payload instruments. A separate contract within the Metop Programme has been placed with Officine Galileo/Alenia Difesa for the three GOME-2 instruments. All other payload instruments are provided to the Metop Programme as customer-furnished instruments via Eumetsat.

MMS-F is responsible for the execution of all tasks performed by the industrial team, including system-level tasks and satellite assembly, integration and testing, and for the Service Module (SVM) with its Electrical Ground Support Equipment (EGSE).

- Among the various contractors involved,
- Dornier Satellitensysteme (DSS)* is responsible for the Payload Module, ASCAT, and GRAS (with Saab-Ericsson)
 - MMS-UK** is responsible for the Service Module mechanical system, and system-support tasks
 - Alenia is responsible for DCS/Search & Rescue mission integration and accommodation hardware.

Subcontractors, at unit or subsystem level, have been selected on the basis of heritage, or after competition. Figure 5 shows the current industrial team.

* Now Astrium GmbH
**Now Astrium Ltd.

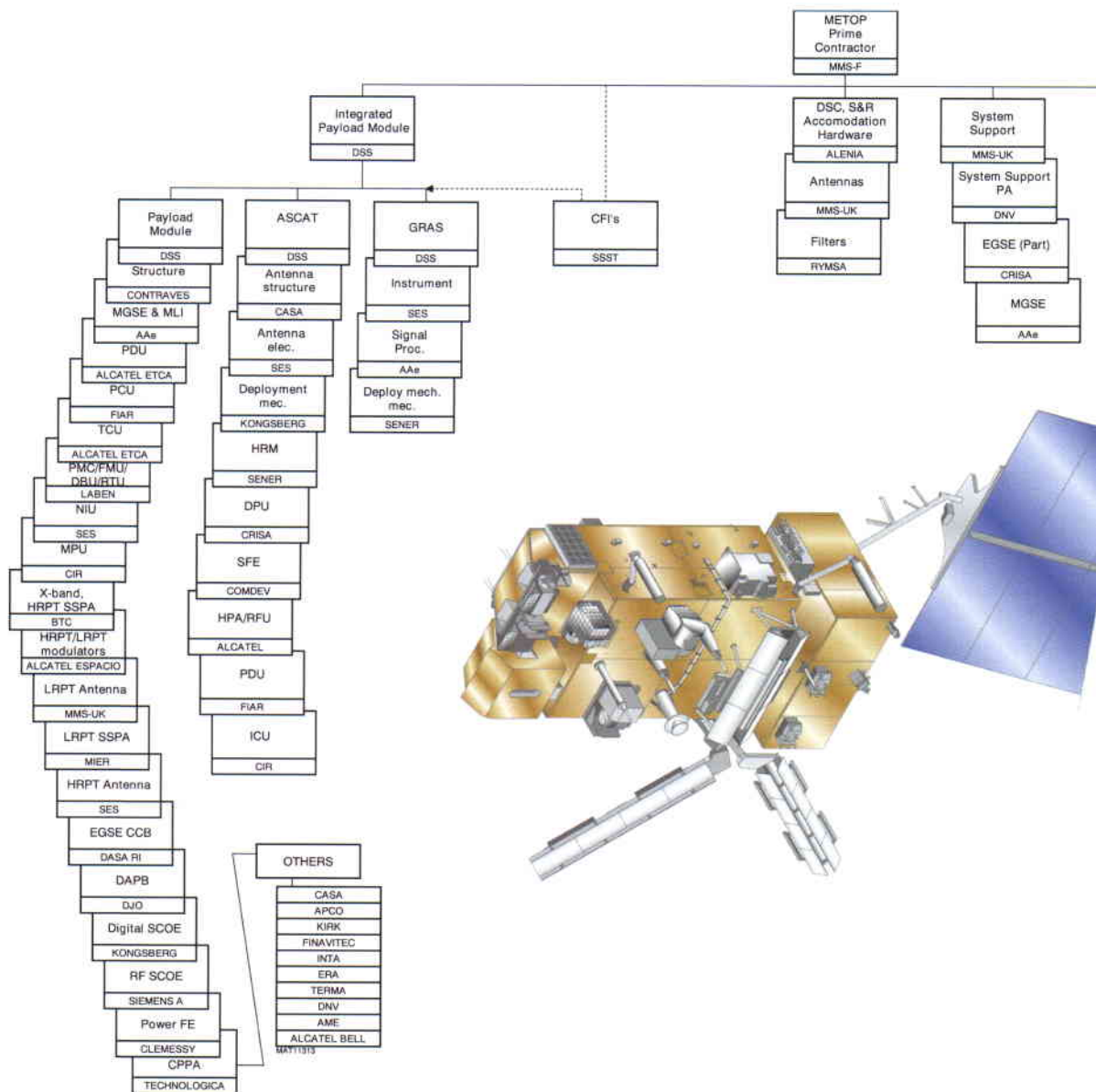


Figure 5. The Metop industrial organisation

Context of the mission

The Metop satellite and its payload embody a great deal of heritage, which has two primary benefits. The heritage of the satellite (especially the SVM) and its equipment have enabled significant cost savings in the development programme, while the heritage of the payload and services is an essential element in the efficient exploitation of the mission data. Almost all payload elements have direct and operational precursors, the only exception being the GRAS instrument, and even this is the operational follow-on to an in-orbit experiment. The transitional instruments in the first group above, commonly called the ATOVS package, supplemented by the DCS/S+R and SEM, are directly recurrent from the US satellites and have a strong heritage both in terms of hardware provision as well as in the processing and exploitation of the data. Amongst these, the MHS instrument is being

developed within the same broad time-frame as Metop-1, but it is intended to be a direct replacement for the AMSU-B and, furthermore, it will fly before Metop on at least one US satellite.

The ASCAT depends on the same physical principle as the scatterometers on ERS-1 and ERS-2, and the higher level processing of the data is equivalent. Hence it may be rapidly adopted as an operational instrument, as the ERS-2 instrument is today. However, it has two swaths compared to the one of ERS and also uses a different radar technique, such that the data pre-processing needs to be newly developed. The GOME-2 is also strongly related to the equivalent instrument on ERS-2, again leading to many advantages in terms of procurement, development of operational data processors, and existing user-experience in the data exploitation.

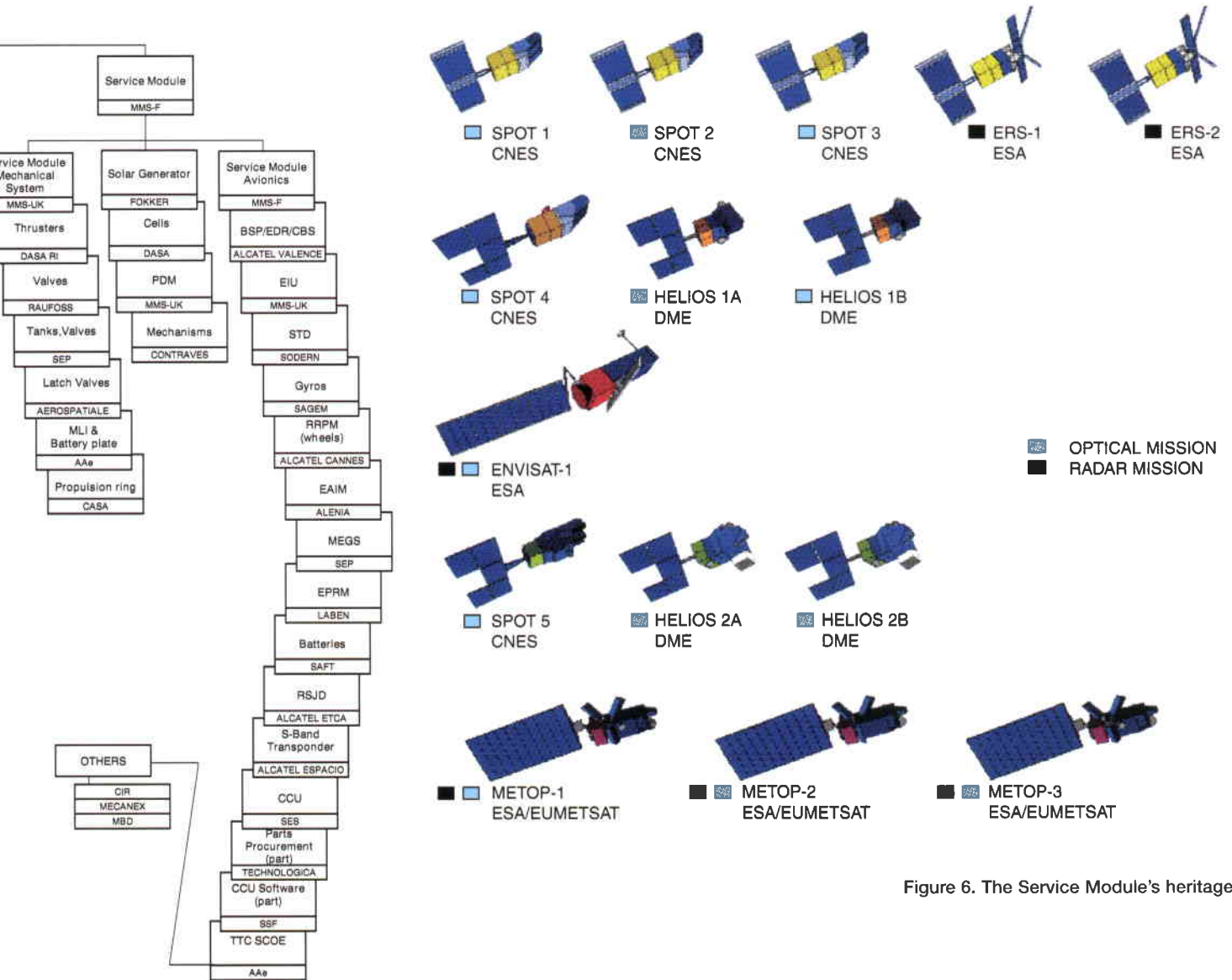


Figure 6. The Service Module's heritage

MMS has more than twenty years of experience in the development of low-Earth-orbit service modules which is of direct benefit for Metop. Regular upgrades to the Spot-1 concept have been performed to meet higher performance requirements and to maintain up-to-date avionics and technologies. A cumulated 46 year lifetime in orbit has been achieved today with 8 satellites (ERS-1 and 2, Spot-1, 2, 3 and 4, and Helios-1A and 1B) using the same SVM concept (Fig. 6). The Spot-1 SVM completed its 14th year of operation last year. ERS-1 operated very successfully for almost 9 years.

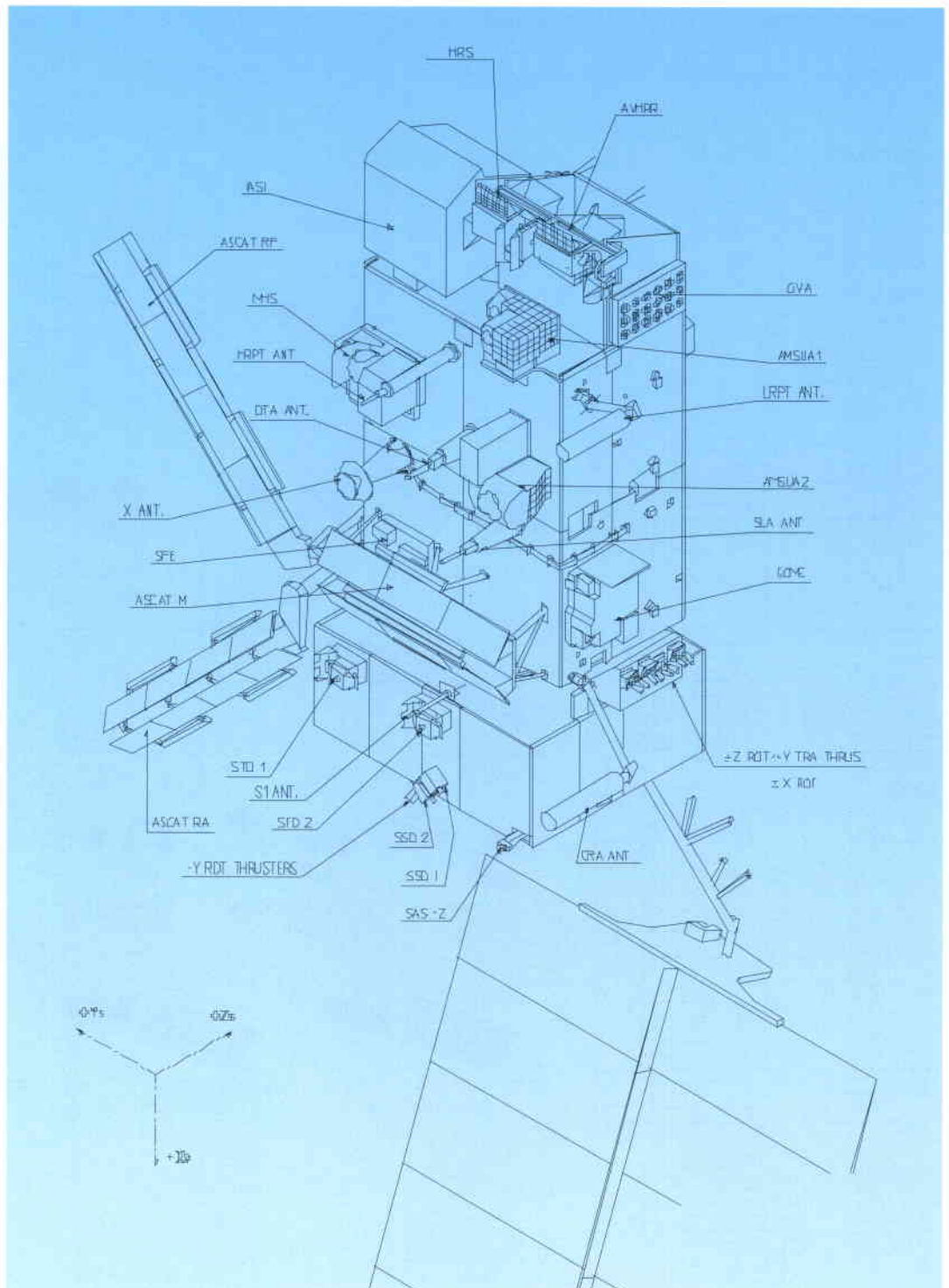
Overall architecture of the satellite

In order to accommodate the mission, and to ease the development as well as the verification process, the satellite's overall design is based on a modular approach, which relies upon two largely independent modules, the Payload Module and the Service Module. Figure 7 shows the Metop in-flight configuration.

The Payload Module (PLM)

The PLM provides the main supporting structure for both the payload instruments and the payload support systems. Instrument sensors and antennas are mounted on the

Figure 7. Metop's in-flight configuration



external panels, while most of the electronics units are accommodated inside the PLM.

The accommodation of a large complement of instruments is a significant design driver for the overall PLM configuration, with many constraints originating from instrument fields of view, antenna patterns, and thermal radiators having to be accounted for. In addition to the instrument units, the PLM also houses all of the avionics necessary to ensure:

- power regulation for the US instruments: as these instruments need a 28 V regulated power bus not available from the SVM; a dedicated power control unit is provided by the PLM
- power distribution: each unit or instrument is powered through a switchable and protected line, provided by specific PLM units
- command and control: a dedicated data bus, based on the European On-Board Data Handling Standard (OBDH), is used by the PLM. The Payload Module Computer (PMC) receives commands from the SVM and interfaces with the European instruments ICUs (Instrument Control Units) and MPU (MHS PLM adaptation Unit), as well as with a specific PLM unit for the US instruments
- handling of scientific data consisting of acquisition, formatting, encryption, storage, and transmission to ground of CCDS packetised data through the HRPT (High-Rate Picture Transmission), LRPT (Low-Rate Picture Transmission), and X-band links.

The Service Module (SVM)

The SVM provides all the standard service functions, like:

- attitude and orbit control, to maintain accurate Earth-pointing during the various operational modes, and to perform orbit acquisition and maintenance
- propulsion, for orbit and dedicated manoeuvres, as well as propellant storage
- electrical power generation, through the solar array, storage, conditioning, and overall distribution
- distribution of on-ground and on-board generated commands, and collection of house-keeping telemetry data for transmission to ground through the S-band link
- central on-board software for telemetry generation, telecommand processing, and various application functions (e.g. thermal control, on-board surveillance, automatic command sequencing).

The mechanical subsystem is derived from the Envisat Service Module. It is a box-shaped structure that interfaces with both the launch vehicle and the PLM. Interfaces between the

two modules have been standardised as much as possible, and kept to a minimum. Thermal exchanges between the two modules are very limited, mechanical interfaces basically consist of the two modules connection, electrical interfaces are limited to power and OBDH bus, plus solar-array deployment and pyrotechnics needs, data exchanges use telemetry and telecommand packets.

The satellite overall dimensions (in metres) are close to 6.3 (high) by 3.4 x 3.4 (transverse section) in launch configuration, and 17.6 x 6.6 x 5.0, after solar-array and antenna deployment.

Electrical architecture

Modularity and standardisation are the main design drivers for the electrical architecture (Fig. 8). The design offers simple interfaces, and makes use of existing hardware developed in the frames of Spot-5 for the SVM and Envisat for the PLM.

Power generation, storage and distribution

Electrical power is generated by an eight-panel solar array derived from Envisat. Energy storage is provided by five batteries, which allow operation in the launch and early orbit phase (LEOP), eclipse and contingency modes. The primary power bus is an unregulated bus, which is distributed to both the SVM and PLM units. The 28 V power regulation needed by the US instruments is performed by a dedicated PLM unit (PCU).

Command and control

The command and control functions are distributed throughout the spacecraft, and also have to accommodate a range of interface requirements from the heritage instruments. The Metop-specific equipment and instruments use the European OBDH interfaces, while the MHS uses the MIL-STD-1553 interface. Both of these are high-level command and control interfaces allowing for intelligence within the instruments. The heritage instruments from NOAA have a much simpler interface with distributed signal lines.

The distributed command and control architecture features the following elements:

- The primary spacecraft computer is within the SVM and is responsible for the interface to the ground segment and control of the equipment in the SVM and for the overall security of the mission.
- Command and control of the payload is performed by the PLM Computer (PMC), which is connected to the SVM computer via the SVM OBDH bus. This computer controls a specific OBDH bus within the PLM.

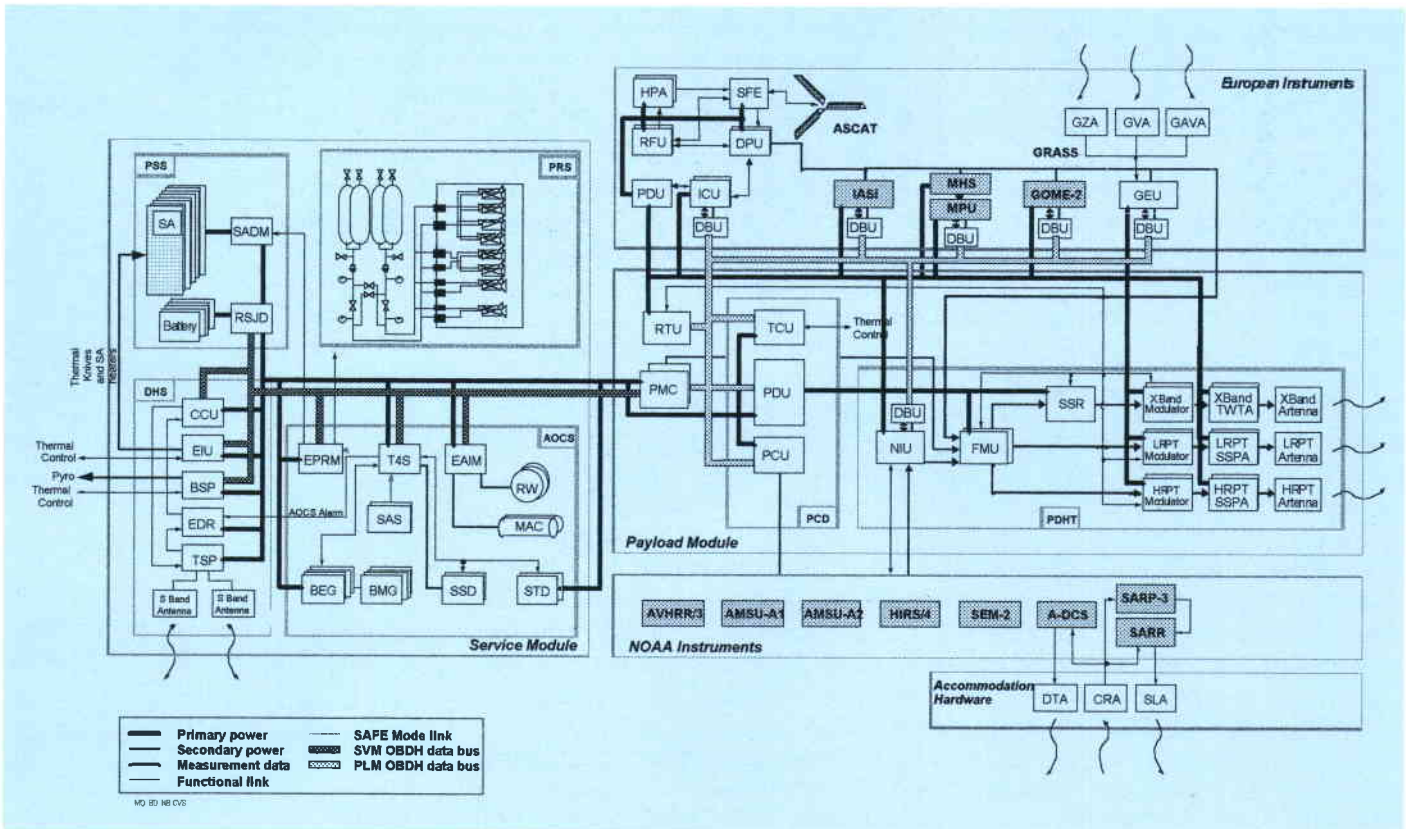


Figure 8. Metop's electrical architecture

- The 'European' instruments (ASCAT, GRAS, GOME, IASI) each include an intelligent Instrument Control Unit (ICU) which communicates with the PMC.
- The MHS communicates via a specific adaptation unit, MPU, or MHS Protocol Unit, which performs the translation between the MHS MIL-STD 1553 bus and the PLM OBDH. The MPU also provides the science-data interface.
- The NOAA Interface Unit (NIU) emulates the Tiros-spacecraft-type interfaces required by the NOAA instruments. It includes its own ICU, which performs the command and control function as well as packaging the NOAA instrument data into CCSDS packets. It also performs the AVHRR data compression.

Payload data handling and transmission

The science data from the payload is provided in the form of CCSDS packets at a wide range of data rates, ranging from 1.5 Mbps for IASI to 160 bps for SEM. The PMC also provides some additional packets required for data exploitation:

- Position and time data derived from the GRAS.
- A copy of the full spacecraft housekeeping telemetry.
- A text 'administration message' which is uplinked and stored on board, providing the facility to broadcast information to remote users.

All of these data streams are multiplexed and provided on three channels going to the on-board recorder, the HRPT, and LRPT direct-broadcast subsystems. Encryption is possible for the direct-broadcast services. Only a subset of the packets is provided to the LRPT.

The Solid-State Recorder is based on the Cluster and Envisat design, and has a capacity of 24 GB at end-of-life. This is sufficient for slightly more than one full orbit of data. The X-band subsystem provides a direct 70 Mbps transmission link to ground during visibility periods, dumping the data stored during the previous orbit to ground.

Telemetry, tracking and command

Two antennas allowing omni-directional coverage interface with the S-band transponder by means of a 3 dB hybrid coupler. Each transponder consists of a diplexer, a receiver and a transmitter.

Attitude and orbit control

The AOCS architecture is based around three units performing the interface between the SVM OBDH bus and the sensors and actuators. A first unit (T4S) interfaces with the Earth and Sun sensors, and with the gyros; the EAIM provides the interface with the reaction wheels and the magnetotorquers; the EPRM ensures the necessary command and acquisition capability for the propulsion subsystem, and also interfaces with the solar-array drive mechanism.

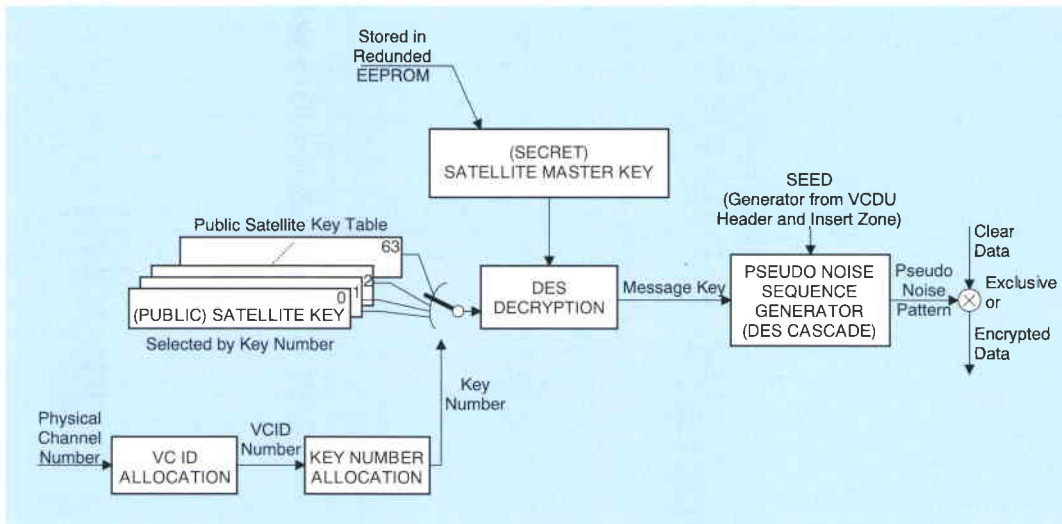


Figure 9: Metop's encryption scheme

In all nominal modes, the AOCS software is part of the SVM central flight software. In Sun-pointed safe mode, the AOCS function is autonomously ensured inside the T4S unit by the survival electronics, which feature an independent computer.

Mission-specific features

High-Rate and Low-Rate Picture Transmission (HRPT/LRPT)

The Metop satellite continuously records its data on-board, but it also provides a continuous direct data-broadcast service, with two simultaneous signals. The HRPT service operates with a microwave link at L-band with the full data content as recorded on-board (at 3.5 Mbps). This service is very similar to the existing service from the NOAA satellites and enables regional meteorological organisations to receive all data relevant to their area in real time. The LRPT service is more innovative and replaces the APT service provided today by the NOAA satellites. It is an analogue broadcast at VHF, providing low-resolution AVHRR images to several thousands of users equipped with small, inexpensive receivers. This system has enabled local cloud patterns to be displayed easily, for example in schools. The digital LRPT service retains the VHF frequency and bandwidth of the APT service, but provides three channels of AVHRR data at the full instrument spatial and radiometric resolution, through the use of a modified JPEG compression scheme. To minimise the effect of ionospheric scintillation at VHF, a powerful interleaving and modulation scheme has been developed which will make the system strongly resistant to data drop-outs, which in the analogue system would result in missing scan lines.

Encryption

In order to limit data access, Metop provides facilities to encrypt data for LRPT and HRPT channels. The encryption scheme is selective

on virtual channels and users. Also, there are separate keys for LRPT and HRPT.

The encryption is based on the principle shown in Figure 9. The encryption itself is performed by doing an exclusive OR between each VCDU Data Unit zone and a pseudo-noise pattern. As this operation is fully reversible, the data at ground are decrypted by using the same pseudo-noise pattern with an exclusive OR with data. The pseudo-noise pattern that is the basis for the encryption is created from:

- The secret Master Satellite Key (MSK), which is stored on board and cannot be transmitted to ground via telemetry.
- The Public Satellite Keys, which can be uploaded from the ground periodically to ensure sufficient secrecy and to control data access. On Metop, there is a table of 64 different possibilities. For each encryption process, there is a suitable telecommand in order to select the appropriate key.

These two keys are processed through a Data Encryption Standard (DES) algorithm (decryption part) in order to get the Message Key.

Compression

The AVHRR scanning mirror rotates at 360 rpm, producing five lines (one per channel) of Earth-view samples every 1/6 sec. The samples are 10 bits wide and each Earth-view line contains 2048 pixels (1 pixel is about 1 km), which means a data rate of 2048 (samples) x 3 (spectral bands) x 6 (lines per second) x 10 (bits per sample) = 369 kbps. As the allocated data rate for AVHRR/LRPT is 40 kbps, global factor-10 data compression is required. The following convention has been adopted for the compression (Fig. 10):

- The AVHRR/LRPT will contain only three spectral compressed images and one calibration data packet. Five spectral channels are inside HRPT.

Figure 10. Metop's compression scheme: AVHRR data

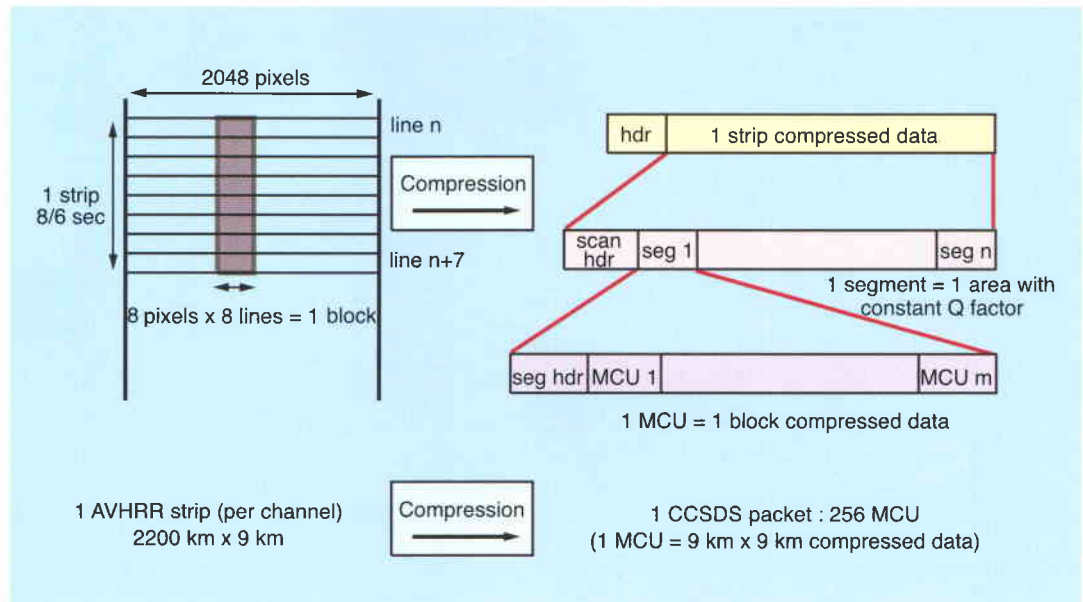


Table 3. Metop's data interface with ground

| Data Description | Frequency Domain | Useful Bit Rate |
|-----------------------------|----------------------|-------------------------|
| TT&C uplink | S-band 2053.4 MHz | 2000 bps in NRZ/PSK/PM |
| TT&C downlink | S band 2230 MHz | 4096 bps in SP-L/PSK/PM |
| Global Data Stream downlink | X-band 7750-7900 MHz | 70 Mbps in QPSK |
| LRPT downlink | VHF 137.1 MHz | 72 kbps in QPSK |
| HRPT downlink | L-band 1701.3 MHz | 3.5 Mbps in QPSK |

- The compression is applied to the 10-bit data sample words.
- The compression algorithm is a modified JPEG to accommodate a fixed compression rate and a continuous instrument data rate.

An AVHRR image can be divided into strips (8 lines). The compressed part of the strip will be transmitted in the user data field of one CCSDS packet. The strips are divided into segments. Inside a segment, a constant Q factor is applied. Finally, each segment is divided into blocks of 8 pixels x 8 lines. A compressed block is called a Minimum Coded Unit (MCU). There will be four packets (three channels and one calibration) every 8/6 seconds (1 strip lasts 8/6 sec). The global number of MCUs is $2048/8 = 256$. The number of segments can be programmed from the ground, albeit with a potential impact on image quality since a constant Q factor is applied on one segment.

Communications links

The satellite provides data transmission to and from the ground with the characteristics defined in Table 3, and as described previously, in S-band (TT&C), L-band (HRPT), VHF (LRPT)

and X-band (global data dump). In addition to these links, Metop provides an Advanced DCS (Argos) service and a Search & Rescue (SARR/SARP) service with the following frequencies:

- A-DCS data reception at 401.65 MHz
- A-DCS data transmission at 466 MHz
- SARR beacon-signal reception at 121.5, 243 and 406.05 MHz
- SARP-2 data reception at 406.05 MHz (common with SARR)
- SARR data transmission at 1544.5 GHz.

These links are performed by means of an antenna farm comprised of the following elements:

- X-band transmit antenna
- S-band TT&C receive/transmit antenna
- LRPT VHF transmit antenna
- HRPT L-band transmit antenna
- CRA: Combined Receive Antenna (uplink)
- SLA: Search and Rescue L-band transmit antenna
- DTA: DCS transmit antenna.

One major consequence of these various space-to-ground links, combined with numerous RF instruments (AMSU A1, AMSU A2, MHS, GRAS, ASCAT), is the fact that ensuring RF compatibility within the satellite is a challenging design requirement leading to an extensive test campaign and a dedicated development approach.

ASCAT – Metop’s Advanced Scatterometer

R.V. Gelsthorpe

Earth Observation Programmes Development Department, ESA Directorate of Application Programmes, ESTEC, Noordwijk, The Netherlands

E. Schied

Dornier Satellitensysteme*, Friedrichshafen, Germany

J.J.W. Wilson

Eumetsat, Darmstadt, Germany

Introduction

Wind scatterometers already flown on ESA’s ERS-1 and ERS-2 satellites have demonstrated the value of such instruments for the global determination of sea-surface wind vectors. These highly successful instruments – part of the Active Microwave Instrument (AMI) – were conceived about twenty years ago. During the intervening period, there has been a considerable evolution in the capabilities of spaceborne hardware.

ASCAT is an advanced scatterometer that will fly as part of the payload of the Metop satellites, which in turn form part of the Eumetsat Polar System. It is developed by Dornier Satellitensysteme under the leadership of Matra Marconi Space, the satellite Prime Contractor, for ESA. From its polar orbit, ASCAT will measure sea-surface winds in two 500 km wide swaths and will achieve global coverage in a period of just five days.**

The Advanced Scatterometer, known as ASCAT, is the successor to these instruments, and will be flown as part of the payloads of Metop-1, -2 and -3. It represents advances in increased coverage, reduced data rate and power-efficient low-mass technology.

Principles of wind scatterometers

Wind scatterometers are instruments that are used to infer data on wind speed and direction from radar measurements of the sea surface. They rely for their operation on the fact that winds moving over the sea influence the radar backscattering properties of its surface in a manner that is related to wind speed and wind direction. Everyday experience of the sea surface suggests a variation of scattering with wind intensity: we observe a mirror-like surface with no wind, small ripples in gentle airs, and a rough surface under high-wind conditions.

Figure 1 indicates the form of the variation of backscattering coefficient with relative wind direction (at a fixed incidence angle) for a range of wind speeds.

If an instrument were to be constructed that determined the sea-surface backscattering coefficient from a single look direction, the overlapping nature of the curves would limit its capabilities to providing a rather coarse estimate of wind speed and no information on wind direction. The earliest successful spaceborne wind scatterometer, that of Seasat, used two dual-polarised antennas pointed at 45 and 135 deg with respect to the satellite’s direction of flight to determine sea-surface scattering coefficients from two directions separated by 90 deg. The scattering characteristics of areas in the coverage region were firstly determined via the forward-looking antenna and subsequently, by virtue of the along-track motion of the satellite, via the rearward-looking antenna. Pairs of measurements so obtained could then be fitted to curves like those of Figure 1 to derive estimates of both wind speed and wind direction.

A weakness exists in two-beam single-polarisation scatterometers which Seasat sought to overcome, with only limited success, by use of dual polarisation. Owing to the shape of the backscatter functions shown in Figure 1, two-beam scatterometers are capable of producing a number of alternative solutions for wind speed and direction from the same set of measurement data. As an illustration, consider the case of measuring a real 16 m/s upwind – the two beams of the instrument would observe the characteristic at points A and would indicate a scattering coefficient of around -8.7 dB. The yellow curve in Figure 1

*Now Astrium GmbH.

**Now Astrium SAS.

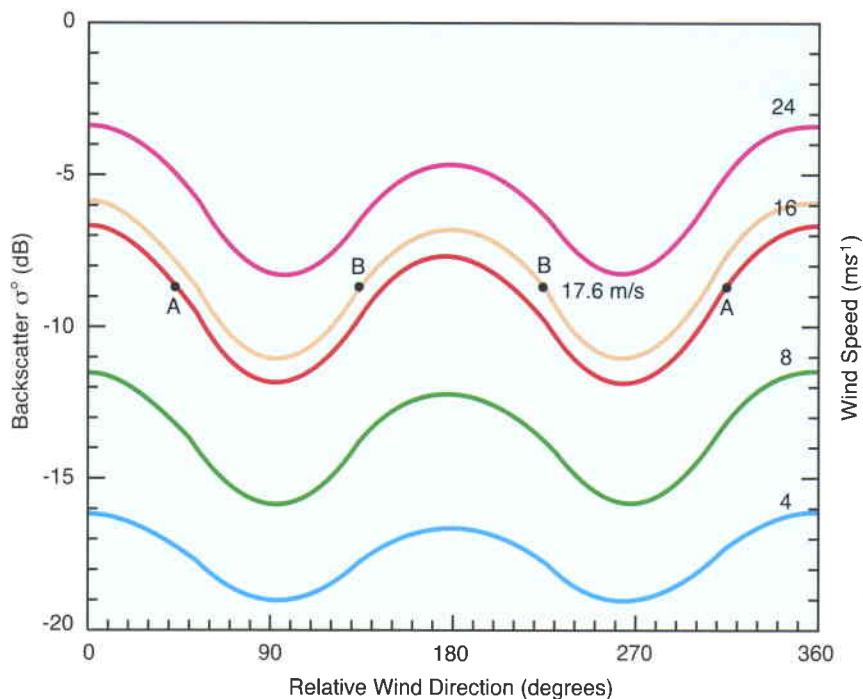


Figure 1. Variation of scattering coefficient with wind direction (35 deg incidence)

also has a pair of points at -8.7 dB separated by 90 deg and represents an ambiguous solution to the wind-measurement problem in the form of a 17.6 m/s downwind. In order to overcome this ambiguity problem, a third beam oriented at 90 deg to the flight direction was introduced into the design of the scatterometers flown on ERS-1 and -2. This configuration has proven very effective, leading to a typical ambiguity rejection skill of 97%.

Figure 2. A typical scatterometer data product over land: the image shows the multi-year mean scattering coefficient at 40 deg incidence angle (courtesy of by V. Wismann and K. Boehnke)

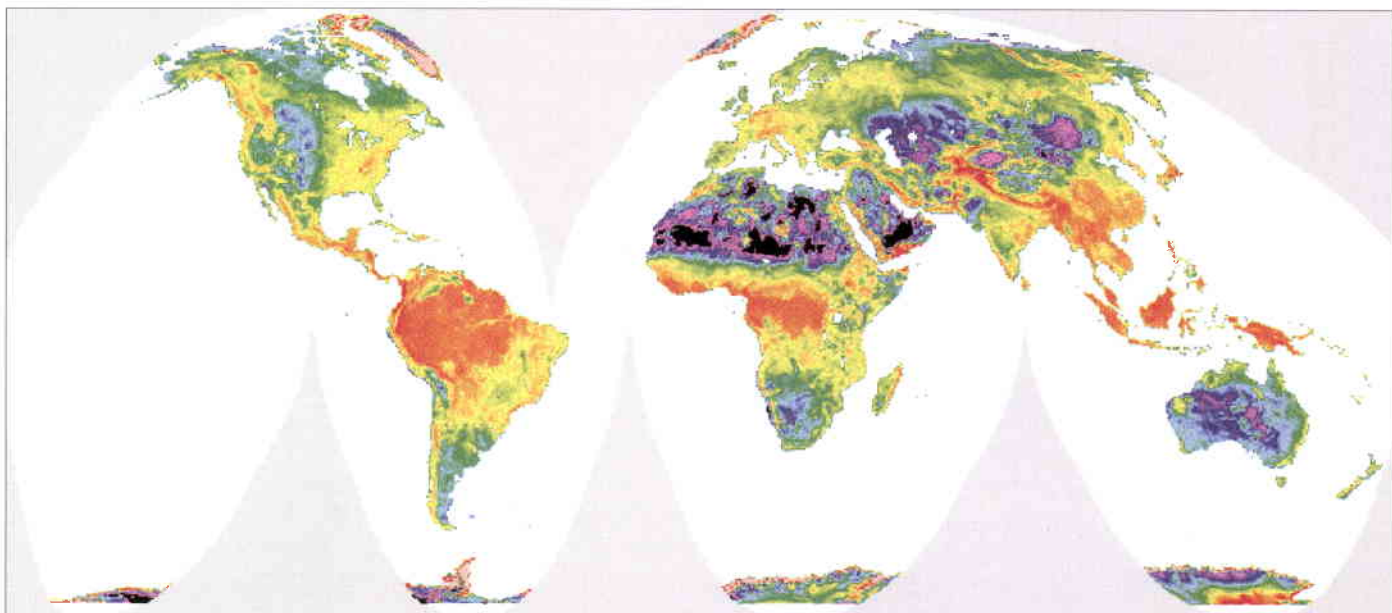
In addition to their intended use for wind determination, the ERS scatterometers have been applied in both sea and land applications with objectives as diverse as monitoring of sea ice, snow, geophysics, soil moisture and vegetation. Figure 2 is a typical product over land. The advanced capabilities of ASCAT will

inevitably continue to expand the range of emerging scatterometer applications.

Key elements in the specification of ASCAT

The engineering specifications of both the ERS and Metop scatterometers derive from a geophysical requirement to determine wind vectors over a coverage region consisting of 50 km-resolution cells. Determination of speeds in the range 4 – 24 m/s with an accuracy of 2 m/s (or 10%) and directions with an accuracy of ± 20 deg is required. Table 1 shows the key engineering performances of the ASCAT and the ERS scatterometers, which meet these requirements, and how the performance has evolved in respect of the following:

- Coverage: ASCAT offers twice the coverage of the instrument flown on ERS. Its twin swaths are offset to the left and right side of the satellite’s ground track by about 384 km, and each offers full performance over a width of 500 km. This is especially important for the Metop mission, where quasi-global coverage on a daily basis is needed.
- Spatial resolution: Although driven by the requirement for 50 km spatial resolution, ASCAT also offers, on an experimental basis, the possibility of increased spatial resolution: a data product with 25 km spatial resolution will be produced in addition to the 50 km product.
- Radiometric accuracy and inter-beam stability: In order to meet the stringent requirements on wind speed and direction, it was necessary on ERS to apply strict control on overall gain variations in the instrument and on gain variations between its beams. Although the terminology differs somewhat between the ERS and Metop scatterometers, the same fundamental requirements apply: radiometric accuracy controls the extent to which the



ensemble of beams may be allowed to vary, and inter-beam stability controls the maximum extent by which the gain of any pair of beams may vary. The use of an on-board calibration network is of great value in this context, but satisfying these specifications still represents one of the most challenging problems of the ASCAT design.

- Radiometric resolution and ambiguities: In order to perform wind extraction on a reliable basis, it is important to limit the level of random errors in the measured data. The specification on radiometric resolution limits the level of such errors in the measurement due to the effects arising from speckle (the statistical behaviour of the radar target) and finite signal-to-noise ratio. The need to provide adequate radiometric resolution is a factor in the dimensioning of antenna gain, transmitter power and receiver noise figure. A second factor leading to random errors in the measured data is ambiguity energy. This is spurious energy arising from outside the measurement cell. The need to control ambiguities imposes constraints on the antenna side-lobe performances.

ASCAT's operating principle

In contrast to the scatterometers used on ERS, which relied on the transmission of continuous-wave pulses with durations of around 100 μ sec and peak powers of several kilowatts, ASCAT transmits linear frequency-modulated pulses with a markedly longer duration of around 10 msec, at a relatively low peak power of 120 W.

Echo signals are received by the instrument and may be thought of as a large number of superimposed echo pulses arriving over a range of times corresponding to the width of the instrument swath; signals outside the area of interest are largely suppressed by the antenna side-lobe pattern. The received echo is mixed with a suitably delayed pulse, which is a frequency-modulated replica of the transmitted signal. Figure 3 illustrates the principle of the mixing process for two echo pulses with flight

Table 1. Key engineering performance parameters for ASCAT and the ERS scatterometers

| Performance Parameter | Unit | ASCAT | ERS |
|--|------|---------------------------------|--|
| Coverage: | | | |
| Number of swaths | | 2 | 1 |
| Full performance width | km | 500 | 400 |
| Reduced performance width | km | 550 | 500 |
| Length | km | continuous | continuous |
| Mid-swath inclination | deg | 37.6 | 29.3 |
| Spatial Resolution: | | | |
| Nominal | km | 50 | 45 |
| Experimental | km | 25 | none |
| Radiometric accuracy | dB | 0.57 | - |
| Common mode stability | | - | 0.57 |
| Interbeam stability | dB | 0.46 | 0.46 |
| Radiometric resolution at minimum cross wind | % | 3.0 – 9.9 | 8.5 – 9.7 |
| Radiometric resolution at | % | 3.0 | 6.5 – 7.0 |
| Ambiguity contribution | % | 1 (near swath) 3 (far swath) | included in radiometric resolution specification |

times t_1 and t_2 ; because of the linear frequency modulation, the pulses are offset from the local oscillator pulse for the duration of the echo by frequencies f_1 and f_2 , respectively. These frequency differences allow the discrimination of signals originating at different ranges. For the real received echo, the mixer output is a spectrum of signals, which is present for a time corresponding to the time that the transmit pulse is present within the swath. By sampling the mixer output in time and Fourier-transforming the time series into a frequency series, the frequency spectrum may be extracted from the data and the height and frequency of its spectral lines may be interpreted in terms of power and range, respectively.

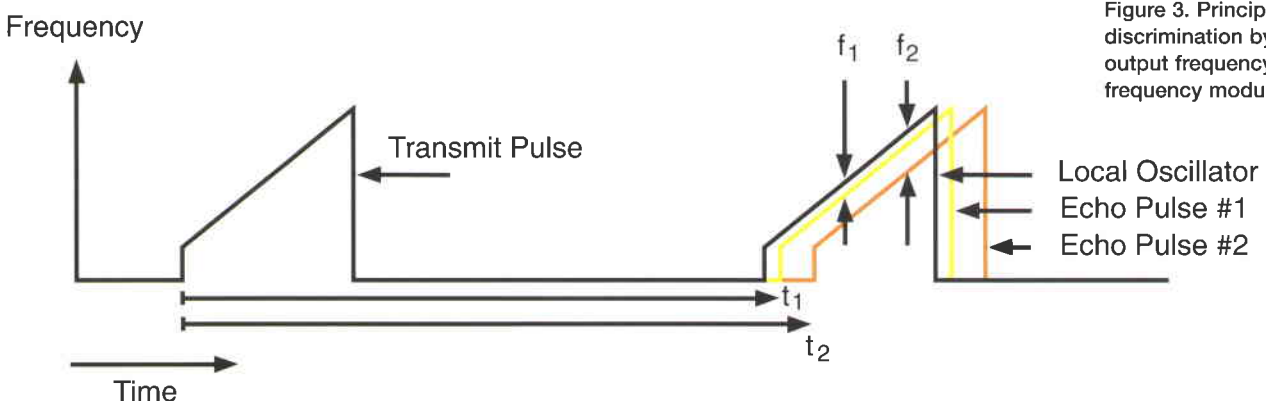


Figure 3. Principle of range discrimination by mixer output frequency in a linear frequency modulation radar

Figure 4. Processes occurring within a single pulse-repetition interval

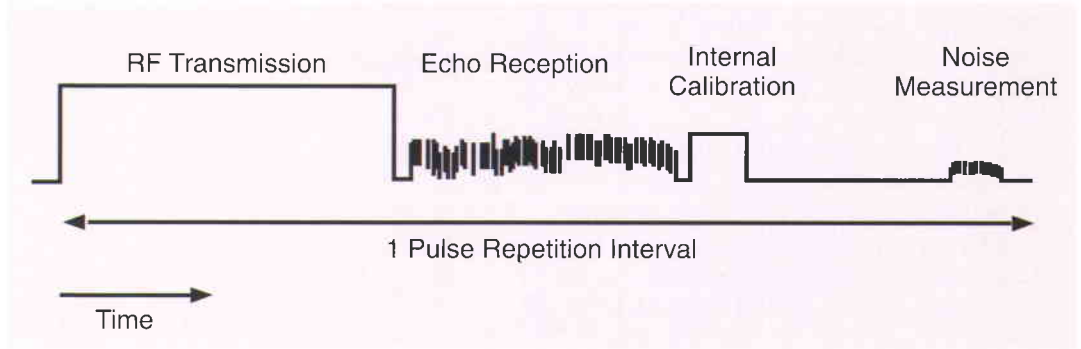
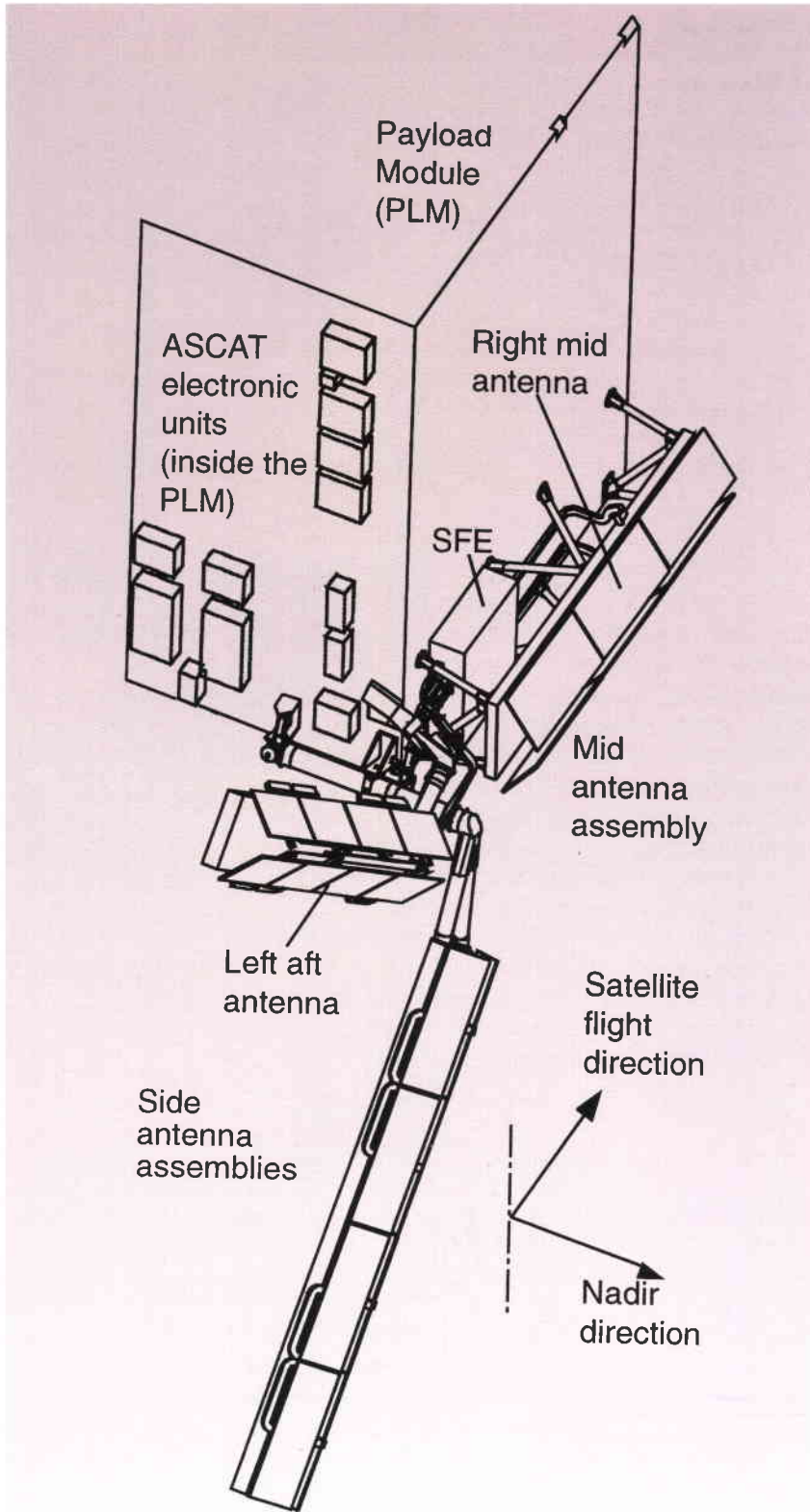


Figure 5. The ASCAT hardware on the Payload Module



In addition to the processing of echo signals, the instrument also performs an internal calibration process within each pulse repetition interval. This consists of a measurement of the output power during the transmit pulse, the injection into the receiver of a signal proportional to the transmit pulse at a point in the inter-pulse period, and monitoring of the magnitude of this signal at the receiver output. This gives an indication of how the combination of transmitter power and receiver gain is varying and allows changes in these parameters to be compensated.

Also contained within the pulse-repetition interval is a period after all echoes have decayed, during which the receiver noise output is monitored. This enables the contribution of the receiver noise to the radar measurement to be estimated and a correction performed. Figure 4 shows the time-lining scheme of the processes occurring within a single pulse-repetition interval.

Because ASCAT is a dual-swath instrument, it has a total of six antennas, three looking to each of the two swaths. In operation, the transmit-receive cycle outlined above is performed by each of the six antennas in turn over a total period of approximately 0.2 sec. Data from each pulse-repetition interval is processed on board to yield instrument data packets, which either contain echo and ancillary data or noise measurement data. This on-board processing, in the case of both packet types, involves a considerable compression of the raw data and results in a reduction in the instrument raw data rate of around 1.4 Mbit/sec to a 55 kbit/sec data stream for delivery to the satellite payload data-handling and transmission system, thereby simplifying the on-board data handling.

On-board hardware

The ASCAT hardware on the Payload Module (PLM) is shown in Figure 5, where the dominating elements are the three ASCAT antenna assemblies mounted outside the Module. All electronics boxes are located inside the Payload Module with the exception of the

Scatterometer Front-End electronics (SFE), which is located below the mid-antenna assembly.

A block diagram of the ASCAT constituent elements is shown in Figure 6: black shadows indicate the existence of a redundant unit. Although the SFE contains only one set of the wave-guide elements, it does have some internal redundancy – there are two low-noise amplifiers, two sets of control electronics, and redundant coils in its switching circulators.

The following paragraphs briefly describe the various hardware elements of the ASCAT instrument and indicate their major functions and some of the design considerations. The numerical performance data given in Table 2 are taken from the results of engineering-model testing and are typical values at about room temperature, which is close to the expected in-flight temperatures of the units.

Antennas

ASCAT has six antennas, which are mounted in pairs in a V-shaped configuration on the three antenna assemblies. The two mid antennas, fixed-mounted on the Payload Module, point in an across-track direction towards the right and the left swaths with respect to the flight direction. In contrast to the mid assembly, the two side assemblies are deployed after the launch by motors. They are then latched in well-defined positions such that the antenna beams are oriented at ± 45 deg with respect to the mid beams.

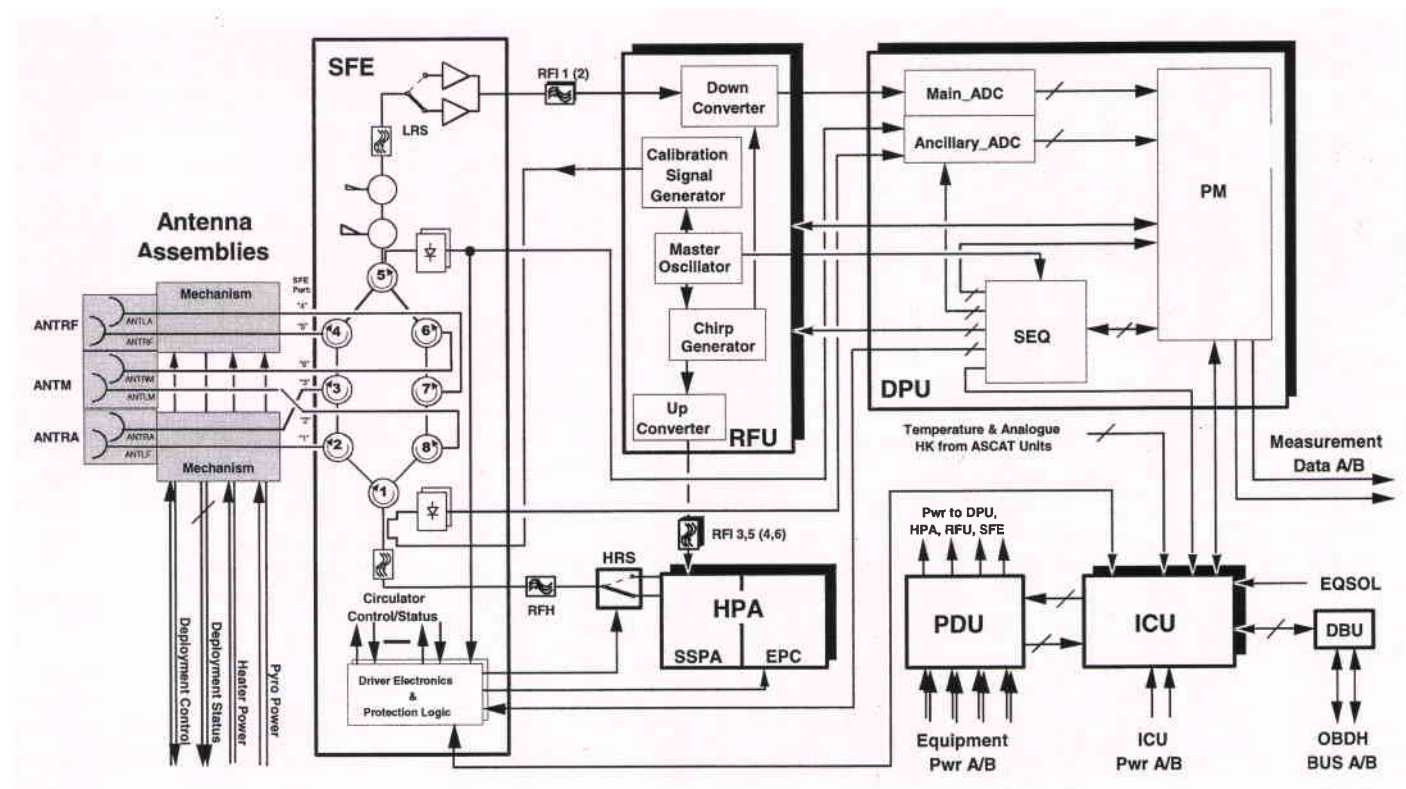
All six antennas are slotted-waveguide arrays manufactured from aluminium. The main considerations for the electrical design have been high gain to ensure an adequate link budget, and low gain slopes, high gain stability and high pointing stability to minimise radiometric errors. Side-lobe performance has also driven the antenna design in order to minimise the reception of echo signals from outside the desired measurement cells.

In addition, the design had to take account of electromagnetic scattering from the satellite. Early analysis showed that the pattern of the right mid antenna was distorted by reflections from the Payload Module surface, and that of the left fore antenna by reflections from the solar array. The mid-antenna problems were solved by minimising the antenna back radiation and by the introduction of a deflector on the Payload Module to reduce the pattern distortion further. The success of this method was proven by tests of the mid-antenna development model on a full-scale satellite mock up.

For the side antennas, the pattern has been constrained by the need to minimise side lobes in the solar-array direction. This has a consequent negative impact on the gain slope, and a compromise has been necessary between the latter and side-lobe suppression in order to maintain acceptable performances in terms of both radiometric accuracy and ambiguity.

Another important parameter is antenna gain

Figure 6. The constituent elements of ASCAT



stability, which is ensured a combination of low antenna-temperature variation over the orbit and low antenna-gain sensitivity to temperature. The former is achieved by careful design of the antennas' passive thermal-control elements. The aperture surfaces are covered with a combination of aluminium tape and silver paint in a carefully selected ratio in order to achieve good thermal stability over the orbit. Good thermal control is the basis for low thermal gradients within the antenna assemblies, which keeps the aperture surface stable and leads to high pointing stability. Electrically, stable gain performance is promoted by splitting the antenna aperture into sub-panels with short waveguide elements.

SFE

Figure 6 includes a schematic representation of the contents of the Scatterometer Front End. Central to the unit is a matrix of eight switching circulators, which allows each of the six antennas to be operated in turn, with the sequence repeating after all six antennas have been exercised.

Each pulse-repetition interval has four phases with a dedicated setting of the circulators, i.e. high-power signal transmission, echo reception, internal calibration and noise power measurement. During the transmit phase, the ferrite circulators route the transmit pulse towards the desired antenna. At the same time, another part of the SFE measures both the transmitted signal power via a directional 'calibration' coupler and a forward power detector, and the reflected signal power via a second directional coupler and a reflected power detector. The pair of measurements may be used to correct the measurement data for power reflected at the antenna interface. During the transmit period, it is necessary to protect the SFE low-noise amplifier from damage by transmit leakage signals. This is achieved by the activation of a shutter, a pair of switches between the switch matrix and the low-noise amplifier. In the receive phase, the shutter is opened to allow the reception of the echo from the ground.

During the calibration phase, the switch matrix is reconfigured so that a calibration signal that is injected into the SFE at the calibration coupler is routed towards the receiver. This coupler is a key element of the ASCAT internal calibration system, which allows the correction of variations in transmit power and receiver gain. The coupling coefficient of the calibration coupler is the reference for the internal calibration loop, and it is therefore vital that this coupling coefficient remains stable over temperature and over the instrument lifetime.

The coupler is a metallic waveguide component, the electrical stability of which depends on its geometry which, in turn, depends on temperature. It is therefore manufactured from Invar. Like the other waveguide elements, it is silver-plated internally for good electrical conductivity.

The last phase in every pulse-repetition interval is the noise power measurement. It starts after all echoes from the ground have ended. The circulators are reset in this phase to the receive configuration, which ensures correct noise power subtraction.

A further important element of the SFE is the low-noise amplifier, which as the first active element of the receive chain has an important role in determining the system noise figure.

RFU

The Radio Frequency Unit generates the low-level transmit signal (which drives the high-power amplifier); it also generates the calibration signal and provides the echo down-conversion and amplification within the receive module.

Signal generation within the RFU is based on the use of a thermally controlled crystal oscillator. All clock signals for the ASCAT timing and the radio-frequency signals for up- and down-conversions are derived from the crystal frequency.

The chirped signals necessary for the transmitter and receiver are generated within a digital chirp generator. Start frequencies and chirp slopes are freely selectable by digital control words. A set of chirp parameters is transmitted to the RFU after start-up and allows selection of the desired signal characteristics during the measurement phase. In nominal operation, three different chirp signals are used for the three antenna types, as well as a continuous-wave signal for internal calibration.

Another important function of the RFU is in gain and level setting. It provides an injected calibration signal which is matched to the detected level of the transmit pulse with a resolution of 0.03 dB and is updated every pulse repetition interval. The transmit signal level also is adjustable by appropriate on-board parameter setting and the receiver section, which down-converts the signals to the baseband, also amplifies the signal with an adjustable gain.

HPA

The ASCAT High Power Amplifier (HPA) consists of two separate hardware items, an electronic power conditioner and a solid-state

power amplifier. Amplification is performed by GaAs FET transistors, and the high output power is achieved by combining the outputs of parallel transistors.

The main design requirements of the HPA are to generate sufficient output power at as high an efficiency as possible with a constant output level over the pulse's duration. In order to be compatible with other instruments on the satellite, harmonic and spurious outputs from the amplifier are tightly controlled.

DPU

The Digital Processing Unit digitises the analogue echo data and the transmitted and reflected power data using three analogue-to-digital converters; it also processes these data. It also controls the ASCAT calibration loop and generates the instrument timing signals.

After digitisation of the DPU input signals, the main echo processing steps are: windowing of the digital samples, Fourier transformation, squared-modulus detection, data compression and finally formatting of the data, together with time stamps and further auxiliary data, into data packages.

In parallel with the data processing, the DPU adjusts the calibration signal level within the RFU on the basis of readings from the ancillary ADC. In addition, there is a two-way communication with the ICU in order to acquire the timing and temperature information for inclusion within the measurement data packets, and to pass housekeeping telemetry parameters to the ICU for instrument monitoring.

The unit provides a large number of timing signals, which control the circulators of the SFE, perform chirp selection, RFU triggering, HPA gating and control the digital processing. The on-board software is controlled by a set of parameter tables. There is a special external calibration mode for the instrument that is obtained by reloading the sequencer parameter table that controls the instrument timing. The parameter tables allow great flexibility in instrument operation and, as they can be changed in flight, the ASCAT timing can be easily modified if that should ever be deemed necessary.

PDU

The Power Distribution Unit switches the power lines for the ASCAT unit and provides the unregulated voltage to the ASCAT units. Its main functions are switching unit power lines according to the instrument redundancy selected, and monitoring the voltages and currents of the different units.

ICU

The Instrument Control Unit provides the interface between the Payload Module controller and the ASCAT instrument. Its main functions are to handle and process commands and timing signals from the controller, to monitor telemetry from the different ASCAT units, to initiate recovery actions where necessary, and to provide the housekeeping data.

Ground processing, calibration and data products

In flight, the ASCAT instrument is only intended to operate in two modes, namely 'measurement mode' or 'calibration mode'. Normal operation will be in measurement mode, and calibration mode will only be used during certain limited periods in the satellite's lifetime specifically assigned to the observation of external calibration transponders.

During measurement-mode operation, the ASCAT instrument generates two types of data packet for each antenna beam, echo packets and noise packets. Noise packets are produced less frequently than echo packets because more extensive on-board averaging along-track is carried out for noise reception windows compared to that for echo reception windows. These two types of data packets are interleaved in the data stream given to the operational ground processor.

For instrument measurement-mode ground processing, the echo and noise packets are split into two different streams. Noise packets are used as part of the instrument calibration process to estimate the shape of receiver-chain spectral-transfer characteristic and also to compute and subtract receiver noise power. These items must be determined before the relevant lines of echo data can be processed.

During calibration-mode operation, the ASCAT instrument also generates echo and noise packets. In this mode, the instrument is configured to prevent on-board along-track averaging of echoes. In order to suppress ground echoes, the calibration transponder delays its echo so that it is received in the reception window following the one in which reception would normally take place. The transmitted pulse preceding this reception window is transmitted from one of the other antennas directed away from the transponder. The transponder echo is therefore received together with only thermal noise. During overflight of a transponder, four or five samples are obtained through an along-track cut through the antenna gain pattern. The overall in-flight antenna gain pattern and the orientation

of each antenna beam can be determined when a sufficiently large number of azimuth cuts have been obtained which are suitably distributed in elevation.

The fundamental approach, which will be adopted for ground processing in the operational ground processor, is the use of automatic baseline procedures and baseline algorithms, which can, where necessary, be modified or overridden manually. This approach ensures, in particular, that calibration information is only introduced or modified in a fully controlled fashion.

The operational data products from ASCAT are classified by level according to how much processing has been performed: the Level-0 product is all relevant raw data, the Level-1A product is reformatted raw data with supplemental information for subsequent processing appended, and the Level-1B product is calibrated sigma-zero data at 25 km and 50 km spatial resolution (and full-resolution sigma-zero fields). The operational ground processing of ASCAT data is partitioned into five steps: (i) Raw data association and validation, (ii) Level-1A processing, (iii) Production of full-resolution sigma-zero data, (iv) Level-1B processing and (v) Product formatting.

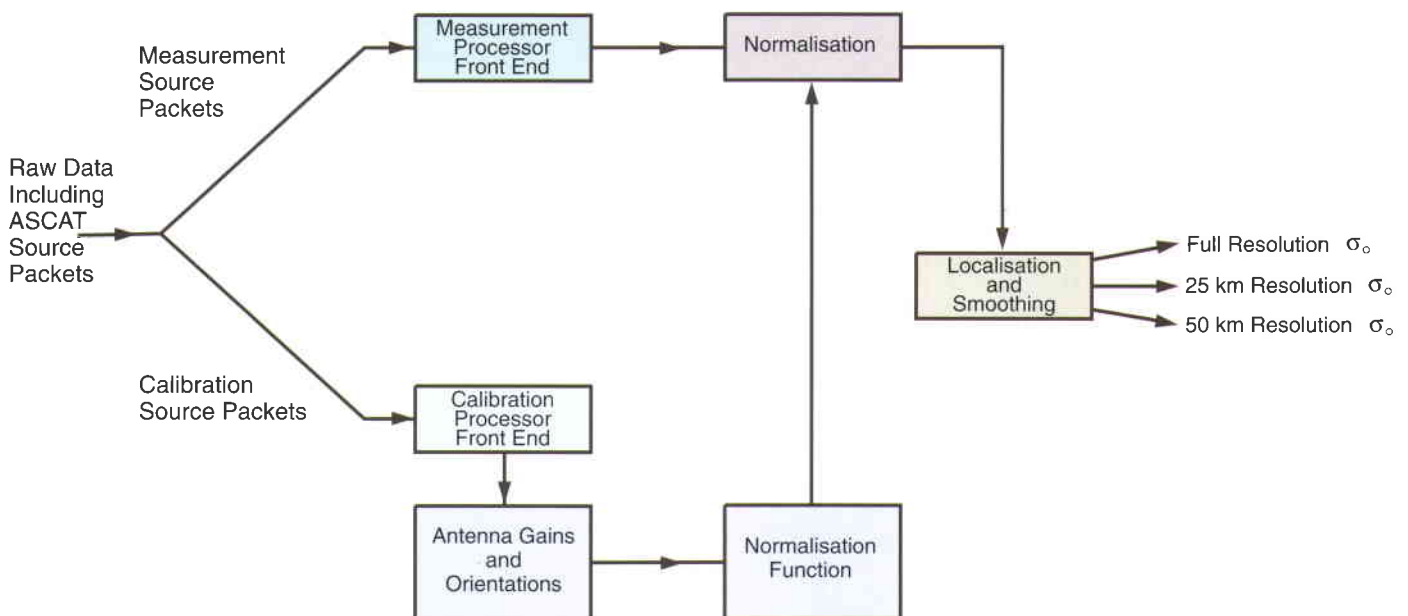
The central chain algorithms required for converting the source-packet echo data into sigma-zero triplet products are presented below in greater detail and are depicted in Figure 7. The echo data is first corrected to compensate for the shape of the receiver-chain spectral transfer characteristic. An estimate of

the receiver noise power is then subtracted and the resulting signal is divided by the power-gain product, which compensates for variations in transmitted radio-frequency power and receiver-chain gain. The power gain products are computed for each line of source-packet echo using various power measurements made by the instrument for internal-calibration purposes.

The resulting signal is then divided by a normalisation function, which converts the signal-power values to sigma-zero values; this function varies with both across-track and orbital position. The normalisation function is essentially determined by summing up the contributions to the power at a particular discriminator frequency from all elemental areas on the surface of the Earth. Each contribution is appropriately weighted by a factor accounting for slant range, antenna gain pattern and orientation, incidence angle, instrument configuration, etc. The normalisation function is computed as a function of discriminator signal frequency and orbit time, and is then stored as a look-up table since its determination is computationally very heavy. If any of the various contributing elements are changed, the look-up table has to be recomputed.

After the normalisation process, spatial coordinates are associated to the sigma-zero values, which allows localisation in terms of latitude and longitude and along-track and across-track position. First, the relation between slant range and discriminator signal frequency is established. Then, the slant range and orbital position allow the corresponding position on the surface of the Earth to be

Figure 7. Outline of ASCAT Ground Processor central-chain algorithms



determined using an Earth model and a model of the satellite's orbit and attitude. Finally, the full-resolution sigma-zero data is smoothed to generate the Level-1B products with the desired spatial and radiometric resolutions. This is done by use of a two-dimensional weighting function, which is centred at the position where the smoothed sigma-zero value is to be produced. The raw sigma-zero data are weighted according to their position within the weighting-function envelope and summed; this sum is then normalised with respect to the weighting function. It is expected that the weighting function will be a product of two one-dimensional Hamming functions, one across- and the other along-track. The size of this function will vary with swath position.

Two fully radiometrically calibrated products will be produced for ASCAT, namely a 50 km spatial-resolution product and a 25 km spatial-resolution product. These two products will be distributed in near-real-time to key users (including the national weather services of the Eumetsat Member States and the Eumetsat Satellite Application Facilities), in addition to being archived at Eumetsat itself. A product containing all the raw data (either the Level-0 or the Level-1A product) will also be permanently archived at Eumetsat (to allow reprocessing to be performed in future, if required).

The stability and quality of the ASCAT products will be monitored by observing various natural targets and via transponder measurements. In addition, various instrument and processor-derived parameters will be monitored in order to detect any anomalous instrument behaviour.

Expected in-flight performance

The ASCAT performance parameters are applicable to the measured backscattering coefficients, provided in the radiometrically calibrated product. These results depend not only on the actual instrument hardware and design, but also on the ground-processing algorithms and the external calibration. The performance analysis considers error contributions from all of these areas.

Table 2 summarises the predicted performance parameters for the nominal measurement mode (50 km-resolution cells) and for the high-resolution mode (goal of 25 km resolution). Several of the engineering parameters depend on the different antennas or on the location of the measurement cell within the swath: in such cases, a range is given which covers the different cases.



ASCAT Industrial Participation

| | |
|-------------------------------------|---|
| Alcatel Espace (F) | - HPA, RFU |
| Alcatel ETCA (B) | - EPC |
| Alcatel Space Switzerland (CH) | - ICU, EGSE (part) |
| Alcatel Space Norway (N) | - RFU (part) |
| Alenia (I) | - PDU |
| CASA (E) | - Antenna mechanical/thermal, harness |
| Comdev Europe (UK) | - SFE, EGSE (part) |
| Crisa (E) | - DPU, EGSE (part) |
| Dornier Jenoptik (D) | - EGSE (part) |
| Dornier Satellitensysteme (D) | - Instrument design, integration, ICU software Ground processor prototype (part) |
| Kongsberg Defence and Aerospace (N) | - Antenna deployment mechanism |
| Kongsberg – Spacetek (N) | - Ground processor prototype (part) |
| Saab Ericsson Space (S) | - Antenna electrical |
| Sener (E) | - Antenna hold-down and release mechanism |

Table 2. Predicted performance of the ASCAT engineering model in nominal and high-resolution mode

| Performance Parameter | Unit | Nominal mode | High-resolution mode |
|--|-------|---|---|
| Spatial resolution | km | 50 | 25 to 37 |
| Spectral resolution | 1/km | 0.0195 | |
| Sampling interval | km | 25 | 12.5 |
| Radiometric resolution at low wind (minimum back scattering) | % | 2.5 to 7.1 | 6.0 to 17.6 |
| Radiometric resolution at high wind (maximum back scattering) | % | 2.0 to 2.7 | 5.0 to 9.1 |
| Radiometric accuracy | dB pp | 0.47 to 0.55 | 0.48 to 0.56 |
| Interbeam radiometric stability | dB pp | 0.33 to 0.41 | 0.33 to 0.41 |
| Ambiguity under worst case scenario | % | 0.34 to 3.3 | 0.34 to 3.3 |
| Dynamic range (backscatter coefficients on the ground at near swath and far swath) | dB | -8.6 to 4.3 (near) -28.6 to -8.8 (far) | -8.6 to 4.3 (near) -28.6 to -8.8 (far) |
| Aliasing error | % | 0.08 | 0.08 |
| Centre frequency | GHz | 5.255 | 5.255 |
| Swath length | | continuous | continuous |
| Swath width (full performance) | km | 500 | 500 |
| Swath width (reduced performance) | km | 550 | 550 |
| Incidence angle mid near at H_{min} | deg | 25 | 25 |
| Localisation accuracy | km | 4.4 | 4.4 |
| Polarisation | | vertical | vertical |
| Cross polarisation | dB | >20 | >20 |

GOME-2 – Metop's Second-Generation Sensor for Operational Ozone Monitoring

J. Callies, E. Corpaccioli, M. Eisinger, A. Hahne & A. Lefebvre

Metop Project, Earth Observation Projects Department, ESA Directorate of Application Programmes, ESTEC, Noordwijk, The Netherlands

GOME's success on ERS-2

GOME was the only new instrument selected for inclusion in ERS-2's payload compared with ERS-1, and therefore had to live with the resources provided by the system margins established for its predecessor. Consequently, not all performance features that were scientifically desirable could be implemented. In particular, the available science data telemetry bandwidth imposed rigid constraints. Nonetheless, the instrument basically accomplished all of its mission objectives (see ESA SP-1151, SP-1212 and Earth Observation Quarterly No. 58).

The Global Ozone Monitoring Experiment (GOME) was first launched on ESA's ERS-2 spacecraft on 20 April 1995. It is still operating extremely successfully, providing ozone and other valuable data even two years beyond its original design lifetime. As the only European ozone-monitoring instrument with an actual flight heritage, GOME was therefore selected for the Metop series of satellites being jointly developed by ESA and Eumetsat for operational meteorology and climate monitoring. The phasing between the ERS-2 and Metop development schedules has been such that many 'lessons learnt' could be implemented to improve the sensor's design, calibration and data processing. In addition, various spacecraft- and launcher-imposed modifications have meant that eventually almost no subsystem has remained totally unchanged. The changes made to the sensor itself have also resulted in changes to the calibration philosophy and to the processing of the scientific data. The new features of this second-generation sensor, known as GOME-2, are presented here.

GOME lead scientist Prof. J. Burrows' conclusion was:

"GOME-1 has successfully passed its initial validation phase and demonstrated its capability to provide valuable information about the state of the earth's atmosphere... Continuous improvement of the quality of the data is necessary and is an ongoing activity, which will enable GOME to make an optimal contribution to important and challenging issues such as long-term trend analysis of atmospheric composition."

Comparison with ground-based observations of total ozone columns shows good agreement (within 2–4%) at northern mid-latitudes, which is within the common error bar of both sets of measurements. GOME has shown that it can continue the monitoring and documentation of the ozone distribution started by the TOMS series of instruments. Its potential to provide global-distribution data for nitrogen dioxide, bromine oxide, chlorine dioxide, sulphur dioxide and formaldehyde has been demonstrated (see Fig. 1). Ozone-profile retrieval is highly demanding, but the available results clearly confirm GOME's ability to deliver new information on ozone vertical distribution in both the troposphere and stratosphere of our planet.

A GOME near-real-time campaign lasting from December 1999 until May 2000 was set up to support the three major measurement campaigns SOLVE/EUROSOLVE, THESEO 2000 (Third European Stratospheric Ozone Experiment), and TOPSE (Tropospheric Ozone Production about the Spring Equinox), all of which are aimed at increasing our knowledge of ozone chemistry in the Arctic. The near-real-time data products derived from the GOME spectral data encompass ozone total columns and profiles, total columns of NO₂ and BrO, and slant columns of OCIO. Regular GOME images (mainly ozone) can be found at the web sites of the University of Bremen (D), KNMI (NL), and DLR/DFD (D). The list of retrieved products is complemented by a GOME-based solar activity index (based on the Mg II line) and some limited aerosol information.

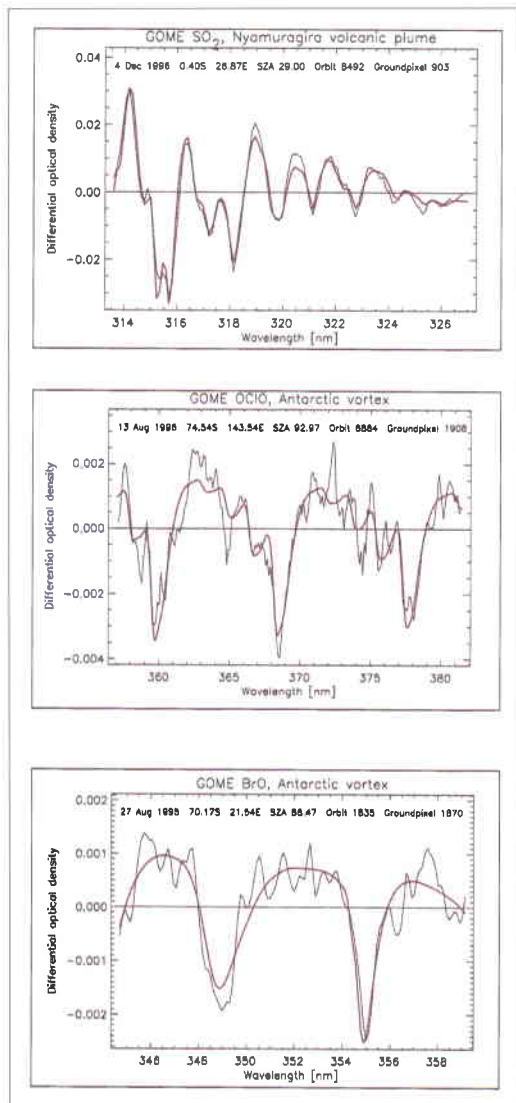
The Metop environment

Quite a number of changes to the GOME instrument design have been imposed by the fact that Metop is a very different satellite from ERS-2, designed for a different orbit, and launched by a different launcher (Ariane-5). The new orbit imposes a different viewing angle to

the Sun, for in-orbit calibration purposes, and some moderate changes in the instrument's thermal environment.

Because of the presence of sensitive microwave receivers on Metop, stringent radio-frequency compatibility requirements are imposed on the satellite and its instruments. For the specific bands used by the Search and Rescue payload, the maximum tolerable emissions from GOME-2 are 70 dB lower than what was acceptable on ERS-2.

Whilst the GOME instrument on ERS-2 was interfaced with the satellite avionics via the ATSR instrument's main electronics, on Metop GOME-2 will have its own Instrument Control Unit (ICU) with interfaces to the satellite's power distribution, OBDH bus, and science data handling subsystems. These changes are not very obvious in the instrument's physical appearance (only a moderate increase in the size of the electronics boxes is noticeable), but have a significant impact on its internal architecture and design.



So, although at first glance appearing virtually unchanged, nearly all subsystems had to be redesigned and needed re-qualification to demonstrate their compatibility with the new environment.

GOME-2 for Metop

The feedback from five years of GOME-1 operations and data evaluation, and the environmental and accommodation constraints imposed by satellite, orbit and launcher, have led to a significant number of detailed changes, but with the basic concept still being retained. Their detailed implementation is addressed here for each of the main subsystems affected.

As a general principle, the GOME-2 instrument collects light arriving from the Sun-illuminated Earth's atmosphere and decomposes it into its spectral components. In order to provide both the required spectral coverage from 240 to 790 nm and a good spectral resolution, as well as ensuring a proper stray-light level in channels 1 and 2, the instrument is set up as a double spectrometer. It consists of the following

Figure 1. GOME-DOAS fit results for SO₂, OCIO and BrO, together with the corresponding reference spectra

Table 1. GOME-2's main characteristics

| | | |
|------------------------------|---|----------------|
| Spectrometer type | Double monochromator with pre-disperser prism and four holographic gratings | |
| Spectral range | 240 – 790 nm | |
| Field of view | 0.286 deg (across-track) x 2.75 deg (along-track) 4 km x 40 km | |
| Entrance slit | 0.2 mm (across-track) x 9.6 mm (along-track) | |
| Channels and resolution | 1: 240 - 315 nm | 0.24 - 0.29 nm |
| | 2: 311 - 403 nm | 0.26 - 0.28 nm |
| | 3: 401 - 600 nm | 0.44 - 0.53 nm |
| | 4: 590 - 790 nm | 0.44 - 0.53 nm |
| Polarisation Monitoring Unit | 200 detector pixels 312 – 790 nm in 12 programmable bands Spectral resolution: 2.8 nm @312 nm to 40 nm @ 790 nm | |
| Viewing modes: | ± 1920, ± 960, ± 480, ± 360, ± 240, ± 120 km | |
| Solar | Fixed angle once per day | |
| Lunar | Fixed varying angle, ~ 6 times per year | |
| Spectral calibration | Fixed angle (once per day to once per month) | |
| White Light Source | Fixed angle (once per day to once per month) | |
| Dark signal | Fixed angle (night side of the orbit) | |
| Spatial resolution | 40 km x 40 km (960 km swath and integration time of 0.1875 s) 40 km x 5 km (for polarisation monitoring) | |
| Data rate | 400 kbit/s (GOME-1: 40 kbit/s) | |
| Mass | 73 kg (GOME-1: 55 kg) | |
| Power | 58 W (avg) (GOME-1: 32 W) | |
| Dimensions | Zenith nadir 656 mm, across-track 848 mm, velocity 468 mm | |

functional blocks: Spectrometer, Polarisation Monitoring Unit, Calibration Unit, Focal-Plane Assemblies, Scan Unit and Command and Data Handling Unit.

The Spectrometer

The optical design of the GOME-2 main spectrometer is almost a carbon copy of the GOME-1 concept. The major change between the two instruments is driven by the accommodation of the more complex Polarisation Monitoring Unit (PMU) of GOME-2 (Fig. 2). There have also been a number of minor improvements to the design.

The GOME-2 spectrometer is an across-track scanning spectrometer covering the 240 to 790 nm wavelength region in four different channels. A Scan Mirror directs the light emitted from the Sun-illuminated atmosphere into an anamorphic telescope. The telescope is designed to match the two directions of the instantaneous field of view (0.286 deg across-track and 2.75 deg along-track) to the two directions of the entrance slit (0.2 x 9.6 mm²). In addition, the Scan Mirror can point to two internal calibration light sources and the Sun diffuser. The increase in slit width from 0.1 mm for GOME-1 to 0.2 mm for GOME-2 was necessary to avoid spectral undersampling.

Behind the entrance slit, the light is collimated by an off-axis parabolic mirror ($f = 200$ mm) onto the double Brewster/pre-disperser prism configuration, which generates the s- and p-polarised light beam for the Polarisation Monitoring Unit and produces the pre-dispersion for the main spectrometer (Fig. 3). An off-axis parabolic mirror ($f = 125$ mm) focuses the dispersed beam onto the channel separator prism. The pair of parabolas forms a relay system with a magnification of 0.625. The band separator is a quartz prism, the first surface of which is partially coated with a reflective coating (for channel 2) and a transmission coating (for channel 1). The light for channels 3 and 4 passes the prism edge, and a dichroic filter separates it into the two channels. To avoid the slow but steady outgassing of this coating experienced with GOME-1, it was manufactured using plasma ion-assisted deposition technique to provide high-temperature stability.

The four channels are built from a collimating off-axis parabolic mirror, a grating and a focusing objective that images the spectrum on the detector. Each collimator/objective combination forms a main channel relay of magnification 0.4. The combined magnification of the optical path is 0.25, ensuring that the image of the entrance slit is completely imaged

on the detector array. The optical analysis shows that even taking aberration into account, the photometric barycentre of the spots relevant to the maximum field of view falls within the detector pixel dimensions. The margin between the barycentre and the outline of the detector is sufficient to absorb the manufacturing tolerances of the optical elements. This design therefore guarantees a field-of-view overlap between the main channels and those of the polarisation unit.

All refractive optics are made of quartz (Suprasil 1) and are multilayer-coated for maximum efficiency and low stray light. The off-axis parabolas are made of aluminum, nickel-coated and machined with a single-point diamond turning technique. Polishing then achieves a surface quality compliant with the low-stray-light application in the ultraviolet.

The four holographic gratings have demanding requirements in term of stray-light reduction and diffraction efficiency, and so only master gratings can be used. The stray-light performance of the UV channel requires that the grating blanks have a micro-roughness of better than 0.5 nm RMS. The groove density is determined by the angles of incidence, which are adjusted to the required densities of 3600 l/mm (channel 1), 2400 l/mm (channel 2) and 1200 l/mm (channels 3 & 4). Particular care is taken to avoid and shield against false light generated with the recording set-up. The symmetrical photoresist groove profile is transformed to a sawtooth-like shape by ion-beam etching. Due to the high spectrometer angles of 45 to 50 deg, the efficiency very much depends on the shape of the groove profile. The polarisation sensitivity of the GOME-2 gratings is considerably lower than for GOME-1. The dispersed light is focused by a four-lens objective onto a silicon linear detector array in the Focal-Plane Assembly.

The new Polarisation Monitoring Unit

Nadir-looking space-borne spectrometers have only two options for treating the atmospheric polarisation of the incoming light. Either the polarisation information is destroyed by scrambling, as in the American TOMS and SBUV-type instruments and the Dutch/Finish OMI instrument, or the polarisation has to be measured with sufficient accuracy to correct for the polarisation dependence of the instrument. The benefit of the latter approach is that the polarisation detector information can also be used for other purposes such as cloud or aerosol detection, or for high spatially, low spectrally resolved atmospheric-radiance measurements.

The new polarisation unit monitors the 312 to 790 nm range using 200 detector pixels with a spectral resolution that varies from 2.8 nm at 312 nm to about 40 nm at 790 nm, with an integration time of 23 ms. Both the s- and p-

polarised parts of the light will be measured simultaneously. As GOME-2's data rate is limited, the information from the 200 detector pixels is co-added on board to form 12 programmable bands.

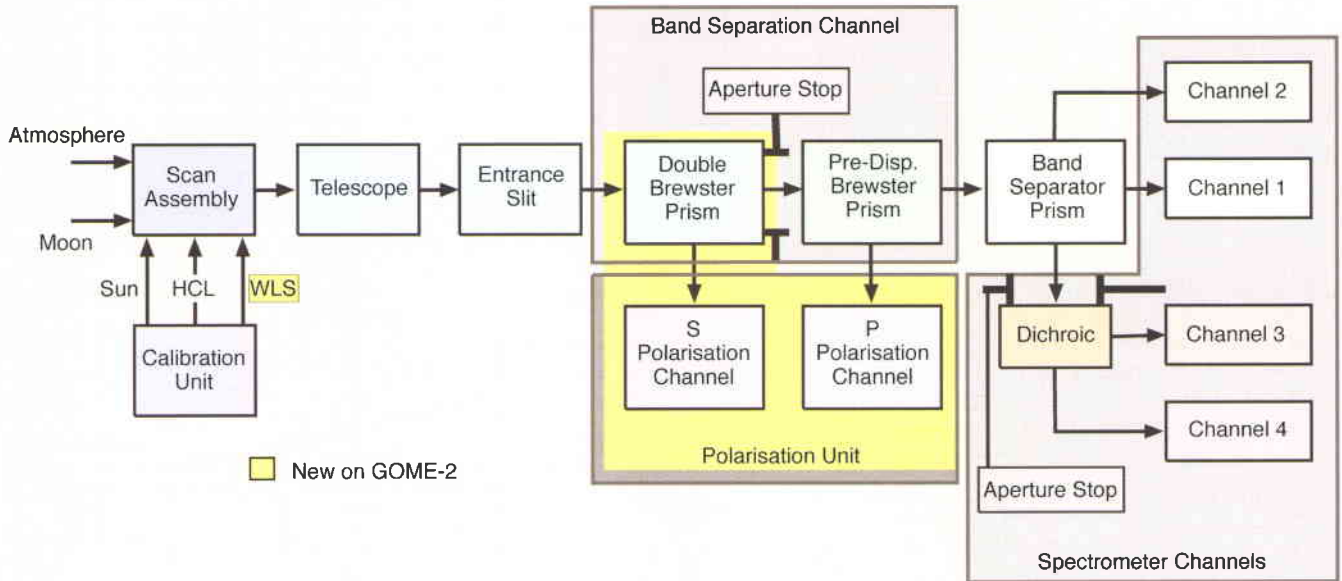


Figure 2. Block diagram of GOME-2 optics, with the differences compared with GOME-1 highlighted

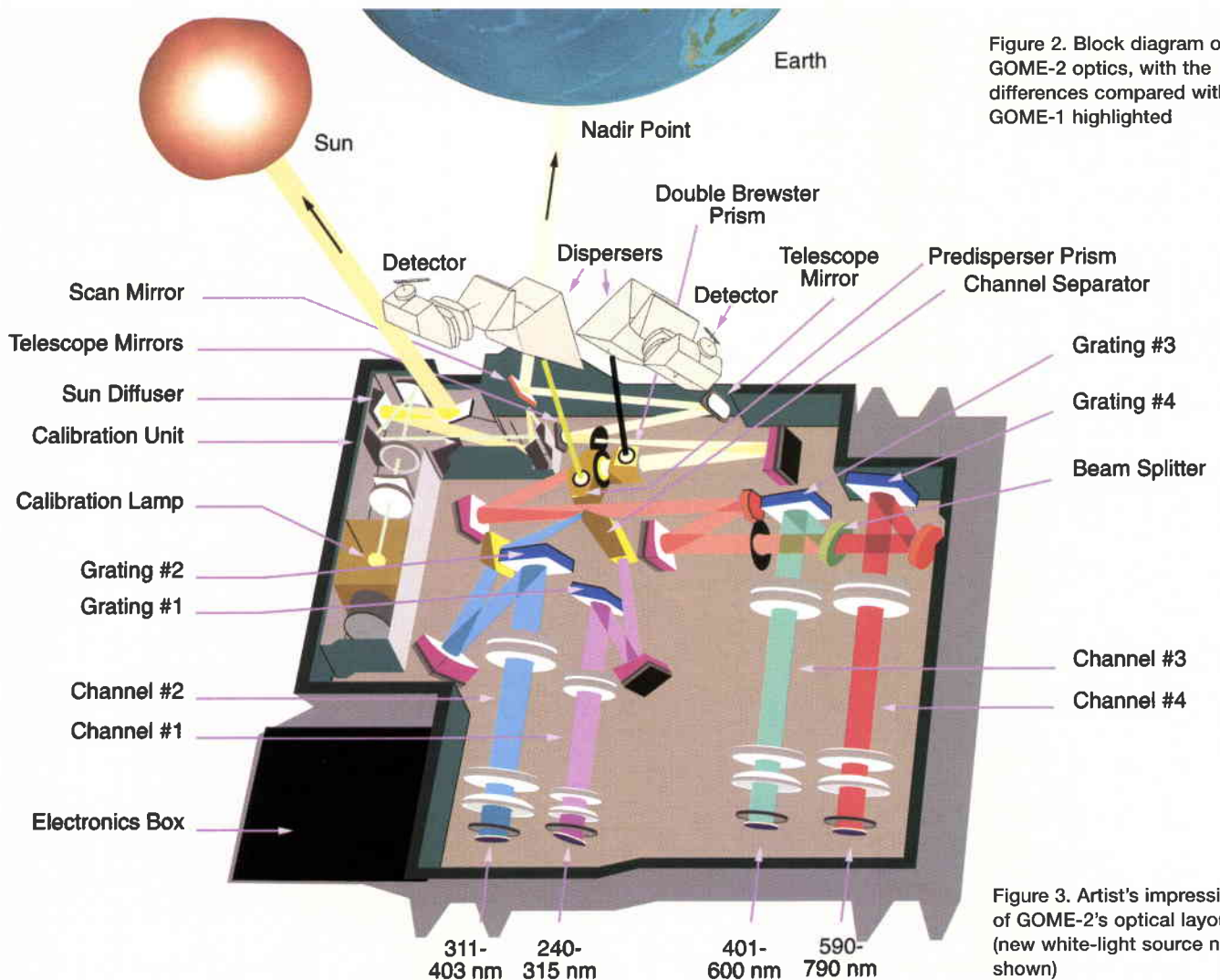


Figure 3. Artist's impression of GOME-2's optical layout (new white-light source not shown)

The design drivers for this new subsystem have been the optical identities of the s- and p-channels, to ensure identical fields of view for both these and the main channel, using the same detector array as the latter. Given the need for a compact lightweight system, a trade-off comparison was made of a grating solution and a prism solution. The latter proved both simpler and more robust, and was therefore selected.

As shown in Figure 4a, the collimated mirror (200 mm) beam passes through a double Brewster prism that extracts the s-polarised light into the s-channel. This light leaves the prism group orthogonal to the optical bench.

The prism group (Fig. 4b) consists of two prisms with two parallel surfaces tilted at the Brewster angle, thereby compensating the wedge effect for the main channels. The light of the main channels enters a pre-disperser prism like that on GOME-1, which generates the p-polarised beam and pre-disperses the light of the main channel. In the two polarisation channels, a two-prism disperser disperses the light and redirects it again parallel to the optical bench. A dioptric focusing objective ($f = 48$ mm) forms, together with the 200 mm parabolic mirror, a relay of magnification 0.24. The field of view (FOV) overlap between the main channels and the two PMU channels is thereby guaranteed. For

Figure 4a. Block diagram of the new Polarisation Monitoring Unit (PMU) optics

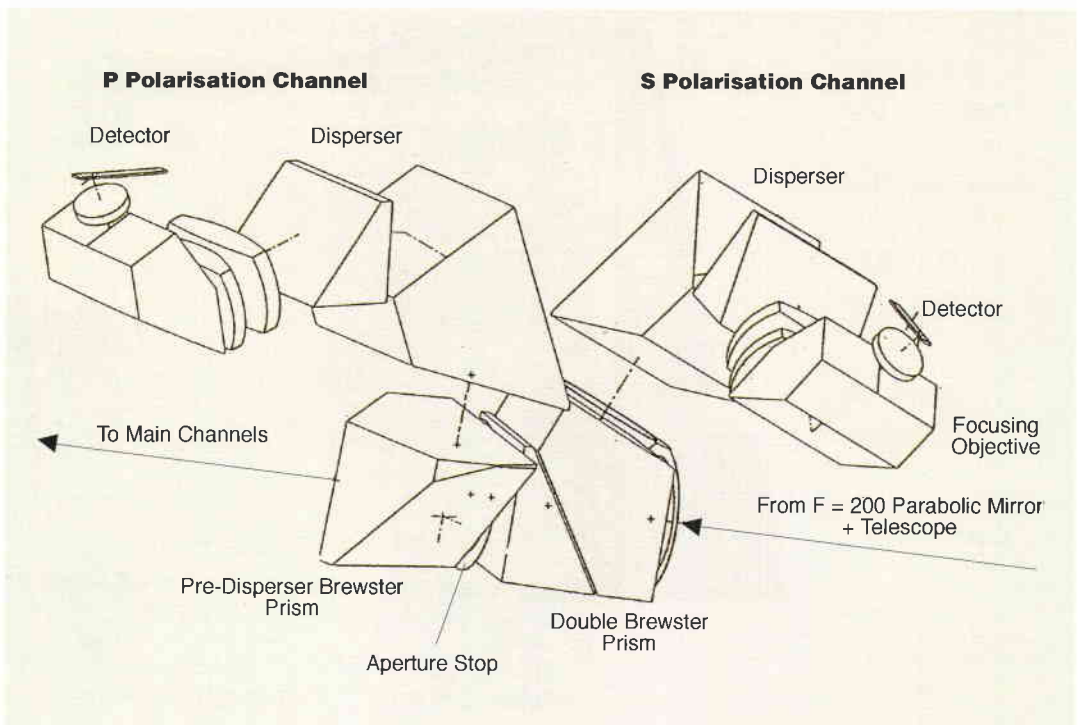
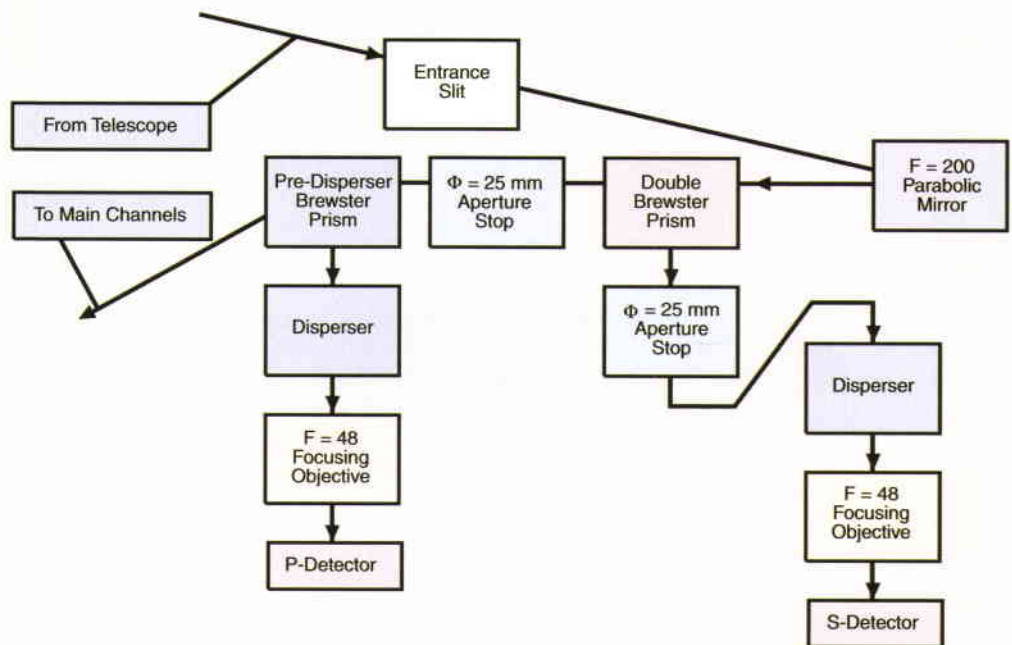


Figure 4b. The PMU detailed optics

accommodation reasons, an additional prism has been placed between the lenses and the detectors. The detector array is tilted by 30 deg in spectral dispersion to compensate for chromatic aberrations.

The Calibration Unit

The demanding radiometric-accuracy requirements for the instrument call for in-orbit calibrations. The unit contains two light sources, one of which offers well-isolated spectral lines in the required wavelength range, and a quartz tungsten halogen lamp (White Light Source, WLS) for a broad-band continuum. The WLS is used to monitor the etalon that is present on the cooled Reticon detectors, due to freezing water vapour on the protective SiO₂ layer. Although this etalon stabilises in vacuum, it is irritating during the ground calibration and for the mapping of key calibration data between the on-ground calibration and the in-orbit situation. The spectral light source is a hollow cathode lamp (Pt anode/Cr cathode) filled with a mixture of neon and argon. Adding argon to the gas mixture increases the number of spectral lines in channel 3 and reduces the very strong neon lines in the near-infrared, which would otherwise be saturated.

The Calibration Unit is complemented by a diffuser, which allows a solar calibration to be performed. Due to the orbital geometry, the Sun can be seen via the solar calibration port once per orbit. As with GOME-1, the diffuser is well protected against the hostile space environment and the harsh ultraviolet radiation by a mesh that attenuates the flux and a shutter that opens only for a Sun calibration. GOME-1 experience shows that one solar calibration per day is sufficient and no degradation of the Sun diffuser itself has been detected in 4.5 years.

The beams of the three sources leave the Calibration Unit at different angles (Fig. 5) and the sources can therefore be separated by proper selection of the Scan Mirror position.

The Focal-Plane Assemblies

GOME-2 has a total of six Focal Plane Assemblies (FPAs), four devoted to the main spectrometer channels and two to the new polarisation channels. The basic design for the four main-spectrometer FPAs is very similar to that for GOME-1, with titanium being used for the structure and a quartz window on the side where it is assembled on the spectrometer objective. Each FPA contains a random-access linear silicon photodiode array, consisting of 1024 elements each 2.5 x 0.025 mm² (type Reticon RL 1024 SRU), which is reverse-biased and operates in charge accumulation mode.

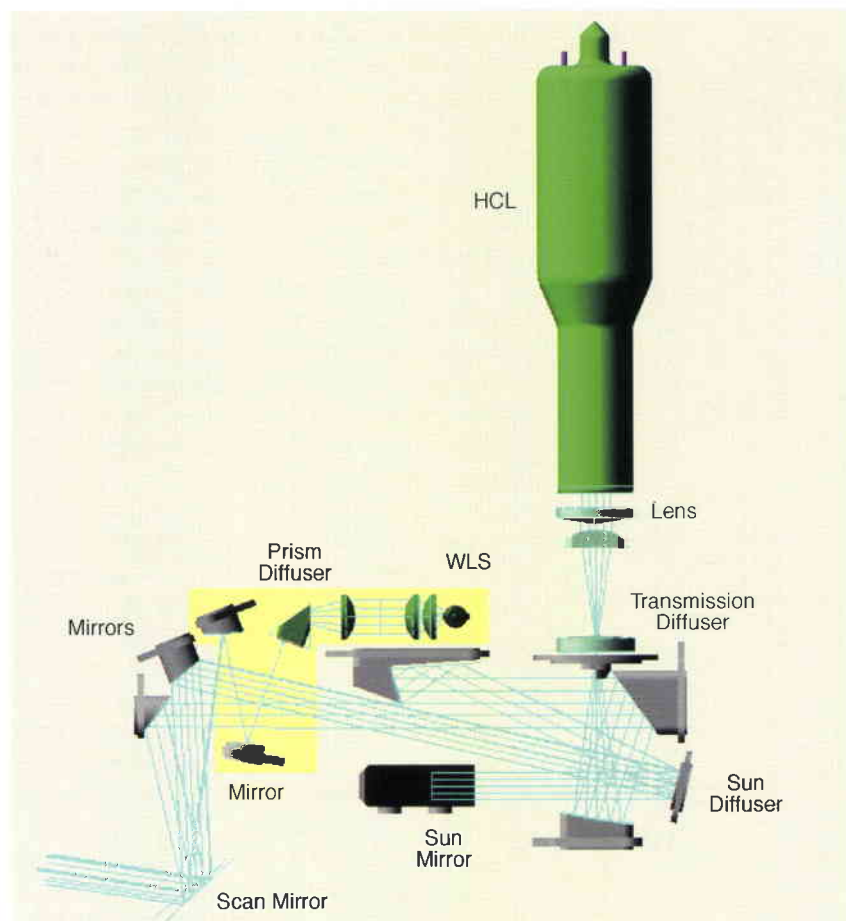


Figure 5. The Calibration Unit optics (new WLS part highlighted in yellow)

To achieve maximum sensitivity, the detector has to be cooled to -38°C by means of a thermoelectric cooler, glued directly on the bottom face of the detector itself. To reject the heat generated by the cooler, a low-resistance thermal path to the main GOME-2 radiator is provided by two heat pipes, and some specially designed parts to absorb the effects of thermal expansion. The detector temperature is controlled in closed loop by a suitable electronic circuit inside the Command and Data Handling Unit; the actual target temperature can be programmed in-flight to any value between ambient and -38°C . Based on GOME-1 experience, stability is better than $\pm 0.1^{\circ}\text{C}$.

To avoid ice formation during ground testing, each FPA has a vacuum-tight enclosure containing the detector and cooler. This enclosure can be evacuated via a system of pipes on the bottom of the optical bench and a tap on back of the instrument, which will be removed just before launch, allowing the FPAs to evacuate naturally during the ascent phase.

The FPA electronics is split onto two boards. The first carries the charge amplifier, made up of a dual-FET differential stage and a low-noise amplifier. To achieve maximum noise immunity, this board is installed on the rear of the vacuum enclosure, just 3 cm from the detector. The second board is mounted on top of the

spectrometer objective, and contains some filtering circuits, the 16-bit A/D converter and the interfaces. Thanks to the modular approach, each FPA can be tested and trimmed at module level before final integration on the instrument. Testing has shown that, due to their careful design, the FPA electronics have low noise and a dynamic range of about 30 000.

There are 255 integration times possible, ranging from 93.75 msec to more than 1 h. In channels 1 and 2, two different integration times can be selected for two bands of the detector; and the border between the two bands is in-flight programmable.

The two Polarisation Monitoring Unit FPAs are slightly different. Due to the less-demanding detection performance needs and the more stringent requirements on mechanical accommodation, no closed-loop thermal control has been implemented. Consequently, neither the thermal link to the radiator nor the vacuum-tight enclosure is present, with very beneficial effects in terms of mass savings and structural robustness. The detector is anyway cooled in open-loop configuration to about 0°C by a thermoelectric element, which rejects heat to the main optical bench through the PMU mechanics. Although not stabilised, the detector temperature is kept low enough for the dark current effect to be neglected in this particular case. The detection electronics is the same as for main-channel FPAs. Integration time will normally be fixed at 23.4 msec, and the spectral information will be grouped in 12 fully programmable bands. The integration time can be programmed as per the main-channel FPAs during calibration phases.

The Scan Unit

To perform global Earth coverage, GOME-2's instantaneous on-ground field of view has to be scanned in the across-track direction. This function is performed by a subsystem called the Scan Unit (SU) containing a rotating mirror, situated optically in front of the spectrometer, and its related mechanics and electronics. The unit's design is strongly based on the positive experience acquired with GOME-1, with some improvements in terms of functionality and reliability.

The SU is physically subdivided into two assemblies: the Mechanical Assembly (SUMA) and the Electronics Assembly (SUEA). The SUMA is almost identical to that of GOME-1, with a rotating mirror installed on an axis actuated by a brushless three-phase motor. A major improvement with respect to the GOME-1 design is the presence of a wireless angular-position resolver; which removes all

electrical connections between fixed and rotating parts, leading to a notable reliability gain.

Another positive consequence of such a design is the possibility to perform continuous (360 deg) rotations of the Scan Mirror at a speed of 10 rpm. This feature, exercised every now and then, will allow redistribution of the lubricant that could accumulate in some parts of the bearing races due to wear, so recovering the original smoothness and precision of movement. Another minor improvement is better confinement of the debris generated by the bearing wear itself.

The SUEA is a separate box, which contains all of the electronics needed for closed-loop control of the scan mirror angular position. It is able to implement five scan profiles at constant angular speed (as per GOME-1) and five new scans, compensating for the Earth's curvature and providing a constant linear scan speed on the ground. A new wide-amplitude scan corresponding to 1920 km on the ground is also implemented, which will allow complete Earth coverage in 1.5 days. All scans are completely in-flight reprogrammable, allowing an almost unlimited choice of profiles. The basic scan timing is 4.5 sec for the forward scan and 1.5 sec for the flyback.

The mirror movements are synchronised with the global instrument timings (detector integration times, etc.). In the event of a failure in the synchronisation interfaces, the Scan Unit can autonomously perform a pre-programmed series of operations, in order to partially recover the mission. The Unit's overall performance remains the same as for GOME-1; mirror positioning accuracy in fixed pointing will be better than 0.03 deg (corresponding to about 800 m on the ground), while in scanning modes it will depend on actual speed, but will anyway be better than 0.065 deg.

The Command and Data Handling Unit

All electrical and operational interfaces to GOME-2 (Fig.6) are routed through the Command and Data Handling Unit (CDHU). Within this unit, a primary processor is responsible for all ICU functions such as the reception and expansion of macrocommands, maintenance of history file, monitoring of instrument parameters and preparation of housekeeping telemetry formats. The ICU controls the operation of the Scan Unit via a bi-directional serial interface and provides each of the four FPA thermoelectric coolers with an individual thermal-control loop. A secondary processor controlling the Science Data Management board takes care of science data collection, processing and packetisation.

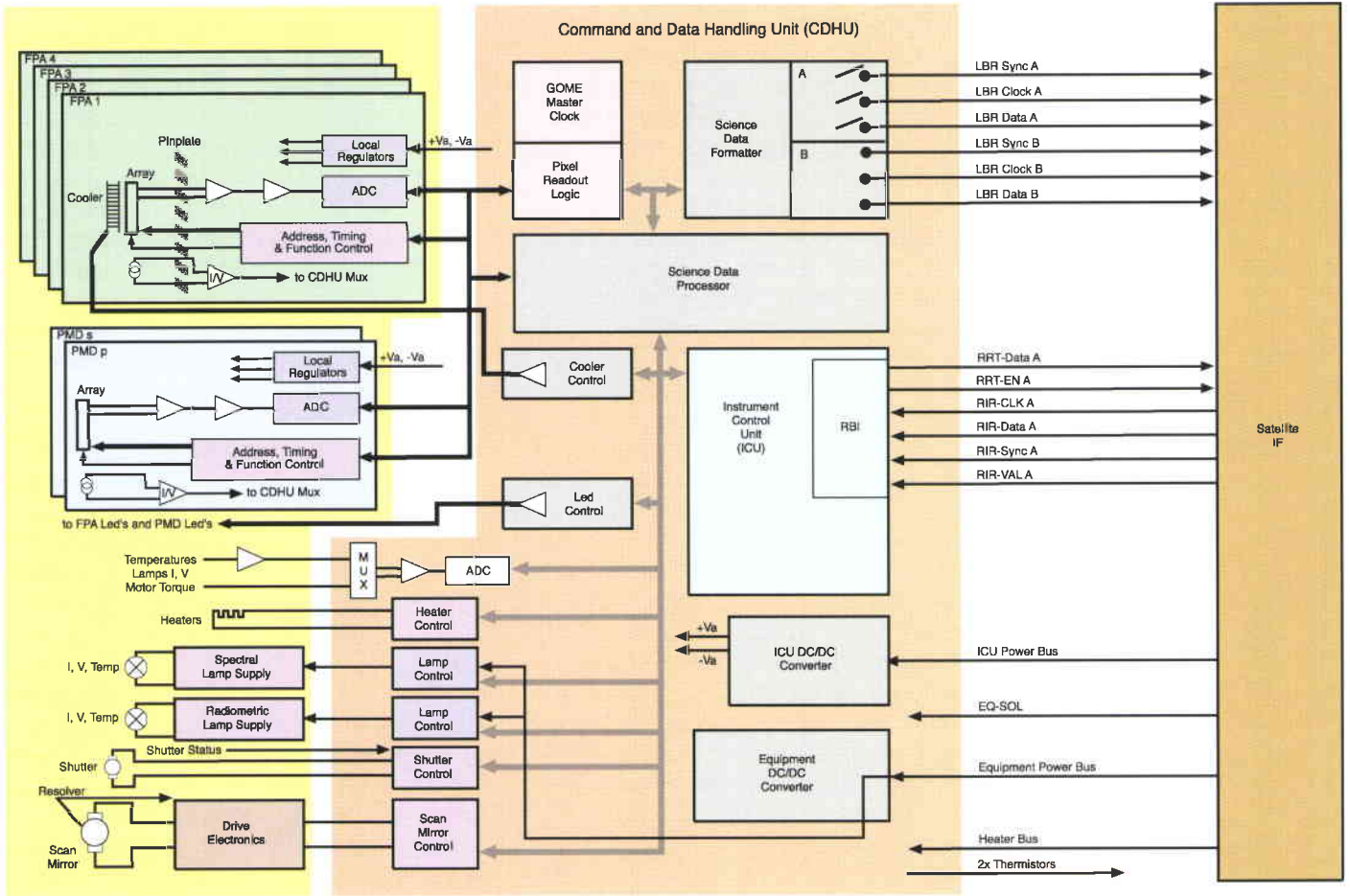


Figure 6. GOME-2 block diagram and electrical interfaces

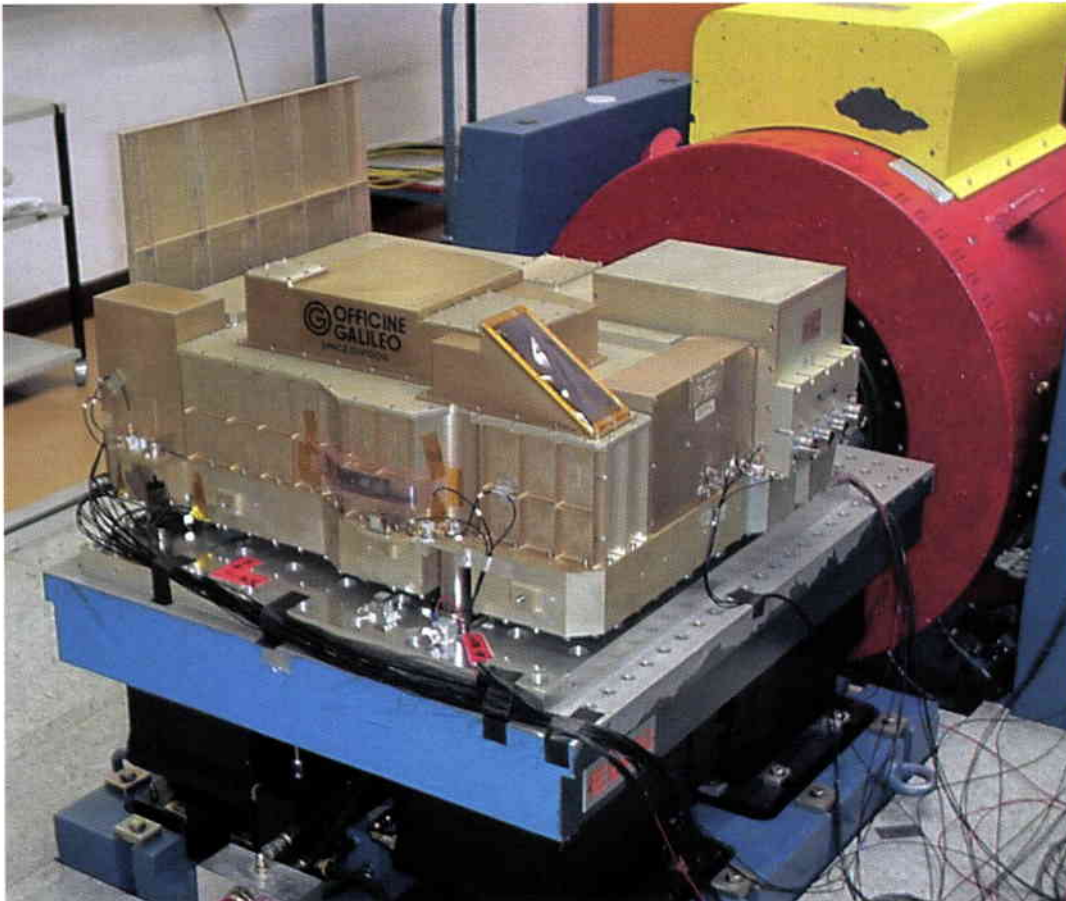


Figure 7. GOME-2 structural model during vibration testing

Pre-flight calibration

Although GOME-2 includes a number of on-board calibration capabilities, a thorough on-ground calibration exercise is required prior to launch. The most important measurements are: the characterisation of the Bi-Directional Scattering Function (BDSF) of the diffuser built into the Calibration Unit; and the characterisation of the polarisation response of the instrument as a function of the different optical paths for solar calibration and Earth nadir viewing, as a function of scan mirror position and wavelength. These calibrations are performed in a thermal-vacuum chamber at the instrument calibration contractor's site (TNO/TPD, NL). A number of additional measurements are made for various purposes, including more comprehensive instrument characterisation and consistency cross-checking. In particular, full radiance and irradiance calibrations using Earth and Sun observation paths are performed with NIST calibrated light sources for the PMU and the main channels. A full characterisation of the instrument's stray-light behaviour, the wavelength calibration, the field of view as well as the instrument response function, is performed as part of the calibration.

Operations

The GOME-2 instrument has many measurement and calibration modes. Moreover, the high variability of the light levels observed by the instrument over each orbit implies that the integration times of the detectors will have to be changed frequently. To limit the command rate, and implement the 36 h autonomy, the timeline concept validated by the GOME-1 experience has been extended. Each timeline now contains 28 different commands to be automatically expanded when required to change integration times, subsystem modes or parameter values. The CDHU will provide 12 predefined timelines, each dedicated to a specific orbit sequence (nominal, calibration, Sun calibration or test). The contents of the default timelines will be changed by macro command if necessary to tune the integration times and the modes sequencing to the actual in-flight conditions.

About once per month, an extensive calibration exercise will be performed, assessing any diffuser degradation, any changes in the dark signal currents and saturation levels of the detectors and making a wavelength mapping as function of the thermal variation. An etalon characterisation is also planned on these occasions. Lunar observations, which are restricted by the Sun-Moon-satellite scanner field of view geometry, will be performed whenever possible.

Data processing

GOME-2 data will be transmitted from the Metop to the receiving stations via an X-band link. From there they will be transmitted to the Core Ground Segment (CGS) at Eumetsat in Darmstadt, Germany, for processing. The CGS is a central facility providing command and control, near-real-time data processing, and data dissemination for the Metop satellites.

In a first processing step, the raw (or level-0) data will be augmented by the geolocation and calibration parameters needed for further processing. Some of these calibration parameters come from the pre-flight calibration of GOME-2, while others will be derived from regular in-flight calibration measurements using the Sun and the on-board lamps as light sources. The calibration parameters are then applied on the raw data in order to obtain calibrated solar irradiance and Earth radiance spectra, together with auxiliary geophysical information, such as polarisation and cloud-fraction data. These level-1 products will then be disseminated by the CGS to Satellite Application Facilities (SAF) and other users for further processing. Specifications and a prototype processor for the GOME-2 level-0 to level-1 processing are currently being developed at DLR in Oberpfaffenhofen (D).

Column amounts of the target trace gases and vertical profiles of ozone will be derived from the GOME-2 level-1 spectra at the Ozone SAF. The aim is to derive the final trace-gas product (level-2) within just three hours of the satellite measurement being made.

In addition to this operational near-real-time processing chain, GOME-2 data will be evaluated by scientific users for their own specific retrieval purposes. Exploitation of the new features that GOME-2 offers compared to GOME-1 will certainly stimulate a number of interesting new possibilities for atmospheric research.

Acknowledgement

Much of the work presented here has been done by the GOME Industrial Team led by Officine Galileo (I), and supported by Laben (I), TNO/TPD (NL), Arcom Space (DK) and Finavitec (Fin). The Ground Processor Prototype (GPP) development is led by DLR/DFD (D) under an ESA/Eumetsat contract. We also gratefully acknowledge the support of the GOME Science Advisory Group, led by Prof. Dr. J. P. Burrows from the University of Bremen (D).

We contribute to preserve



our planet.



Officine Galileo
B.U. Spazio

Marketing Communications:
Via Montefeltro, 8
20156 MILANO, Italy
Phone: ++39.0230242.362
Fax: ++39.0230242.052
e-mail: mkt.space@officine-galileo.finmeccanica.it



Alenia

DIFESA

A FINMECCANICA COMPANY

Since 1995 with GOME on ERS-2 we are mapping ozone and other atmospheric gases.

GOME-2 on METOP will provide enhanced data on an operational basis to improve weather forecasts and to provide climate trends of our planet.

SOLUTIONS FOR A LIVING PLANET

GRAS – Metop's GPS-Based Atmospheric Sounder

M. Loiselet, N. Stricker & Y. Menard

Earth Observation Programmes Development Department,
ESA Directorate of Applications Programmes, ESTEC, Noordwijk, The Netherlands

J.-P. Luntama

Eumetsat, Darmstadt, Germany

Introduction

Occultation methods based on effects connected with the refraction of electromagnetic waves in both the optical and radio-frequency domains have been used by astronomers for numerous investigations of planetary atmospheres over the last decades. The first experiment started with the Mars flyby by Mariner-IV in 1964. Since this first attempt, radio-occultation experiments have been carried by the majority of planetary missions.

GRAS is an atmospheric-sounding instrument that forms part of the payload of the Metop series of meteorological satellites. The three Metop satellites form part of the Eumetsat Polar System (EPS), whose primary mission objectives are operational meteorology and climate monitoring. GRAS measurements will provide atmospheric temperature and humidity profiles, which are intended to be assimilated into Numerical Weather Prediction (NWP) models. Possible future developments involving a fleet of GPS receivers could allow temperature and water-vapour profiles of the atmosphere to be recorded with unprecedented vertical resolution and measurement accuracy for tomorrow's climate models.

The Global Navigation Satellite Systems Radio Occultation Receiver for Atmospheric Sounding, known as GRAS, will use the radio-frequency signals generated by the constellation of satellites of the Global Positioning System (GPS). The validity of this concept was first proven with the launch and successful operation of the GPS/MET experiment by Jet Propulsion Laboratory in 1995. Since then, several missions with onboard radio-occultation GPS receivers have been put into development, including Ørsted, Champ, SAC-C, and Grace. Ørsted was launched in 1999, and Champ is planned to be launched this year. Both missions are precursors, and will pave the way of GRAS to deliver an operational product continuously over 14 years.

Measurement principle

The GPS constellation consists of 24 satellites distributed in six orbital planes around the globe. Each satellite orbit is circular with an inclination of 55 deg, a period of 12 h and an altitude of 20 200 km. A schematic of atmospheric profiling by GPS radio occultation is shown in Figure 1. For the receiver, an occultation occurs whenever a GPS satellite rises or sets and the ray path from its transmitter traverses the Earth's atmospheric limb. With 24 GPS satellites, a single GPS receiver in a near polar orbit at 824 km will observe over 500 occultations per day, distributed fairly uniformly about the globe (Fig. 2).

The fundamental measurement in the GPS limb-sounding technique is the phase delay resulting from transmission of the GPS signal through the atmosphere. Total atmospheric delay is a function of two factors: ray bending due to refraction, and reduced propagation velocity in the atmosphere. The radio signal propagating from the GPS transmitter to the low-Earth-orbiting receiver follows a path through the atmosphere that curves in response to atmospheric refractive-index gradients.

The cumulative effect of the atmosphere on the ray path can be expressed in terms of the total refractive bending angle α , which has a known relationship to the atmospheric Doppler shift. For the Earth's atmosphere, the maximum bending angle is in the order of 36 mrad (2 deg) at the Earth's surface, while at 30 km altitude its magnitude reduces to 0.3 mrad.

The atmospheric Doppler shift, in turn, is determined by taking the time derivative of the observed phase. The variation of α with

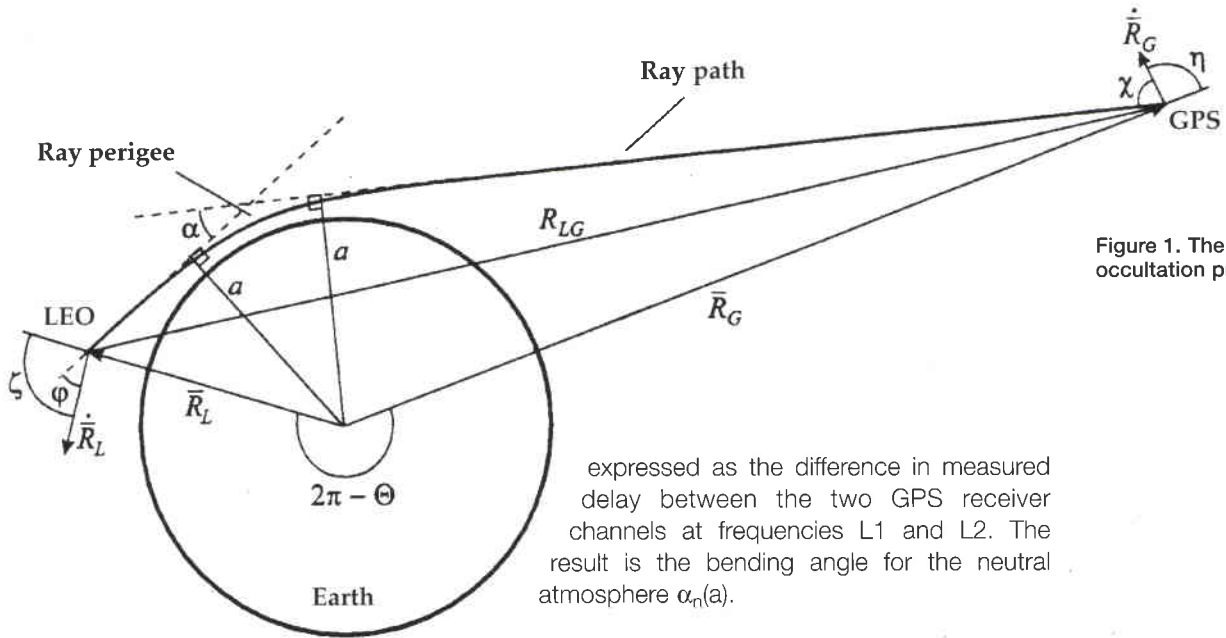


Figure 1. The radio-occultation principle

expressed as the difference in measured delay between the two GPS receiver channels at frequencies L1 and L2. The result is the bending angle for the neutral atmosphere $\alpha_n(a)$.

For an atmosphere with local spherical symmetry (i.e. no significant asymmetric horizontal variations in temperature or moisture) and having determined the bending angle $\alpha_n(a)$ as described above, there is a unique relationship between $\alpha_n(a)$ and $\mu(r)$, the atmospheric refractive index as a function of radius r . The refractive index profile $\mu(r)$ is then derived through an Abel transform of the measurements of $\alpha_n(a)$ obtained over a complete occultation.

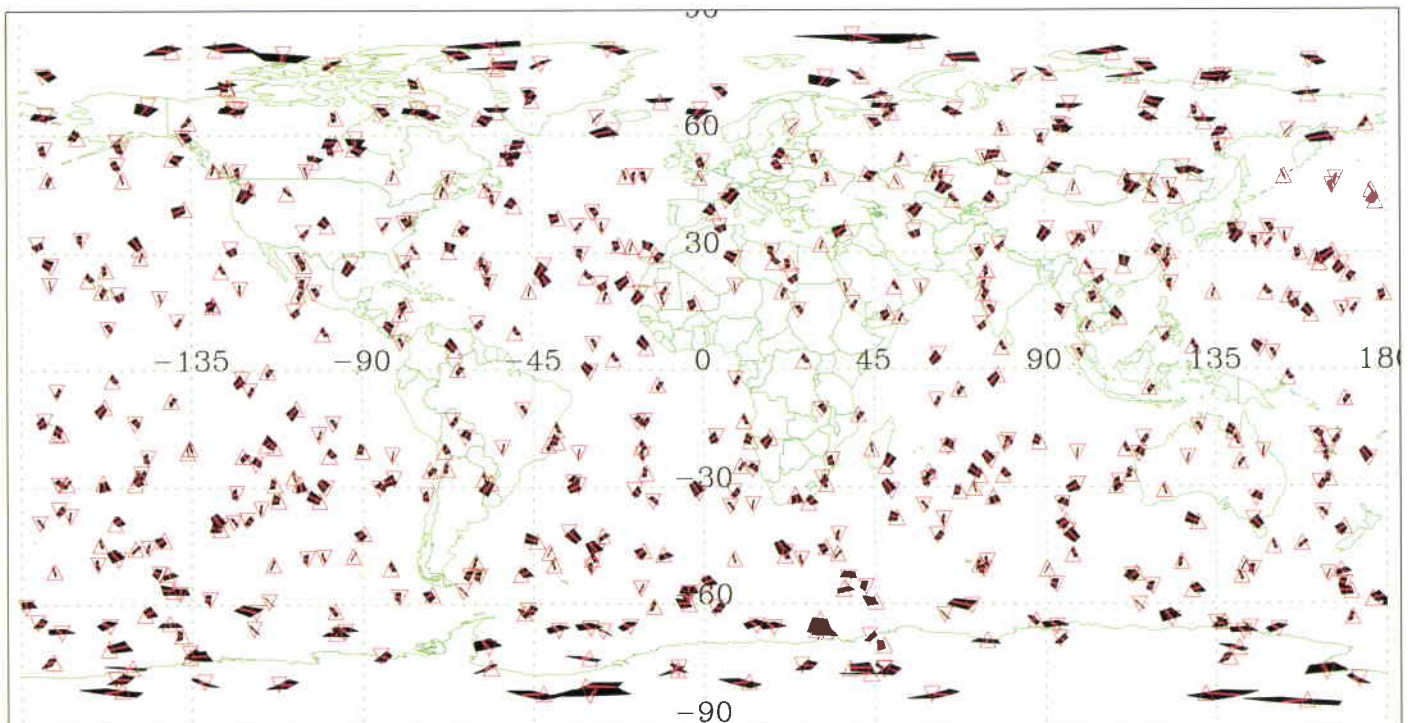
For dry air at the top and above the troposphere, the refraction index can be expressed as a function of temperature and pressure as:

$$N(r) = [\mu(r) - 1] 10^6 = 77.6 P/T$$

experiment geometry can be characterised through the use of an impact parameter (a) defined as the perpendicular distance between the centre of the Earth and the straight line followed by the ray approaching the atmosphere. When combined with precise knowledge of the geometry (obtained concurrently from the navigation channels of the GPS receiver), each phase-data sample can be converted to the corresponding values for α and (a).

To extract information on the neutral atmosphere, propagation delays caused by the ionosphere must be isolated and removed from the signal. The correction required can be

Figure 2. Example of occultations seen by GRAS over a one-day period



Using the equation of state and integrating the equation of hydrostatic equilibrium, the temperature and pressure of the atmosphere for a given altitude can be determined.

Below the tropopause, the procedure described above needs to be modified to account for the presence of water vapour. The index of refraction can be expressed with two terms, the dry and wet terms. The second term, due to water vapour, exhibits considerable variations with location and time and increases considerably close to the Earth's surface.

Figure 3. The GRAS instrument elements on the Metop satellite

The individual contributions to $\mu(r)$ of the dry and wet terms cannot be distinguished uniquely through occultation measurements. Deeper in the troposphere, water-vapour concentrations increase, contributing to 30% of the total refractivity. A planned technique for recovery of the water vapour from measurements of $\mu(r)$ is to use existing temperature analyses from meteorological offices. The accuracy to which lower tropospheric water-vapour profiles can be retrieved has been estimated by Kursinsky et al. at about 20%.

Instrument design

GRAS is a bi-frequency GPS receiver with codeless-mode operating capabilities. A dual-frequency operating instrument is needed for ionospheric correction. The codeless capability is mandatory in order to mitigate the anti-spoofing (encryption of the precise code), which prevents civilian users from benefitting from the P-code on the L2 frequency. The signals of the occulting satellites are received through two

antennas, one dedicated to the rising and one to the setting occultations. Shaped antenna patterns (10 to 12 dB gain) and dedicated radio-frequency front-ends ensure a high sensitivity and the ability to measure at low altitudes in the atmosphere – just a few kilometres – where the atmospheric attenuation due to absorption and diffraction is high.

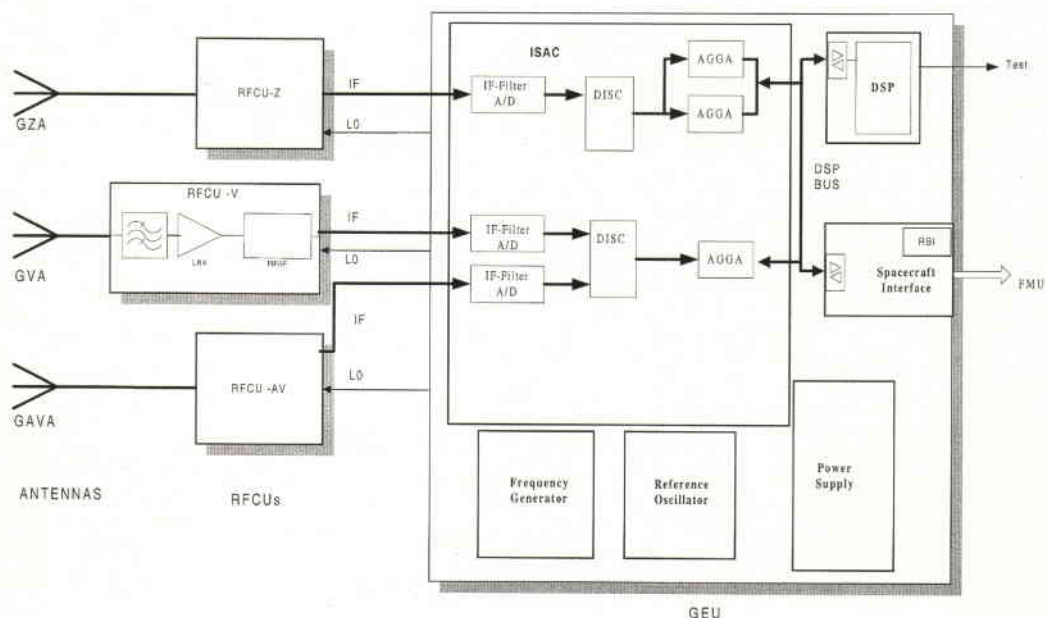
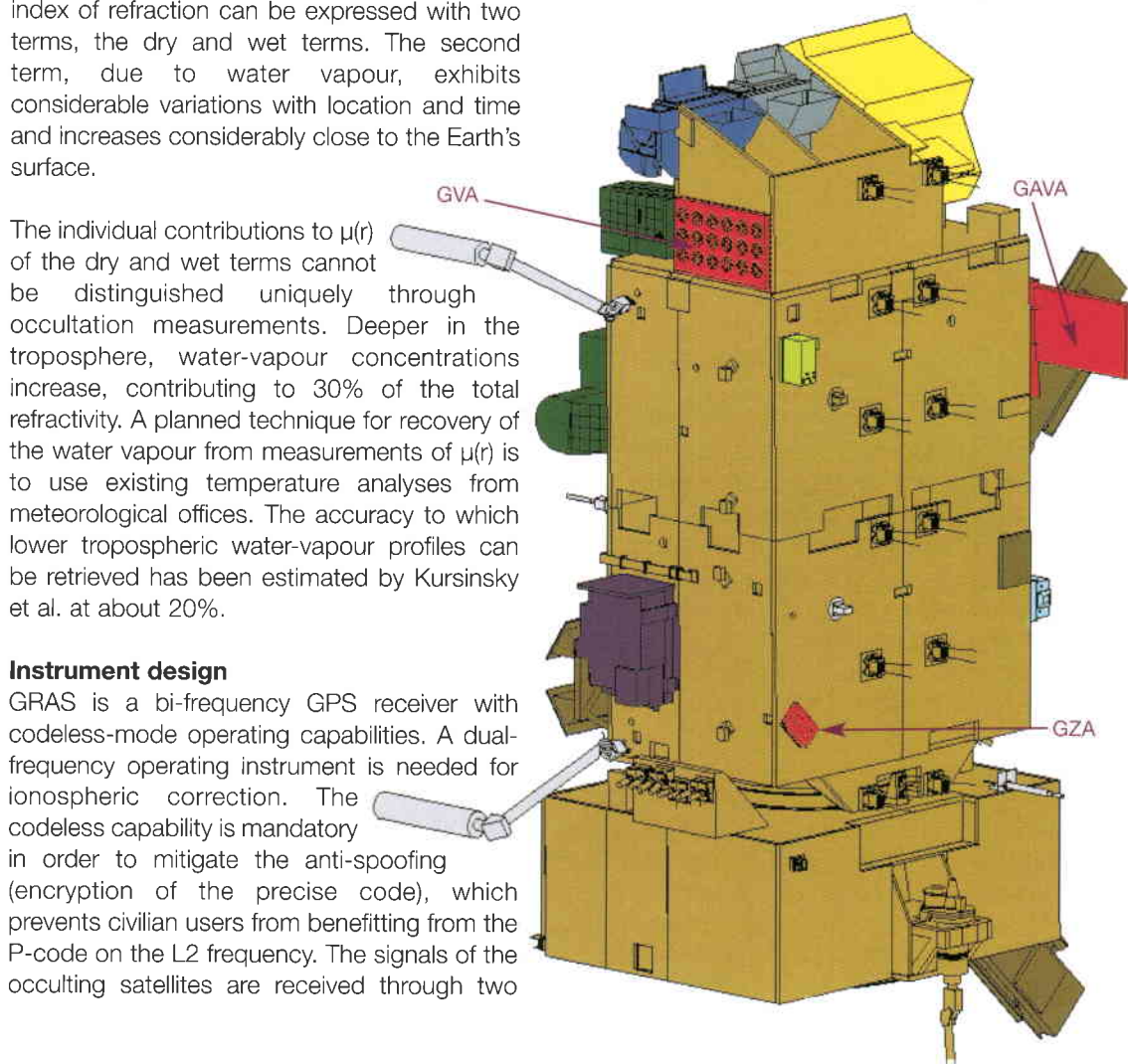


Figure 4. Functional block diagram of GRAS



Figure 5. GRAS's GZA (top) and GVA/GAVA (bottom) antennas



To track the Metop satellite's position, the instrument also operates as a navigation receiver. In this context, it receives GPS signals via a third antenna with hemispherical coverage, pointing at zenith. It acquires and tracks a set of GPS signals through eight bi-frequency channels having codeless capabilities, and uses a limited-precision navigation solution to support the autonomous instrument operation. It also provides the positional data as part of its measurement data to the Payload Module to be transmitted to the ground segment. Within the ground segment, the data are then used to compute the precise orbit of the spacecraft.

The GRAS antennas accommodated on the Metop spacecraft are shown in Figure 3.

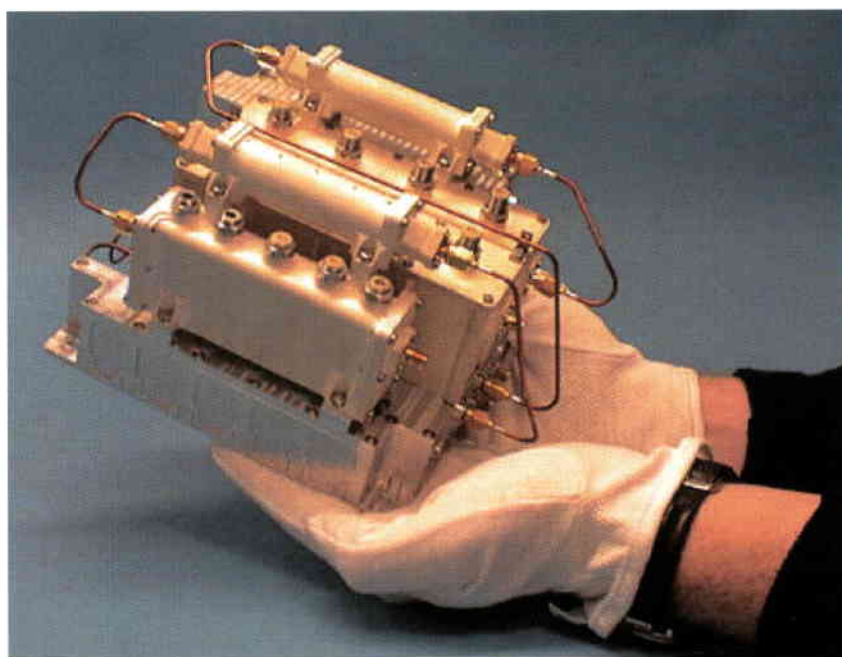
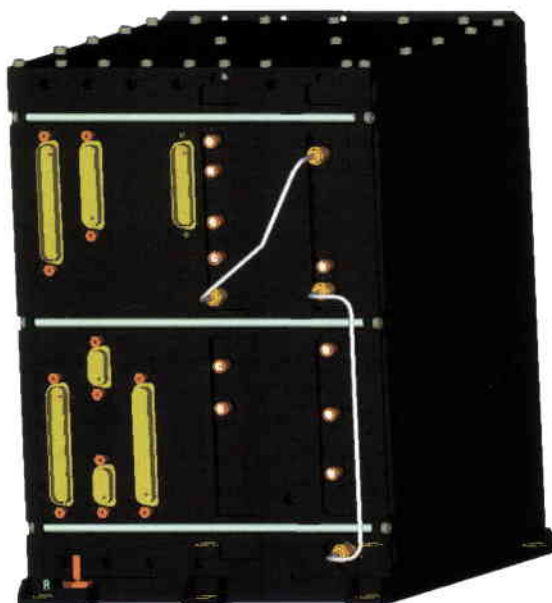


Figure 6. The Radio-Frequency Conditioning Unit (RFCU)



The GRAS instrument (Fig. 4) consists of :

- 3 antennas
- 3 RF Conditioning Units (RFCUs)
- 1 GRAS Electronics Unit (GEU).

The three antennas point in the satellite's velocity, anti-velocity and zenith directions. The velocity and anti-velocity antennas are phased arrays, each containing 18 patches with a shaped antenna pattern optimised for the occultation of the Earth's limb and its atmosphere (Fig. 5).

The RFCU (Fig. 6) consists of two bandpass filters, a low-noise amplifier and a single down-converter stage. The RFC units are accommodated within the Payload Module close to their respective antennas in order to minimise ohmic losses.

Figure 7. The GRAS Electronics Unit (GEU)

The GEU (Fig. 7) is built around three dedicated Advanced GPS GLONASS ASICs (AGGA) and a Digital Signal Processor (DSP). After filtering and a single-stage down-conversion in the RFCU, the signals are digitally down-converted with an 8-bit ADC, and filtered in a DISC ASIC, then sampled at a high rate (141.25 MHz) and delivered to the channel processor. The core of the processor is the AGGA, which simultaneously performs the final down-conversion, de-spreading and correlation of four bi-frequency GNSS channels. It also provides the codeless functionality. It is being developed by ESA and contains functionality for tracking the phase and frequency of code and carrier. The AGGA ASIC provides a number of observables to the DSP, which the latter uses to close the tracking loops and to produce the actual measurement data.

atmospheric measurements with a high accuracy in the stratosphere. The frequency generator provides the necessary frequencies for down-conversion and clock-signal generation using the reference oscillator. The power supply converts primary power to secondary power for the instrument units.

The mass budget for the whole GRAS instrument is around 30 kg, including the harness and deployment mechanism for the anti-velocity antenna. The power consumption in full operation (navigation and occultation signals) is 38 W. The average GRAS data rate is 22 kbit/s, with peaks of up to 60 kbit/s.

Instrument performance

The GRAS instrument's performance requirements are driven by the meteorological community. Near-real-time weather forecasting calls for an accuracy of 1 K in the temperature profile. This is equivalent to an error budget on the bending angle and the atmospheric Doppler of 1.2 μ rad and 3.8 mm/s at 30 km altitude. Two inversion techniques have been used, the geometrical-optics approximation and the back-propagation method. With the former, the signal path is treated as a single ray that curves in accordance with Snell's law. The vertical resolution is then limited by the first Fresnel zone, which is of the order of 1.5 km in the stratosphere and reduces to 300 m in the lower troposphere. The geometrical-optics approximation does not resolve the atmospheric multipath, but the latter is important in the troposphere due to the large gradient in the refractive index (water vapour), which will cause significant error on the sounding profile and will disturb the receiver, even to the point of loss of tracking.

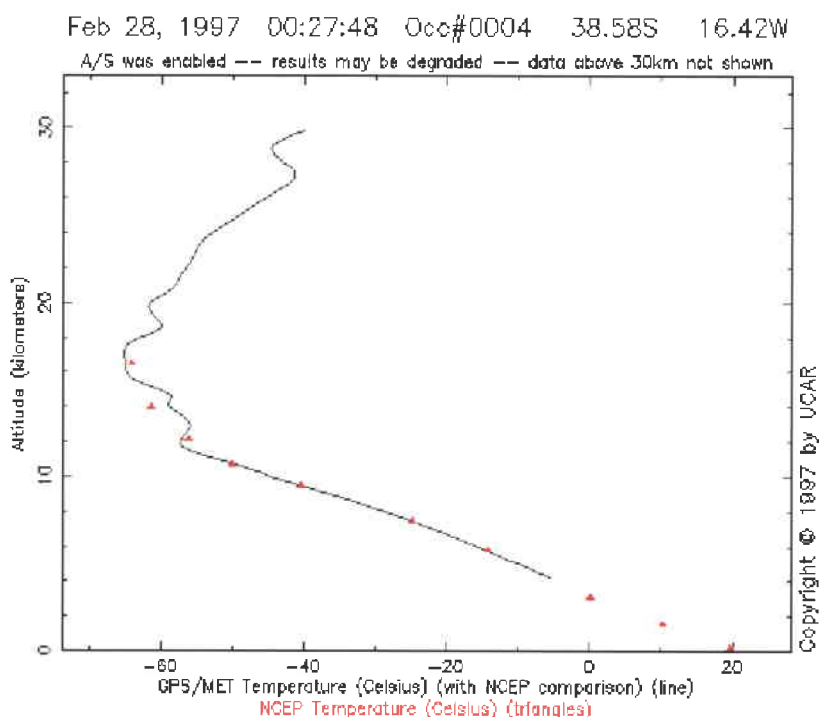


Figure 8. GPS/MET temperature soundings (courtesy of UCAR)

The DSP chip itself (TSC 21020E) has been developed by European space industry under an ESA contract. Its role within the GRAS instrument is to support the Instrument Control Unit software as well as the data-processing software (measurement, signal tracking, navigation solution and time management). The Spacecraft Interface (SCIF) board provides the interface between the DSP bus, the satellite OBDS bus and the Formatting and Multiplexing Unit (FMU) of the Payload Module.

An oven-controlled crystal oscillator is used as a reference oscillator with very stable frequency (Allan variance of 10^{-12}) in order to retrieve

Moreover, as the temperature gradient in the troposphere is of the order of 7.5 K/km, the temperature accuracy requirement cannot be met. By using more advanced techniques that take into account the wave nature of the radio signal, such as the back-propagation inversion method based on Helmholtz equations, the multipath propagation can be resolved and the vertical accuracy improved by a factor 2 to 5 up to 100 m.

The best results in terms of temperature-profile errors are obtained between 5 to 30 km altitude. Below this range, the attenuation due to the water-vapour content of the troposphere penalises the instrument's signal-to noise ratio, while above it residual correction errors due to the ionosphere become predominant.

The horizontal resolution of the radio-occultation technique is limited by the limb-sounding approach itself, and is of the order of 100 km in the troposphere and 300 km in the stratosphere.

A GPS/MET temperature sounding is plotted in Figure 8. The temperature profile retrieved with the geometrical-optics approximation technique is in good agreement with the radiosonde profiles provided by the NCEP and within 1 K from 16 to 5 km altitude, where the receiver stops tracking the signal. GRAS should provide better performances both in the high stratosphere and in the low troposphere, since the antenna gain of the occultation channels has been set at over 10 dB, while for GPS/MET it was only 3 dB.

Accurate retrieval of atmosphere parameters requires the implementation of several corrections. First of all, the positions and velocities of the GPS and Metop satellites have to be determined with accuracies of 1 m and 0.1 mm/s, respectively. This will be done using the navigation signals delivered by the instrument. In addition, a clock error correction needs to be implemented in order to correct for the dithering of the GPS clock, called selective availability (SA), and the long-term drift of the crystal clock onboard the GRAS receiver. For this correction, a double differential technique will be implemented using a network of 12 to 30 tracking ground stations. ESA already controls six tracking ground stations equipped with GPS receivers as part of the International GPS Service for Geodynamics (IGS) network. The occultation data will also need a clock correction to mitigate the GPS clock dithering signals (SA). This will be done using a single-differential technique, which is preferable to a double-differential approach if GRAS's master oscillator is stable over 100 sec. It will also be better in terms of its effect on the variance of the signal by root square of two, whilst the GPS

satellite clock bias and drift errors will also be cancelled.

The effect of the ionosphere can be seen as an extra signal path length of the order of 50 to 80 m, depending on the frequency, solar activity and diurnal cycle. A fine correction will be achieved in the classical way using the bi-frequency capability of the receiver. Unfortunately, the codeless mode, which is less sensitive than a single channel, will lose track at an altitude of around 10 km, leaving the receiver to operate with only one frequency. At this altitude, the extra path length due to the atmosphere is already of the order of 130 m, and a less accurate ionospheric correction is good enough. This correction will be performed by extrapolation of the ionospheric data (Total Electron Content, TEC) measured during the sounding of the stratosphere. Multipath due to appendages on the Metop spacecraft has been minimised. GRAS antenna accommodation has been carefully optimised, but a residual effect will remain which will be part of the total bending-angle error budget.

The processing of the occultation and the navigation data, as well as the data from the fiducial ground station, will be performed in the Level-1b ground processor. A Ground Processor Prototype (GPP) is being developed to validate the Level-1b algorithms, and to verify the end-to-end performance of the data chain. An extensive pre-launch characterisation of the instrument is planned to fully characterise its transfer function. After launch and during the satellite commissioning phase, the instrument performances will be verified and validated.

The near-real-time products

The GRAS Level-1 products (Table 1) are processed in the Eumetsat Polar System (EPS) Core Ground Segment (CGS) located at Eumetsat in Darmstadt, Germany. Level-1b products from the EPS GRAS mission will be

Table 1. GRAS Level-1 and Level-2 products

Level 1 products

- Residual phase data
- Sounding occultation table
- Navigation data
- Total bending angle as a function of the impact parameter at L1 and L2
- Ionospheric corrected total bending angle (first-order correction)
- TEC
- Auxiliary data
- Earth orientation parameters
- Observation error characteristics

Level 2 products

- Refractivity profiles
- Temperatures profiles
- Moisture profiles
- Pressure profiles
- Integrated precipitable water vapour
- Temperature and humidity retrieval parameters
- Observation error characteristics
- TEC

disseminated to the operational users of meteorological data within 2 h 15 min of the observation. All GRAS Level-1 products are to be archived and will be available to users via the Unified Meteorological Archive and Retrieval Facility (UMARF) from the EPS CGS.

Applications

Numerical Weather Prediction

Assimilation of GRAS observations into NWP models is the most important operational application for the data produced by the instrument. GRAS observations combine high vertical resolution and high absolute accuracy with global coverage and good long-term stability. These features complement the existing and planned meteorological observation systems very well.

The trend in Numerical Weather Prediction is towards using variational assimilation. This technique suits GRAS observations very well as it enables the assimilation of observation quantities that are not model variables. For GRAS data, this means that the observations can be assimilated either as Level-1 or as Level-2 products, providing an opportunity to optimise the system performance in terms of both complexity and accuracy. However, assimilation of the GRAS data into NWP models requires a deep understanding and good characterisation of the observation errors.

Because of the low horizontal resolution, GRAS observations can be expected to be most valuable in global forecasting over the short-to-medium range (1–10 days). They should also have a positive impact on regional and mesoscale forecasting by providing information over the sparsely observed ocean areas. Also, the boundary conditions from the global models to the regional and mesoscale models will be more accurate due to the impact of GRAS data on the global models.

Climate monitoring

The basis for climate monitoring is databases populated with accurate global measurements of the atmospheric characteristics over a long period of time. The 14-year EPS GRAS mission is a very good starting point for building up an archive of radio-occultation data. The long-term stability and self-calibration features of the GRAS instrument support the objectives of climate-monitoring applications.

Unfortunately, the climate-monitoring requirements are very demanding in terms of temperature resolution (0.1 K), which is one order of magnitude better than currently requested for NRT weather predictions. Recent studies have demonstrated that a constellation

of six satellites with GPS/GLONASS receivers, or 12 satellites with GPS only, is the minimum necessary in order to attain the objectives set by the climate community. GRAS on Metop might therefore be considered a first step, but many companion GPS receivers are needed in orbit in order to match the climate needs.

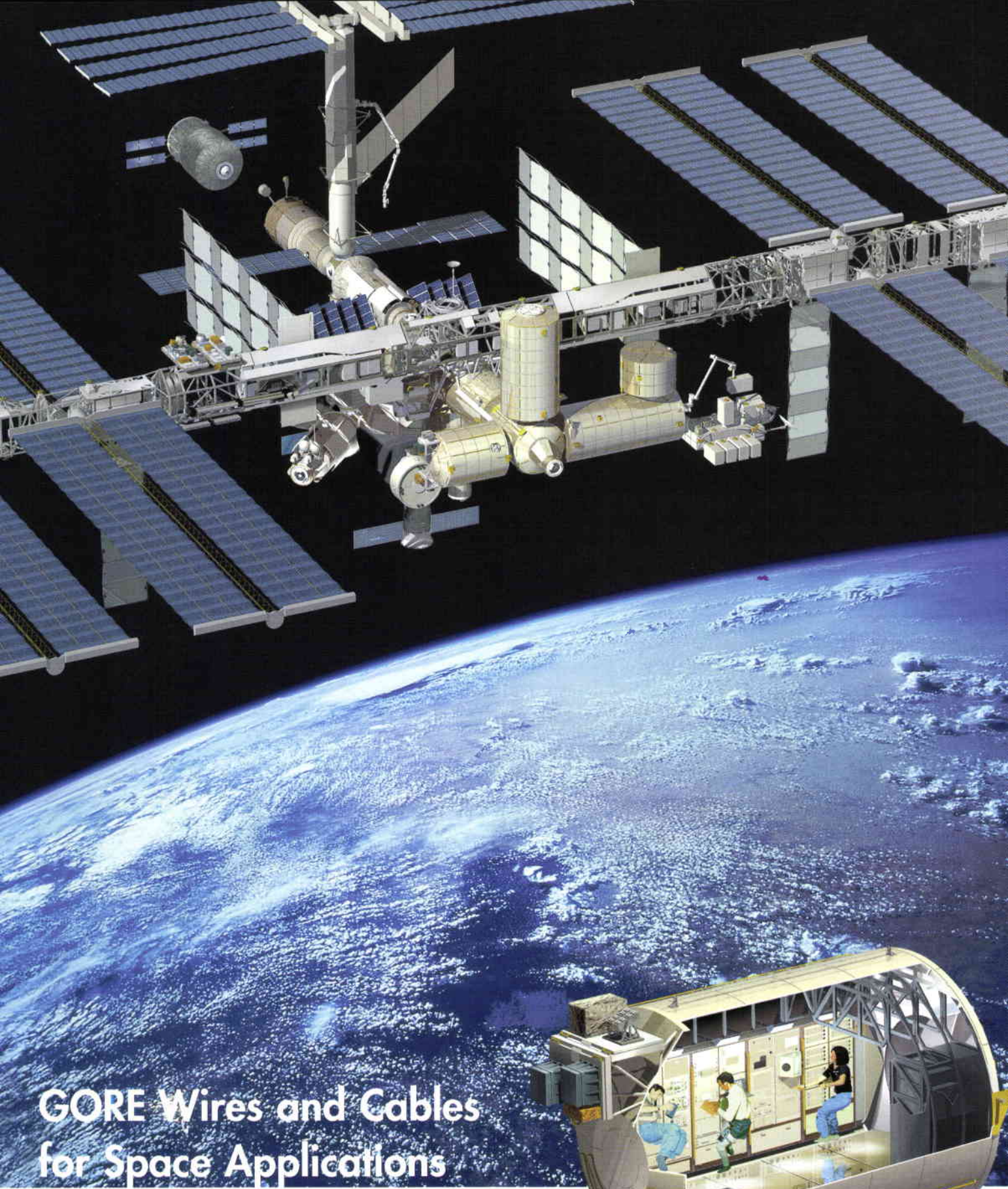
Other applications

Study of the heat exchange between the stratosphere and troposphere requires accurate measurements of the temperature profile across the tropopause. This phenomenon takes place at tropical latitudes and in regions where the sparse radiosonde network cannot provide enough data for the verification of theories and models. The very good temperature-measurement accuracy provided by GRAS at the locations where no permanent radiosonde or lidar measurement network exists will enable the verification and further study of many atmospheric theories and models.

Conclusions

The GRAS instrument on Metop, as part of the EPS system, will provide an unrivalled set of high-quality atmospheric sounding data with a vertical accuracy ranging from 1 km down to 100 m at low altitude. In addition, GRAS provides a unique opportunity to establish the height of the tropopause with a vertical accuracy of better than 1 km.

The GRAS instrument capitalises on the experience gained with its precursor GPS/MET, and its improved design allows it to better fulfil the mission objectives. The instrument is designed around a DSP chip and an ASIC, which have been developed under ESA contract. Their utilisation and adequacy within a GPS receiver has been validated with an instrument breadboard. Small-satellite radio-occultation missions, and in particular Champ, will pave the way for the setting up and utilisation of the ground infrastructure necessary for the clock correction and the precise orbit determination.



GORE Wires and Cables for Space Applications

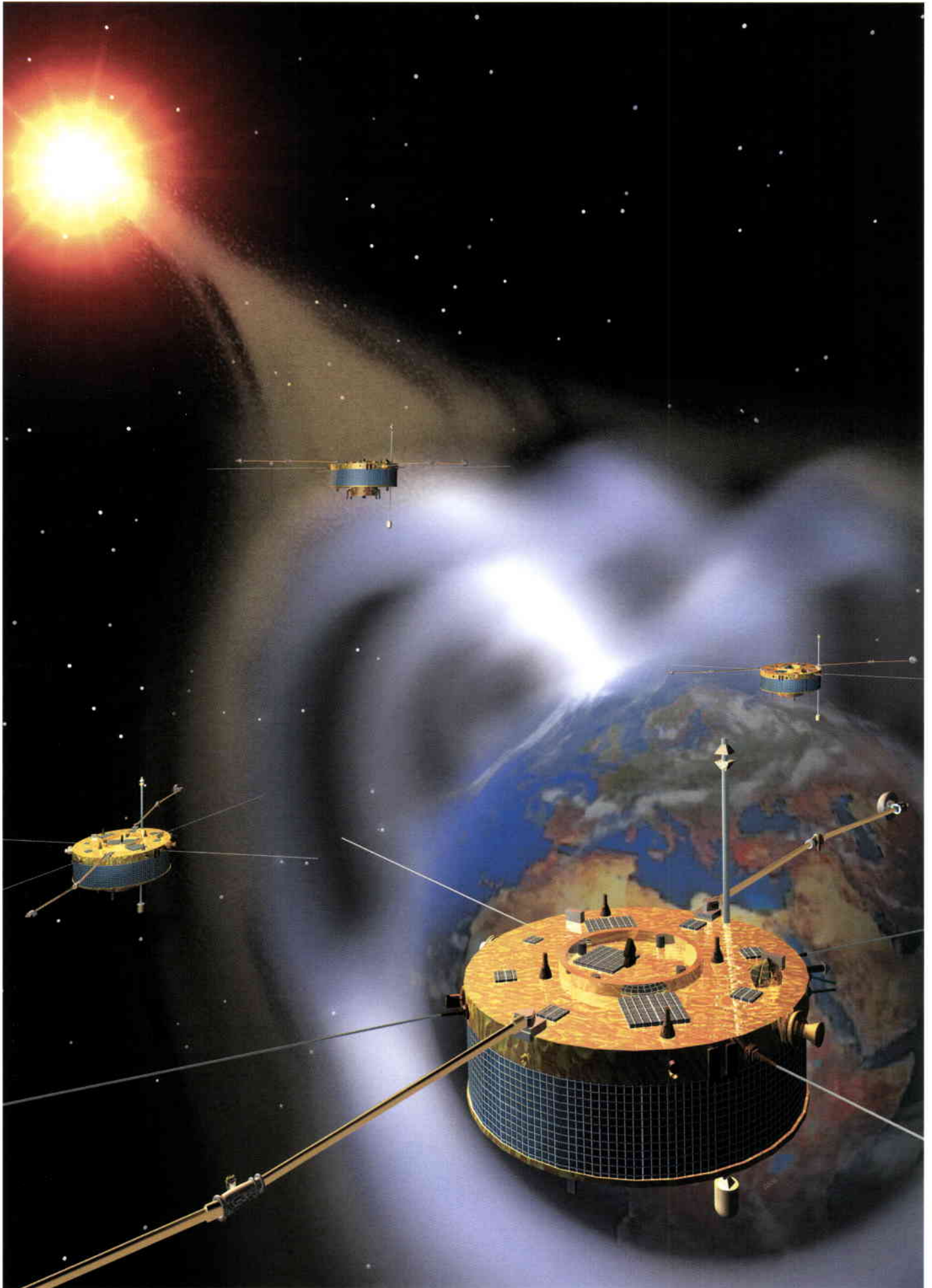
Over twenty years of technological experience, Gore has proved competence in space applications for many milestones of space missions, such as Moon Landing, Spacelab, EURECA, ERS1 + 2, Italsat, SAX, SPOT, ISO, Envisat, XMM, Metop, Integral, scientific research in space, Columbus.

As a special cable supplier we support you in planning the next step into space. Call us now.

TEL.: +49/91 44/6 01-0 • FAX: +49/91 44/60 14 53
W. L. GORE & ASSOCIATES GMBH • NORDRING 1 • D-91785 PLEINFELD / GERMANY



©1999 W. L. GORE & Associates GmbH. Illustrations: David Ducras



The Cluster-II Mission

– Rising from the Ashes

The Cluster II Project Team

Scientific Projects Department, ESA Directorate of Scientific Programmes,
ESTEC, Noordwijk, The Netherlands

In June and July of this year, four Cluster-II spacecraft will be launched in pairs from Baikonur Cosmodrome in Kazakhstan (Fig. 1). If all goes well, these launches will mark the culmination of a remarkable recovery from the tragic loss of the original Cluster mission.

In June 1996, an explosion of the first Ariane-5 launch vehicle shortly after lift-off destroyed the flotilla of Cluster spacecraft. Now, just four years later, this unique Cornerstone of ESA's Horizons 2000 Science Programme has been

rebuilt and is ready to complete the mission to the magnetosphere planned for its predecessors.

From concept to reality

The Cluster mission was first proposed in November 1982 in response to an ESA Call for Proposals for the next series of science missions. It grew out of an original idea from a group of European scientists to carry out a detailed study of the Earth's magnetotail in the equatorial plane. This idea was then developed into a proposal to study the 'cusp' regions of the magnetosphere with a polar orbiting mission.

The Assessment Study ran from February to August 1983 and was followed by a Phase-A definition study, which was presented to the scientific community in late 1985. At this time, the proposal included one 270 kg 'mother' spacecraft, carrying 46 kg of scientific payload, together with three smaller companions, each weighing 217 kg and carrying a payload of

Four years ago, the first Cluster mission was lost when the maiden flight of Ariane-5 came to a tragic end. Today, through the combined efforts of the ESA Project Team, its industrial partners and collaborating scientific institutions, the Cluster quartet has been born again. A two-year programme of investigation into the Sun-Earth connection will begin this summer when ESA's Cornerstone mission to the magnetosphere lifts off from Baikonur. Flying in formation over the Earth's polar regions, Cluster-II will carry out the first three-dimensional exploration of near-Earth space ever attempted.



Figure 1. The four Cluster-II spacecraft in the clean room at IABG in Munich (D), in November 1999

26 kg. This quartet would be launched into an elliptical polar orbit of $4 \times 22 R_E$ (Earth radii)*.

At the same time, a parallel Phase-A study was also undertaken for the Solar and Heliospheric Observatory (SOHO) mission to study the Sun and solar wind. After the ESA Science Programme Committee (SPC) approved the Agency's Horizon 2000 long-term science plan, the combined Cluster and SOHO missions were selected as the Solar-Terrestrial Physics (STP) Cornerstone, the first major science project of the new programme.



Figure 2. Debris from the Cluster spacecraft being collected after the Ariane-501 launch failure

Prior to the final definition of the Cluster mission, a proposal was made to use the first Cluster spacecraft in place of a planned NASA satellite called Equator. This would have involved a launch into an equatorial orbit by a US launch vehicle for an initial one-year mission. The remaining three Cluster spacecraft would then have been launched by ESA into polar orbits, where they would later be joined by the original 'equatorial' spacecraft. This concept was eventually abandoned after consideration of expected payload degradation during one year in equatorial orbit and difficulties in inter-calibration of the four sets of scientific instruments after launch.

The final baseline Cornerstone, renamed the Solar-Terrestrial Science Programme (STSP), was defined as a two-thirds/one-third co-operative endeavour between ESA and NASA, with most of the American participation allocated to SOHO. Cluster was expected to benefit from a 'free' launch on the first test flight (V501) of the newly developed Ariane-5 booster.

After several minor delays, Ariane-501 lifted off from Kourou on 4 June 1996, carrying its

payload of four Cluster satellites. Unfortunately, the launcher's maiden flight lasted just 37 seconds before intense aerodynamic loads resulted in its break up and initiation of the automatic destruct system. Debris from the Cluster spacecraft was scattered across the mangrove swamps near the launch site (Fig. 2).

The phoenix rises from the ashes

It seemed to all concerned that 10 years of work had come to naught. However, in July 1996, after considering possible ways of recovering at least some of the unique science from the mission, ESA, with the approval of its Science Programme Committee, decided to build a fifth Cluster satellite.

Appropriately named 'Phoenix', after a mythical Arabian bird that was burnt on a funeral pyre and then was reborn by rising from the ashes, this spacecraft was to be identical to the original Cluster spacecraft. It would be based on the Cluster structural model and equipped with flight spares of the experiments and subsystems prepared for the Cluster mission. New equipment, such as the harness, wire booms and radial booms, would only be manufactured when necessary. By taking advantage of the existing hardware, together with the knowledge and experience gained in the original programme, Phoenix was expected to be fully integrated and tested by mid-1997, opening the way for a launch later that year.

This rapid response to the launch failure soon gave way to a longer term strategy. An awareness that the scientific objectives of the Cluster mission could not be met by a single spacecraft led to proposals to rebuild three or four full-size Cluster spacecraft, or to launch three smaller satellites alongside Phoenix.

Although these proposals had significant implications for an ESA science budget that was already fully committed, it was accepted that the costs of a full rebuilding programme would be much lower, since the spacecraft had already been through a complete cycle of design, development and testing. In addition, designing and developing completely new, albeit smaller, spacecraft, would jeopardise the objective of constructing the new satellites as soon as possible, so that they would be available to study the Sun during the peak of the solar cycle, which was expected in the year 2000.

On 3 April 1997, the SPC agreed that the potential science return from a full Cluster re-flight was so important that a further three near-replicas of the original spacecraft would be built, in addition to Phoenix (Fig. 3).

* The Earth's equatorial radius $R_E = 6378$ km

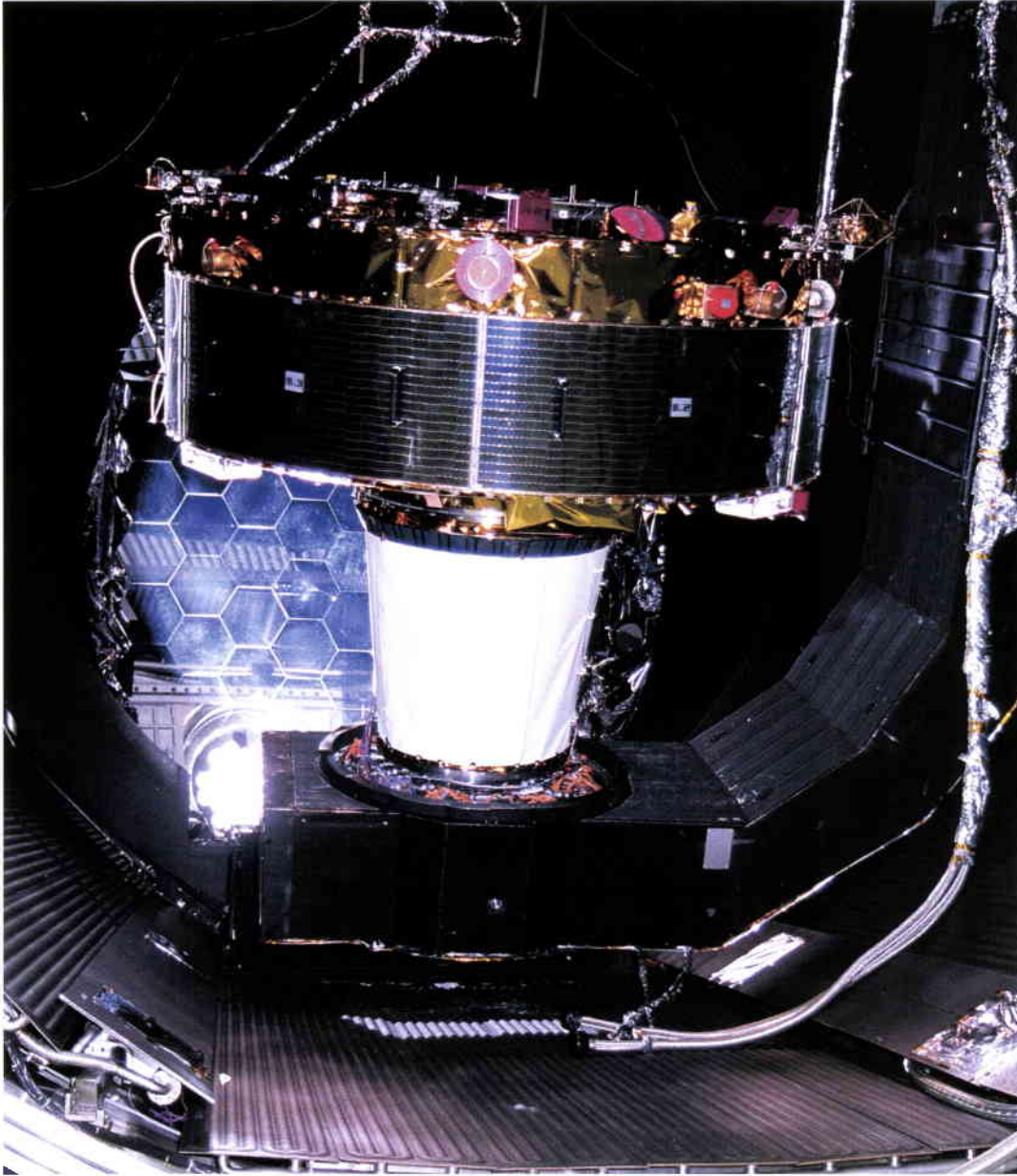


Figure 3. Phoenix (FM 5) on the test stand at IABG in Munich (D)

Dubbed flight models (FM) 5 to 8, these spacecraft have now completed their assembly and integration test programme, and were transported to Baikonur Cosmodrome in April of this year.

Anatomy of a Cluster-II spacecraft

Construction of the Cluster and Cluster-II spacecraft has been a major enterprise for European industry. Manufacturing companies in almost all of the 15 ESA Member States, and in the United States, have provided hardware for these projects. The prime contractor is the German company Dornier Satellitensysteme, but many other companies have also participated (Fig. 4).

All of the spacecraft have been assembled in the giant clean room at Dornier's Friedrichshafen plant, and then sent to IABG in Ottobrunn, near Munich, for intensive acoustic, thermal-vacuum and magnetic testing.

The first spacecraft to be completed by Dornier was FM 6, which was then transported to IABG in March 1999. It was followed at regular intervals by FM 7, then FM 8 and FM 5. All four spacecraft were briefly brought together for a press briefing at IABG in November 1999, and the test programme for the final satellite, FM 5, was completed in March 2000.

The spacecraft have been assembled by hand from thousands of individual parts. Built into each 550 kg satellite are six propellant tanks, two pressure tanks, eight thrusters, 80 m of pipework, about 5 km of wiring, 380 connectors and more than 14 000 electrical contacts.

When fully loaded with fuel, a Cluster-II spacecraft weighs approximately 1.2 tonnes. Each spacecraft is shaped like a large drum, 1.3 m high and 2.9 m in diameter (Fig. 5). In the centre is a cylinder with an aluminium honeycomb structure covered with a skin of

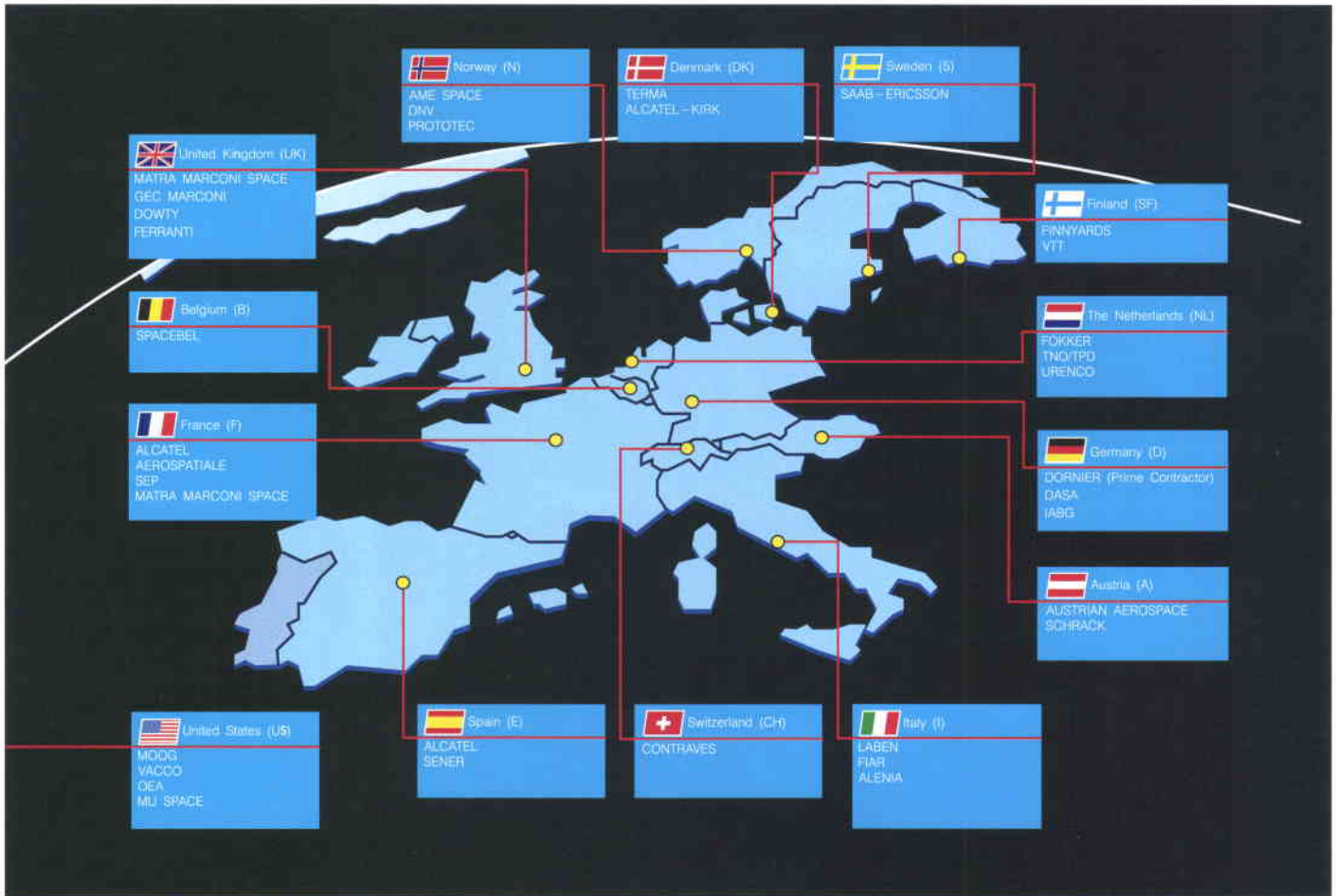


Figure 4. Major industrial contractors involved in Cluster

carbon-fibre-reinforced plastic. The equipment panel inside this cylinder supports the main engine, two high-pressure tanks and other parts of the propulsion system.

Six spherical fuel tanks made from titanium are attached to the outside of this central cylinder. The fuel they carry (MMH and MON1) accounts for more than half the launch weight of each spacecraft. Most of this fuel will be consumed soon after their launch, during the complex manoeuvres required to reach their operational orbits. Each spacecraft also carries eight 10 N thrusters – four radial and four axial – for smaller changes of orbit.

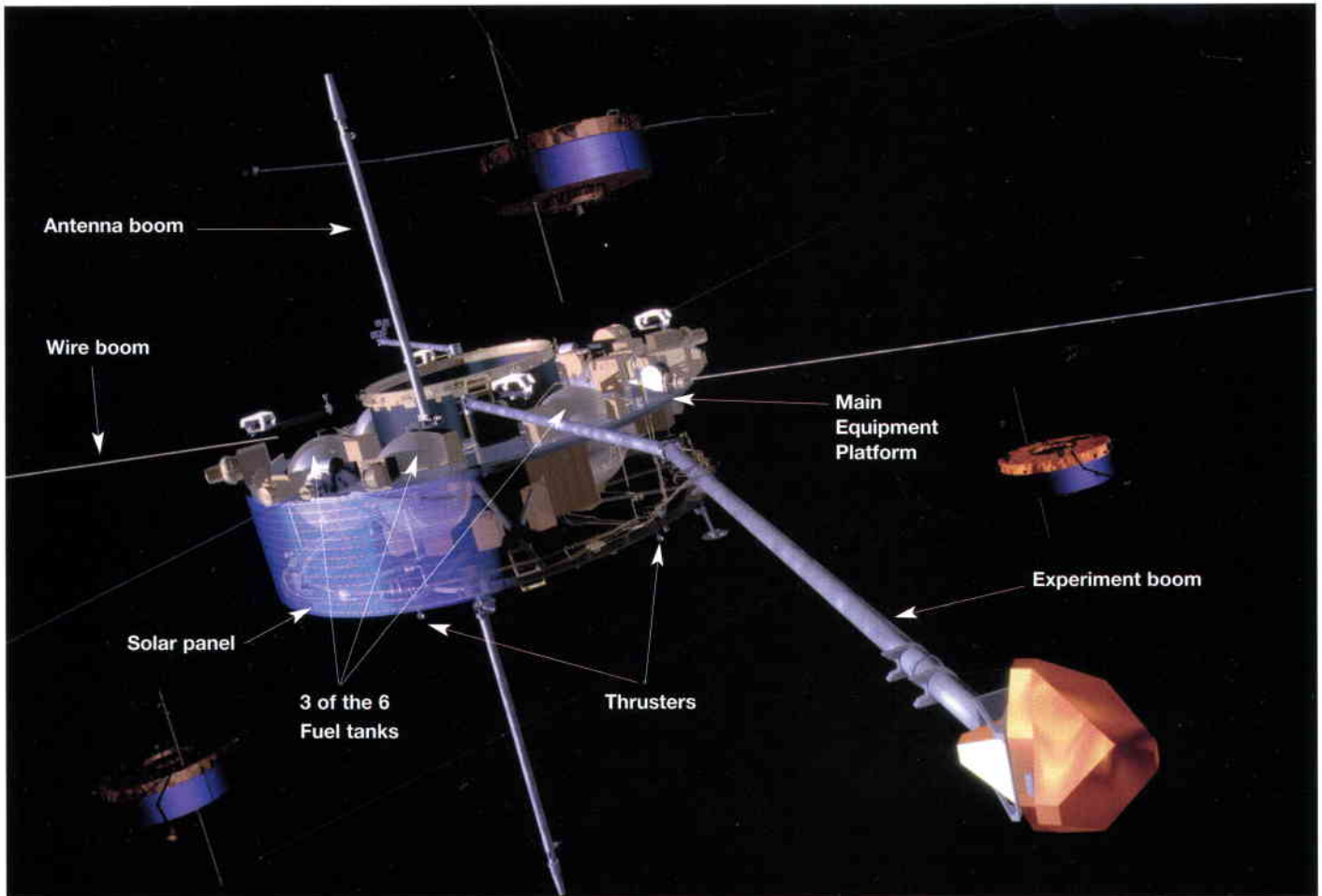
Table 1. Spacecraft vital statistics

| | |
|---------------------|--------------|
| Diameter | 2.9 m |
| Height | 1.3 m |
| Mass | 1200 kg |
| Propellant | 650 kg |
| Scientific payload | 71 kg |
| Solar-array power | 224 W |
| Battery capacity | 80 Ah |
| Power to payload | 47 W |
| Spin rate | 15 rpm |
| Operational mission | 2 yr |
| Telemetry downlink | 2–262 kbit/s |

Around the central cylinder is the main equipment platform. It consists of an aluminium-skinned honeycomb panel, which is reinforced by an outer aluminium ring. Most of the subsystems, such as the power and computer processing hardware, are attached to its lower surface, while the science experiments are placed on top. Electrical power is provided by six curved solar panels attached around the outside of the platform. Five silver-cadmium batteries supply power during the four-hour-long eclipses when the spacecraft enter Earth's shadow.

Various rod-shaped booms open out once the satellite reaches orbit. They include two single-hinged antennas for communications and two 5 m, double-hinged booms on the satellite's upper surface which carry sensors that would otherwise be disturbed by the spacecraft. There are also four 50 m-long wire booms, which deploy horizontally when the spacecraft begins to spin. These measure the changing electrical fields around each spacecraft.

Although all of the Cluster-II spacecraft are outwardly similar in appearance, the present-day Phoenix is an unusual combination of the old and the new. At its heart is the first spacecraft structure ever manufactured during the original Cluster programme back in 1992,



Never intended to fly in space, this main body was used for a variety of shock tests and eventually grabbed some limelight at the 1995 Paris Air Show.

Phoenix also differs slightly from its companions by having the original Cluster analogue transponder and signal amplifier. However, no hardware from the four Clusters that were lost has been used again. To all intents and purposes, Phoenix can be considered to be a new spacecraft.

The other three Cluster-II spacecraft are identical, but even they differ slightly from the original satellites. Significant modifications made to the overall design include the addition of a solid-state data recorder with a larger memory; two new computer boxes, a new high-power digital transponder, and experiment booms which have been slightly shortened to fit inside the protective fairing on the Soyuz rocket. Various other components that are no longer manufactured have also been replaced.

The same applies to the scientific payload. Under the first Cluster revival plan, Phoenix was to have carried spare experiments, but most of its science instruments have now been completely rebuilt. It was decided that, since it was necessary to make three new units for

each experiment, it would be just as easy to make four.

One unusual addition to FM 5 and FM 7 (the upper spacecraft on each stack) is a small Visual Monitoring Camera, with which it is hoped to capture views of the lower spacecraft and its Fregat stage shortly after each pair separate in orbit.

Dual launches from Kazakhstan

The Cluster-II spacecraft are scheduled to be flown to Baikonur Cosmodrome, Kazakhstan on board two Antonov aircraft in early April. There, they will spend the next few months in the various launch-preparation and launcher-integration facilities, undergoing final checks and fuelling. The spacecraft will then be integrated to the launch vehicle, after which the entire assembly will be transported to the launch pad by rail car, in a horizontal position. The Soyuz is then lifted upright, ready for fuelling and lift-off. Launch will take place from Pad 6, which has been specially modified to handle a Soyuz with a Fregat upper stage.

The four satellites will be put into orbit, in pairs, by two Soyuz rockets provided by the Russian-French Starsem company (Fig. 6). The Soyuz is a more powerful version of the Semyorka rockets, which launched the world's first

Figure 5. Cut-away view of the Cluster spacecraft

Figure 6. Soyuz-Fregat lifts off from Baikonur at the start of its first qualification flight on 9 February 2000 (courtesy of Starsem)



Figure 7. Cutaway view of Soyuz-Fregat

Figure 8. Artist's impression of Fregat with two Cluster spacecraft above the Earth (courtesy of NPO Lavotchkin)

satellite in 1957 (Sputnik) and the first spaceman in 1961 (Yuri Gagarin). Between them, the various versions of the booster have successfully completed more than 1650 launches. Although the Soyuz first flew in 1963, it is still used to orbit both manned and unmanned spacecraft. Upgraded versions of the booster are in the pipeline, ensuring its continued service well into the new century, and its future operations will include delivering crews and cargo to the International Space Station.

When the Cluster-II mission was approved by ESA's Science Programme Committee in April 1997, it appeared that a launch on a European Ariane rocket would be too expensive. The only feasible solution, bearing in mind the project's financial constraints, was to launch the spacecraft using two Soyuz launch vehicles, each equipped with a newly designed Fregat upper stage (Fig. 7). The contract for launch of the Cluster-II satellites was eventually signed on 24 July 1998 at ESA Headquarters in Paris.

Although a similar system has been fitted on nearly 30 interplanetary spacecraft, including the Phobos probes to Mars, the Fregat has not previously been flown on a Soyuz vehicle. Before finally committing itself to the dual Cluster-II launches, ESA has insisted on two qualification flights of the Soyuz-Fregat combination.

The first of these was successfully completed on 9 February 2000. The mission was performed according to the predefined schedule and Fregat performed the first two requested engine burns, placing its payload into the expected orbit. Preliminary analysis of the parameters received from the Fregat showed a



very good accuracy, with values very close to the specification.

A second validation flight, involving a dummy satellite with the same mass as a pair of Cluster-II spacecraft, followed on 20 March. This also proved to be highly successful, clearing the way for the dual Cluster-II launches in June and July.

Built by the Russian Lavotchkin industrial complex, the Fregat has a single-chamber main engine, which can be restarted up to 20 times, and four groups of three 50 N hydrazine thrusters to provide attitude control.



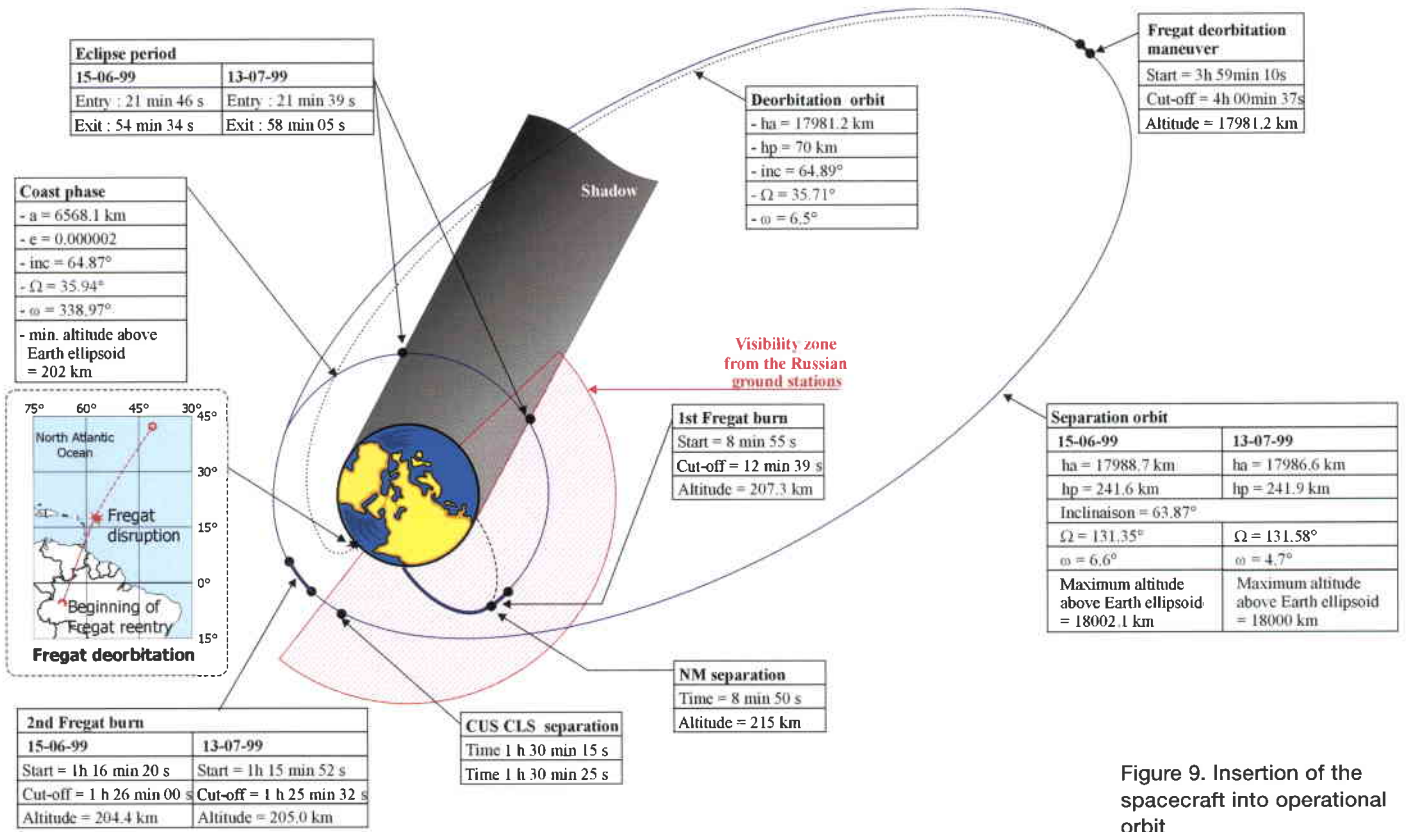


Figure 9. Insertion of the spacecraft into operational orbit

Into orbit

The first pair of Cluster-II satellites (FM 6 and 7) are currently set for launch in mid-June 2000, to be followed by the second pair one month later. The Soyuz launcher will place the upper stage and its Cluster-II payload into an orbit inclined at 64.8° to the equator. The fairing is jettisoned during operation of the Soyuz third stage. Once it reaches the correct altitude, 8 min 48 sec after lift-off, the Fregat payload assist module and its two Cluster-II spacecraft will separate from the booster (Fig. 8). The Fregat main engine will fire almost immediately to achieve a circular orbit of approximately 200 km altitude. About one hour later, the Fregat engine will fire again to inject the spacecraft into a 200 km x 18 000 km elliptical orbit (Fig. 9).

The two satellites will then be released, one after the other. They will use their own on-board propulsion systems to reach the final operational orbit. This involves changing their orbital inclination from 64.8° to 90°, while raising the highest point above the Earth (apogee) to 119 000 km and the lowest point (perigee) to 19 000 km. To do this, each Cluster-II spacecraft main engine will perform six major manoeuvres. These orbital changes are made possible by the large amount of onboard fuel, which makes up approximately half of each satellite's launch mass.

Once they reach their operational orbits, the spacecraft will fly in tetrahedral formation around the Earth. The relative distances

between them may be adjusted from a minimum of 200 km to a maximum of 18 000 km by firing their onboard thrusters. Their separation will depend on the characteristics of the particular region of near-Earth space that is being studied and the spatial resolution that the scientists require.

The 57 h elliptical orbit has been selected so that the spacecraft will travel over the planet's polar regions and investigate all of the key near-Earth plasma regions within the magnetosphere (Fig. 10). Operations will begin several months after launch, when orbital checkout, commissioning and calibration of instruments are completed.

This means that, during the first part of the mission (in the northern hemisphere's winter), the spacecraft will pass over the polar cusp and spend a considerable amount of time during each orbit exposed to the solar wind when they venture beyond the magnetosphere. Six months later, when the Earth is on the opposite side of the Sun, the quartet will remain inside the Earth's magnetosphere and explore the electromagnetic environment more than 100 000 km down the magnetotail.

All regions of interest will be crossed again during the second year of operations, though, with the benefit of previous experience, the science team will have the option to investigate some of them more intensively by modifying the quartet's orbital configuration.



Cluster-II: Scientific Objectives and Data Dissemination

C. Ph. Escoubet

Space Science Department, ESA Directorate of Scientific Programmes, ESTEC, Noordwijk, The Netherlands

Scientific objectives

The study of the interaction between the solar wind, the extension of the solar atmosphere, and the magnetosphere, the cavity that contains the Earth magnetic field, is a key element in the Solar Terrestrial Science Programme (Fig. 1). One example of this interaction is the direct entry of solar-wind particles into the magnetosphere through the polar cusps (Fig. 2). These consist of two magnetic funnels, one in each hemisphere, which focus the solar-wind particles. The polar cusps, located near the geomagnetic poles, are the 'windows' through the Earth's magnetic shield for high-energy solar particles.

The solar-wind particles (mainly electrons and protons) enter the broad outer cusp, which has a diameter of approximately 50 000 km, and then follow the converging magnetic field down to the ionosphere, where the cusp size shrinks to about 500 km. This converging magnetic field allows the study of a very large area of the magnetopause through a limited region of space inside the cusps.

Another example of the interaction of the solar wind with the magnetosphere is the acceleration of plasma in the magnetotail during geomagnetic substorms. The enormous, tapering magnetotail is a large reservoir of both solar-wind and ionospheric particles. Under some circumstances, for instance when the solar wind causes the interplanetary magnetic field to reverse in polarity from north to south, the magnetotail releases a large amount of particles towards the Earth.

Both mechanisms - particles entering in the polar cusps and substorms - produce aurorae when the precipitating particles, electrons and

The Cluster-II mission is designed to study the near-Earth space environment in three dimensions. This will be the first scientific mission with four identical spacecraft flying together in the Earth's environment. The relative distance between the four spacecraft will vary between 200 and 18 000 km, according to the scientific region of interest. Cluster-II and the Solar and Heliospheric Observatory (SOHO) together make up the Solar Terrestrial Science Programme, the first 'Cornerstone' of ESA's Horizons 2000 long-term science plan.

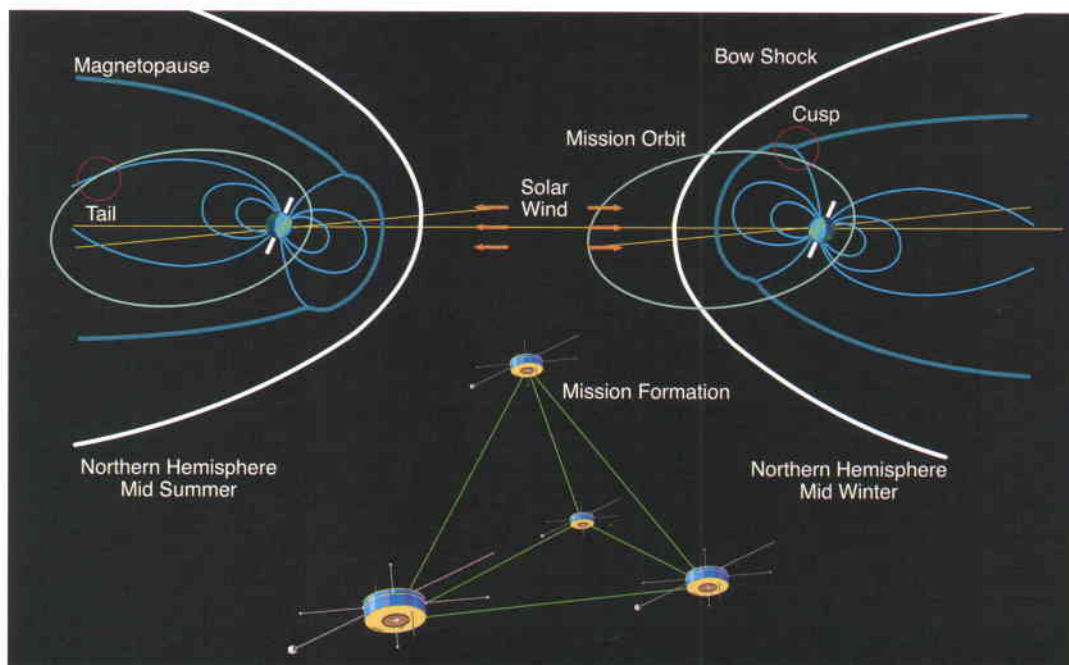


Figure 1. Artist's impression of the Sun-Earth interaction to be studied by the four Cluster spacecraft

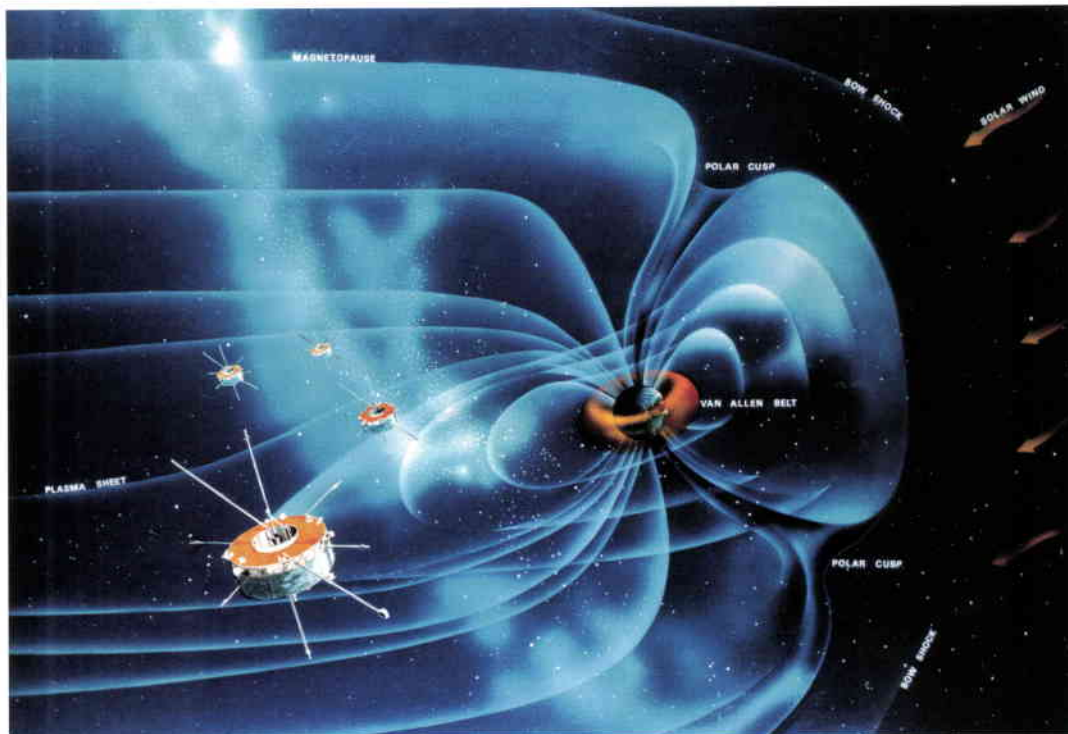


Figure 2. Artist's impression of the Cluster orbit and the main regions/boundaries of the Earth's magnetosphere

ions, hit the neutral gas of the atmosphere. Sometimes these particles are very energetic and can have dramatic effects on human activities, for example disruption of electrical power and telecommunications and also serious anomalies in the operation of satellites, particularly at the geostationary orbit.

Cluster will determine the physical processes involved in this interaction between the solar wind and the magnetosphere by visiting key regions like the polar cusps and the magnetotail. The four Cluster spacecraft will map the plasma structures contained within these regions in three dimensions. In addition, the simultaneous four-point measurements provided by the satellites will permit scientists to derive differential plasma quantities for the first time. For example, the density of current flowing around the spacecraft will be derived from the magnetic-field measurements taken at four points in space.

The Cluster instrumentation has state-of-the-art capability to measure electric and magnetic fields together with electron and ion distribution functions. The four Cluster spacecraft are identical and each carries 11 instruments (Table 1), giving a total of 44 instruments, a record for a space mission. The instruments are located on the upper external ring of the spacecraft or on radial booms to allow a free field of view for each of them (Fig. 3).

To make accurate intercomparisons between the same instruments on the four spacecraft, it is necessary to make the best absolute measurements. The goal of the PEACE

Table 1. The Cluster-II instruments and their Principal Investigators

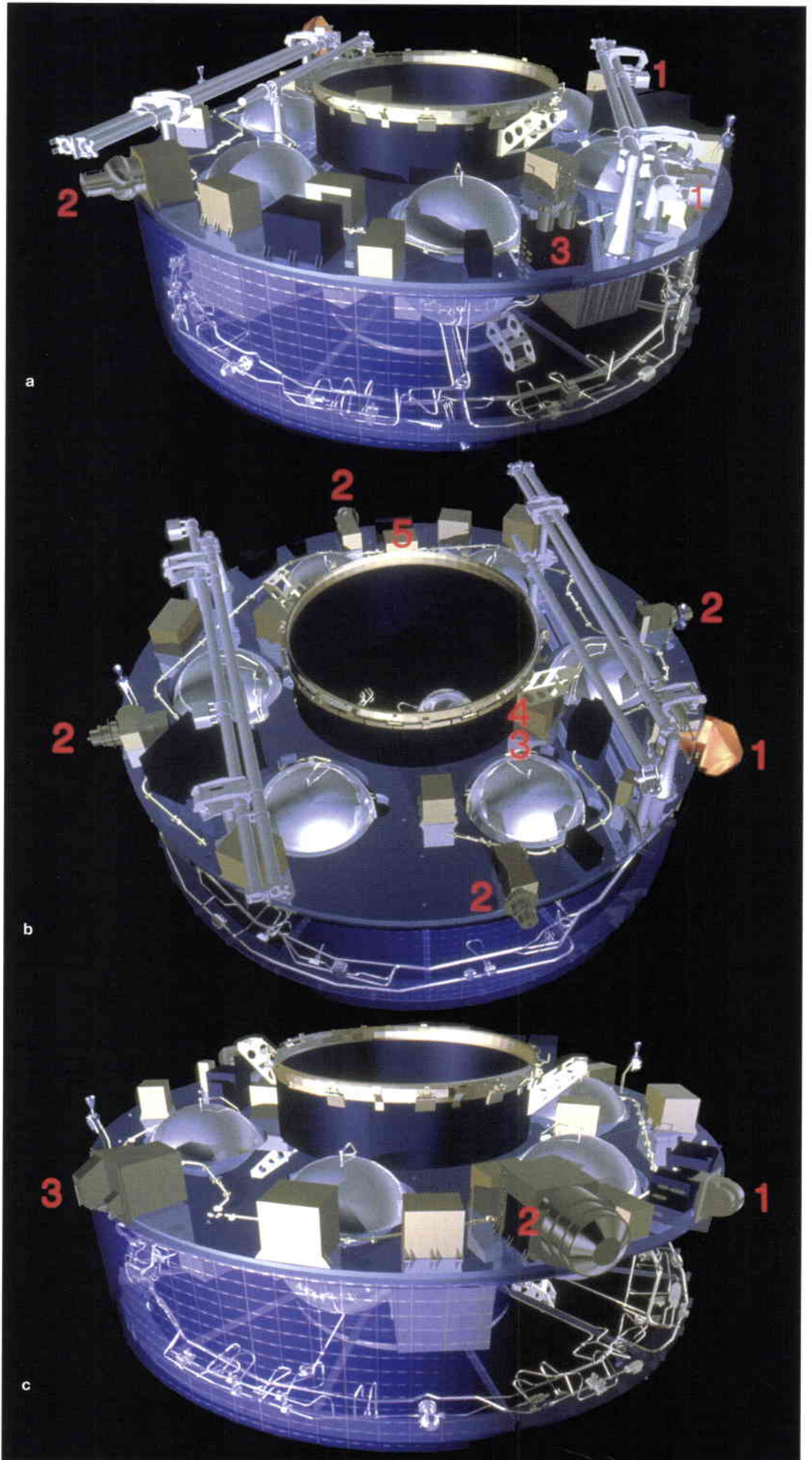
| Instrument | Principal Investigator |
|--|--------------------------------|
| ASPOC (Spacecraft potential control) | W. Riedler (IRF, A) |
| CIS (Ion composition) | H. Rème (CESR, F) |
| EDI (Plasma drift velocity) | G. Paschmann (MPE, D) |
| FGM (Magnetometer) | A. Balogh (IC, UK) |
| PEACE (Electrons) | A. Fazakerley (MSSL, UK) |
| RAPID (High-energy electrons and ions) | B. Wilken (MPAe, D) |
| DWP * (Wave processor) | H. Alleyne (Sheffield, UK) |
| EFW * (Electric field and waves) | G. Gustafsson (IRFU, S) |
| STAFF * (Magnetic and electric fluctuations) | N. Cornilleau-Wehrin (CETP, F) |
| WBD * (Electric field and wave forms) | D. Gurnett (IOWA, USA) |
| WHISPER * (Electron density and waves) | P. Décréau (LPCE, F) |

* Wave Experiment Consortium (WEC)

electron sensor, for example, is to achieve a 1% accuracy for the measurements of the density, temperature and velocity of electrons. Being able to achieve these goals has required perfect manufacturing of the instrument and its very precise calibration on the ground, to be supplemented later by a calibration in space. The results of the calibrations on the ground are shown on Figure 4. It is clear that all four models are all very similar and the small residual differences will be taken into account when comparing the measurements made in space.

In the case of the Flux Gate Magnetometer (FGM), an overall single instrument accuracy of 0.1% is required. In addition to ground calibration, a special magnetic-cleanliness programme was conducted to achieve a spacecraft magnetic background of less than 0.25 nT at the magnetometer position (5 m from the spacecraft).

Figure 3. The instruments on the Cluster spacecraft



a: 1 FGM, 2 EDI and
3 ASPOC

b: 1 STAFF, 2 EFW, 3 DWP,
4 WHISPER and 5 WBD

c: 1 PEACE, 2 CIS and
3 RAPID

The measurement of electromagnetic waves requires a very high timing accuracy for each spacecraft. The guaranteed accuracy is ± 2 ms, although we can expect even better precision during the mission. Since this accuracy would not be sufficient to compare waves measured on the four spacecraft, the Wave Experiment Consortium (group of 5 instruments) has developed special algorithms which, together with the use of transputers with parallel processing, achieve an accuracy of a few microseconds.

The ideal spacecraft configuration for measuring plasma structures in three dimensions is a tetrahedron (triangular pyramid) with a spacecraft at each corner. Unlike the Egyptian pyramids, where the base is a square, the base of the Cluster tetrahedron will be triangular and the distances between the spacecraft identical. Unfortunately, this shape cannot be maintained all along the orbit due to orbital mechanics effects, and we have to target it to specific regions of interest. It has been shown, however, that if we form the tetrahedron at two places along the orbit, for instance at the northern and southern cusp, then the configuration stays very close to a tetrahedron over a major part of the orbit (Fig. 5).

Key advances in plasma physics will be achieved using the four Cluster spacecraft. A first example is the measurement of the electric

Figure 5. Cluster orbit and spacecraft configuration with respect to magnetospheric models at the beginning of the mission when the polar cusp is crossed (a), and 6 months later when the magnetotail is crossed (b). For clarity, the interspacecraft distances have been enlarged by a factor 30 in panel (a), and by a factor 2 in panel (b)

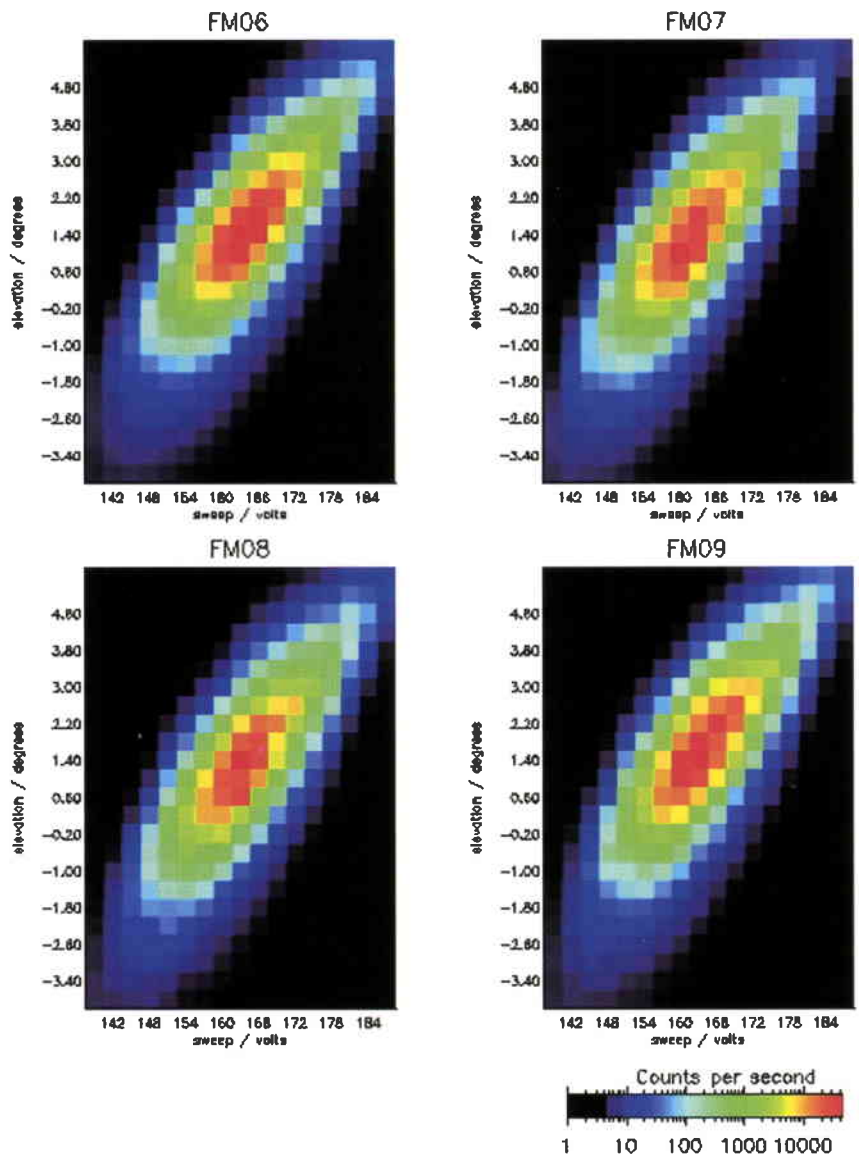
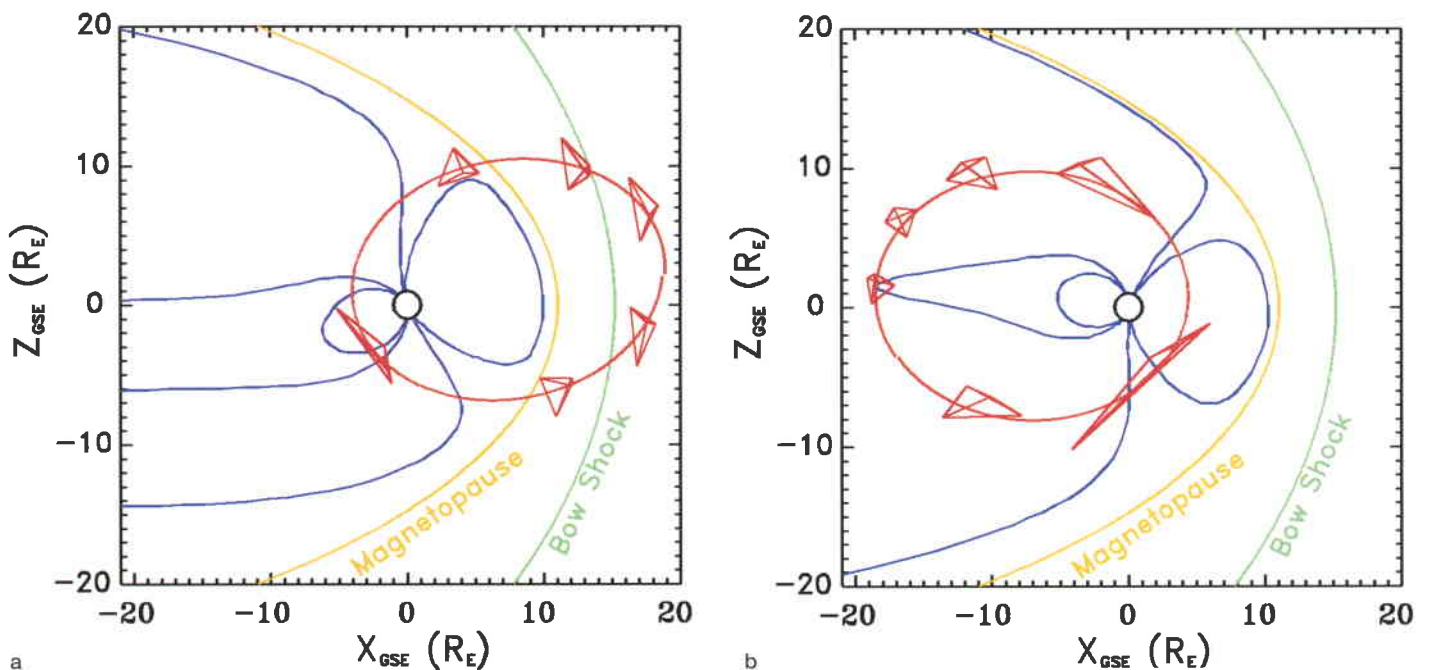
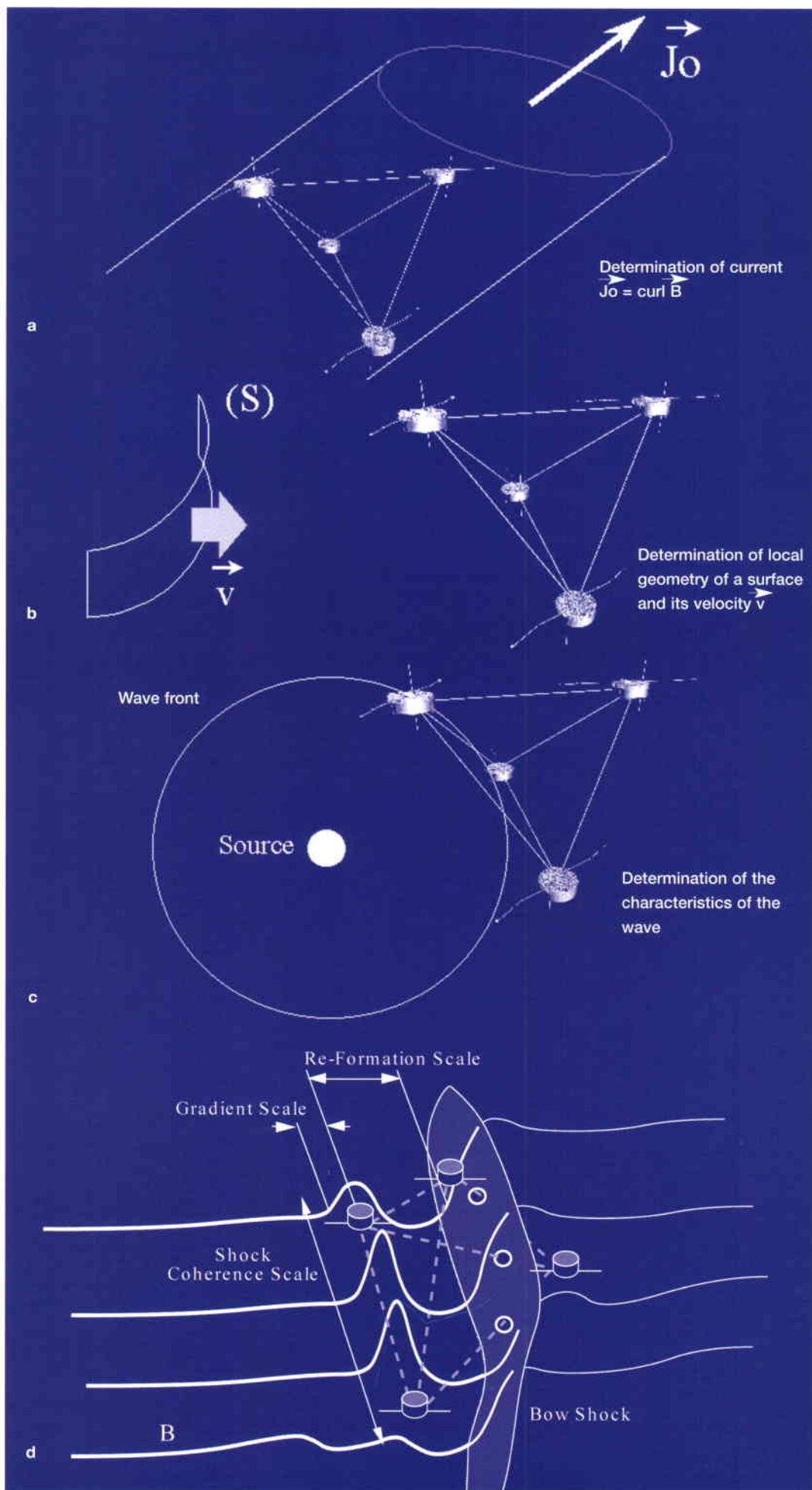


Figure 4. Flux of electrons detected by the four PEACE instruments when bombarded by an electron source (Courtesy of PEACE Calibration Team, MSSL/UCL)

Figure 6. Examples of Cluster-specific capabilities (Panel (d) courtesy of E. Moebius, Univ. of New Hampshire)



current J flowing through the Cluster fleet and given by Ampere's law, $\text{curl } B = \mu_0 J$ (Fig. 6a). The measurement of the difference of B between the four spacecraft will give curl B and then J .

The currents are key parameters in magnetospheric physics because they are present in all regions and contribute to the magnetosphere's shape. For instance, the magnetopause is a narrow current layer that separates the solar wind from the magnetosphere (Fig. 2). Other quantities can also be derived using this formalism, such as the plasma vorticity, which is given by the curl of the plasma velocity.

Another example is the analysis of discontinuities (Fig. 6b). When the Cluster-II spacecraft cross a boundary like the magnetopause, each of them will determine the normal to that boundary. By combining these measurements, we will obtain information on the boundary curvature, e.g. either convex or concave, and its radius of curvature. In the case of the magnetopause, this information will enhance our knowledge of the interaction between the solar wind and the magnetosphere. Theoretical studies have predicted that when clouds of dense solar-wind particles arrive at the magnetosphere, they can produce an 'indentation' in the magnetopause and eventually penetrate it. The four Cluster spacecraft should tell us if this process exists.

The particle-acceleration processes involved in producing aurorae generate intense electromagnetic emissions. These processes are not yet fully understood and the four Cluster spacecraft will bring us additional information. Using four measurements in space, each giving the direction of the source, we will be able to derive its location, size and speed (Fig. 6c).

A final example of the benefits of four-point measurement analysis is the bow-shock reformation. The bow shock is the boundary where the supersonic plasma from the solar wind is decelerated to a subsonic speed when it encounters the obstacle of the magnetosphere. Depending on the speed of the solar wind, the bow shock moves or reforms itself at another place. Cluster's four spacecraft will enable one spacecraft to be at a former location, another one at the new location and the other two in between (Fig. 6d), so providing new information on the bow-shock reformation process.

Data dissemination

Two centres are in charge of the Cluster-II operations: the Joint Science Operations Centre (JSOC) and the European Space

Operations Centre (ESOC) (see accompanying article by M. Warhaut et al. in this issue).

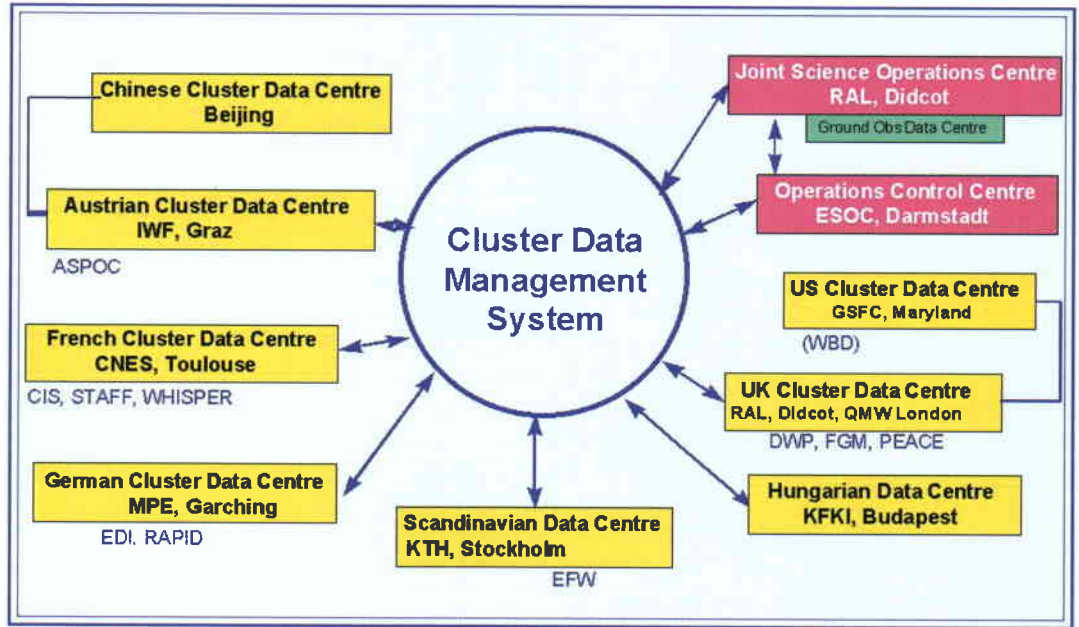
JSOC, located at the Rutherford Appleton Laboratory in the United Kingdom, is coordinating the science operations. Its main task is to merge the input from the individual Principal Investigator (PI) teams into a command schedule. In addition, JSOC will monitor the health of the instruments and disseminate information on the mission. Included in this information is a scientific event catalogue, which will identify the main magnetospheric boundaries (bow shock, magnetopause, neutral sheet, flux transfer events and auroral zone). These data, together with other parameters coming from all instruments, will be accessible to the scientific community through the Cluster Science Data System (CSDS).

This data system has been designed as a distributed system, to enable the joint scientific analysis of data coming from all 44 instruments. The general approach is to have national data centres located near the Principal Investigators (PIs), and thus near the expertise required for processing the data. One of the major tasks of the CSDS is to offer, as a matter of routine, products such as the Summary Parameter Data Base (data products coming from one spacecraft with 60 sec resolution) and the Prime Parameter Data Base (data products coming from the four spacecraft with 4 sec resolution).

Table 2: Cluster-II Principal Investigators (PI) and Co-Investigators (CoI) and the Data Centre locations

| Country | PIs or CoIs Centre | Data |
|-----------------|--------------------|------|
| Austria | 6 | yes |
| Belgium | 2 | |
| China | 4 | yes |
| Czech Republic | 1 | |
| Denmark | 3 | |
| Finland | 4 | |
| France | 39 | yes |
| Germany | 23 | yes |
| Greece | 2 | |
| Hungary | 2 | yes |
| India | 2 | |
| Ireland | 1 | |
| Israel | 1 | |
| Italy | 6 | |
| Japan | 3 | |
| Norway | 11 | |
| Russia | 4 | |
| Sweden | 13 | yes |
| Switzerland | 1 | |
| The Netherlands | 5 | yes |
| United Kingdom | 20 | yes |
| USA | 68 | yes |
| Total: | 221 | |

Figure 7. The Cluster Science Data System (CSDS) architecture



The CSDS consists of eight nationally funded and operated data centres (Fig. 7). In most cases, the data centres produce data products on behalf of the national PI teams. Members of the Cluster-II science community (Table 2) wishing to access the CSDS will do this via their national data centre or via an assigned data centre. It should be noted that all data centres offer the same data products. Scientists from outside the Cluster-II community will also have access to the CSDS, according to the policy on data rights agreed by the Principal Investigators. Full access can be granted to the Summary Parameters.

CDMS is to provide the scientific community with uniform access to CSDS. For the individual data centres, the CDMS offers local file handling, distribution of validated data files to other data centres, data ordering, user administration, catalogue browsing and data-manipulation functions. The CDMS allows a user to browse the CSDS catalogues, fetch prime and/or summary data, manipulate and display prime and summary parameters, and retrieve summary plot files. The CDMS can be accessed with any Web browser.

Figure 8. Web interface of the Cluster Data Management System (CDMS). A user will have access to the Cluster-II data in Common Data Format, ASCII and Summary Plots

The scientists will interact with CSDS via the Cluster Data Management System (CDMS), as shown on Figure 8. The main purpose of the

The CSDS has been designed to allow fast and easy access to all physical parameters measured by the four spacecraft. In addition, the CSDS is fully compatible with data from other magnetospheric and solar missions and will be the perfect tool with which to conduct collaborative studies in the framework of campaigns defined by the Inter-Agency Consultative Group (IACG).

The screenshot shows the web interface of the Cluster II Science Data System. The main heading is 'Data Management System'. Below it is a 'Data Selection' section. A table lists various data sources and their associated parameters and file formats. The table has four columns: Source, Data Type, Descriptor, and Type. Below the table are buttons for 'Group Selection: Primary', 'Apply Group', and 'Submit Query'. At the bottom, there are buttons for 'Check', 'reset selection', 'Reset', 'reset everything', and 'Reset All'.

| Source | Data Type | Descriptor | Type |
|-----------|--------------------|---|------|
| Cluster | Prime Parameters | ASPOC – Active Spacecraft Potential Control | cdf |
| Cluster 1 | Summary Parameters | CIS – Cluster Ion Spectrometry Experiment | gif |
| Cluster 2 | Summary Plots | DWP – Digital Wave Processing Experiment | ps |
| Cluster 3 | JSOC catalogues | EDI – Electron Drift Instrument | bt |
| Cluster 4 | | EFW – Electric Fields and Waves | zip |
| Centroid | | FGM – Flux Gate Magnetometer | |
| | | PEACE – Plasma Electron and Current Experiment | |
| | | RAPID – Imaging Particle Spectrometer | |
| | | STAFF – Spatial/Temporal of Field Fluctuations | |
| | | WHISPER – Sounder and HF Wave Analyser Experiment | |

Conclusion

Monitoring the effect of the Sun on our near-Earth environment is a key task for the upcoming years of solar maximum, and Cluster-II will be the ideal mission with which to undertake this activity. Now, with the Cluster-II launches scheduled to take place in just a few weeks' time and the agreed extension of the SOHO mission, the scientific community is looking forward to the exciting results emanating from these missions as they jointly study the dramatic interaction between the Sun and the Earth's environment.

Cluster-II: Evolution of the Operations Concept

M. Warhaut, S. Matussi & P. Ferri

Mission Operations Department, ESA Directorate of Technical and Operational Support, ESOC, Darmstadt, Germany

Introduction

The preparation of this recovery action for a major space science mission, to be launched four years after the original one, represents a significant engineering and managerial challenge. The need to cap the new mission at less than 50% of its original cost has imposed a rigid discipline in terms of keeping the spacecraft-component and ground-segment facility configurations as close as possible to those used for the original mission. On the other hand, some changes have had to be accepted as inevitable, due for example to a lack of spare parts for the spacecraft, or to keep pace with the continuous evolution in the ESOC ground segment.

The operations concept for the Cluster-II mission has had to evolve with respect to the original Cluster baseline, due mainly to changes in the spacecraft design and the reduction in the number of ground stations from two to only one for routine mission-operations support. The solutions adopted have allowed the overall impact on the ground segment and mission operations to be minimised, whilst still maintaining the scientific data return at the original level.

Cluster-II also suffers from the fact that it will be launched during what was already an extremely busy period for ESOC, with the launch and control of ESA's XMM mission, and the provision of launch support for other external missions (e.g. Meteosat Second Generation). This results in the need to share the existing facilities, in particular the ground stations. Cluster-II has therefore had to accept to use a single dedicated ground station for the mission's routine science operations phase, instead of the two originally foreseen, which has had a significant impact on the operations concept. An additional consequence of the 'year 2000 peak' is the difficulty in re-utilising staff with Cluster experience, most of whom are already supporting other missions.

Space-segment evolution

In re-building the new Cluster spacecraft, there were from the outset various dilemmas

associated with possible or enforced changes in several hardware components. The problem was complicated by the fact that one of the four spacecraft was already completely integrated based on spare parts from the original Cluster programme. This spacecraft, called 'Phoenix' or Cluster-FM5, is identical to the original spacecraft, but slightly different from the next three to be built. The not completely identical spacecraft hardware has meant reduced flexibility during the integration and test phases. In the original Cluster programme, spacecraft units were often exchanged from one spacecraft to another depending on hardware availability and the need to continue specific test activities. This flexibility was one of the keys to the success of the original Cluster integration programme, which ensured the continuation of the complex activities without accumulating significant delays. In addition, it had always been a fundamental assumption underlying the design of the ground segment and the operations concept that all four spacecraft would be indeed identical. The non-availability of original parts already utilised on the Phoenix spacecraft has meant that exceptions have had to be accepted.

The main changes in spacecraft hardware due to unavailability of now obsolete parts are in the telecommunications (TTC) and on-board data-handling (OBDH) subsystem areas. The original TTC high-power amplifier was no longer available and had to be replaced on the three new spacecraft, together with the transponder, by new hardware derived from that developed for ESA's XMM and Integral scientific satellites. A major OBDH change is replacement of the two original solid-state recorders (SSRs) with a single recorder of a new design with a higher recording capacity. No changes in the operating philosophy of the TTC subsystem are required, but the operational database and the related flight-control procedures have been affected. On the other hand, the new SSR allows the way data recording and dumping is managed by the ground to be significantly improved.

As far as the payload is concerned, there will be an identical complement of instruments flying on the four spacecraft, and so at least the instrument hardware will be identical to the original set. The on-board software for several instruments has changed, however, and possible impacts on the ground segment have been carefully analysed, and also checked in the test and verification phase.

It was decided, for cost and schedule reasons, not to change the on-board software of the OBDH central on-board processor, although several patches to improve the final software version were already prepared prior to the original Cluster launch. For Cluster-II, these patches will be loaded on top of the software already burned into the spacecraft PROMs before the launch. For the ground segment, this means safer operations immediately after launch.

The changes in integration approach from the original Cluster programme, introduced to speed up the production work and taking into account the already accumulated experience, had an impact on the testing approach for the ground segment. The traditional final system test for ESOC, the System Validation Test (SVT), in which the ground segment exercises and verifies all command and telemetry functions with the spacecraft flight model, was originally carried out with two spacecraft in parallel. This was done to validate one of the basic features of the Cluster operations, namely the parallelism of control activities on more than one spacecraft. This approach also had the benefit of increasing the test time available to ESOC with the flight hardware. In the original programme, each spacecraft was tested from ESOC for more than 15 working days in total.

For the Cluster-II programme, four separate SVT slots were allocated, each with a single, different flight model and for a maximum duration of four days.

This limited test time imposed the need for a careful trade-off in the selection of subsystems and functions to be addressed, in order to concentrate mainly on those areas in which changes with respect to the original spacecraft were to be expected. This approach relied on the correctness and completeness of the documentation describing the changes, and therefore bore inherent risks. These risks had, however, to be accepted due to the tight project schedule, and were kept within reasonable limits since the overall number of changes introduced into the spacecraft has been small and strictly controlled (Table 1).

Ground-segment evolution

Unlike the problems encountered in re-building the space segment linked mainly to unavailability of parts, the ground segment has had to deal with a continuously evolving infrastructure. This evolution could not be halted for four years to wait for the re-launch of the Cluster mission and then support it with the same systems. Apart from the modernisation of the infrastructure, which is a continuous process and normally only marginally constrained by the needs of the projects using it, one of the problems faced today is rapid obsolescence of computer hardware and software. Workstations, operating systems and, in general, commercial off-the-shelf (COTS) products have an average lifetime of just 18 months, after which the maintenance costs – if maintenance is even supported by the supplier – become far larger than the cost of replacing the item with the latest model or version. This carries with it,

Table 1. Summary of changes to the space segment

| Change | Reason | Impact |
|---|---|---|
| New Transponder/High Power Amplifier for three spacecraft | Old High Power Amplifier not procurable | Different procedures and databases in the TTC area between Phoenix and the rest of the fleet. Upgrade of ESOC software simulator needed |
| New Solid-State Recorder (SSR) | Old Solid-State Recorder (SSR) not procurable. New SSR has higher capacity and greater flexibility of use | Positive impact on operations, since the new SSR allows partial dumps. Upgrade of ESOC software simulator needed |
| Patches to on-board software burned into PROM expensive | Changes in software were necessary, but re-build of full software considered too | Safer LEOP ops compared to original flight (patches to be loaded at launch site). However, no "clean" starting point for software maintenance |
| New payload software | Evolution of scientific knowledge and targets | Database/procedures changes necessary. Heavy SVT re-testing. Minor upgrade of ESOC software simulator |
| Sequential spacecraft integration and testing | Acceleration of production schedule | Parallel SVT on two spacecraft not possible. Limited testing time for new features |

however, the problem of adapting, i.e. 'porting', the application software to the new tools or platforms, with an inherent, non-negligible cost and schedule impact, and with the related risk of not meeting the original specifications.

The Cluster ground segment suffered this problem in all critical areas: ground stations, control system and simulators. A main component of the on-going upgrading process is the porting of the software to new operating systems: from Sun OS to Solaris 2.6 for the ground-station equipment based on Sun workstations, and to higher VAX VMS versions or Alpha stations for the control system and the simulator. The infrastructure changes dictated by software and hardware obsolescence created significant problems in the area of ground-station interfaces in particular. Compromise solutions, mixing the old and the new interfaces, have been adopted to minimise changes to the old baseline. Figure 1 shows the new baseline for all interfaces between the ground stations and the mission-control system managed by a central computer, the Network Control and Telemetry Routing System (NCTRS), located at the Control Centre.

Ground stations are one of the main infrastructure items of the ground segments for the missions supported by ESOC. They are shared by all missions, particularly for the launch and early orbit phases. For these important shared items, it is essential that identical, or at least compatible, interfaces to the mission control systems are used. On the other hand, the Cluster requirements on telemetry and telecommand interfaces to the ground stations are different from those of the other missions that will be supported in the

same time frame, which all utilise packet telemetry and telecommand standards. In the telemetry area, the solution adopted was to port the Cluster telemetry processor software to the new Solaris 2.6 operating system.

The new operating system will allow both the old telemetry processor software (TMP3) and the new software (TMP4) to be run on the same platform, with the required performance. In addition, the change to a new hardware platform (UltraSparc workstations), which very soon became mandatory (maintenance costs for the old Sparc20 platforms were becoming prohibitive) did not imply any additional software adaptation exercise. This solution allowed the installation of identical hardware on all ESA workstations. In order to support different missions, a simple restart of the telemetry processor using different software (TMP3 or TMP4) is required. The telecommand interface to the Control Centre has also changed, but fortunately the solution adopted will allow the utilisation of the new telecommand encoder software and hardware also for the Cluster-II mission, via normal configuration changes.

Another change imposed on the ground stations, this time due to hardware obsolescence, was the development of a new Station Computer (STC), the central local control system for all ground-station units. Its repercussions for Cluster-II lie mainly in the area of the interface to the Mission Planning System (MPS), which produces schedules to be transferred to the station computer for automatic station control. The scheme adopted in the MPS software for the generation of the STC schedules is incompatible with the way schedules are handled in the new station

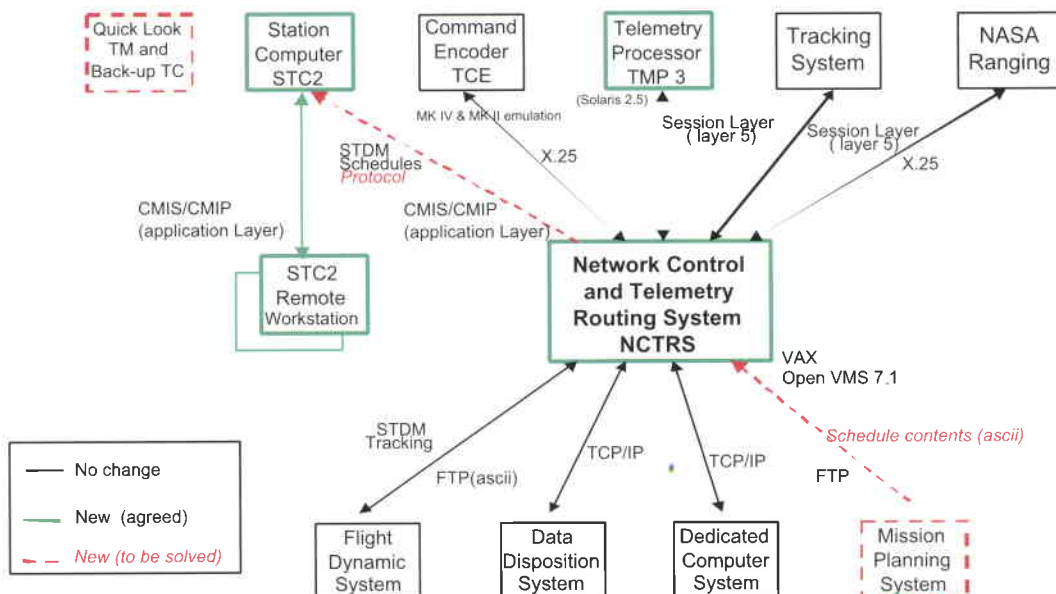


Figure 1. Network Control and Telemetry Routing System (NCTRS) interfaces

computer. The adaptation of this interface involved work on both the STC and the MPS software. The changes in the interfaces between the Control Centre and the ground stations with respect to the original mission are shown in Figure 1.

The fact that one of the two original dedicated ground stations is no longer available triggered a major change in the Cluster-II baseline, which now has only one ground station – at Villafranca, near Madrid (E) – to support the routine science mission phases. A single antenna will therefore be used to control the four Cluster spacecraft sequentially. This change prompted a number of studies and trade-off activities, resulting in an operations concept that provides a significant reduction in operating costs, in terms of both manpower and facilities.

The main antenna to be used at Villafranca, known as VIL-1, is a 15 m dish that operates in S-band at 1.8 – 2.7 GHz (Fig. 2). Formerly used for the IUE and ISO missions, its hardware and electronic equipment have recently been refurbished and upgraded to comply with Cluster-II requirements. Modernisation of VIL-1 involved transporting more than 23 t of equipment from the Odenwald site in Germany, which was a two-week-long road journey. Since its arrival at Villafranca in November 1998, much of the hardware has been replaced, including the 60 dish panels, the subreflector, the antenna equipment room and other parts of the main structure. One of the

Figure 2. The Cluster-II antenna at ESA's Villafranca station, near Madrid (E)



most significant modifications has been the replacement of the servo and tracking systems, necessary because the Cluster-II satellites will move in a highly elliptical orbit and require high-speed tracking. About 0.8 Gbyte of data will be returned each day from the 44 experiments (11 scientific instruments on each of the four spacecraft). Over two years of operations, this adds up to 580 Gbyte (580 000 000 000 byte) of data – equivalent to 290 million pages of printed text. All of the Cluster-II data exchange between Villafranca and ESOC will be via dedicated communications lines.

Another 'victim' of hardware and software obsolescence is the Cluster software simulator. This software tool is based on two computers, a DEC Alpha workstation to simulate the four spacecraft, and a DEC VAX workstation to run the ground-segment models. This separation was needed because of the high computer processing load when simulating four independent spacecraft. The operating system of the VAX used to simulate the ground stations and communication network is no longer maintained by the manufacturer and needed to be upgraded. For this and other reasons, it was decided to port the Cluster ground models also to the new Alpha workstations, upgrading to the latest VMS operating system, rather than maintain the obsolete software. Furthermore, the Cluster simulator had to be updated to follow the spacecraft design modifications and ensure that it is functionally representative of the behaviour of the new Cluster-II spacecraft. The impact of the spacecraft changes on the software simulator was confined to the transponder and SSR. Changes in the payload had only a small overall effect on the simulator.

The Control Centre facilities at ESOC (Fig. 3) have also been affected in that the original Cluster Dedicated Control Room (DCR) now has to be shared with the XMM project, which is already using it. The original room was designed for a double controller position, each in charge of two spacecraft and with parallel operations via the two Cluster dedicated ground stations. The room included eight identical spacecraft control workstations and two station control workstations. Thanks to the use of a single ground-station antenna for Cluster-II, it will be possible to use a single station computer workstation in the DCR. Also, fewer spacecraft control workstations will be available. This constraint will be acceptable because only one spacecraft will be in



Figure 3. The Main Control Room at ESOC

visibility of the ground segment at any given moment, allowing a single spacecraft controller to carry out all the necessary real-time operations. In this case, no more than four workstations will be needed for spacecraft-control activities.

The ground-segment changes are summarised in Table 2.

Mission operations concept evolution

The tight budgetary constraints on the mission have imposed many changes on the Cluster-II operations scenarios, including the launches by Russian Soyuz-type vehicles from Baikonur (Kazakhstan). The launch scenario foresees two Soyuz launchers, enhanced with a dedicated fourth upper stage, each carrying a

stack of two Cluster spacecraft. There is a four-week interval between the two launches.

Because of the difference in latitude between Baikonur (52 deg) and Kourou (5 deg), the timelines for the Launch and Early Orbit Phase (LEOP) and the Transfer Orbit Phase (TOP) to the final operational orbit look very different from those for the original Cluster mission. For the Cluster-II initial operations phase, the ESA ground stations of Kourou (Fr. Guiana), Perth (W. Aus.), Kiruna (Sweden) and Villafranca (Spain), plus the DSN Canberra (Aus.) station will be available. The LEOP/TOP operations timeline will be defined such that critical activities (such as orbit manoeuvres) on the two spacecraft are not executed in parallel. This reduces the size of the mission operations

Table 2. Summary of ground-segment changes

| Change | Reason | Impact |
|--|---|--|
| MCS VAX software ported to Alpha | Lack of maintenance support for old versions | None expected |
| TMP software ported to Solaris 2.6 operating system | Compatibility of TMP hardware platform with other missions | None expected |
| New station computer (STC 2) | STC-1 hardware obsolescence | Changes in mission-planning software to adapt to new STC schedule handling |
| Software simulator porting from VAX VMS to Alpha | Lack of maintenance support for old versions | None expected |
| Single ground-station support for routine science ops. phase | Heavy ESOC workload imposes sharing of ground station with other missions; cost reduction | Operations concept modified; upgrade of mission planning software required; ops. manpower reduction. |
| Reduction of floor space in Dedicated Control Room | Heavy ESOC workload imposes sharing of OCC facilities with other missions | Only possible thanks to revised ops. concept (sequential and not parallel spacecraft control) |

team needed and allows a better distribution of the available expertise across the two shifts. Once the first pair of spacecraft have been put into their final operational orbit, the second pair will be launched and a second LEOP/TOP phase will begin. The operations related to the second launch will be complicated by the presence of the first pair of spacecraft, which will need to be monitored and controlled from time to time by the same operations team.

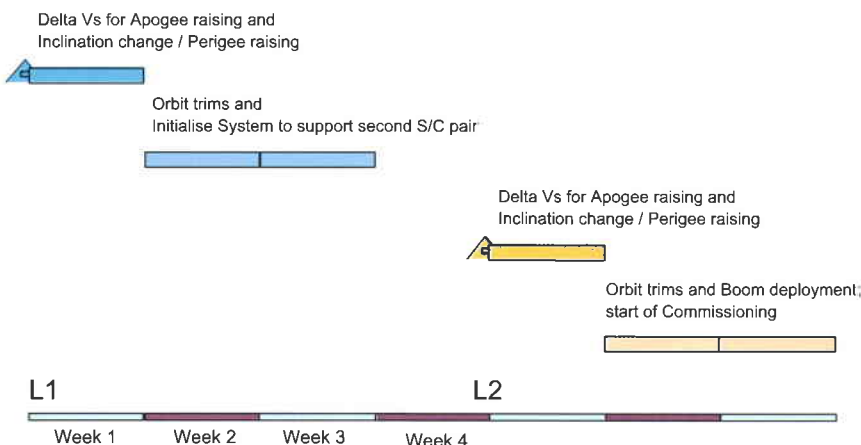
Figure 4 is a schematic of the LEOP/TOP operations timeline, and how these critical phases for the two launches are connected. L1 is the time of launch of the first spacecraft pair, L2 the second launch, nominally four weeks later.

The deployment of spacecraft appendages (instrument and lower-antenna booms) and the start of payload-commissioning activities for all four spacecraft only takes place once the full constellation has been achieved, i.e. all spacecraft are in the initial operational orbit. The reduced ground-station availability has imposed a major change in the Commissioning and Verification Phase (CVP) operations. Originally these operations were to be executed in parallel for two spacecraft, using the two dedicated ESA ground stations. For Cluster-II, the single mission-dedicated station in Villafranca (E) will be used, augmented by the DSN Canberra station. As the ground coverage of the two stations is almost complementary, CVP operations for the four spacecraft will be executed sequentially, but covering almost 24 hours of real-time activities per day. The new mission plan for this phase is still being finalised, but it is expected that all activities can be covered in a time comparable to that assumed for the original mission (12 to 14 weeks). The current baseline is to start CVP operations on the first pair of spacecraft only after the second pair have completed their LEOP/TOP activities.

As already mentioned, during the Mission Operations Phase (MOP) in which the scientific observations will be performed, only one ground station (Villafranca) will be used for science data recovery, and the baseline is to use a single antenna to serve all four spacecraft. This is a major change in the operations scenario compared with the original mission, which used two ground stations, each one permanently dedicated to two spacecraft. It implies that, on average, each spacecraft is visible from the ground station for only half of the time that was previously available. Studies have been performed to analyse how much science data can be recovered with this new configuration, and what on-board storage is required for the new Solid State Recorder (SSR) in order to compensate for the reduced spacecraft visibility. The results show that it will still be possible to recover the same quantity of science data that was specified in the original Cluster Master Science Plan (MSP). However, some changes must be implemented in the ground segment to cope with the reduced visibility periods, such as the doubling of the data-link capacity between the station and the Control Centre, and the possibility to execute partial dumps of the SSR stored telemetry data. With the latter possibility, it is feasible to exploit every single visibility slot, thereby maximising the science data return. Partial dumps can only be performed in forward mode, i.e. older data first, to avoid the need for reconstituting the temporal sequence of science and house-keeping data. This is also a change from the original Cluster approach, which was to dump all data from the SSR in reverse order, involving a modification of the ground software that processes the dumped data.

An advantage of using a single ground station controlling the four spacecraft in sequence is that routine mission operations can be executed by a single spacecraft controller position, compared to the two of the original mission, significantly reducing costs. Defining the size and timing the recruitment of the mission control team for a recovery mission is always difficult. The danger is to underestimate the unavoidable changes required in the operational documentation, such as the flight control procedures, and the modifications to the control system, and therefore implement a late build-up of a, perhaps undersized, flight control team. The case of the Cluster-II mission is complicated by the fact that only 3 of the original 23 members of the Cluster control team will participate in the new mission. The problem of maintaining the expertise and skills that were available in the original team is partly mitigated by the fact that many of the initial team members are still available at ESOC, having

Figure 4. The LEOP/TOP timeline



moved to other projects. Part-time involvement of some experts from the original Cluster mission is therefore already a reality, and will continue until the critical phases of the mission are over.

Conclusion

The preparation of a ground segment and mission-operations concept for the Cluster-II recovery mission, heavily affected by severe cost and schedule constraints, was driven by the basic premise of trying to avoid any change to the original baseline. At the same time, the unavoidable 'environmental' changes, such as the replacement of obsolete parts in the spacecraft or the adaptation to the new ground-segment infrastructure items, have had to be taken into account.

In some cases, changes were imposed purely by the need for cost savings, including the change to a single ground station for controlling the routine phases of the mission. Thanks to the upgrades to spacecraft data-storage capacity

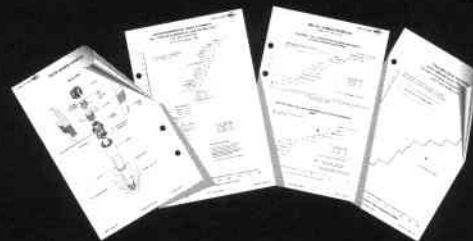
and functionality and to an improved mission control concept, significant cost reductions in terms of manpower requirements and facilities utilisation have been achieved without impacting the overall science data return.

Acknowledgements

The work described in this article was carried out on all sides – science, industry, project and operations – by small teams of 'veterans' of the original Cluster mission, using their reservoir of skills and knowledge accumulated over several years of being dedicated to this project. The realisation of a recovery mission within the limited resources assigned to the Cluster-II project is only possible thanks to the work of many more people – the hundreds of scientists, technicians and engineers who originally developed, integrated and tested the Cluster spacecraft, payload and ground segment, and who left the project for many different reasons after the failed launch. To these people in particular the authors are sincerely grateful. 

AIRCLAIMS 

You shouldn't be in the Space Business without us



Space Review is the industry reference manual for space launch systems. Supplied in a loose leaf hard-copy format and updated monthly, it provides:

- Reliability trends and failure rates of launchers
- Past and future launches
- Successes/failures in the launching and positioning of satellites
- In-orbit failures and insurance losses

Airclaims Ltd. Cardinal Point,
Newall Road, Heathrow Airport,
London, England TW6 2AS.
United Kingdom

www.airclaims.co.uk
Tel: +44 (0) 20 8 897 1066
Fax: +44 (0) 20 8897 0300

ARIANE 5 (502)

SpaceTrak[®] is a user friendly commercial space database. Updated monthly, it gives the World's Space Industry the answers it needs at the touch of a button.

Features include:

- Satellite histories from pre-launch to re-entry and retirement
- Satellite and launcher technical data
- Unbiased reliability data for all current launchers
- Queries on in-orbit failures and insurance losses
- Future schedule of all known launches



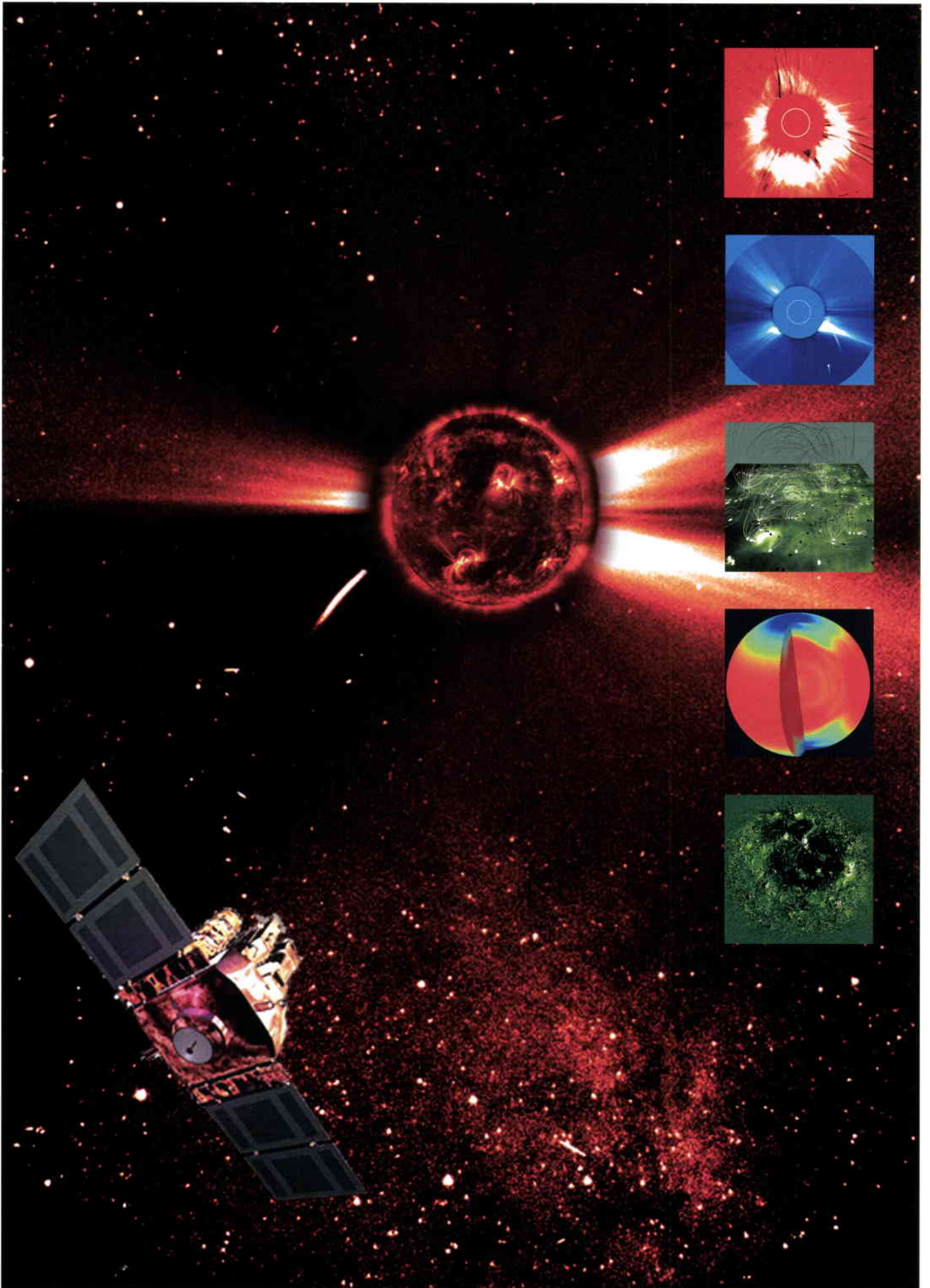
FREE DEMO CD



For a FREE DEMO CD and details contact:
Isabel Pessoa-Lopes (Space Analyst)
E-mail: ipl@airclaims.co.uk

For a FREE DEMO CD and details contact:
David Todd (Space Analyst)
E-mail: dt@airclaims.co.uk

www.airclaims.co.uk
Please quote ADVEB1



Four Years of SOHO Discoveries – Some Highlights

B. Fleck, P. Brekke, S. Haugan & L. Sanchez Duarte

Solar System Division, ESA Space Science Department, NASA/GSFC,
Greenbelt, Maryland, USA

V. Domingo

Department of Astronomy and Meteorology, University of Barcelona, Spain

J.B. Gurman & A.I. Poland

Laboratory for Astronomy and Solar Physics, NASA/GSFC,
Greenbelt, Maryland, USA

The SOHO mission

SOHO, the Solar and Heliospheric Observatory, is an international cooperative project by ESA and NASA to study the Sun, from its deep core to the outer corona, and the solar wind. It carries a complement of twelve sophisticated instruments (Table 1) developed and furnished by twelve international Principal Investigator (PI) consortia involving 39 institutes from fifteen countries (Belgium, Denmark, Finland, France,

work stations in the SOHO Experimenters' Operations Facility (EOF) at NASA/Goddard Space Flight Center, from where they can command their instruments in near real time. From the outset SOHO was conceived as an integrated package of complementary instruments, being once described as an 'object-oriented, rather than an instrument-oriented mission'. There is therefore great emphasis on coordinated observations. Internally, this is facilitated through a nested scheme of planning meetings (monthly, weekly, daily), and externally through close coordination and data exchange for special campaigns and collaborations with other space missions and ground-based observatories over the Internet.

Since its launch on 2 December 1995, the Solar and Heliospheric Observatory (SOHO) has provided an unparalleled breadth and depth of information about the Sun, from its interior, through the hot and dynamic atmosphere, out to the solar wind. Analysis of the helioseismology data from SOHO has shed new light on a number of structural and dynamic phenomena in the solar interior, such as the absence of differential rotation in the radiative zone, subsurface zonal and meridional flows, sub-convection-zone mixing, a possible circumpolar jet, and very slow polar rotation. The ultraviolet imagers and spectrometers have revealed an extremely dynamic solar atmosphere in which plasma flows play an important role. Evidence for an upward transfer of magnetic energy from the Sun's surface toward the corona has been found. Electrons in coronal holes have been found to be relatively 'cool', whereas heavy ions are extremely hot and have highly anisotropic velocity distributions. The source region for the high-speed solar wind has been identified and the acceleration profiles of both the slow and fast solar wind have been measured.

More than 500 articles have already appeared in the refereed literature and over 1500 articles in conference proceedings and in other publications. Here, we can only touch upon some selected highlights.

Global structure and dynamics of the solar interior

Just as seismology reveals the Earth's interior by studying earthquake waves, solar physicists probe the inside of the Sun using a technique called 'helioseismology'. The oscillations detectable at the visible surface are due to sound waves reverberating through the Sun's interior. These oscillations are usually described in terms of normal modes (identified by three integers: angular degree l , angular order m , and radial order n). The frequencies of the modes depend on the structure and flows in the regions where they propagate. Because different modes sample different regions inside the Sun, one can, in principle, map the solar interior by observing many modes. By measuring precisely the mode frequencies, one

Germany, Ireland, Italy, Japan, The Netherlands, Norway, Russia, Spain, Switzerland, United Kingdom, and the United States). Detailed descriptions of all twelve instruments, the science operations and data products, as well as a complete mission overview, can be found in ESA Bulletin No. 87.

SOHO has a unique operating mode that provides a 'live' display of data on the scientists'

Table 1. The SOHO scientific instruments

| | Investigation | Principal Investigator |
|--------|---|--|
| GOLF | Global Oscillations at Low Frequencies | A. Gabriel, IAS, Orsay, France |
| VIRGO | Variability of Solar Irradiance and Gravity Oscillations | C. Fröhlich, PMOD Davos, Switzerland |
| MDI | Michelson Doppler Imager | P. Scherrer, Stanford University, USA |
| SUMER | Solar Ultraviolet Measurements of Emitted Radiation | K. Wilhelm, MPAe Lindau, Germany |
| CDS | Coronal Diagnostic Spectrometer | R. Harrison, RAL, Chilton, UK |
| EIT | Extreme-Ultraviolet Imaging Telescope | J.-P. Delaboudinière, IAS, Orsay, France |
| UVCS | Ultra-Violet Coronagraph Spectrometer | J. Kohl, SAO, Cambridge, USA |
| LASCO | Large-Angle Spectroscopic Coronagraph | R. Howard, NRL, Washington, USA |
| SWAN | Solar Wind Anisotropies | J.-L. Bertaux, SA, Verrières, France |
| CELIAS | Charge, Element and Isotope Analysis System | P. Bochsler, Univ. of Bern, Switzerland |
| COSTEP | Comprehensive Supra-Thermal and Energetic-Particle Analyser | H. Kunow, Univ. of Kiel, Germany |
| ERNE | Energetic and Relativistic Nuclei and Electron Experiment | J. Torsti, Univ. of Turku, Finland |

IAS : Institut d'Astrophysique Spatiale
 PMOD : Physikalisch-Meteorologisches Observatorium Davos
 RAL : Rutherford Appleton Laboratory
 MPAe: Max-Planck-Institut für Aeronomie

SAO : Smithsonian Astrophysical Observatory
 NRL : Naval Research Laboratory
 SA : Service d'Aeronomie

can infer the temperature, density, elemental and isotopic abundances, interior mixing, interior rotation and flows, even the age of the Solar System, and pursue such esoteric matters as testing the constancy of the gravitational constant.

Interior rotation and flows

The nearly uninterrupted data from SOHO's Michelson Doppler Imager (MDI) yield oscillation power spectra with an unprecedented signal-to-noise ratio that allow the determination of the frequency splittings of the global resonant acoustic modes of the Sun with exceptional accuracy. These data confirm that the decrease in angular velocity Ω with latitude seen at the surface extends with little radial variation through much of the convection zone, at the base of which is an adjustment layer, called the 'tachocline', leading to nearly uniform rotation deeper in the radiative interior (Fig. 1). Furthermore, a prominent rotational shearing layer in which Ω increases just below the surface is discernible at low- to mid-latitudes.

The MDI team has also been able to study the solar rotation closer to the poles than has been achieved in previous investigations. The data have revealed that the angular velocity is distinctly lower at high latitudes than previously extrapolated from measurements at lower latitudes based on surface Doppler observations

and helioseismology. Moreover, they found evidence of a submerged polar jet near latitudes of 75°, which is rotating more rapidly than its immediate surroundings (red oval near the poles in Fig. 2).

Alternating zonal bands of faster and slower rotation (± 7 m/s) at a depth of 2 – 9 Mm appear to coincide with an evolving pattern of 'torsional oscillations' reported from earlier surface Doppler studies (Fig. 2). Clear evidence of the migration of these zonal flows towards the equator has been found, and a recent study has established that these banded flows are not merely a near-surface phenomenon. Rather, they extend downward at least 60 Mm (some 8% of the total solar radius) and thus are evident over a significant fraction of the nearly 200 Mm depth of the solar convection zone (Fig. 3).

Long-lived velocity cells extending over 40–50° of longitude, but less than 10° of latitude, have been identified with the elusive 'giant cells' by Beck et al.. Their suprisingly large aspect ratio may be a consequence of the Sun's differential rotation, whereby larger features are broken up by rotational shear.

High-precision MDI measurements of the Sun's shape obtained during two special 360° roll manoeuvres of the SOHO spacecraft have

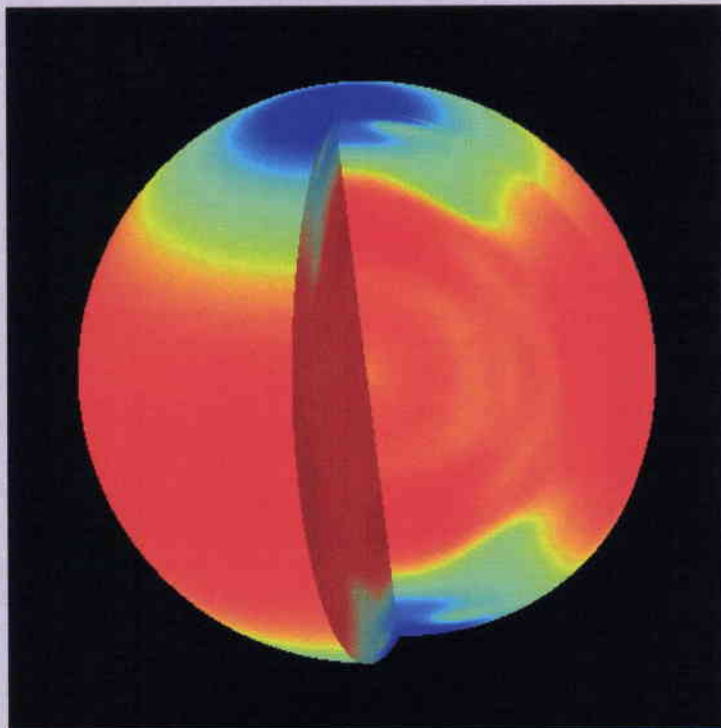


Figure 1. Solar interior rotation. Red indicates the fastest rotating material, dark blue the slowest (courtesy of SOHO/MDI Consortium)

Figure 2. Variations in solar motion. This false-colour image represents the difference in speeds between various areas on the Sun, both at the surface and in the interior. Red - yellow is faster and blue slower than average. On the left side of the image, the light-yellow bands are zones that are moving slightly faster than their surroundings. The cutaway on the right side of the image reveals speed variations in the interior of the Sun. Only the outer 30% of the Sun's interior where the variations are more certain is shown. The red ovals embedded in the green areas at the poles are the newly discovered polar plasma 'jet streams'. They move approximately 10% faster than their surroundings, and each is about 25 000 km across, large enough to engulf two Earths (courtesy of SOHO/MDI Consortium)

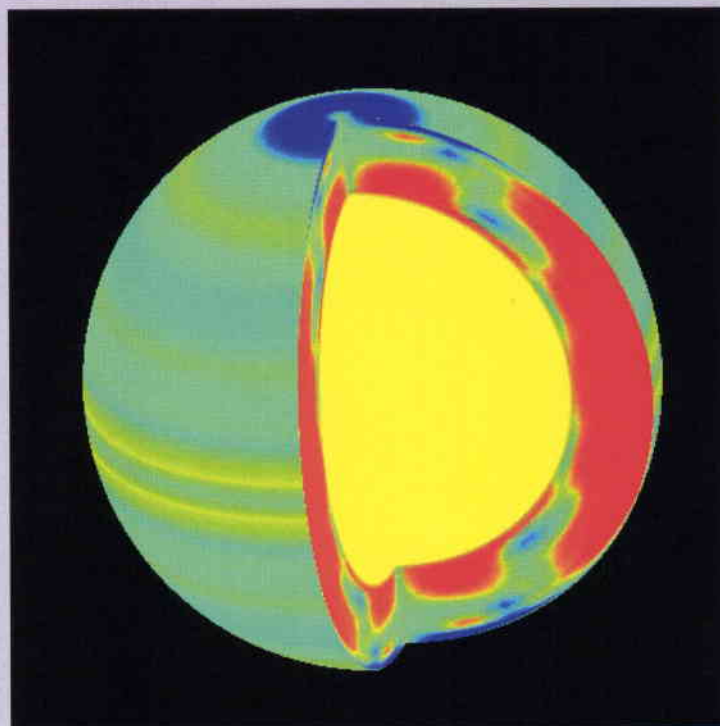
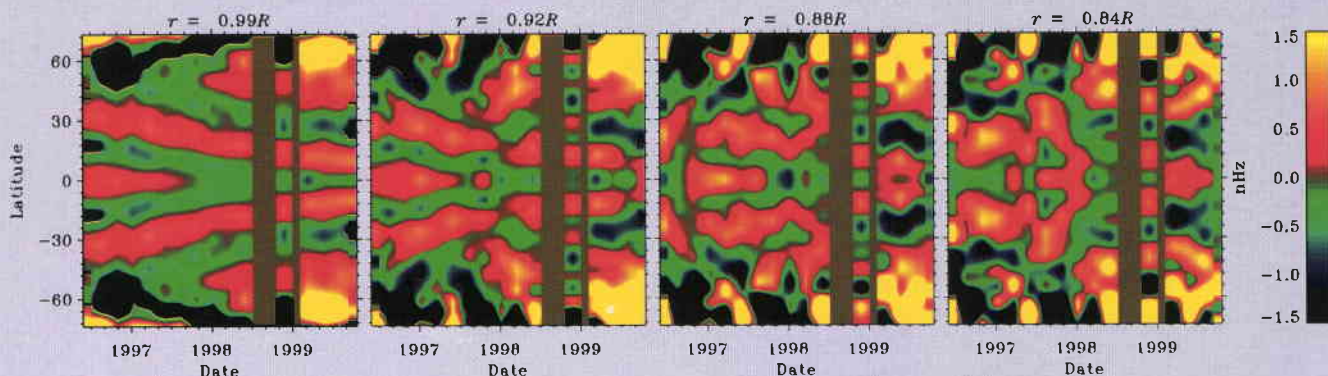


Figure 3. Migrating banded zonal flows: variation of rotation rate with latitude and time at four different depths in the convection zone. The uniform olive-green vertical bands indicated time periods when no data were available from SOHO (during the summer of 1998 due to the temporary loss of the spacecraft, and in January 1999 when SOHO was in safe mode after a gyroscope failure). The colour bar indicates the dynamic range in nHz of the angular velocity (from Howe et al.)



produced the most precise determination of solar oblateness ever. These measurements unambiguously rule out the possibility of a rapidly rotating core, and any significant solar-cycle variation in the oblateness.

Interior sound-speed profile

The unprecedented accuracy of helioseismic data from SOHO's MDI, GOLF and VIRGO instruments has enabled substantial improvements in models of the solar interior, and has even shown the importance of considering mixing effects, which turn out to solve existing riddles in the isotopic composition of the Sun.

Figure 4 is quite remarkable in that there is very good agreement between the measured sound speed and the model throughout most of the solar interior. Except for the conspicuous bump at about 0.68 R_⊙ (the location of the transition from the radiative zone into the convection zone), the difference is less than 0.2%, suggesting that our understanding of the mean radial stratification of the Sun is reasonably accurate.

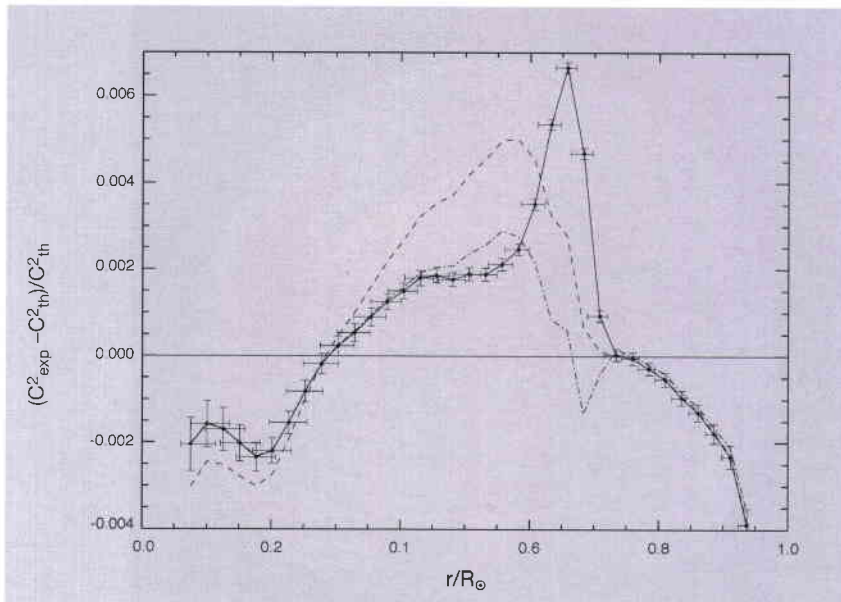


Figure 4. Relative differences between the squared sound speed in the Sun as observed by GOLF and MDI and a reference model (solid line), as well as two models including macroscopic mixing processes in the tachocline (dashed and dash-dotted lines) (from Brun et al.)

In order to resolve this discrepancy at 0.68 R_⊙ and the failure of recent updated standard models to predict the photospheric lithium abundance, Brun et al. introduced a new term – macroscopic mixing below the convective zone – into the standard stellar structure equations. They showed that the introduction of this ‘tachocline layer mixing’ significantly improves the agreement with the helioseismic data and photospheric abundance data. In particular, the anomalous bump in the sound-speed plot is practically erased (see the dash-dotted line in Fig. 4).

Local-area helioseismology

In conventional helioseismology, most results

are obtained from a global-mode analysis. With the availability of high-spatial-resolution data from MDI, interest in studying the Sun's local structure has grown rapidly. As a result, several new techniques are being developed, including helioseismic holography, ring-diagram analysis and time-distance helioseismology.

Helioseismic holography

Originally proposed by Roddier in 1975 (though not as ‘holography’) and developed over the last few years mainly by Lindsey & Braun, this technique has been applied to MDI data to render acoustic images of the absorption and egression of sunspots and active regions. These images have revealed a remarkable acoustic anomaly surrounding sunspots, called the ‘acoustic moat’, which is a conspicuous halo of enhanced acoustic absorption at 3 mHz. At 5–6 mHz, on the other hand, a prominent halo of enhanced acoustic emission, called ‘acoustic glory’, was found surrounding active regions. Helioseismic holography techniques can be applied to render images of supposed acoustic sources that can be sampled at any desired depth. This technique has recently been applied by Lindsey & Braun to derive the first seismic images of the far side of the Sun, from MDI data (Fig. 5).

Ring-diagram analysis

The second technique, known as ‘ring-diagram analysis’, is based on the study of three-dimensional power spectra of solar p-modes on a part of the solar surface. Several groups have applied this technique to MDI data to determine near-surface flows in the Sun. A remarkable meridional flow from the equator to the poles was found in the outermost layers of the convection zone, reaching a maximum of 25–30 m/s at approximately 30° latitude. No change of sign of the meridional flow has been measured, i.e. no evidence of a return flow has been detected in this depth range. The rotation rate determined with the ring-diagram technique agrees well with that from global modes, and the measurements could be extended closer to the surface, providing new insight into the shear layer immediately beneath the surface.

Time-distance helioseismology

The third, and perhaps most exciting and most promising new technique for probing the three-dimensional structure and flows beneath the solar surface is called ‘time-distance helioseismology’ or ‘solar tomography’. It measures the travel time of acoustic waves between various points on the surface. In a first-order approximation, the waves can be considered to follow ray paths that depend only on a mean solar model, with the curvature of the ray paths

being caused by the increasing sound speed with depth below the surface. The travel time is affected by various inhomogeneities along the ray path, including flow, temperature inhomogeneities, and magnetic fields. By measuring a large number of travel times between different locations and using an inversion method, it is possible to construct three-dimensional maps of the subsurface inhomogeneities.

One of the most successful applications of time-distance helioseismology has been the detection of large-scale meridional flows in the solar convection zone. Meridional flows from the equator to the poles have been observed before on the solar surface in direct Doppler-shift measurements. The time-distance measurements by the Stanford MDI team provided the first evidence that such flows

By applying this new technique to high-resolution MDI data, Duvall et al. were able to generate the first maps of horizontal and vertical flow velocities as well as sound-speed variations in the convection zone just below the visible surface (Fig. 6). They found that in the upper layers, 2–3 Mm deep, the horizontal flow is organised in supergranular cells, with outflows from the cell centres. The characteristic size of these cells is 20–30 Mm and the cell boundaries coincide with the areas of enhanced magnetic field. The supergranulation outflow pattern disappears at a depth of approximately 5 Mm, suggesting that the depth of the supergranular layer is less than one quarter of the characteristic horizontal size of the cells (20–30 Mm).

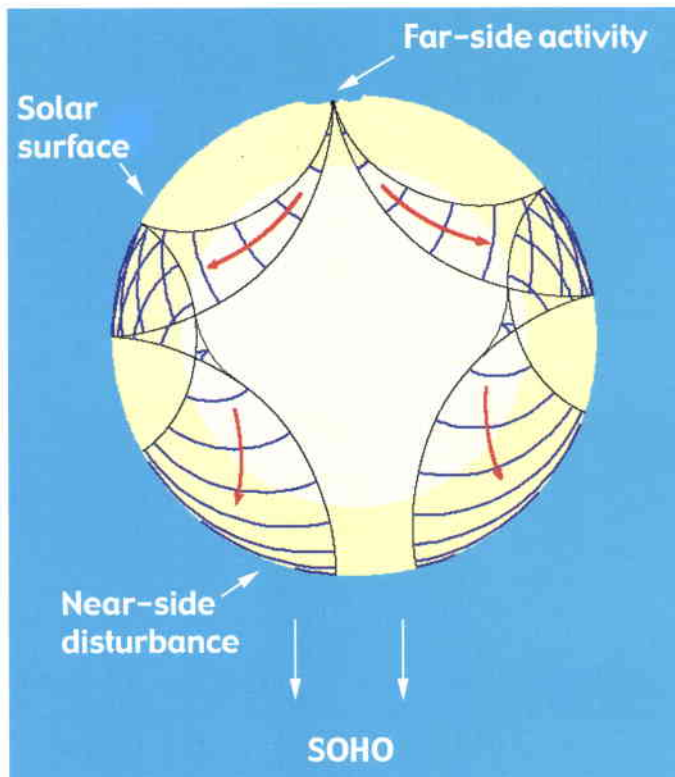


Figure 5a. Cross-section of the solar interior illustrating the wave configuration of two-skip far-side seismic holography. Sound waves from the far side of the Sun are reflected internally once before reaching the front side, where they are observed with MDI

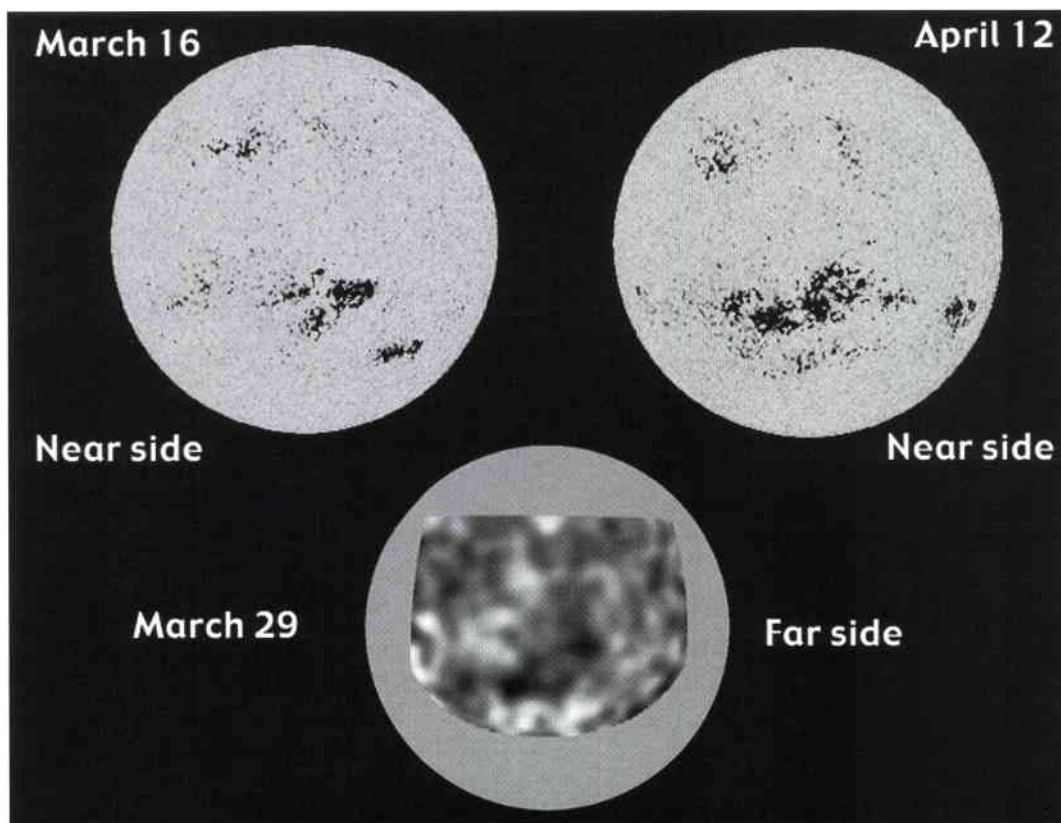
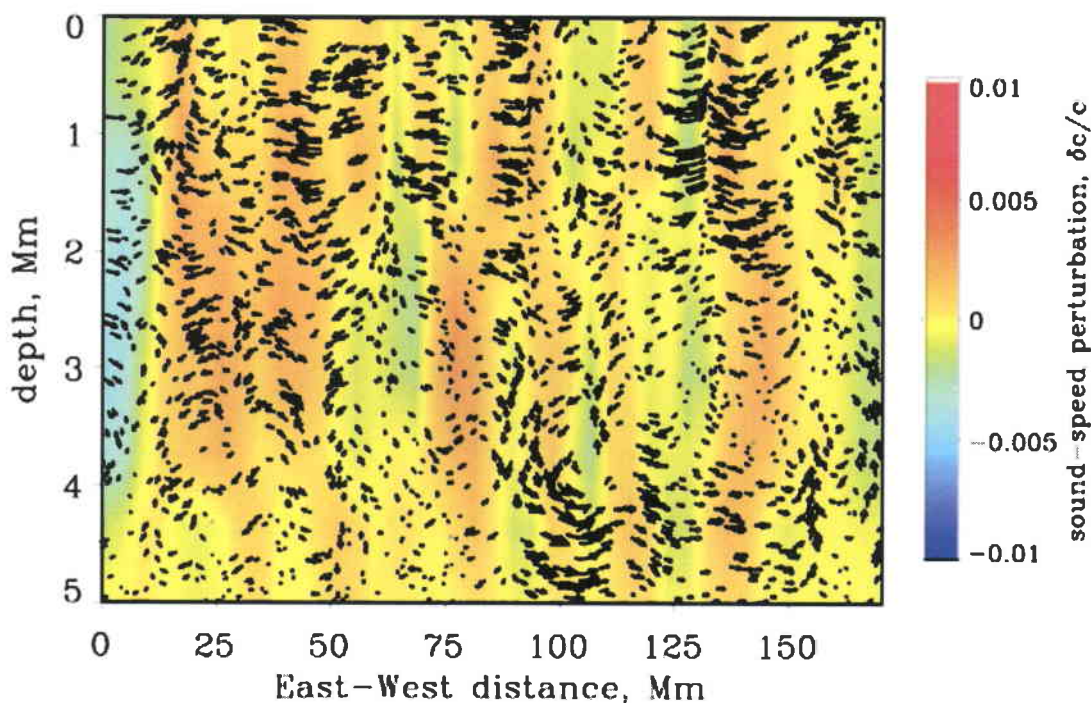


Figure 5b. The upper two images show the magnetic field strength measured with MDI while the active region was facing the Earth - before and after being holographically imaged on the far side, shown in the lower image (from Lindsey & Braun)

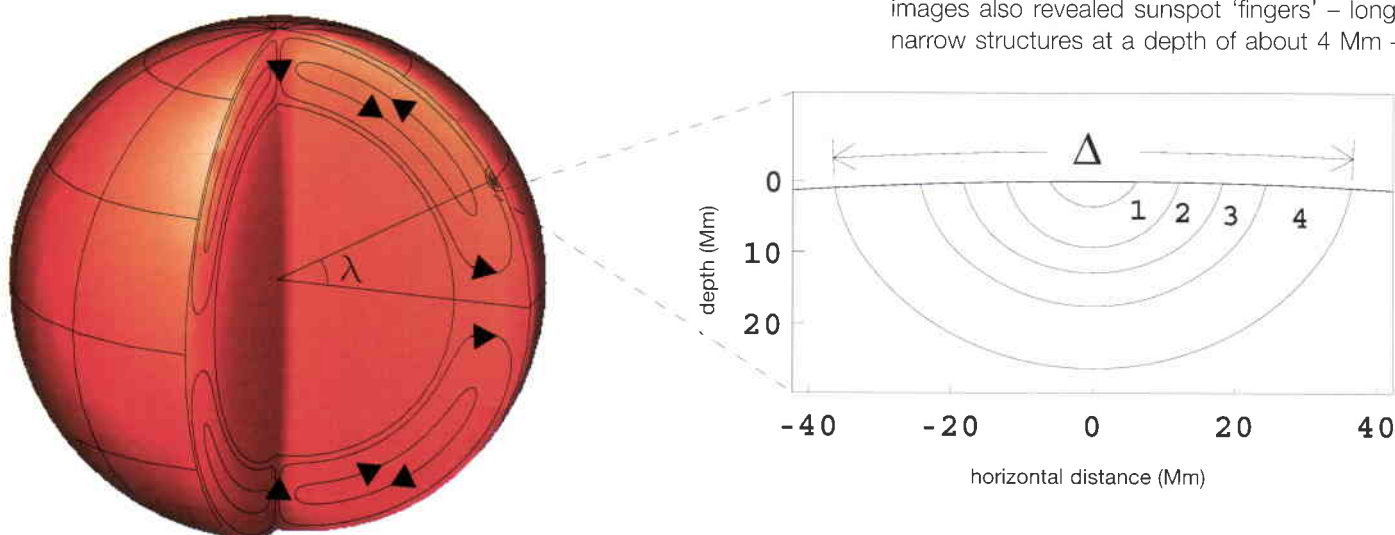
Figure 6. A vertical cut through the upper convection zone showing subsurface flows and sound speed inhomogeneities (from Kosovichev et al.)



persist to great depths (Fig. 7), and therefore may play an important role in the 11-year solar cycle. They found the meridional flow to persist to a depth of at least 26 Mm, with a depth-averaged velocity of 23.5 ± 0.6 m/s at mid-latitude. More recently, they extended these measurements to a depth of $0.8 R_{\odot}$ without finding any evidence of a return flow. Continuity considerations led them to estimate the return flow below $0.8 R_{\odot}$ at approximately 5 m/s, which might actually be detectable in the future, providing a useful constraint for dynamo theories.

quickly through the upper 18 Mm of the convection zone. They estimate the speed of emergence at about 1.3 km/s, which is somewhat higher than predicted by earlier theories. Wave speeds vary in the emerging active region by about 0.5 km/s. The observed development of the active region suggests that the sunspots are formed as a result of the concentration of magnetic flux close to the surface. The Stanford team also presented time-distance results on the subsurface structure of a large sunspot observed on 20 June 1998 (Fig. 8). The wave-speed perturbations in the spot are much stronger than in the emerging flux (0.3–1 km/s). At a depth of 4 Mm, a 1 km/s wave-speed perturbation corresponds to a 10% temperature variation (approx. 2800 K) or to a 18 kG magnetic field. Beneath the spot, the perturbation is negative in the subsurface layers and becomes positive further down in the interior. Their tomographic images also revealed sunspot ‘fingers’ – long, narrow structures at a depth of about 4 Mm –

Figure 7. The geometry of the time-distance analysis of subsurface meridional flows (from Giles et al.)



which connect the sunspot with surrounding pores of the same polarity. Pores with the opposite polarity are not connected to the spot.

MDI has also made the first observations of seismic waves from a solar flare, opening up possibilities for studying both the flares and the solar interior. During the impulsive phase of the X2.6-class flare of 9 July 1996, a high-energy electron beam caused an explosive evaporation of chromospheric plasma at supersonic velocities. The upward motion was balanced by a downward recoil in the lower chromosphere, which excited propagating waves in the solar interior. On the surface, the outgoing circular flare waves resembled ripples from a pebble thrown into a pond (Fig. 9). The seismic wave propagated at least 120 000 km from the flare's epicentre, with an average speed of about 50 km/s on the solar surface.

Transition-region dynamics

Explosive events and 'blinkers'

Several types of transient events have been detected in the quiet Sun. High-velocity events in the solar transition region, also called 'explosive events', were first discovered in the early eighties based on ultraviolet observations with the High-Resolution Telescope-Spectrometer (HRTS) rocket payload. They have large velocity dispersions, approximately ± 100 km/s, i.e. velocities are directed both towards and away from the observer causing a strong broadening of the spectral lines observed.

Explosive events have been studied extensively by a number of authors using SUMER data, and several results support the magnetic reconnection origin of these features. Innes et al. have reported explosive events that show spatially separated blue- and red-shifted jets and some that show transverse motion of blue and red shifts, as predicted if reconnection was the source (Fig. 10). Comparisons with magnetograms from MDI and those obtained at ground-based solar observatories have also provided evidence that transition-region explosive events are a manifestation of magnetic reconnection occurring in the quiet Sun.

Harrison et al. have presented a comprehensive study of EUV flashes, also known as 'blinkers'.

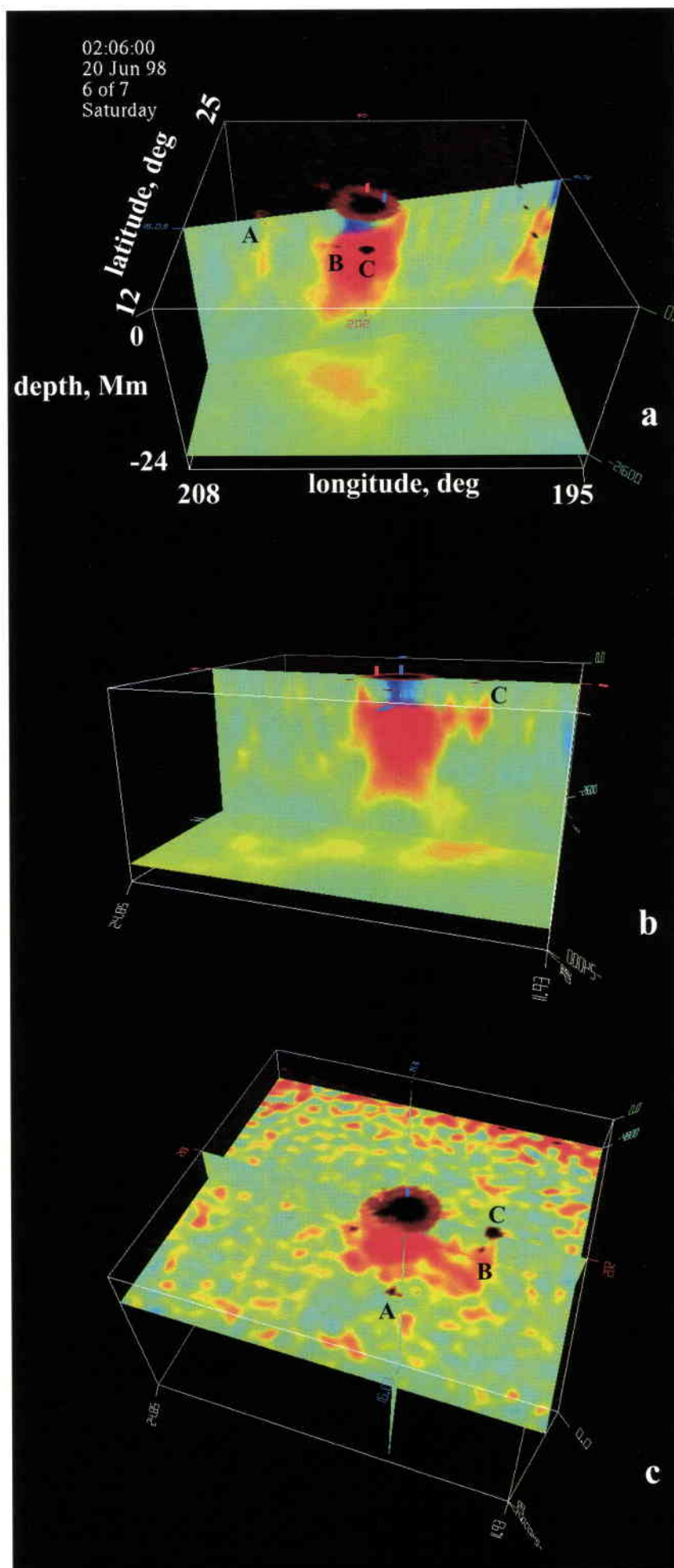


Figure 8. The subsurface sound speed perturbations in a sunspot region observed on 20 June 1998 by MDI. The horizontal size of the box is 13 deg (158 Mm), the depth is 24 Mm. The horizontal cut in panels (a) and (b) reaches down to a depth of 21.6 Mm, while in panel (c) it is 4.8 Mm deep. Positive variations are shown in red, negative variations in blue. Scaling: ± 1 km/s (from Kosovichev et al.)

Figure 9. Seismic waves ('sun quake') produced by a solar flare on 9 July 1996 (from Kosovichev & Zharkova)

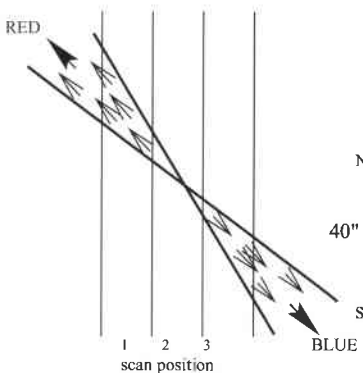
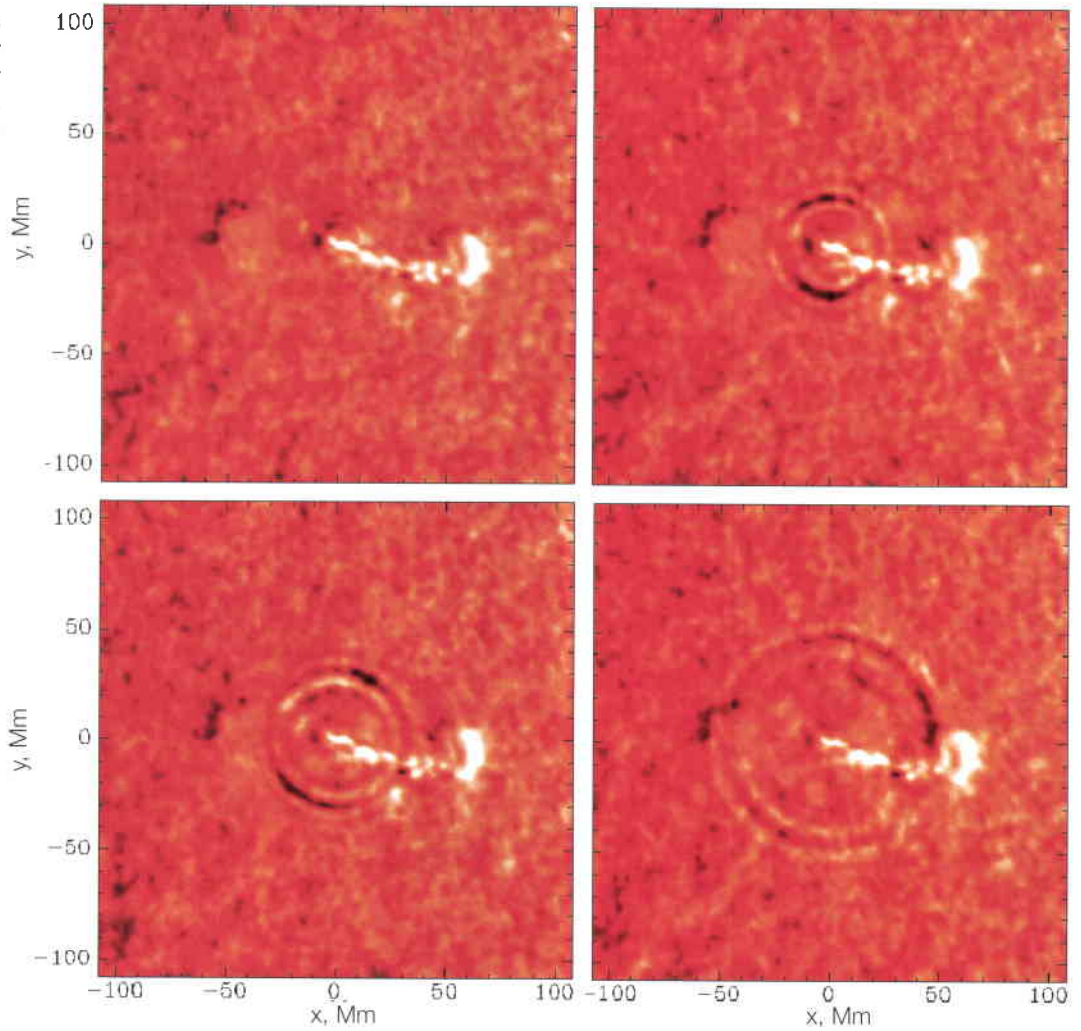
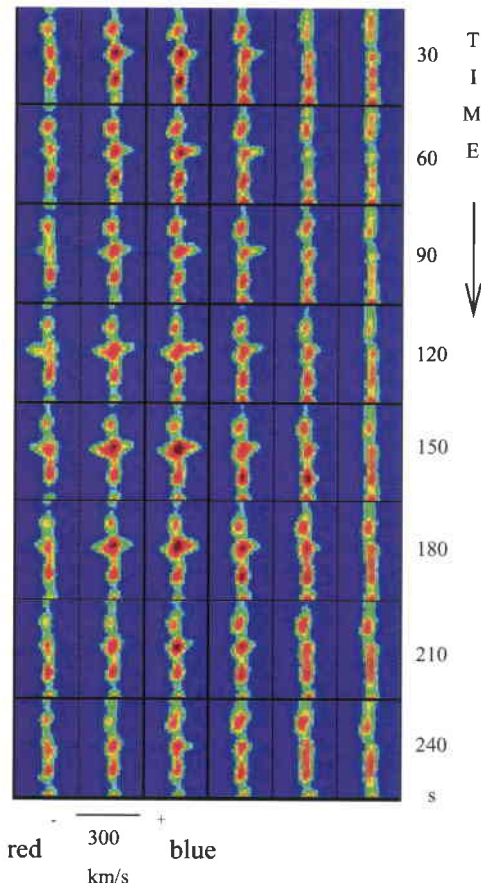


Figure 10. Bi-directional plasma jets observed by SUMER in Si IV 1393 Å in June 1996 and a schematic of the plasma flow (from Innes et al.)



which were identified in the quiet Sun network as intensity enhancements of order 10–40% using CDS (Fig. 11). They have analysed 97 blinker events and identified blinker spectral, temporal and spatial characteristics, their distribution, frequency and general properties, across a broad range of temperatures, from 20 000 to 1 200 000 K. The blinkers are most pronounced in the transition region lines O III, O IV and O V, with modest or no detectable signature at higher and lower temperatures. A typical blinker lasts about 1000 s, but due to a long tail of longer duration events the average duration is 2400 s. Comparisons with plasma cooling times led to the conclusion that there must be continuous energy input throughout the blinker event. There are about 3000 blinker events in progress at any given time. Remarkably, line ratios from O III, O IV and O V show no significant change throughout the blinker event, suggesting that the intensity increase is not a temperature effect, but is predominantly caused by increases in density or filling factor. The thermal-energy content of an average blinker is estimated as 2×10^{25} erg.

While the explosive events appear as extremely broad line profiles with Doppler shifts of

CDS-SOHO – December 4, 1997 – QUIET SUN BLINKER

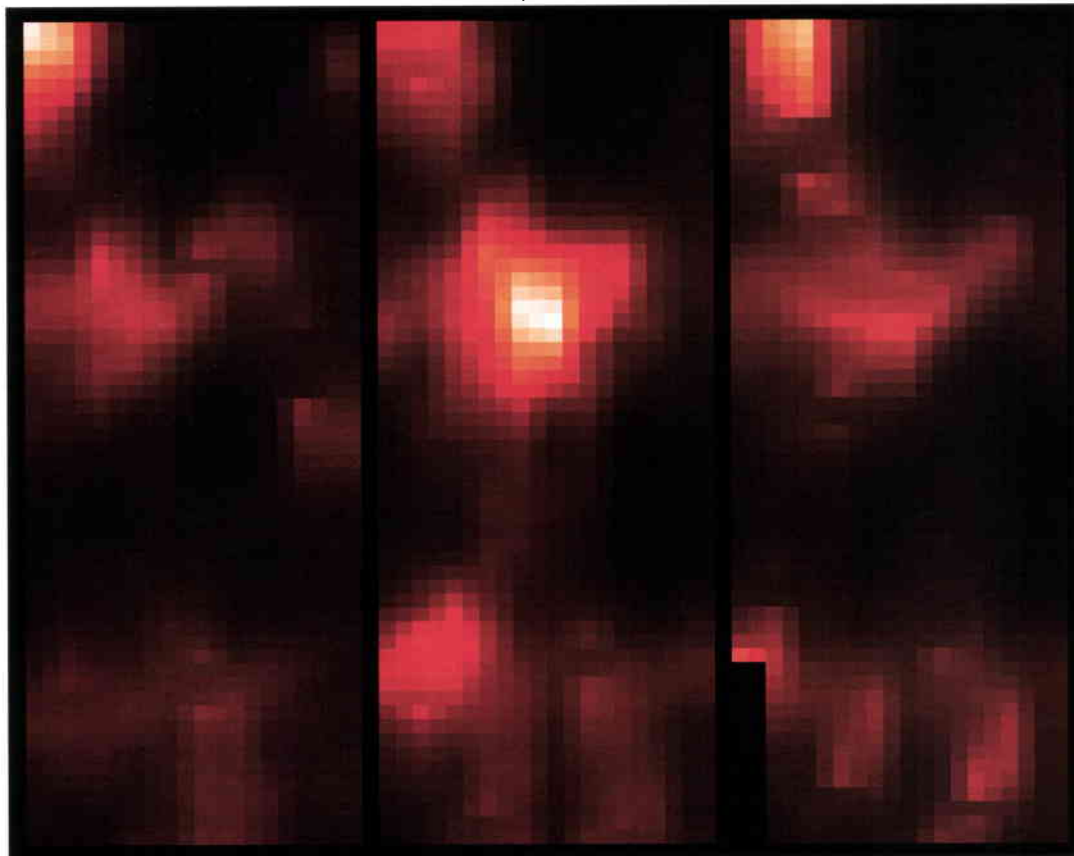


Figure 11. 'Blinker' event observed by CDS in OV 629 Å ($T \approx 230\,000$ K). The area shown covers $30\,000 \times 74\,000$ km². The three images are minutes apart (from Harrison et al.)

± 150 km/s without significant brightenings, spectral-line fits to CDS data have so far revealed no clear velocity shifts, or only modest velocities up to a maximum of 20 km/s. Typically, the explosive events are short-lived (approx. 60 s), small scale (about 2 arcsec) and occur at a rate of 600 s^{-1} over the Sun's surface. While both types of event appear fairly common, they are seemingly of two different classes and further analysis is needed to establish the relationship between the two phenomena.

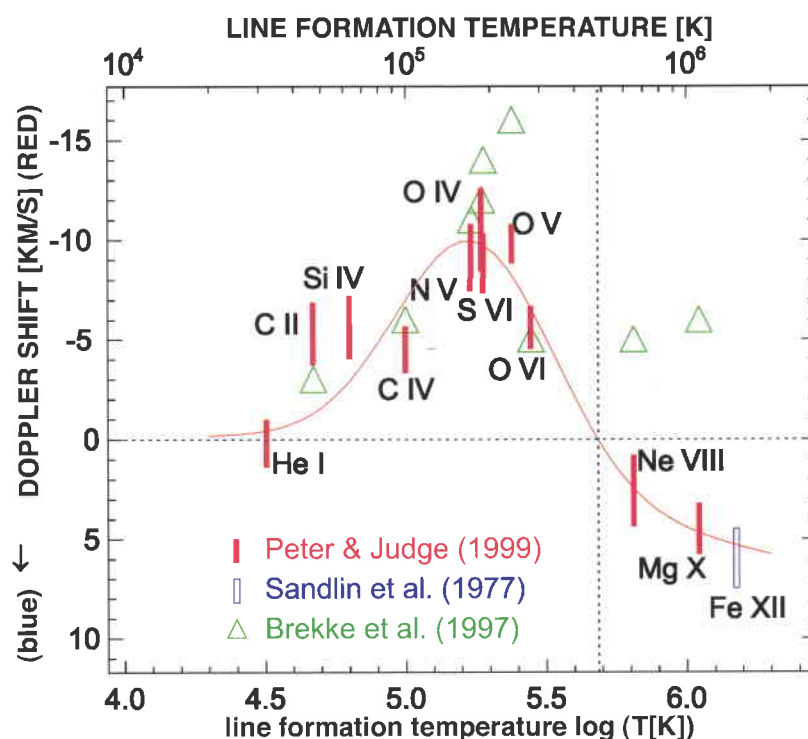
Doppler-shifted emission in the transition region

It has long been known that the UV emission lines originating from the transition region of the quiet Sun are systematically redshifted relative to the underlying chromosphere. In earlier investigations the magnitude of the redshift has been found to increase with temperature, reaching a maximum at $T \approx 10^5$ K, and then to decrease sharply towards higher temperatures. Systematic redshifts have also been observed in stellar spectra of late-type stars, first with the International Ultraviolet Explorer (IUE) satellite and more recently with the Hubble Space Telescope. Below temperatures of about 1.6×10^5 K, the line redshifts of the Sun, α Cen A, α Cen B, and Procyon are all very similar.

Early SOHO observations extended the observable temperature range and suggested that the average redshift persists to higher

temperatures than most previous investigations suggested. Shifts of 10 to 16 km/s were observed in lines formed at $T = 1.3\text{--}2.5 \times 10^5$ K (Fig. 12). Even upper transition region and coronal lines (O VI, Ne VIII, and Mg X) showed systematic redshifts in the quiet Sun corresponding to velocities around 5 km/s.

Figure 12. Variation of the Doppler shift at disc centre with formation temperature of the line. The solid line is a by-eye fit to the Doppler shifts (from Peter & Judge)



More recent investigations using SUMER observations have revisited this problem, addressing possible errors in the rest wavelengths of lines from highly ionised atoms (e.g. Ne VIII, Na IX, Mg X, Fe XII). Using full-disc scans from SUMER and assuming that all mass or wave-motion effects on the limb cancel out statistically, new rest wavelengths for Ne VIII and Mg X have been established, leading to blueshifts of 2.5 km/s and 4.5 km/s, respectively, at disc centre.

These recent results suggest that the upper transition region and lower corona appear blue-shifted in the quiet Sun, with a steep transition from red- to blue-shifts above 5×10^5 K. This transition is significant because it has major implications for the transition region and solar-wind modelling, as well as for our understanding of the structure of the solar atmosphere.

The network

Early models of the solar atmosphere assumed that the temperature structure of the upper atmosphere was continuous, with a thin transition region connecting the chromosphere with the corona. This depiction now appears too simplistic. Rather, it seems that the solar atmosphere consists of a hierarchy of isothermal, highly dynamic loop structures. Of particular interest in this context is the network, which is believed to be the backbone of the entire solar atmosphere and the basic channel of the energy responsible for heating the corona and accelerating the solar wind.

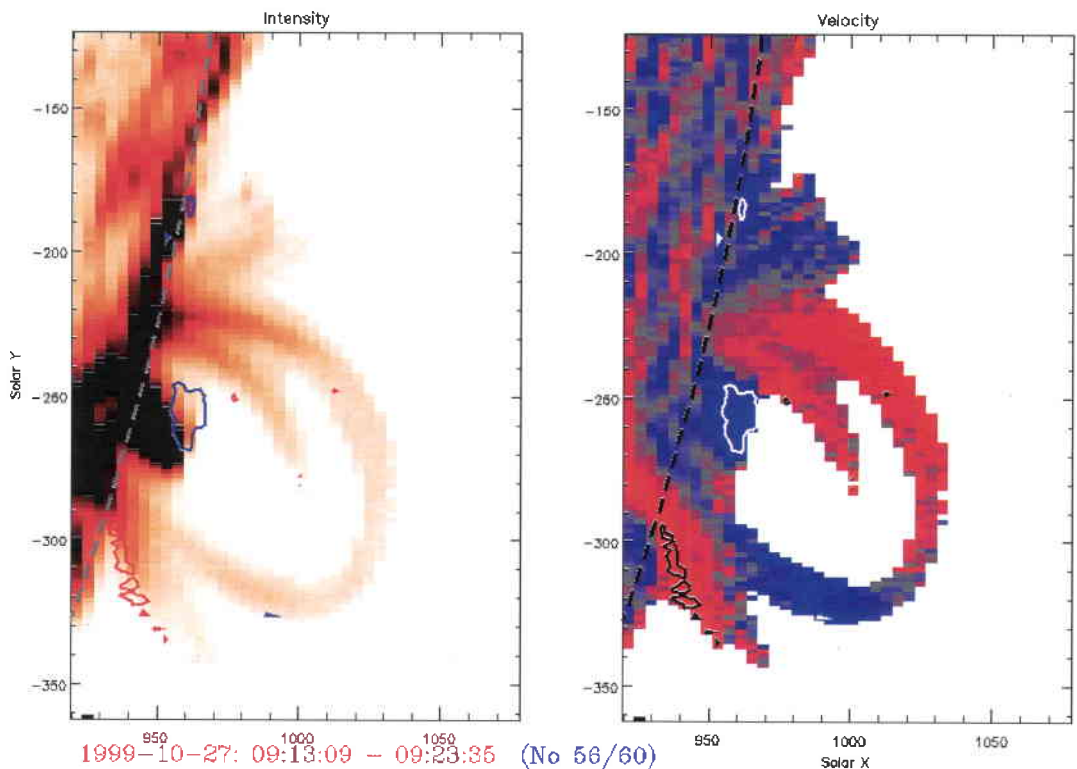
Patsourakos et al. have used CDS data to study the width variation of the network with temperature. They found that the network boundaries have an almost constant width up to about 250 000 K (where the network contrast is also strongest) and then fan out rapidly at coronal temperatures. The network in the lower transition region is about 10 arcsec across and spreads to about 16 arcsec at 1 MK. These results are in very good agreement with Gabriel's transition region-corona model, dating from 1976.

Active-region dynamics

EIT, SUMER and CDS observations have clearly demonstrated that the solar transition region and corona are extremely dynamic and time variable in nature. Large line shifts of up to 60 km/s were observed with CDS in individual active region loops (Fig. 13). High Doppler shifts are common in active-region loops and strong shifts are present in parts of loops for temperatures up to 0.5 MK. Regions with both red and blue shifts are seen. While typical values correspond to velocities of ± 50 -100 km/s, shifts approaching 200 km/s have been detected. At temperatures $T > 1$ MK, i.e. in Mg IX 368 Å or Fe XVI 360 Å, only small shifts are seen. The high Doppler shifts therefore seem to be restricted to the transition region.

Brynildsen et al. studied 3-min transition-region oscillations above sunspots by analysing time series recorded in O V 629 Å, N V 1238 Å and 1242 Å, and the chromospheric Si II 1260 Å line in NOAA 8378. The 3-min oscillations that

Figure 13. Coronal Diagnostic Spectrometer (CDS) raster images showing the intensity and velocity distribution of transition-region plasma in AR8737 on the south-west limb in October 1999. Six emission lines were observed simultaneously, of which one is shown here (O V 629 Å, formed at about 230 000 K). Doppler shifts corresponding to a velocity greater than ± 40 km/s (144 000 km/h) are fully red/blue. Contours outline areas with velocities exceeding ± 50 km/s (180 000 km/h) (courtesy of T. Fredvik & O. Kjeldseth-Moe)



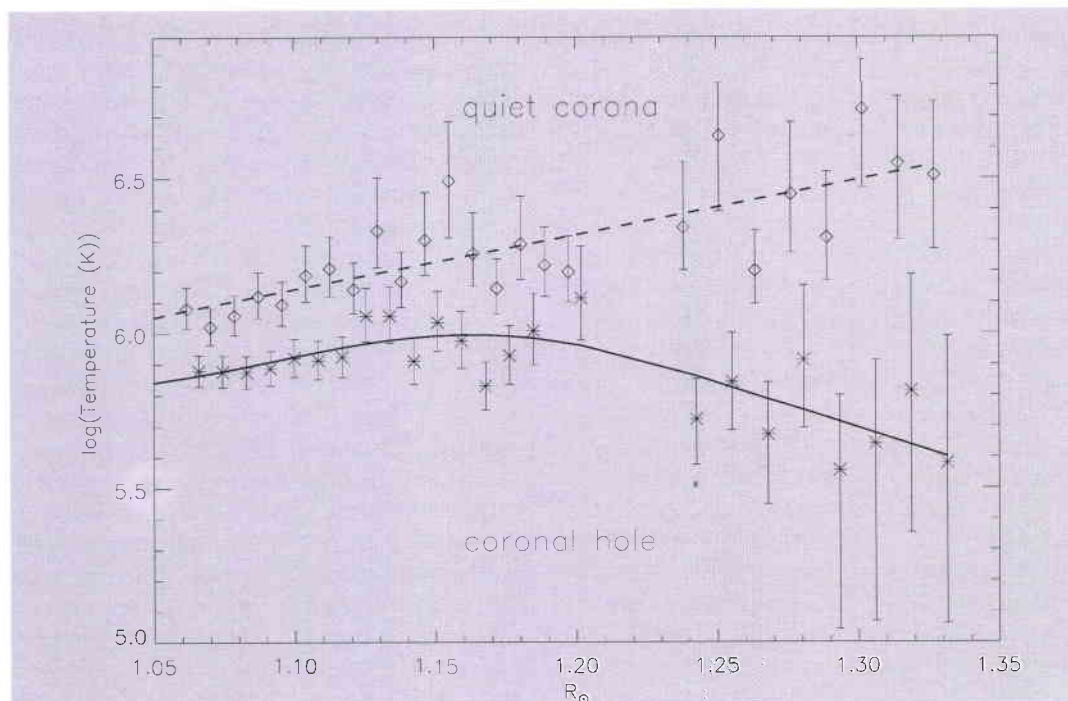


Figure 14. Temperature gradient measurement in the quiet corona (equatorial west limb) and the north polar coronal hole (from David et al.)

they observed above the sunspot umbra show: (a) larger peak line intensity amplitudes than reported previously, (b) clear signs of nonlinearities, (c) significant oscillations in line width, and (d) maxima in peak line intensity and maxima in velocity directed towards the observer that are nearly in phase. They also performed a simple test and calculated the velocity oscillations from the intensity oscillations (which, to a first approximation for optically thin lines, is proportional to ρ^2) using a standard text-book equation for simple nonlinear acoustic waves. The agreement with the observed velocity is astounding, providing convincing evidence that the oscillations that they observed are upward-propagating, nonlinear acoustic waves.

One of the most surprising results from SOHO has been the extremely broad coronal profiles of highly ionised elements such as oxygen and magnesium (Fig. 15). Kohl et al. and Cranmer et al. have presented a self-consistent empirical model of a polar coronal hole near solar minimum, based on H I and O VI UVCS spectroscopic observations. Their model describes the

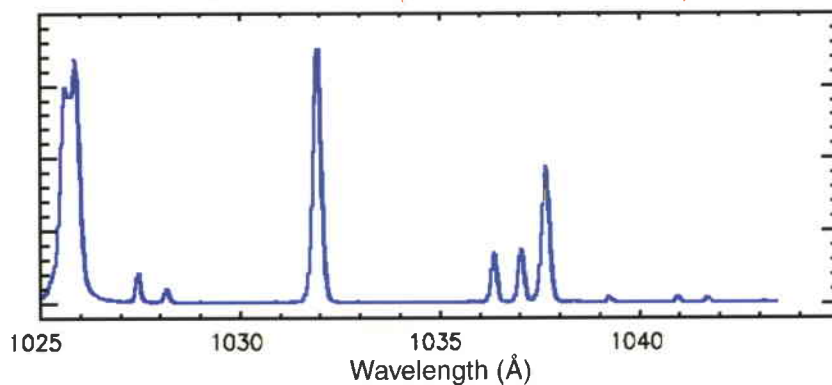
Figure 15. Line profile of O VI from UVCS observations in a polar coronal hole (lower panel) compared to disc observations from SUMER. The broad O VI line widths indicate velocities of up to 500 km/s, equivalent to a thermal-motion kinetic temperature of 200 million K. Narrow peaks in the lower panel are due to stray light (from Kohl et al.)

Corona

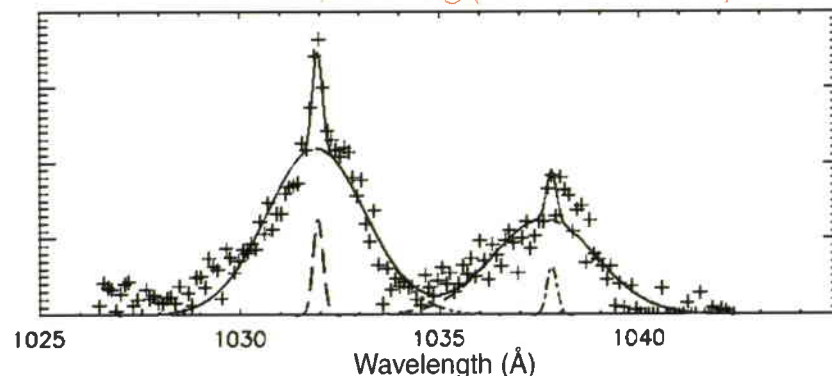
Coronal-hole temperature and density measurements

Using the two SOHO spectrometers CDS and SUMER, David et al. have measured the electron temperature as a function of height above the limb in a polar coronal hole (Fig. 14). Temperatures of around 0.8 MK were found close to the limb, rising to a maximum of less than 1 MK at $1.15 R_{\odot}$, then falling to around 0.4 MK at $1.3 R_{\odot}$. In equatorial streamers, on the other hand, the temperature was found to rise constantly with increasing distance, from about 1 MK close to the limb to over 3 MK at $1.3 R_{\odot}$. With these low temperatures, the classical Parker mechanism for solar-wind acceleration cannot alone explain the high wind velocities, which must therefore be due to the direct transfer of momentum from MHD waves to the ambient plasma.

Solar Disk (SOHO/SUMER)



N. Pole, $2.1 R_{\odot}$ (UVCS/SOHO)



radial and latitudinal distributions of the density of electrons, H I and O VI, as well as the outflow velocity and unresolved anisotropic most probable velocities for H I and O VI.

Polar plumes

Wilhelm et al. have determined the electron temperatures, densities and ion velocities in plumes and interplume regions of polar coronal holes from SUMER spectroscopic observations of the Mg IX 706/750 Å and Si VIII 1440/1445 Å line pairs. They find the electron temperature T_e to be less than 800 000 K in a plume in the range from $r = 1.03$ to $1.60 R_\odot$, decreasing with height to about 330 000 K. In the interplume lanes, the electron temperature is also low, but stays between 750 000 and 880 000 K in the same height interval. Doppler widths of O VI lines are narrower in the plumes ($v_{1/e} \approx 43$ km/s) than in the interplumes ($v_{1/e} \approx 55$ km/s). Thermal and turbulent ion speeds of Si VIII reach values up to 80 km/s, corresponding to a kinetic ion temperature of 10^7 K.

These results clearly confirm that the ions in a coronal hole are extremely hot and the electrons much cooler. They also clearly demonstrate that local thermal equilibrium does not exist in polar coronal holes, and that the assumption of Collisional Ionisation Equilibrium (CIE) and the common notion that $T_e \approx T_{ion}$ can no longer be made in models of coronal holes.

It seems difficult to reconcile these low electron temperatures measured in coronal holes with the freezing-in temperatures deduced from ionic charge composition data. The freezing-in concept, however, assumes that the adjacent charge states are in ionisation equilibrium. A critical reevaluation of this concept appears to be justified.

Previously, plumes were considered to be the source regions for the high-speed solar wind. Given the narrower line widths in plumes and the absence of any significant motions there, Wilhelm et al. suggested that the source regions of the fast solar wind are the interplume lanes rather than the plumes, since conditions there are far more suitable for a strong acceleration than those prevailing in plumes.

Heating processes

A promising theoretical explanation for the high temperatures of heavy ions and their strong velocity anisotropies is the efficient dissipation of high-frequency waves that are resonant with ion-cyclotron Larmor motions about the coronal magnetic-field lines. This effect has been studied in detail by Cranmer et al., who have constructed theoretical models of the

non-equilibrium plasma state of the polar solar corona using empirical ion velocity distributions derived from UVCS and SUMER. They found that the dissipation of relatively small-amplitude high-frequency Alfvén waves (10–10 000 Hz) via gyro resonance with ion cyclotron Larmor motions can explain many of the kinetic properties of the plasma, in particular the strong anisotropies, the greater than mass-proportional temperatures, and the faster outflow of heavy ions in the high-speed solar wind. Because different ions have different resonant frequencies, they receive different amounts of heating and acceleration as a function of radius, which is exactly what is required to understand the different features of the H I and O VI velocity distributions. Furthermore, because the ion-cyclotron wave dissipation is rapid, the extended heating seems to demand a constantly replenished population of waves over several solar radii. This suggests that the waves are generated gradually throughout the wind, rather than propagating up from the base of the corona.

In addition to measuring velocity and intensity oscillation, MDI also measures the line-of-sight component of the photospheric magnetic field. In long, uninterrupted MDI magnetogram series, a continuous flux emergence of small bipolar regions has been observed. Small magnetic bipolar flux elements are continually emerging at seemingly random locations. These elements are rapidly swept by granular and mesogranular flows to supergranular cell boundaries where they cancel and replace existing flux. The rate of flux generation of this 'magnetic carpet' (Fig. 16) is such that all of the flux is replaced in about 40 hours, with profound implications for coronal heating on the top side and questions of local field generation on the lower side of the photosphere. Estimates of the energy supplied to the corona by 'braiding' of large-scale coronal fields through small-scale flux replacement indicate that it is much larger than that associated with granular braiding.

Coronal Mass Ejections

LASCO has been collecting an extensive database for establishing the best statistics ever on coronal mass ejections (CMEs; Fig. 17) and their geomagnetic effects. St.Cyr et al. have reported the properties of all 841 CMEs observed by the LASCO C2 and C3 white-light coronagraphs from January 1996 through the SOHO mission interruption in June 1998 and compared those properties with previous observations by other instruments. The CME rate for solar-minimum conditions was slightly higher than had been reported for previous solar cycles, but both the rate and the

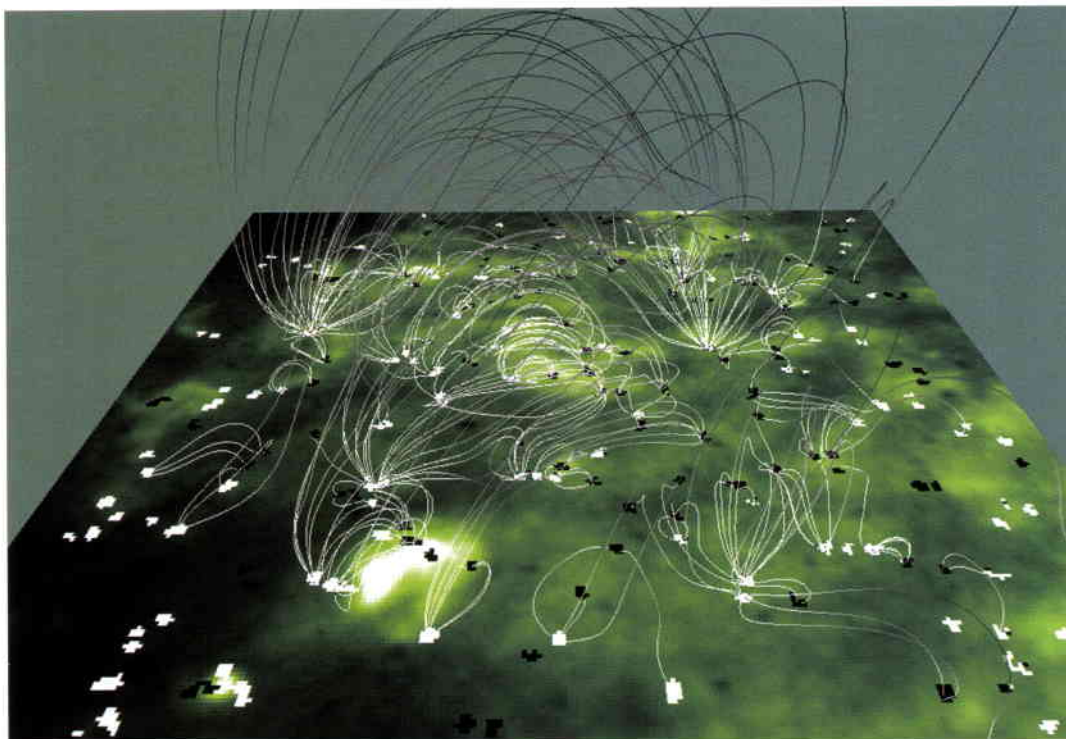


Figure 16. Magnetic carpet. Model of magnetic field lines based on MDI magnetograms, superimposed on an image of the solar corona in Fe XII 195 Å from EIT (courtesy of SOHO/MDI Consortium)

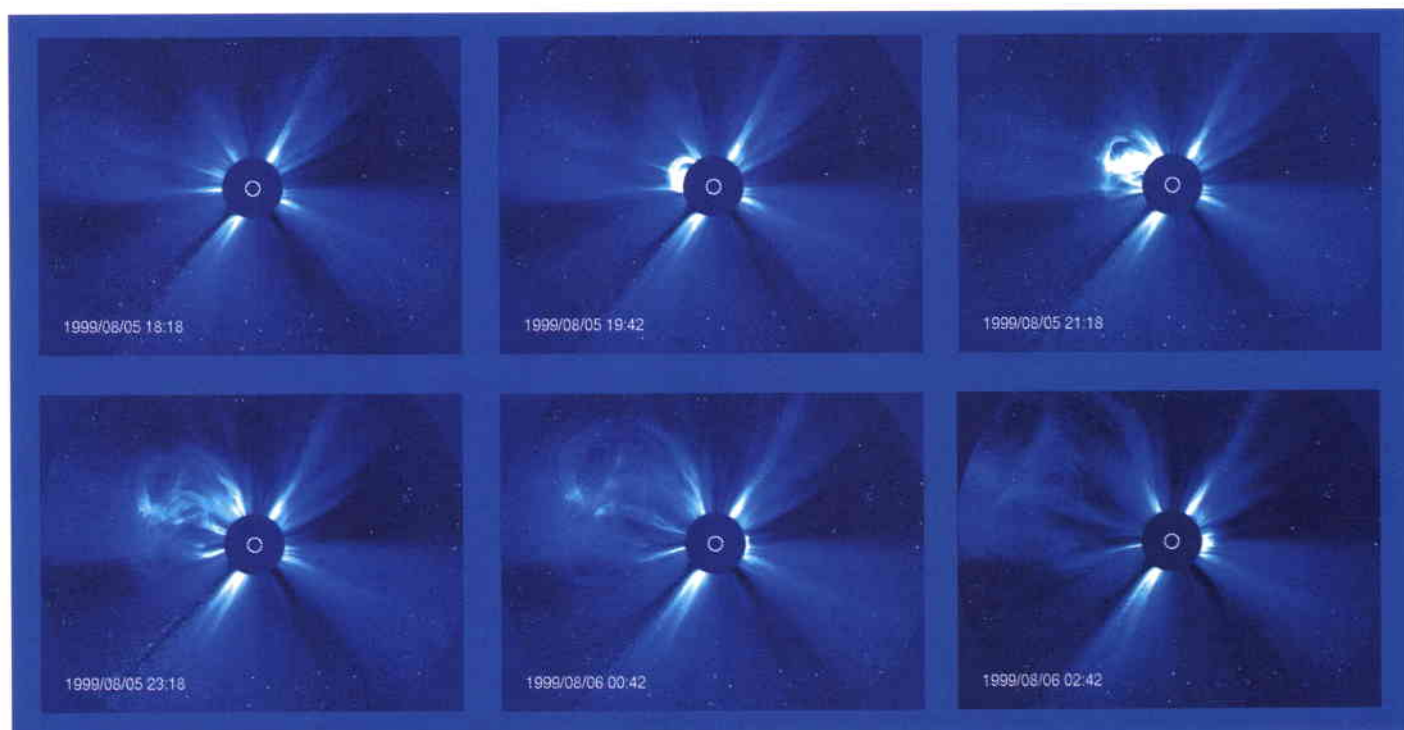


Figure 17. Progress of a Coronal Mass Ejection (CME) observed over an 8 h period on 5-6 August 1999 by LASCO C3. The dark disc blocks the Sun so that the LASCO instrument can observe the structures of the corona in visible light. The white circle represents the size and position of the Sun (courtesy of SOHO/LASCO Consortium)

distribution of apparent locations of CMEs varied during this period as expected. While the pointing stability provided by the SOHO platform in its L-1 orbit and the use of CCD detectors have resulted in superior brightness sensitivity for LASCO over earlier coronagraphs, they have not detected a significant population of fainter (i.e. low-mass) CMEs. The general shape of the distribution of apparent sizes for LASCO CMEs is similar to those of earlier reports, but the average (median) apparent size of 72° (vs. 50°) is significantly larger. St.Cyr et al. have also reported on a population

of CMEs with large apparent sizes, which appear to have a significant longitudinal component directed along the Sun-Earth line, either toward or away from the Earth. These are the so-called 'halo CMEs' (Fig. 18). Using full-disc EIT images, they found that 40 out of 92 of these events might have been directed towards the Earth. A comparison of the timing of those events with the Kp geomagnetic storm index in the days following the CME showed that 15 out of 21 (71%) of the Kp > 6 storms could be accounted for as SOHO LASCO/EIT front-side halo CMEs. Three more Kp storms may have

Figure 18. Massive 'halo' CME as recorded by LASCO C2 on 17 February 2000. Displayed here is a so-called 'running difference' image, showing the variation in brightness from one frame to the next (courtesy of SOHO/LASCO Consortium)

been missed during LASCO/EIT data gaps, bringing the possible association rate to 18 out of 21 (86%).

EIT has discovered large-scale transient waves in the corona, also called 'Coronal Moreton Waves' or 'EIT waves', propagating outward from active regions below CMEs. These events are usually recorded in the Fe XII 195 Å bandpass, during high-cadence (< 20 min) observations. Their appearance is stunning in that they usually affect most of the visible solar disc (Fig. 19). They generally propagate at speeds of 200–500 km/s, traversing a solar diameter in less than an hour. Active regions distort the waves locally, bending them towards the lower Alfvén speed regions. On the basis of speed and propagation characteristics, the EIT waves were associated with fast-mode shock waves. Another interesting aspect of these coronal Moreton waves is their association with the acceleration and injection of high-energy electrons and protons, as measured, for example, by COSTEP and ERNE.



Figure 19. Sequence of EIT difference images showing the intensity (density) enhancement and following rarefaction associated with a shock wave expanding across the solar disc from the site of the origin of a CME, recorded on 12 May 1997. A halo CME was observed by LASCO. These images were formed from the differences of successive images in the emission lines of Fe XII near 195 Å; this ion is formed at temperatures of about 1.5 million degrees. The wave front travels at speeds of ~ 300 km/s, typical of a fast mode Alfvén shock in the lower solar corona (from Thompson et al.)

Solar wind

Origin and speed profile of the fast wind

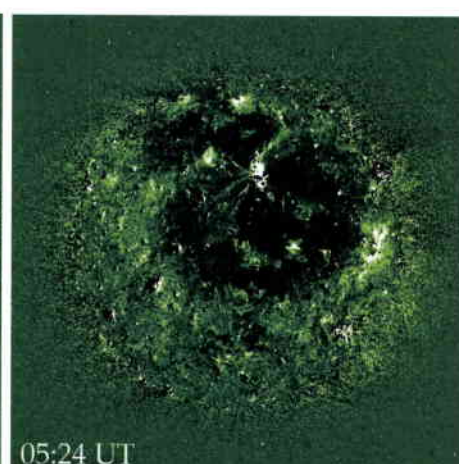
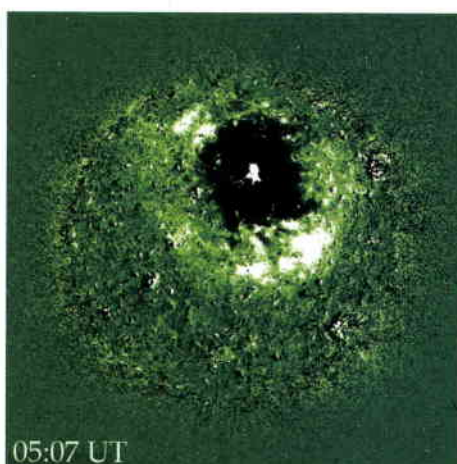
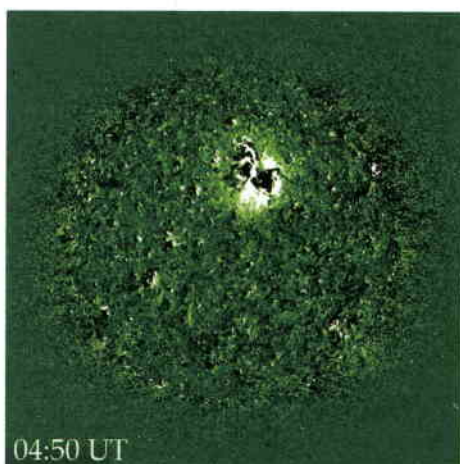
Coronal-hole outflow velocity maps obtained with the SUMER instrument in the Ne VIII emission line at 770 Å show a clear relationship between coronal-hole outflow velocity and the chromospheric network structure (Fig. 20), with the largest outflow velocities occurring along network boundaries and at the intersection of network boundaries. This can be considered the first direct spectroscopic determination of the source regions of the fast solar wind in coronal holes.

Proton and O VI outflow velocities in coronal holes have been measured by UVCS using the Doppler dimming method. The O VI outflow velocity was found to be significantly higher

than the proton velocity, with a very steep increase between 1.5 and 2.5 R_{\odot} , reaching outflow velocities of 300 km/s at around 2 R_{\odot} (Fig. 21). While the hydrogen outflow velocities are still consistent with some conventional theoretical models for polar wind acceleration, the higher oxygen flow speeds cannot be explained by these models. A possible explanation is offered by the dissipation of high-frequency Alfvén waves via gyroresonance with ion-cyclotron Larmor motions, which can heat and accelerate ions differently depending on their charge and mass.

Speed profile of the slow solar wind

Time-lapse sequences of LASCO white-light coronagraph images give the impression of a continuous outflow of material in the streamer belt. Density enhancements, or 'blobs', form near the cusps of helmet streamers and appear to be carried outward by the ambient solar wind. Sheeley et al., using data from the LASCO C2 and C3 coronagraphs, have traced a large number of such 'blobs' from 2 to over 25 solar radii. Assuming that these 'blobs' are carried away by the solar wind like leaves on



the river, they have measured the acceleration profile of the slow solar wind, which typically doubles its speed from 150 km/s near 5 R_{\odot} to 300 km/s near 25 R_{\odot} . They found a constant acceleration of about 4 ms^{-2} through most of the 30 R_{\odot} field-of-view. The speed profile is consistent with an iso-thermal solar-wind expansion at a temperature of about 1.1 MK and a sonic point near 5 R_{\odot} .

Solar-wind composition

Using data from the CELIAS/MTOF sensor, the CELIAS team has made the first in-situ determination of the isotopic composition of calcium and nitrogen in the solar wind. These measurements are important for studies of stellar modelling and Solar System formation, because the present-day solar Ca isotopic abundances are unchanged from their original isotopic composition in the solar nebula. The isotopic ratios $^{40}\text{Ca}/^{42}\text{Ca}$ and $^{40}\text{Ca}/^{44}\text{Ca}$ measured in the solar wind were found to be consistent with terrestrial values. The isotope ratio $^{14}\text{N}/^{15}\text{N}$ was found to be 200 ± 60 , indicating a depletion of ^{15}N in the terrestrial atmosphere compared to solar matter.

Ion freeze-in temperatures were measured by CELIAS/CTOF with a time resolution of 5 min. These measurements indicate that some of the filamentary structures of the inner corona observed in $\text{H}\alpha$ survive in the inter-planetary medium as far as 1 AU.

The unprecedented time resolution of the CELIAS/CTOF data has allowed a fine-scaled study of the elemental Fe/O ratio as a function of the solar-wind bulk speed. Since Fe is a low First Ionisation Potential (FIP) element and O a high-FIP element, their relative abundance is diagnostic for the so-called 'FIP fractionation process'. The Fe/O abundance shows a continuous decrease with increasing solar-wind speed by a factor of two between 350 km/s and 500 km/s, in correspondence with the well-established FIP effect.

Comets

SOHO is not only providing new measurements about the Sun. On 4 February 2000, SOHO discovered its 100th comet, 93 of which belong to the Sun-grazing Kreutz family (Fig. 22). A particular feature is the presence of a dust tail for only a few Sun grazers. Analysis of the light curves is used to investigate the properties of the nuclei (size, fragmentation, destruction) and the dust production rates.

Thanks to rapid communication from the LASCO group and the near-real-time observing capabilities of the SOHO instruments, UVCS could make spectroscopy measurements of

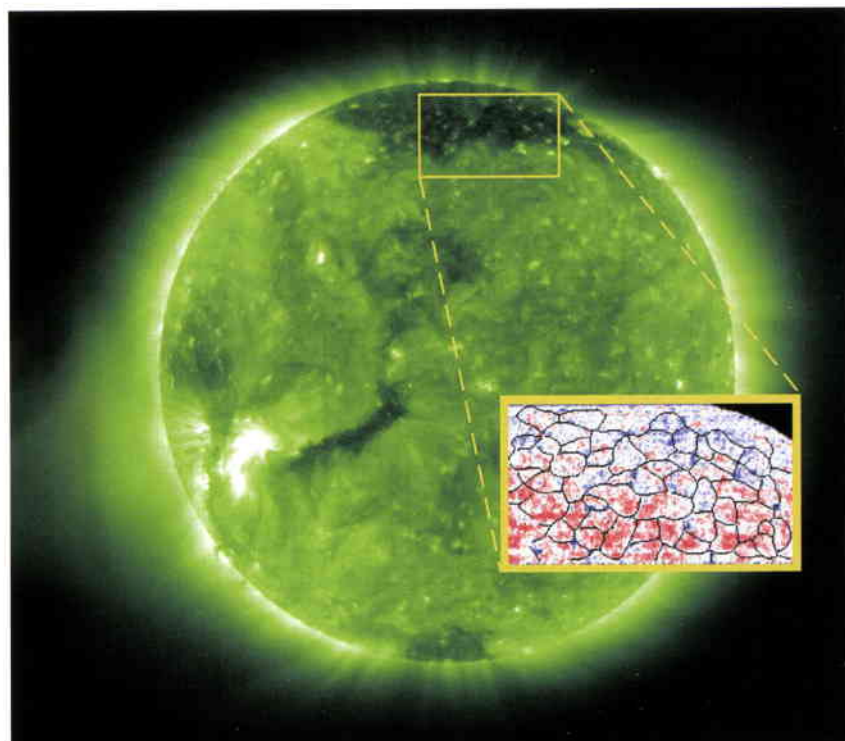


Figure 20. Source regions of the fast solar wind. Background: EIT full-Sun image taken in the emission line of Fe XII 195 Å, revealing gas at 1.5 million degrees shaped by magnetic fields. Bright regions indicate hot, dense plasma loops with strong magnetic fields, while dark regions imply an open magnetic field geometry, and are the source of the high-speed solar wind. The 'zoomed-in' or 'close-up' region shows a Doppler velocity map of plasma at about 630 000 K at the base of the corona, as recorded by SUMER in the Ne VIII emission line at 770 Å. Blue represents blue shifts or outflows and red represents red shifts or downflows. The blue regions are inside a coronal hole, or open magnetic field region, where the high-speed solar wind is accelerated. Superposed are the edges of 'honeycomb-shaped' patterns of magnetic fields at the surface of the Sun (from Hassler et al.)

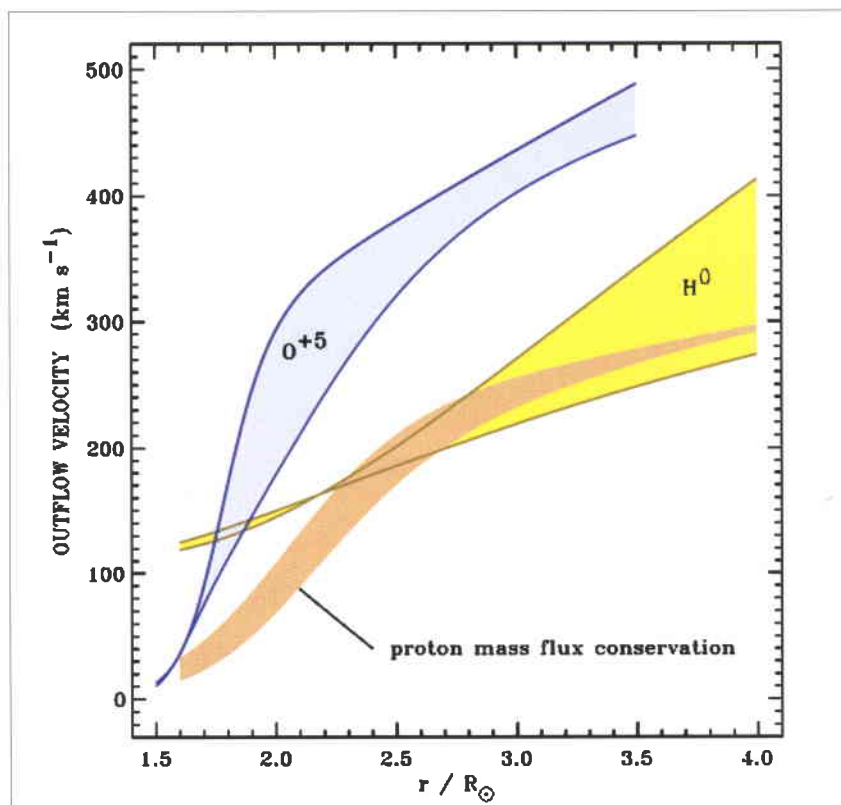


Figure 21. Empirical outflow velocity of O VI and H I in coronal holes over the poles (from Kohl et al.)

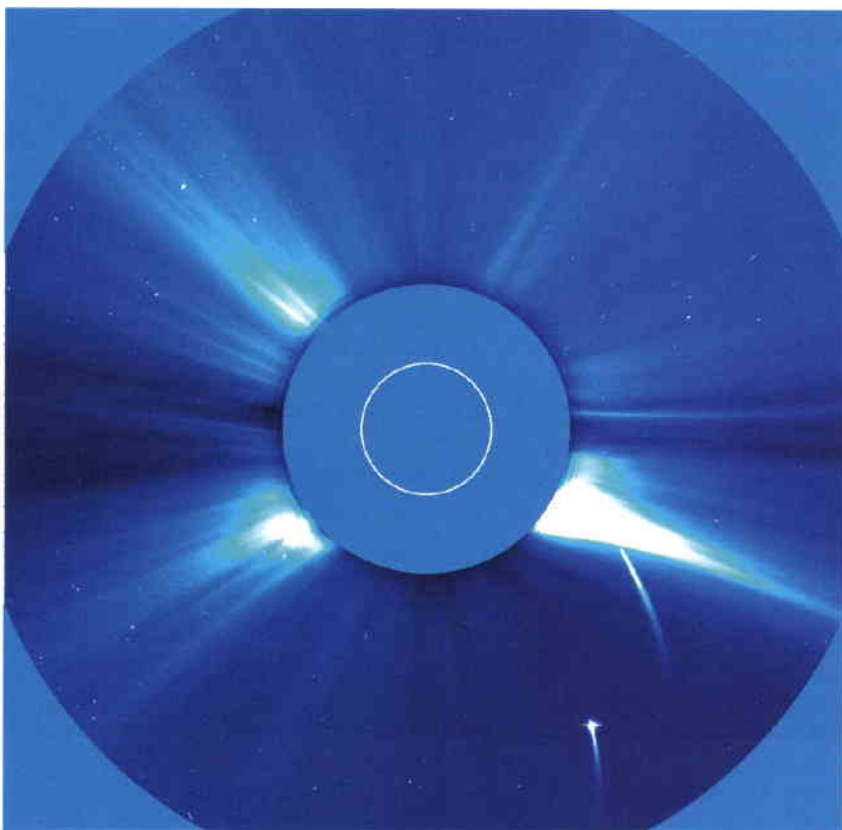


Figure 22. LASCO sees two comets plunge into the Sun. In a rare celestial spectacle, two comets were observed by the LASCO coronagraph plunging into the Sun's atmosphere in close succession, on 1 and 2 June 1998. Science instruments on SOHO have discovered more than 100 comets, including many so-called 'Sun grazers', but none in such close succession (courtesy of SOHO/LASCO Consortium)

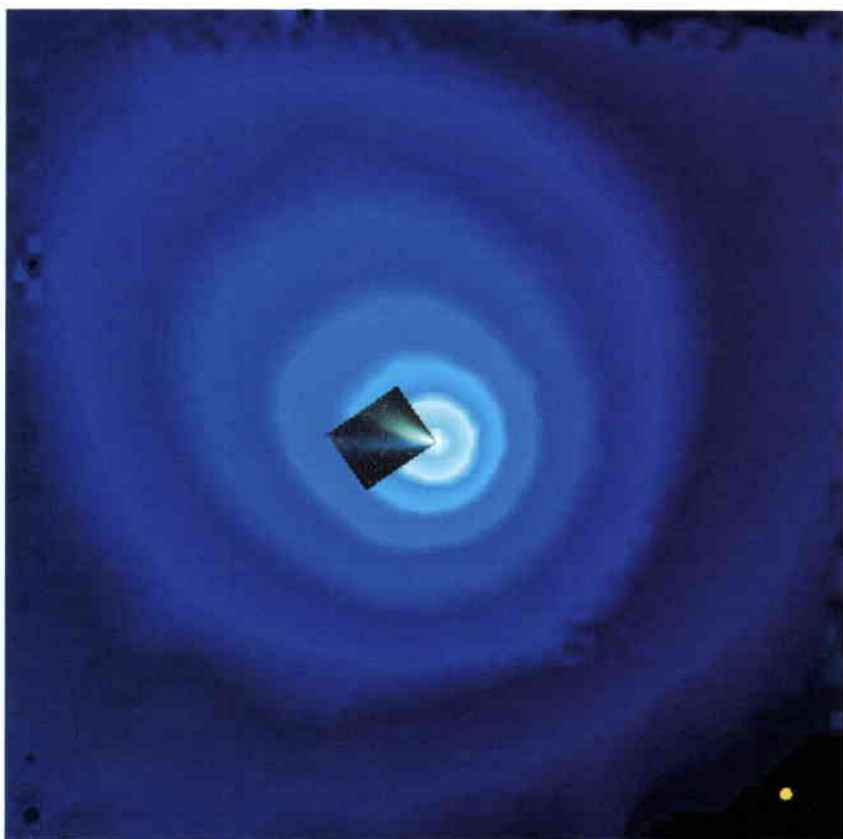


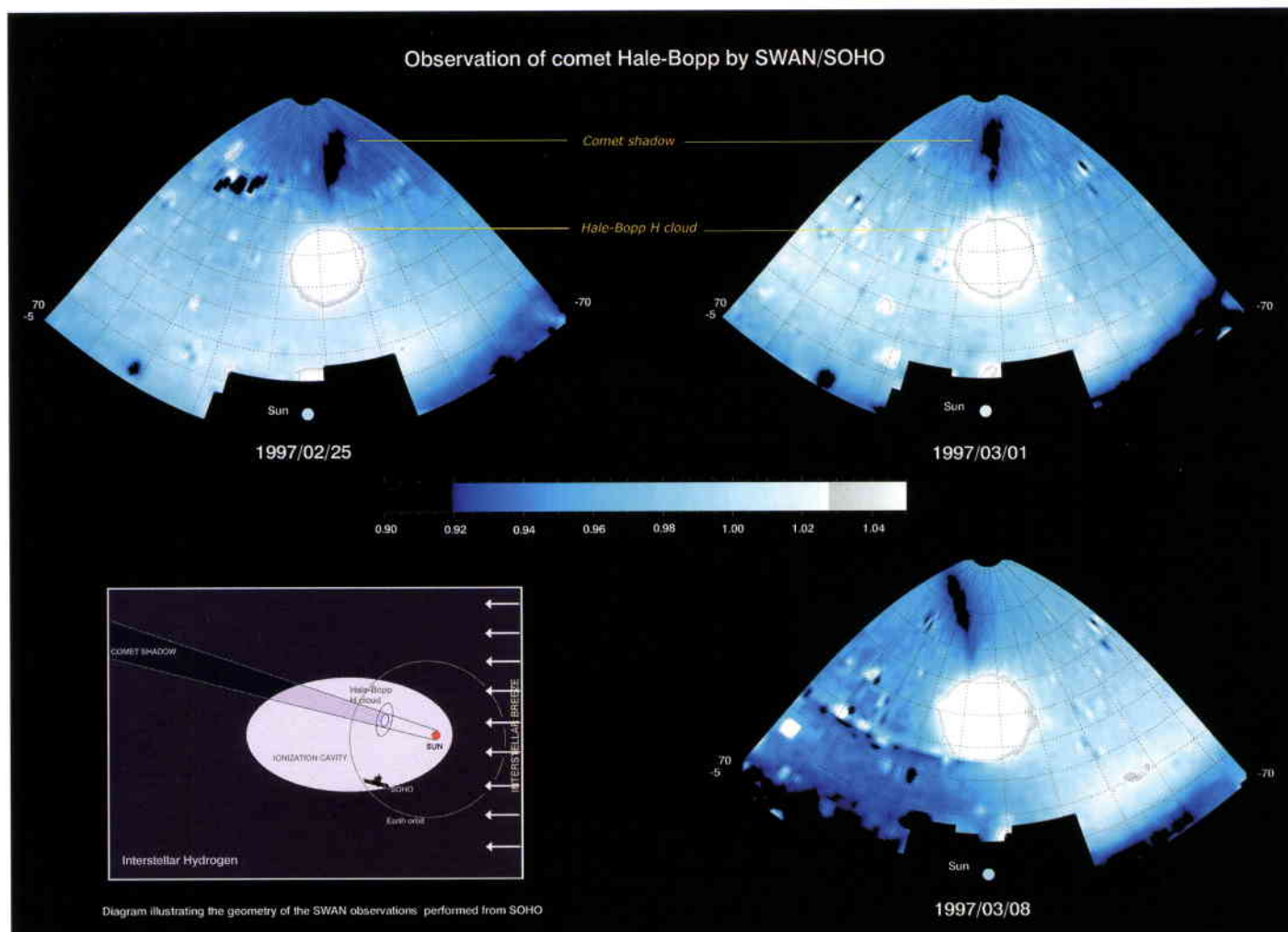
Figure 23. SWAN H I Ly- α image of the huge cloud of hydrogen surrounding comet Hale-Bopp when it neared the Sun in the spring of 1997. The small yellow dot shows the Sun to scale (from Combi et al.)

several comets on the day of their discovery. UVCS measurements of comet C/1996Y1 obtained at $6.8 R_{\odot}$ confirmed the predictions of models of the cometary bow shock driven by mass-loading as cometary molecules are ionised and swept up in the solar wind. From the width and shift of the line profiles, the solar-wind speed at $6.8 R_{\odot}$ could be determined (640 km/s). The outgassing rate of the comet was estimated at 20 kg/s, implying an active nucleus area of only about 6.7 m in diameter and a mass of about 120 000 kg.

Comets are surrounded by large clouds of hydrogen, produced by the break-up of water molecules evaporating from the comets' ice. The solar-wind mapper SWAN sees these large clouds of hydrogen glowing in the light of the H I Lyman- α line. The huge cloud of hydrogen surrounding Comet Hale-Bopp (Fig. 23) during its perihelion passage in the spring of 1997 was more than 100 million kilometres wide, diminishing in intensity outwards (contour lines). It far exceeded the great comet's visible tail (inset photograph). Although generated by a comet nucleus perhaps only 40 km in diameter, the hydrogen cloud was 70 times wider than the Sun itself (yellow dot to scale) and ten times wider than the hydrogen cloud of Comet Hyakutake observed by SWAN in 1996. The water evaporation rate of Hale-Bopp was measured by SWAN at more than 200 million tons per day. Comet Wirtanen, the target for ESA's Rosetta mission (2003), pumped out water vapour at a rate of 20 000 tons a day during its most recent periodic visit to the Sun, according to the SWAN data. SWAN has also seen something else extraordinary – the biggest shadow ever observed in our Solar System, namely that of a comet projected on the sky behind it (Fig. 24).

Heliosphere

The Sun is moving through the Local Interstellar Cloud (LIC) at about 26 km/s. The solar wind builds a cavity, the heliosphere, within the ionised gas component of the LIC. The neutral atoms (e.g. He) of the LIC, on the other hand, enter the heliosphere unaffected. The He flow properties are now well-constrained from a series of measurements ($v_{\text{He}} = 25.5 \pm 0.5$ km/s, $T_{\text{He}} = 6000 \pm 1000$ K). These values are in agreement with the LIC velocity and temperature deduced from stellar spectroscopy. Hydrogen, on the other hand, is expected to be affected by coupling with the decelerated plasma via charge-exchange. Neutral hydrogen heating and deceleration therefore provides a measurement of this coupling and, in turn, of the plasma density in the LIC, which is responsible for most of the heliosphere's confinement.



The SWAN team, analysing data from absorption cells, found hydrogen temperatures T_0 of $11\,500 \pm 1500$ K, i.e. significantly above the temperature of the interstellar He flow (6000 ± 1000 K), requiring strong heating of more than 3500 K at the heliosphere interface. Part of this excess temperature is probably due to radiative-transfer effects.

The apparent interstellar hydrogen velocity in the up- and downwind direction was measured to be -25.4 ± 1 km/s and $+21.6 \pm 1.3$ km/s, respectively, with the most precise determination (since model-independent) of the H flow direction. The new estimate of the upwind direction from SWAN measurements is 252.3 ± 0.73 deg and 8.7 ± 0.90 deg in ecliptic coordinates, which is off by about 3–4 deg from the He flow direction. The SWAN team speculates that this might be a sign of an asymmetry in the heliospheric interface due to the ambient interstellar magnetic field.

Comparing the above hydrogen temperature and velocity measurements by SWAN with heliospheric models leads to an estimate of the interstellar plasma density of $n_e \approx 0.04$ cm⁻³. It is interesting to note that the plasma frequency for $n_e \approx 0.04$ cm⁻³ is 1.8 kHz, i.e. exactly the

value of the remarkably stable cut-off frequency observed by Voyager.

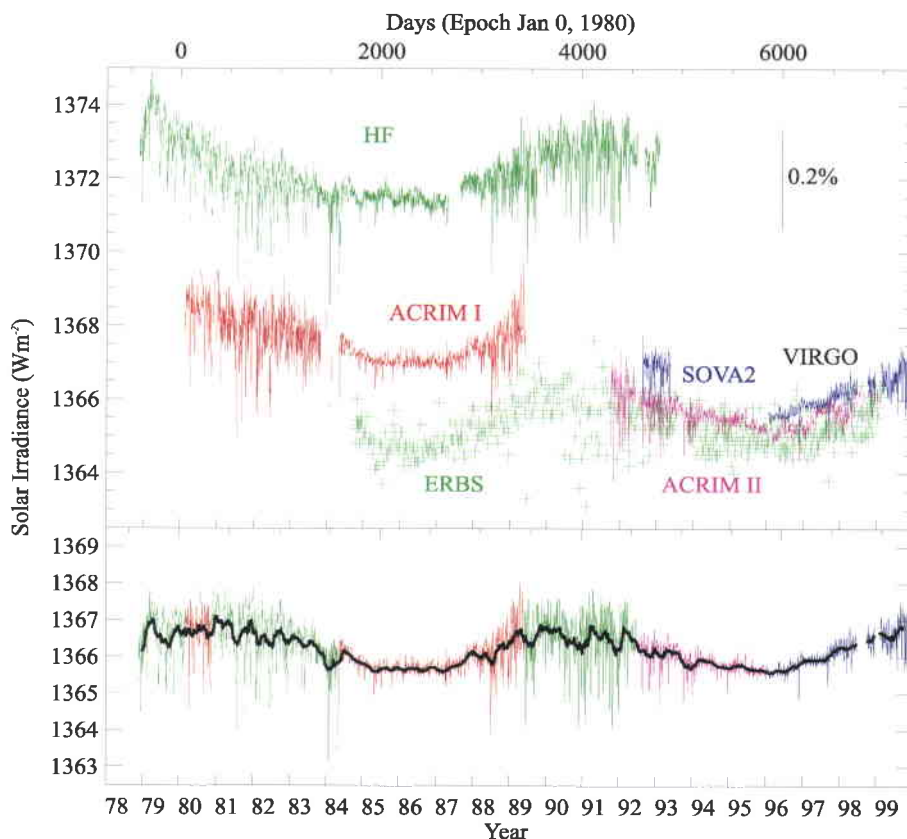
Of particular interest for future studies might be the temperature minimum measured between the upwind and downwind directions. Classical models predict a monotonic increase in the line-of-sight temperature from upwind to downwind. The authors interpret this behaviour as first evidence of the existence of two distinct populations at different velocities, as predicted by some heliosphere/interstellar-gas interface models. If confirmed, this should provide a good diagnostic of the interface.

Total solar irradiance variations

The VIRGO instrument on SOHO extends the record of Total Solar Irradiance (TSI) measurements into cycle 23. In Figure 25, measurements from six independent space-based radiometers since 1978 (top) have been combined to produce the composite TSI over two decades (bottom). They show that the Sun's output fluctuates during each 11-year sunspot cycle, changing by about 0.1% between maxima (1980 and 1990) and minima (1987 and 1997) in solar activity. Temporary dips of up to 0.3% and a few days duration are the result of large sunspots passing over the

Figure 24. SWAN observations of comet Hale-Bopp's shadow (courtesy of SOHO/SWAN Consortium)

Figure 25. Total solar irradiance variations from 1978 to 1999. The data are from the Hickey-Frieden (HF) radiometer of the Earth Radiation Budget (ERB) experiment on Nimbus-7 (1978-1992), the two Active Cavity Radiometer Irradiance Monitors (ACRIM I and II) aboard the Solar Maximum Mission (1980-1989) and the Upper Atmosphere Research Satellite (1991-), respectively, and the VIRGO radiometers on SOHO (1996-). Also shown are the data from the radiometer on the ERB (1984-), and SOVA2 as part of the Solar Variability Experiment on the European Retrievable Carrier (1992-1993) (from Quinn and Fröhlich)



visible hemisphere. The larger number of sunspots near the peak in the 11-year cycle is accompanied by a general rise in magnetic activity that creates an increase in the luminous output which exceeds the cooling effects of sunspots. Offsets between the various data sets are the direct result of uncertainties in the absolute radiometer scale of the radiometers ($\pm 0.3\%$). Despite these biases, each data set clearly shows varying radiation levels that track the overall 11-year solar activity cycle.

Conclusions

SOHO set out to tackle three broad topics in solar and heliospheric physics: the structure and dynamics of the solar interior, the heating and dynamics of the solar corona, and the acceleration and composition of the solar wind. In all three areas, its observations have allowed great strides to be made in our understanding of the diverse physical processes at work in our Sun. This has been made possible by the comprehensive suite of state-of-the-art instruments mounted on the superb and stable SOHO spacecraft, operating from the unique vantage point of the L1 halo orbit.

In such complex areas of research as solar physics, progress is not made by just a few people acting in a vacuum. The scientific achievements of the SOHO mission are the results of a concerted, multi-disciplinary effort by a large international community of solar scientists, involving sound investments in

space hardware, coupled with a vigorous and well-coordinated scientific operation and interpretation effort. The interplay between theory and observations has already provided many new insights and will continue to do so for many years.

With the wealth of SOHO data already in the archive (and many more data yet to come, hopefully well beyond the next solar maximum), we should be able to unravel even more of the mysteries of our closest star.

Acknowledgements

The great success of the SOHO mission is a tribute to the many people who designed and built this exquisite spacecraft and these excellent instruments, and to the many people who diligently work behind the scenes to keep it up and running. Special thanks go to: Harold W. Benefield and his AlliedSignal Flight Operations Team; Helmut Schweitzer and Jean-Philippe Olive from the ESA/MMS Technical Support Team; the Science Operations Co-ordinators Laura Roberts, Joan Hollis and Piet Martens; Craig Roberts, John Rowe and their colleagues from Flight Dynamics, the colleagues from DSN, and, last but not least, to Francis Vandembussche and his recovery team for making a miracle come true!

The Second Report by ESA's Long-Term Space Policy Committee (LSPC)

G. Naja

Directorate of Strategy and Technical Assessment, ESA, Paris

Background

The Long-term Space Policy Committee was created by the ESA Council in 1993 and submitted its First Report to the ESA Council at Ministerial Level in Toulouse (F) in October 1995. It was unanimously endorsed by the Ministers, who requested that the Committee continue its reflections and prepare a Second Report as a framework for a long-term European Space Policy.

The Second Report by ESA's Long-term Space Policy Committee has provided the Agency's Member States with a comprehensive framework for long-term strategic thinking and decision making on European space policy. Many of the ideas proposed in the Action Plan contained in this Second Report are already being pursued and put into practice within the Agency.

The Committee thus worked from 1996 to early 1999 to prepare that Second Report. In it, three 'challenges' have been identified that Europe has to face now, at the dawn of the new century. The first is the 'Challenge of Independence' – to ensure that Europe is not strategically dependent in particular key areas like navigation, information services or peace-keeping. The second is the 'Challenge of Planetary Management' – to secure Europe's leading position in the worldwide effort directed towards achieving a better understanding of our planet, a cleaner environment, and sustainable development for all to share. The third is the 'Challenge Beyond': in a longer term perspective, humanity will have to expand into space and to use its resources, and Europe must be a major player in this

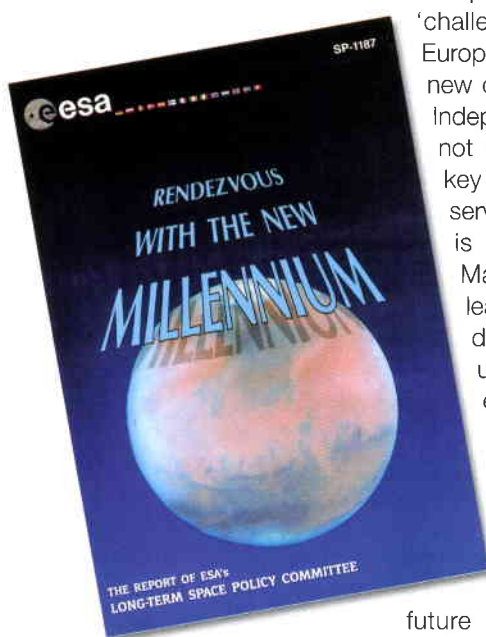
future effort. The Committee's work highlighted the fact that Europe needs an ambitious space policy and programmes to respond properly to these three challenges and to play a role on the world stage commensurate with its economic weight and cultural heritage.

The Committee also drew up an 'Action Plan' as an integral part of its Report. Tomorrow's successes depend on actions initiated today, and the LSPC's Action Plan therefore aims to deliver a clear sign that Europe has understood the upcoming challenges and is preparing to face them. The twenty actions proposed are modest in funding, but each represents a first step in a promising field in which Europe must demonstrate and establish its presence.

This Second Report, together with its Action Plan, was presented to the ESA Council Meeting at Ministerial Level in Brussels in May 1999. The Ministers welcomed the Report and invited the Director General 'to prepare and submit to the Council at Delegate Level an assessment and implementation plan for the actions listed in the Report'. A proposal for the implementation of the LSPC's Action Plan was therefore presented to and discussed at the ESA Council meeting on 14 December. Delegations generally welcomed the implementation plan. A number believed, however, that since no new money could be made available, there was a need to prioritise within existing budgets and that the different Actions should therefore be considered, discussed and decided upon by the appropriate Programme Boards. Council also requested that it be given a report at a subsequent meeting on the progress of those discussions in the various Programme Boards, and the Actions that are starting to be implemented as a result.

Why must Europe invest in space?

Over the forty years of the space era, space has already transformed daily life, thanks to the quality and efficiency of such space-based services as telecommunications, broadcasting, weather forecasting and navigation. Space has also enabled quantum leaps to be made in our knowledge of our planet and of the Universe, fulfilling scientists' wildest aspirations. Indeed, space data have modified our view of Earth and have led to a new understanding of our planet and the complex interactions of its oceans,



The LSPC's First Report (ESA SP-1187, October 1995)



The LSPC's Second Report
(ESA SP-2000, May 1999)

land masses and atmosphere. Space systems have thus become crucial to the understanding and management of our planet, to the provision of goods and services in the global marketplace, and to regional and global security and peacekeeping. They are also the source of a large number of highly skilled jobs: space employs about 35 000 people directly in Europe, and an estimated 400 000 indirectly.

The LSPC's basic assumption was that in the 21st Century an enlarged European Union will want to play a leading political and economic role commensurate with its size, wealth and cultural heritage. In order for Europe to fulfil this role, a full space capability is essential, including the associated industrial capabilities. A full space capability means the freedom to access space and to define, build and operate complete space systems in all strategic areas. As the American example shows, this capability is increasingly being used as an instrument for and integral part of overall political, economic and military leadership.

Europe already possesses certain elements of this capability, in particular in the fields of science, launchers and applications, but these need to be sustained and expanded as a basis for continued success. However, Europe is falling behind in key applications of space technology, in which it must acquire real strategic independence. Europe must also continue to be a leading partner in global cooperation on space systems for research into and monitoring of the Earth's ecosystem. Beyond that, Europe has to be able to lead in some areas of future commercial space applications. Success in the potentially huge

space market requires forward-looking policies and investments that go beyond short-term commercial concerns.

Last but not least, in order to prepare itself for the future Europe must also invest in ideas and concepts that will lay the foundations for as yet unforeseen applications, and contribute to its future as a leading global power in the 21st Century.

It was against this background that the LSPC identified its three main challenges that Europe will have to face and respond to in the next few years. The short-term challenge – the Challenge of Independence – is clear. Europe has to consolidate and expand its overall space capability, avoiding reliance on others in strategic areas of space. The medium-term challenge – the Challenge of Planetary Management – aims at responding to threats to the planet's environment. Europe must be a major and responsible player in the worldwide effort to ensure the sustainability of civilisation on planet Earth. The longer-term challenge – the Challenge Beyond – is for Europe to play its role in the future exploitation of the resources of space and man's expansion into the Solar System.

To start to respond to these challenges, the Committee's Action Plan contains 'Twenty Actions for Year 2001'. Each of these twenty initiatives includes a first step that can be implemented quickly and at moderate cost (see Tables 1, 2 and 3).

Proposed implementation of the Action Plan

The Action Plan itself can be organised around three key themes, which are the following:

Global security

This theme involves the traditional meaning of 'security', as well as newer concepts of environmental security in the widest sense. Thus it also involves all actions aimed at promoting a clean and safe environment for Earth and human activities. The relevant LSPC-proposed actions are: Action 5 - European Systems for Security and Peacekeeping, Action 9 - Space Monitoring of Compliance with Environmental Regulations, Action 10 - Disaster Warning from Space, Action 11 - Space Weather, Action 12 - Space Debris, Action 13 - Threat of Cosmic Collision, and Action 17 - Weather Modification from Space.

Exploration

This theme involves all Actions relating to the longer-term objective of exploration of the Solar System, working towards an eventual manned

Table 1. Global Security Actions

| Action | Implemented/On-going | Supplementary Action | Follow-on Steps |
|---|---|--|---|
| European Systems for Security and Peacekeeping (5) | Synergy assessments (SAR images utilisation), contacts with WEU | Technological studies for dual-use | Technological developments |
| Space Monitoring of Compliance with Environmental Regulations (9) | Study on Kyoto Protocol requirements. Needs for space observations | Enlarging on-going study to include air-based elements | |
| Disaster Warning from Space (10) (earthquakes and volcanoes) | Numerous pilot projects (ERS) on disaster management and prediction | Study on earthquake-prediction methodology. Similar study for volcanic eruptions | Operational-service feasibility study |
| Space Weather (11) | Workshop autumn 1999; start of a study on space-weather programme; ESA internet server established | Next step: extension of data-distribution infrastructure for operational service, extension of orbital data-gathering means | |
| Space Debris (12) | Coordination meetings with partners; maintenance of database; study on forecasting and mitigation means | Increased effort on development of mitigation measures and of independent means of verification | |
| Threat of Cosmic Collision (13) | Study of global network for research on NEOs; IMPACT workshop (adoption of Torino Scale); assessment of spaceborne system; use of ISS | Host the Spaceguard Central Node in ESRIN; study feasibility of an annual contest between European astronomers for detection of close NEOs | |
| Weather Modification from Space (17) | SE&U study: use of microwave energy from space | International Workshop on the subject | Assessment study, including risk assessment |

Table 2. Exploration Actions

| Action | Implemented/On-going | Supplementary Action | Follow-on Steps |
|---|--|--|--|
| Search for Earth-like Planets (1) | IRSI/Darwin mission-feasibility studies; discussions with NASA on international cooperation; experiments for ISS | | Large interdisciplinary workshop |
| Innovative Space Station Utilisation (3) | Activities on ISS as assembly platform; use of inflatable technologies; ISS Utilisation Conference | Session of ISS Utilisation Conference dedicated to innovative uses | |
| Small Business Innovation Initiative (7) | ESA SME Initiative | | Increase financial level of SME Initiative |
| Micro-miniaturisation Technology Initiative (8) | EC's Network for Excellence for Functional Microsystems; TRP axis; GSTP; GSP studies | | |
| Telepresence Demonstration Project (14) | Numerous studies and activities concerning Mars exploration in GSP, TRP, GSTP; robotic activities within ISS Programme | Check applicability of on-going studies and activities to robotic Moon exploration | Demonstration programme |
| European Lunar Initiative (15) | Lunar Exploration and Exploitation Conference in July 2000 | | |
| Space Energy and Resources | System-level study in SE&U study performed | Technological watch, study of demonstration opportunities | Phase-A/B study of demonstration mission |

Table 3. Enabling Factors and Organisational Aspects

| Action | Implemented/On-going | Supplementary Action | Follow-on Steps |
|---|--|---|---|
| Cheaper Access to Space (2) | FLTP studies and activities | Feasibility study on airborne launch systems, semi-reusable | Joint venture with international partners |
| Future Navigation Services (4) | On-going activities on EGNOS and Galileo programmes | Call for ideas within ARTES for innovative applications | |
| Creation of a European Telecom. Regulatory Body (6) | | Re-open the question together with EC; technical support to be provided by ESA | |
| European Space Education Programme (18) | Office for Education Project Outreach Activities | Progressive raising of financial level of activities. Organisation of a "Space Day" in European schools | |
| Public Awareness Initiative (19) | ESA Image Study; implementation of study recommendations | Further implementation of recommendations of the Study; creation of country desks. Revision of ESA Web Site | |
| European Space Policy Institute (20) | Informal contacts taken regarding location | Call for Proposals from Member States for hosting the Institute | |

mission. It therefore also includes Actions aiming at encouraging and stimulating innovation, whether by use of the Space Station or by a specific programme focusing on small- and medium-sized enterprises. The relevant LSPC-proposed actions are: Action 14 - Telepresence Demonstration Project, Action 15 - European Lunar Initiative, Action 16 - Space Energy and Resources, Action 7 - Small Business Innovation Initiative, Action 8 - Micro-miniaturisation Technology Initiative, Action 3 - Innovative Space Station Utilisation, and Action 1 - Search for Earth-like Planets.

Enabling factors and organisational aspects

This third theme involves conditions for success of the European space programme in general. The Actions concerned are very diverse in nature and content: for instance the creation of a regulatory body for telecommunications, the reflection on future commercial services associated with a European Navigation Satellite Programme, a European Space Education Programme, and low-cost access to space investigating airborne launchers. This theme therefore embraces: Action 2 - Cheaper Access to Space, Action 4 - Future Navigation Services, Action 6 - Creation of a European Telecommunications Regulatory Body, and Actions 18, 19 and 20 - European Space Education Programme, Public-Awareness Initiative and European Space Policy Institute.

Clearly, several Actions are of a general nature and of strong interest to the Agency and the European space community. A number of Actions have already been started while the LSPC was still completing its work, based on

the Committee's reflections. Supplementary actions have to be initiated rapidly.

The three accompanying tables summarise for each group of Actions – global security, exploration, enabling factors and organisational matters – what is already in progress and what 'Supplementary Actions' need to be initiated rapidly. Ways of funding these Supplementary Actions will be proposed at a future Council. The 'Follow-on Steps' identify the work that remains to be done once the Supplementary Actions have been completed.

Conclusion

Successful implementation of the LSPC's proposed Action Plan is essential for the overall future of space activities in Europe. History has shown on numerous occasions that those nations that cease to explore and conquer the unknown, usually for economic reasons, ultimately lose out both politically and economically. Indeed space is not only about return on investments, but also about new dimensions to be explored and new discoveries to be made, thus responding to one of man's deepest needs. Moreover, the history of space endeavours has proved that the greatest technological advances, eventually leading to spin-offs and wealth-generation in other economic sectors, are often achieved in the most far-reaching programmes. If Europe wants to play a global role in economic development, peace-keeping, protection of the environment, and information collection and distribution, successful implementation of the LSPC's Action Plan could well prove to be a critical factor.

ASAR – Envisat’s Advanced Synthetic Aperture Radar

Building on ERS Achievements towards Future Earth Watch Missions

Y-L. Desnos

Earth Observation Applications Department, ESA Directorate of Application Programmes, ESRIN, Frascati, Italy

C. Buck, J. Guijarro, J-L. Suchail and R. Torres

Envisat System and Payload Division, ESA Directorate of Application Programmes, ESTEC, Noordwijk, The Netherlands

E. Attema

Earth Sciences Division, ESA Directorate of Application Programmes, ESTEC, Noordwijk, The Netherlands

The mission

The Envisat mission is an important element in providing the long-term, continuous data sets that are so crucial for addressing environmental and climate issues. At the same time, it will further promote the transfer of applications of remote-sensing data from experimental to pre-operational and operational exploitation.

Following on from the highly successful ERS-1/2 SARs, which have contributed to major scientific achievements and initiated pre-operational and commercial applications of SAR data, ESA is now ready to launch Europe’s largest remote-sensing satellite to date, carrying an Advanced Synthetic Aperture Radar (ASAR).

The ASAR is an all-weather, day-and-night high-resolution radar-imaging instrument. Compared with the ERS SAR, it features extended observational capabilities, three new modes of operation and improved performances. The ASAR system has been designed to provide continuity with ERS SAR, but also to extend the range of measurements through the exploitation of its various operating modes and the development of new algorithms and data products. The Envisat ground segment will allow the generation of near-real-time and off-line precision images to satisfy the needs of the scientific, institutional and commercial data users.

The mission has both ‘global’ and ‘regional’ objectives, with the corresponding need to provide data to scientific and applications users on various time scales. Important contributions by ASAR to the global mission include:

- measuring sea-state conditions at various scales
- mapping ice-sheet characteristics and dynamics
- mapping sea-ice distribution and dynamics

- detecting large-scale vegetation changes
- monitoring natural and man-made pollution over the oceans.

ASAR is set to make a major contribution to the regional mission by providing continuous and reliable data sets for applications such as:

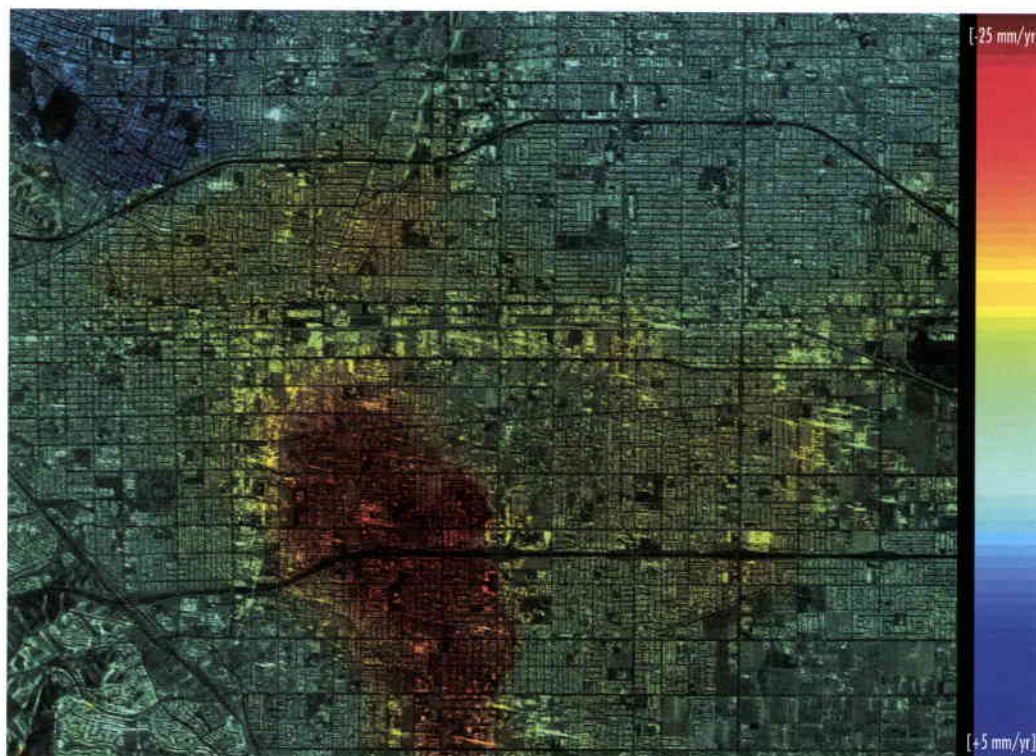
- offshore operations in sea ice
- snow and ice mapping
- coastal protection and pollution monitoring
- ship traffic monitoring
- agriculture and forest monitoring
- soil-moisture monitoring
- geological exploration
- topographic mapping
- predicting, tracking and responding to natural hazards
- surface deformation.

Some of the regional objectives (sea-ice applications, marine pollution, maritime traffic, hazard monitoring, etc.) require near-real-time data products (within a few hours from sensing) generated according to user requests. Some others (e.g. agriculture, soil moisture, etc.) require fast turn-around data services (within a few days). The remainder can be satisfied with offline data delivery. As well as ASAR satisfying specific operational and commercial requirements, there will be major systematic data-collection programmes to build up archives for scientific research purposes.

Land

As a result of observing the land surface with the ERS SARs, a large number of land applications have emerged, several based on

Figure 1. ERS-SAR interferometry estimated displacement over POMONA using the permanent-scatterers technique: June 1992 to January 1999 (courtesy of Politecnico di Milano, Italy)



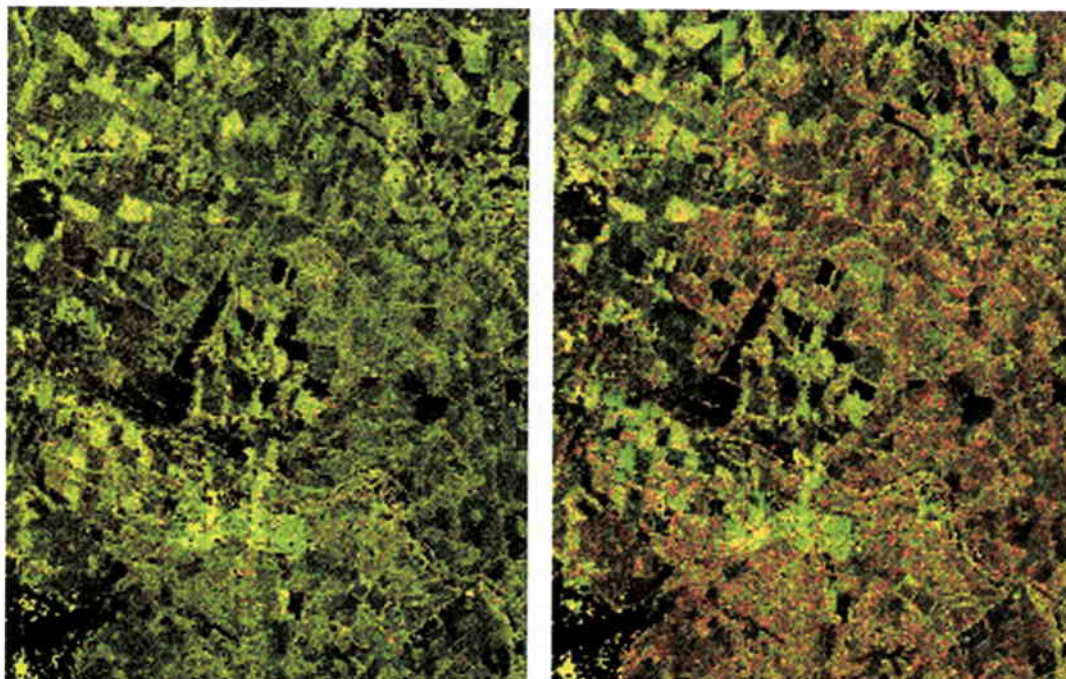
important developments in the field of SAR interferometry. SAR data are being used for agricultural monitoring, forest mapping, geological exploration and flood mapping, while INSAR measurements of topography and small topographic changes are making major contributions to environmental risk assessment involving earthquakes and land subsidence.

ASAR has extended observational capabilities in comparison to the ERS SAR, providing SAR mission continuity as well as benefiting from the results from ERS and other SAR missions. Operating in concert with other Envisat-1 instruments MERIS and AATSR, ASAR provides

essential surface-roughness and land-cover information for the determination of land-surface processes and air/sea interaction for climate studies.

The higher frequency of coverage provided by ASAR will improve greatly the value of SAR data for hazard monitoring, because locally infrequent events such as earthquakes, volcanic eruptions, floods and fires, require intensive observation over short periods. The beam steering mode will also permit (at least) 3-day repeat observations of certain localised events at high spatial resolution. Table 1 shows the average revisit frequency per 35-day orbit

Figure 2. Dual-polarisation SAR images of Thetford Forest (UK), from the SIR-C mission. Left image: HH (green) and VV (red). Right image: HH (green) and HV (red) (courtesy of GEC-Marconi, UK)



cycle as function of latitude and incidence angle (descending tracks only).

The potential value of the Global Monitoring mode is indicated by previous work carried out over land, using the ERS wind scatterometer at 25 km spatial resolution. For local land-cover mapping, ASAR high-resolution products will continue the role already established for ERS SAR in complementing conventional optical images from other satellites, particularly under poor solar-illumination conditions or in cloudy areas. The new features of ASAR include image acquisitions at multiple incidence angles and with dual polarisation, which will open up new possibilities in land-cover classification from SAR.

Ocean and ice

The original focus of the ERS missions was ocean and ice monitoring, and there has been an impressive range of scientific investigations in oceanography, polar science, glaciology and climate research which will be supported by ASAR. These include measurements of ocean surface features (currents, fronts, eddies, internal waves), directional ocean-wave spectra, sea-floor topography, snow cover and ice-sheet dynamics. Operational systems have been developed for mapping sea ice, oil-slick monitoring and ship detection.

Major features of the interaction between the ocean and the atmosphere are the creation of waves and ocean currents by surface winds. Wind and wave data are needed for climatological research, as inputs to meteorological models and for sea-state forecasting in support of marine operations. ASAR will provide observations of surface waves and winds over the ocean.

The ASAR Wave mode combined with a new algorithm called 'inter-look cross-spectral processing', whereby information on the wave propagation direction is computed from pairs of single-look images separated in time by typically a fraction of the dominant wave period, will provide meteorological users with wave directional and geophysical parameters and wind parameters.

Recently, investigations have shown that it is possible to derive wind-speed estimates from SAR data (see Fig. 3). The ASAR Wide Swath mode is of interest in this respect because of its large coverage area and the short revisit period.

Instrument operation

Measurement principle

The radar antenna beam illuminates the ground to the side of the satellite. Due to the satellite's

| Incidence Angle | Latitude | | | |
|-----------------|----------|-----|-----|-----|
| | 0° | 45° | 60° | 70° |
| No Constraints | 5 | 7 | 11 | 16 |
| ± 5° | 3 | 4 | 6 | 9 |
| ± 2° | 1 | 1.4 | 2 | 3 |
| Exact Repeat | 1 | 1 | 1 | 1 |

Table 1. Average revisit cycle per 35-day orbit as a function of latitude and incidence-angle variation, illustrating ASAR revisit time capability (descending path only)

| ASAR LAND APPLICATIONS | Image | Alternating Polarisation | Wide Swath | Global Monitoring |
|-----------------------------|----------|--------------------------|------------|-------------------|
| | HH or VV | HH/VV or VV/VH or HH/HV | HH or VV | HH or VV |
| Vegetation / Agriculture | Lighter | Lighter | Lighter | Lighter |
| Forestry | Lighter | Lighter | Lighter | Lighter |
| Land cover classification | Lighter | Lighter | Lighter | Lighter |
| Cartography | Lighter | Lighter | Lighter | Lighter |
| Topography Geomorphology | Lighter | Lighter | Lighter | Lighter |
| Hydrology / Soil moisture | Lighter | Lighter | Lighter | Lighter |
| Snow cover | Lighter | Lighter | Lighter | Lighter |
| Ice | Lighter | Lighter | Lighter | Lighter |
| Glacier | Lighter | Lighter | Lighter | Lighter |
| Tectonics | Lighter | Lighter | Lighter | Lighter |
| Land transformation process | Lighter | Lighter | Lighter | Lighter |
| Climate studies | Lighter | Lighter | Lighter | Lighter |

Table 2. ASAR modes and land-application themes (lighter colour indicates primary applications)

| ASAR OCEAN APPLICATIONS | Image | Alternating Polarisation | Wide Swath | Global Monitoring | Wave |
|-------------------------|----------|--------------------------|------------|-------------------|----------|
| | HH or VV | HH/VV or VV/VH or HH/HV | HH or VV | HH or VV | HH or VV |
| Weather forecasting | Lighter | Lighter | Lighter | Lighter | Lighter |
| Sea state forecasting | Lighter | Lighter | Lighter | Lighter | Lighter |
| Current modelling | Lighter | Lighter | Lighter | Lighter | Lighter |
| Internal wave modelling | Lighter | Lighter | Lighter | Lighter | Lighter |
| Offshore activities | Lighter | Lighter | Lighter | Lighter | Lighter |
| Ship routing | Lighter | Lighter | Lighter | Lighter | Lighter |
| Ship detection | Lighter | Lighter | Lighter | Lighter | Lighter |
| Fisheries | Lighter | Lighter | Lighter | Lighter | Lighter |
| Sea ice | Lighter | Lighter | Lighter | Lighter | Lighter |
| Oil pollution | Lighter | Lighter | Lighter | Lighter | Lighter |
| Coastal zone | Lighter | Lighter | Lighter | Lighter | Lighter |
| Bathymetry | Lighter | Lighter | Lighter | Lighter | Lighter |

Table 3. ASAR modes and ocean-application themes (lighter colour indicates primary applications)

motion, each target element remains within the illumination beam for a period known as the 'integration time'. As part of the on-ground processing, the complex echo signals received during this integration time are added coherently. This process is equivalent to a long antenna – so-called 'synthetic aperture' – illuminating the target. This synthetic aperture is equal to the distance the satellite has travelled during the integration time.

The along-track (equivalent to the azimuth in the ground processing) resolution obtainable with the SAR principle is half the physical antenna length. The resolution achieved can be

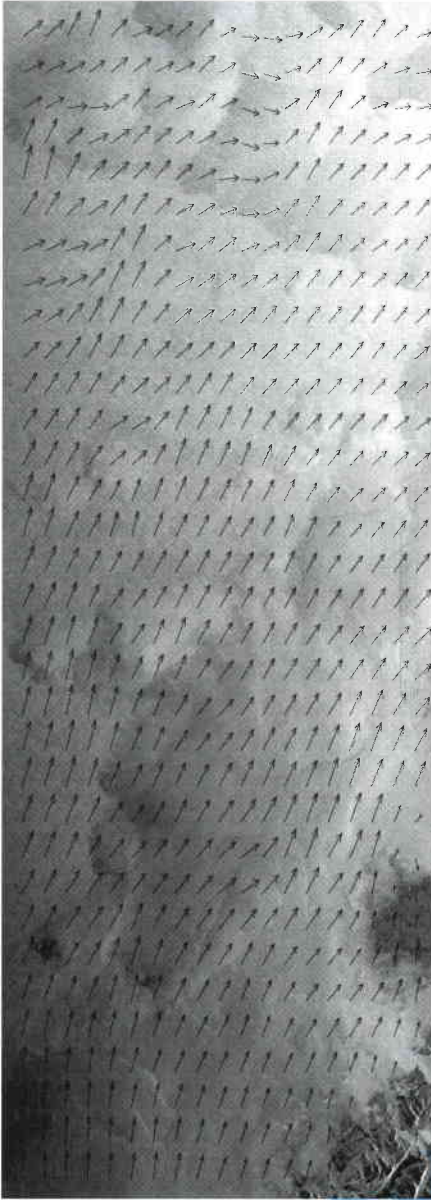


Figure 3. Wind-field estimate from ERS-2 SAR data (courtesy of Norut, Norway)

traded off against other image quality parameters (such as the radiometric resolution).

The across-track or range resolution is a function of the transmitted radar bandwidth. Pulse compression techniques are used to improve the performance taking into account the instrument's peak power capability. The fact that the end-to-end system works coherently means that both the amplitude and the phase relationships between the complex transmitted and received signals are maintained throughout the instruments and the processing chain.

Operating modes

The ASAR instrument is designed to provide a large degree of operational flexibility. The main instrument parameters can be selected by ground command for each of the five operational modes:

- The Image mode generates high-spatial-resolution data products (30 m for precision images) selected from the total of seven available swaths located over a range of incidence angles spanning 15 to 45 deg,

- The Wave mode generates vignettes of 5 km by 5 km, spaced 100 km along-track. The position of the vignette can be selected to alternate between any two of the seven swaths.
- The Wide Swath and Global Monitoring modes are based on the ScanSAR technique using five sub-swaths, and they generate wide-swath products (400 km) with spatial resolutions of 150 and 1000 m, respectively.

These four modes may be operated in one of two polarisations, either HH or VV (the letter first indicates the polarisation of the transmit signal – H for horizontal, V for vertical – and the second the polarisation of the receive signal).

- The Alternating Polarisation mode provides two simultaneous images from the same area in HH and VV polarisations, HH and HV or VV and VH, with the same imaging geometry as the Image mode and similarly high spatial resolution.

The ASAR instrument

The ASAR instrument consists of two main elements: the Central Electronics Sub-Assembly (CESA) and the Antenna Sub-Assembly (ASA).

The active antenna contains 20 tiles with 16 sub-arrays, each equipped with a transmit/receive (T/R) module. The instrument is driven by the Control Sub-System (CSS), which provides the command and control interface to

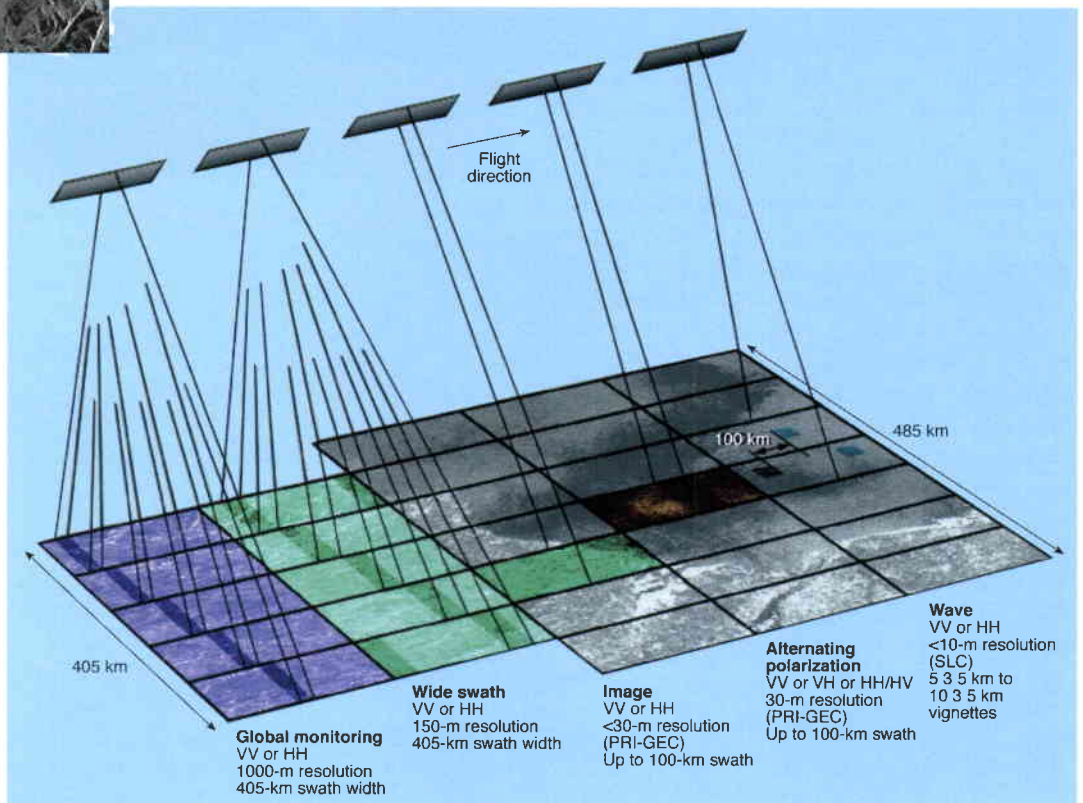


Figure 4. The ASAR operating modes

the spacecraft, manages the distribution of the operational parameters (such as transmit pulse characteristics and antenna beam-set), and generates the instrument operation time line.

The transmit pulse characteristics are set in the Data Sub-System (DSS), the output of which is an up-chirp pulse centred on the IF carrier (124 MHz). In the RF Sub-System (RF S/S) the pulse is up-converted to the RF frequency (5.331 GHz) and amplified. The signal is then passed to the Tile Sub-System (TSS) through a waveguide distribution network (RFPF) and subsequently, within the tile, to each individual T/R module using a microstrip corporate feed. The T/R modules apply phase and gain characteristics according to the pre-selected beam settings transferred from the Control Sub-System and stored in the Tile Control Interface Unit (TCIU).

In receive, the RF-echo signal follows the reciprocal path down to the Data Sub-System, where the raw science data are generated and provided to the spacecraft interface.

Central Electronics Sub-Assembly

The CESA is in charge of generating the transmitted chirp, converting the echo signal into measurement data, as well as controlling and monitoring the whole instrument. Compared to ERS-1 and ERS-2, which use Surface Acoustic Wave (SAW) devices for analogue chirp generation and on-board range compression, ASAR uses digital technologies for on-board chirp generation and data reduction for temporary storage associated with on-ground range compression. A fundamental advantage of using digital chirp

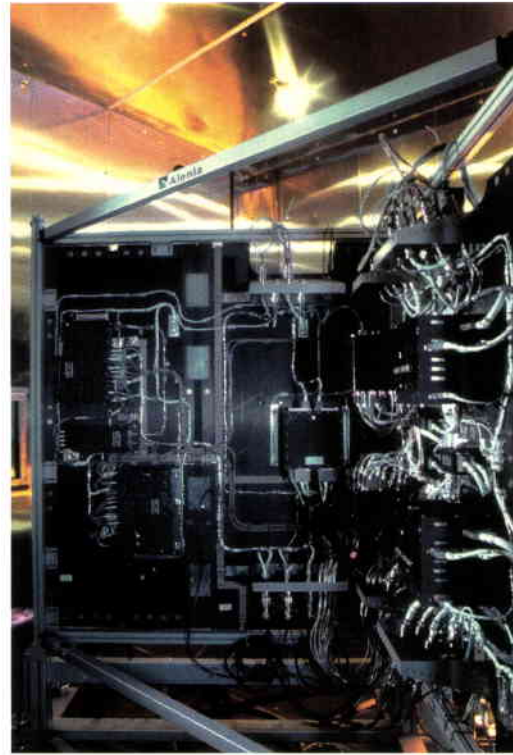


Figure 5. ASAR CESA flight model during thermal testing (courtesy of Alenia, Italy)

generation is the inherent flexibility of such a design, which allows for chirp versatility in terms of pulse duration and bandwidth, thus accommodating efficiently the various requirements associated with the high number of available operational modes and swaths of the instrument.

At reception, the echo signal is first filtered and down-converted in the RF Sub-System, then demodulated into the I & Q components of the carrier. These two signals are then both digitised into 8-bit samples. If required, it is then possible to perform digital decimation of the

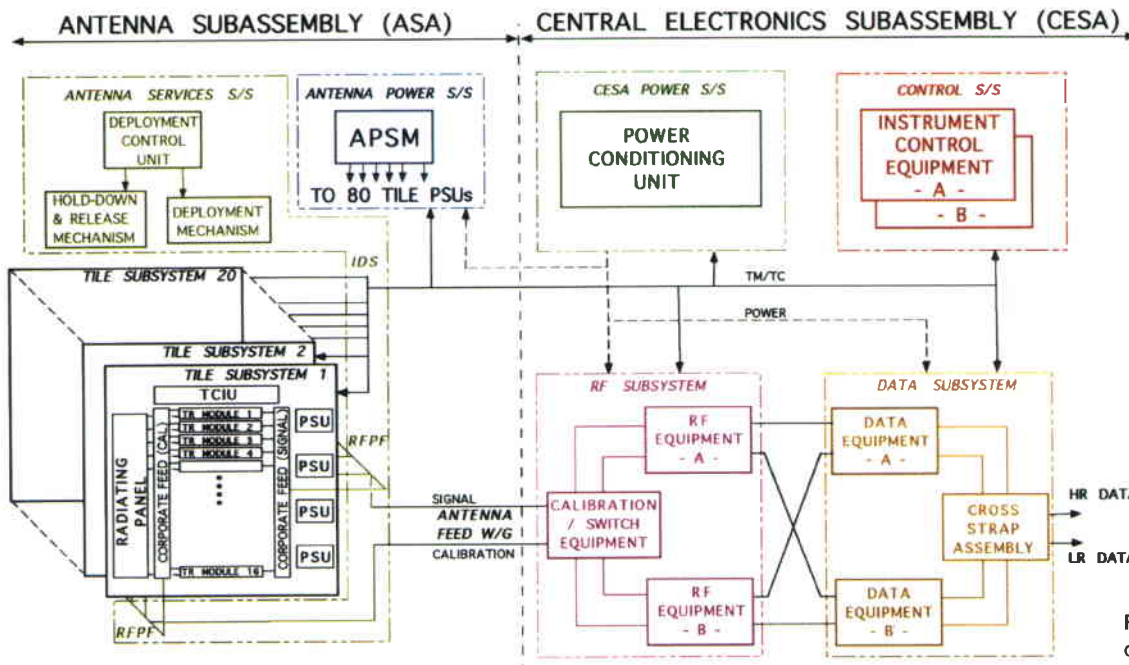


Figure 6. ASAR functional diagram



Figure 7. Flight model of the ASAR antenna (courtesy of Matra Marconi Space, UK)

samples, in order to reduce the data stream, such as in Global Monitoring mode where the transmit bandwidth is low. Following this decimation, a Flexible Block Adaptive Quantiser (FBAQ) compression scheme is applied to the echo samples.

The FBAQ allows the data rate to be maintained within data-transmission requirements without degrading the image quality. This is achieved by using a compression algorithm optimised to the statistics of the radar signal. The FBAQ ASIC that has been developed can be operated in three ways: compression according to the FBAQ algorithm (8 to 4, 3 or 2 bits), bypass or noise (fixed exponent), depending on the type of data to be processed.

In order to optimise raw data transfer, the data equipment also contains science memory, where the echo samples are temporarily stored before their transmission to the on-board recorders.

Active phased-array antenna

The ASAR active antenna is a 1.3 m x 10 m phased array. The antenna consists of five 1.3 m x 2 m panels which are folded for launch. Each panel is formed by four 0.65 m x 1 m tiles

mounted together. The Antenna Sub-Assembly is divided into three sub-systems: the Antenna Services Sub-System (ASS), the Tile Sub-System (TSS) and the Antenna Power Switching and Monitoring Sub-System (APSM).

The antenna is based on a mechanical structure consisting of five rigid Carbon-Fibre-Reinforced Plastic (CFRP) frames and two RF distribution networks of CFRP waveguides running in parallel along the five panels. In launch configuration, the five panels are stowed folded over the fixed central one, and held together by eight hold-down and release mechanisms (HRMs). Each HRM consists of a retractable telescopic tube levered by a secondary mechanism based on non-pyrotechnic technology (kevlar cable and thermal knife).

After release, the panels deploy sequentially around four hinge lines by using stepper motors. Latching is performed by the eight built-in latches to achieve the final antenna planarity of ± 4 mm in orbit. Each of the 20 tiles is a self-contained, full-operating sub-system which includes four Power Supply Units (PSUs), a Tile Control Interface Unit (TCIU), two microstrip RF distribution corporate feeds and 16 sub-arrays of 24 dual-polarised low-loss dispersion-free radiating elements. Each sub-array is connected to a T/R module, with independent connections for the two polarisations. The 16 sub-arrays are mounted together, although thermally and mechanically decoupled, on a radiating panel, which provides both structural and thermal integrity to the tile. The TCIU provides the control functions within the Tile. It performs the local control of the T/R modules, transfers data and interfaces to the Control Sub-System.

Figure 8. The ASAR T/R module (courtesy of Alcatel, France)



| Parameter | Unit | Image | Alternating Polarisation VV/HH, HH/HV, or VV/H | Wide Swath VV or HH | Global Monitoring VV or HH | Wave |
|--|------|--------------|--|------------------------|-------------------------------|--------------|
| Polarisation | | VV or HH | VV/HH, HH/HV, or VV/H | VV or HH | VV or HH | VV or HH |
| Spatial resolution (az. x ra.) * except swath IS1 | m | 28 x 28* | 29 x 30* | 150 x 150 | 950 x 980 | 28 x 30* |
| Radiometric Resolution | dB | 1.5 | 2.5 | 1.5 to 1.7 | 1.4 | 1.5 |
| Point Target Ambiguity Ratio | | | | | | |
| - azimuth | dB | 26 to 30 | 19 to 28 | 22 to 29 | 27 to 29 | 27 to 30 |
| - range | dB | 32 to 46 | 26 to 41 | 26 to 34 | 25 to 32 | 31 to 46 |
| Distributed Target Ambiguity Ratio | | | | | | |
| - azimuth | dB | 23 to 25 | 18 to 25 | 20 to 25 | 25 to 28 | 23 to 25 |
| - range | dB | 17 to 39 | 17 to 39 | 17 to 31 | 17 to 31 | 21 to 48 |
| Radiometric Stability | dB | 0.32 to 0.40 | 0.50 to 0.55 | 0.32 to 0.42 | 0.46 to 0.53 | 0.55 to 0.60 |
| Noise Equivalent σ_0 | dB | -20 to -22 | -19 to -22 | -21 to -26 | -32 to -35 | -20 to -22 |

Each of the 320 T/R modules consists of two (H & V) transmit chains and one common receive chain. For calibration purposes, a coupler (-24 dB) has been implemented at the output of the module to the antenna. For an active antenna, the amplitude and phase characteristics of the T/R modules vary principally as a function of temperature. To handle this, the instrument includes a scheme to compensate for drifts over the temperature range. To this end, the temperature of each T/R module is monitored and utilised by the TCIU to compensate the amplitude and phase settings. This scheme provides the antenna with a high degree of stability.

Qualification of new technologies

In order to guarantee the required operational flexibility and performance, a number of new technologies, processes and components needed to be developed and qualified (from the hybrid line for RF components, to GaAs foundry, parallel-gap welding, etc.).

Performances

The inherent principle of the Synthetic Aperture Radar impedes the direct measurement of ASAR instrument performances on the ground. The selected alternative is computation of the instrument performance characteristics from measurable lower level parameters throughout the various stages of instrument testing.

In the case of ASAR, due to the large number of operating modes and measurement capabilities, the verifications of instrument performances have resulted in an extensive test programme. It has also allowed the determination of an optimal combination of parameters in order to achieve the best overall performance across all operating configurations.

The predicted end-of-life performances for the ASAR instrument are summarised in Table 4. These figures have been derived assuming a

worst-case scenario and demonstrate that the Envisat ASAR mission objectives can indeed be fulfilled.

Instrument calibration

ASAR, unlike the ERS AMI-SAR, is an active antenna and any instabilities in gain and phase characteristics will therefore distort the elevation beam patterns and can contribute

Table 4. ASAR performance summary

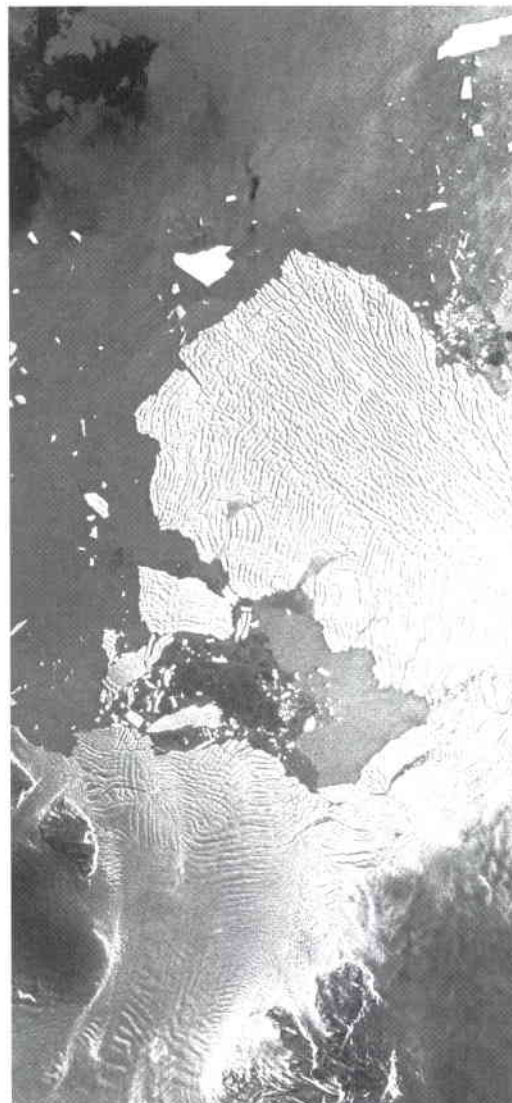


Figure 9. An Image mode medium-resolution product, showing the Walgreen Coast, Antarctica (from ERS raw data)

to radiometric errors in the SAR image. For this reason, a sophisticated scheme for the ASAR's radiometric calibration has been selected, composed of three elements: internal calibration, external calibration and external characterisation.

Internal calibration

The objectives of the ASAR instrument internal calibration are to derive the instrument's internal path transfer function and to perform noise calibration.

During normal operation in any of the ASAR measurement modes, a sequence of calibration pulses is interleaved with normal radar pulses. These pulses characterise the active array in both transmit and receive, on a row-by-row basis.

Figure 10. An Image mode precision product, showing Bathrust Island, Canada (from ERS raw data)



As well as providing internal calibration during the measurement modes, the ASAR includes a special 'module stepping' mode, in which individual T/R module characteristics can be measured. It can be used to investigate T/R module failures and ageing effects. In this mode, only one module is activated at a time in either transmit or receive.

The internal calibration scheme also includes measurements of the instrument noise level. They are taken during the initial calibration sequences at the beginning of a mode. In the modes that have natural gaps in their imaging sequence (i.e. wide-swath and global monitoring modes), noise measurements are also made during nominal operation throughout the mode.

External calibration

The objective of the external calibration is to derive the overall scaling factor. The successful

methodology developed for ERS will be re-used for ASAR.

To this end, four high-precision transponders have been developed, characterised by a 0.08 dB stability and 0.13 dB accuracy. These transponders will be deployed in Flevoland (NL) across the ASAR swath and observed several times during each orbital cycle of 35 days.

Images acquired over suitable regions of the Amazonian rain forest will also be used to derive the in-flight elevation antenna patterns. Absolute calibration factors derived from transponder measurements and across-swath corrections derived from the radar equation will be used to calibrate the final image product.

For the wide-swath mode using the ScanSAR technique, the external calibration approach will be similar to the one used for the narrow-swath mode.

External characterisation

The ASAR has a dedicated External Characterisation mode to monitor all those elements that are outside the internal calibration loop, as well as the calibration loop itself.

In this mode, planned to be operated every 6 months, a sequence of pulses sent by each antenna row in turn is detected by the antenna calibration loop and simultaneously recorded on the ground by a special receiver built into the ASAR calibration transponder. The data recorded in the transponder and that down-linked from the instrument are compared in the ground processor to reveal the relative phase and amplitude of the pulse from each row. These relative amplitudes and phases are used to characterise the row of radiating sub-arrays and the calibration path of the row.

ASAR ground processor

The development of the ASAR processor is based on the following driving concepts:

- The need for users to have identical products irrespective of the processing facility.
- The need to broaden the range of products whilst ensuring the quality of the ERS SAR high-resolution products.
- The capability to cope with the large amount of products to be generated.
- The ability to generate continuous medium and low-resolution products along the orbit (stripline processing, without radiometric or geometric discontinuity).

Following the above concepts, ESA has developed a single ASAR processor able to

| Mode and Product Name | Nominal Resolution (m) | Pixel spacing (m) | Coverage (km) | Product ENL |
|---------------------------------|------------------------|-------------------|---------------|-------------|
| <i>IM precision IMP</i> | 30 x 30 | 12.5 x 12.5 | 56-100 x 100 | 3.9 |
| <i>IM single look IMS</i> | 9slant x 6 | natural | 56-100 x 100 | 1 |
| <i>IM geocoded IMG</i> | 30 x 30 | 12.5 x 12.5 | 100 x 100 | 3.9 |
| IM medium resolution IMM | 150 x 150 | 75 x 75 | 56-100 x 100 | 40 |
| IM browse IMB | 900 x 900 | 225 x 225 | 56-100 x 100 | 80 |
| <i>AP precision APP</i> | 30 x 30 | 12.5 x 12.5 | 56-100 x 100 | 1.9 |
| AP single look APS | 9slant x 12 | natural | 56-100 x 100 | 1 |
| AP geocoded APG | 30 x 30 | 12.5 x 12.5 | 100 x 100 | 1.9 |
| AP medium resolution APM | 150 x 150 | 75 x 75 | 56-100 x 100 | 50 |
| AP browse APB | 900 x 900 | 225 x 225 | 56-100 x 100 | 75 |
| WS medium resolution WSM | 150 x 150 | 75 x 75 | 400 x 400 | 12 |
| WS browse WSB | 1800x1800 | 900 x 900 | 400 x 400 | 57-62 |
| WV imagette & cross spectra WVI | 9slant x 6 | natural | 5x5 to 10x5 | 1 |
| WV cross spectra WVS | - | - | 5x5 to 10x5 | n/a |
| GM image GM1 | 1000 x 1000 | 500 x 500 | 400 x 400 | 12 |
| GM browse GMB | 2000 x 2000 | 1000x1000 | 400 x 400 | 18-21 |

handle data from any of the ASAR modes in near-real-time and off-line. This processor will be installed at the ESA Payload Data Handling Stations (Kiruna in Sweden and ESRIN, Frascati, in Italy), at the Envisat Processing and Archiving Centres (PACs), and at the national stations offering ESA ASAR services. The use of a single processor will ensure product consistency for the users, independent of the ESA processing centre selected (same format and processing algorithm) and will simplify product validation and future product upgrade cycles.

One of the key new features of the ASAR processor is the ability to generate medium-resolution (150 m) and low-resolution (1 km) products with their corresponding browse images in stripline without geometric or radiometric discontinuity. The stripline image products represent processed data from an entire acquisition segment of up to 10 minutes for Image, Alternating Polarisation and Wide Swath modes and up to a complete orbit for Global Monitoring mode. The user can select any segment in the processed stripline.

The processor computes the replica of the transmitted pulse from the calibration-pulse measurements, the row patterns as characterised on-ground and the external characterisation data. The constructed replica tracks variations in the transmit and receive chains and is used to determine the range reference function for range-compression processing.

The ground processor includes a Doppler Centroid Estimator with a specified accuracy of 50 Hz for Image and Wave modes as for ERS and 25 Hz in the ScanSAR modes in order to limit radiometric errors in azimuth.

The ASAR processor will be used to ensure the systematic processing in near-real-time of all received high-rate data to generate medium-resolution and browse products. All Wave mode or Global Monitoring mode data will also be systematically processed in near-real-time.

Furthermore, the ASAR processor will allow high-resolution products to be processed from Image or Alternating Polarisation acquisitions (Precision Image, Single Look Complex or Ellipsoid Geocoded products) in near-real-time or off-line, depending on user requests. The accompanying figures show examples of a Precision Image and a Medium Resolution Product.

The different products, their coverages and qualities are summarised in Table 5.

Data collection and user services

The ASAR instrument modes of operation can be divided into two categories:

- Low-data-rate modes (Global Monitoring and Wave) with an operational capability of up to 100% of the orbit. Both modes are systematically recorded on-board and the on-board recorder is dumped every orbit when visible from an ESA station.
- High-data-rate modes (Image, Alternating Polarisation and Wide Swath) with a maximum operating time of 30 min per orbit (including the ability to operate for up to 10 min in eclipse).

Compared to ERS, the Envisat mission offers improved data recording and transmission capabilities for the ASAR high-data-rate modes:

- 12 minutes of on-board recording
- real-time transmission X-band in visibility of ground stations

Table 5. ASAR products, coverages and qualities

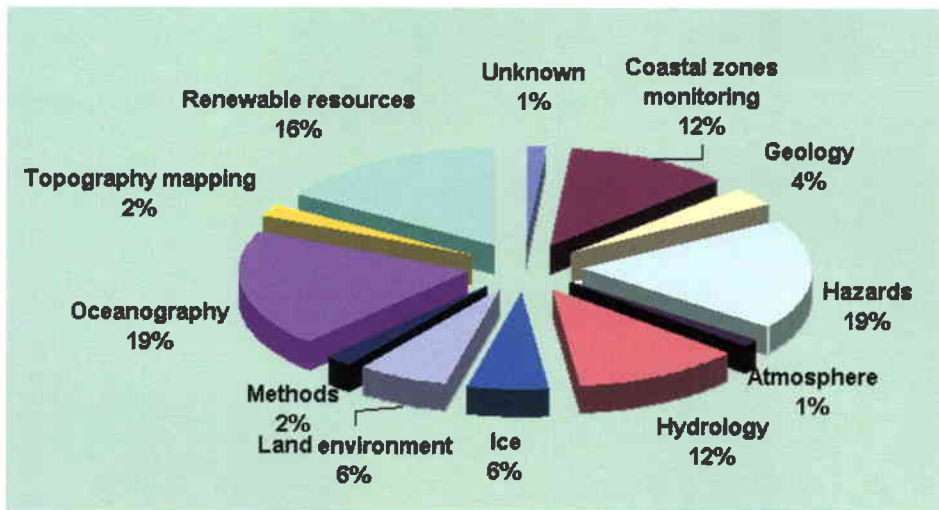


Figure 11. Distribution of ASAR Announcement of Opportunity projects across the different application fields

- real-time transmission or recorded data dump in visibility of ESA X-band ground stations or via ESA data-relay satellite Artemis using Ka-band links.

The instrument will be operated according to the following strategy:

- In response to user requests for Category 2 use (commercial applications).
- In response to user requests for Category 1 use (scientific and demonstration projects).
- For background acquisition, including reference data archive build-up as well as routinely planned data acquisitions (e.g. Wave mode over oceans).

All ASAR high-rate data acquired by ESA facilities will be systematically processed in near-real-time to generate medium-resolution products (~150 m) and browse products. The browses will be available on line via the Envisat User Service. The Envisat Ground Segment will provide a unified service to the users with access – once they are registered – to the full range of ESA services and products.

Users' requests will be supported for inventory searching on already acquired data, as well as for data requiring future acquisitions. Users who have ordered Envisat products will be kept informed of the status and progress of their orders: from acceptance, planning of instrument operation, data-taking, processing and through to product delivery.

Data use for science and applications

The Envisat Announcement of Opportunity (AO) for data exploitation was issued in December 1997, with a deadline for the submission of proposals of end-May 1998. A total of 674 proposals have been accepted, 376 of which involve the use of ASAR (71% science, 24% commercial and 5% Cal/Val). Figure 11 shows the distribution of the ASAR projects across the different fields of application.

Most of the AO proposals involve the use of multiple ASAR operating modes. There is no clear preference for specific swaths or specific polarisations, and different polarisation combinations are requested for all modes. Interferometry is a component of 38% of the projects.

Conclusions

The ASAR instrument is characterised by extensive flexibility, thanks to its five operating modes, the ability to operate in Horizontal and Vertical polarisations, the wide range of elevation angles covered, and the possibility to shape the antenna beam in both transmit and in receive by individually controlling the amplitude and phase of each of the 320 transmit/receive modules.

In order to achieve the required performance and operational flexibility, many new technologies, processes and components have been qualified.

All acquired data will be processed (either in near-real-time or off-line) within the ESA Ground Segment by a single design of processor, to ensure product consistency irrespective of the processing centre. A large number of ASAR products will be routinely produced by ESA and made available to users.

The large number of applications that the instrument will be capable of supporting, illustrated by the responses to the Announcement of Opportunity, qualifies ASAR as a precursor of future Earth Watch missions.

The ASAR instrument test campaign was completed in early February 2000. CESA was subsequently delivered to ESTEC in Noordwijk (NL) and mounted on the Envisat spacecraft. The ASAR antenna was delivered a month later and integrated onto the spacecraft in early March.

Acknowledgements

Many European industries have participated in the effort required to develop the largest single instrument (and associated ground processing chain) ever built in Europe for remote-sensing applications. We limit ourselves here to mentioning only the major industrial contractors: Dornier (Mission Prime), MMS-UK (Instrument Prime), Alcatel Space Industries (Tile S/S), Alenia Aerospazio (CESA) and, for the ASAR Ground Processor, MDA under the direction of Alcatel Space Industries (PDS Prime Contractor).

Earth-Observation Applications of Navigation Satellites

P. Silvestrin

Earth Observation Future Programmes Department, ESA Directorate of Application Programmes, ESTEC, Noordwijk, The Netherlands

Introduction

The development of Earth-observation techniques based on the use of navigation signals can be traced back to the use of GPS in geodetic applications to provide astonishing precision, such as the determination to within a few centimetres of the relative positions of points on the Earth's surface separated by several thousand kilometres. This ultra-precise positioning of fixed GPS receivers is now routinely used as a tool for studying the dynamics of the Earth's crust (e.g. plate tectonics).

In the course of the development of the related models and data-analysis techniques, new geophysical applications have emerged. Meticulous modelling work has shown how

phenomena that were initially considered as measurement perturbations for the original application can later become the observations of interest for new applications. For geodetic positioning, the presence of water vapour (humidity) along the signal propagation path in the troposphere (Fig. 1) is an unavoidable nuisance, because it causes a propagation delay equivalent to a significant additional path (~ 0.4 m in humid regions). On the other hand, it is possible to derive this water-vapour content to about 1 kg/km² from the excess-path estimates, which can be determined via the geodetic analysis with about 1 mm accuracy. This provides an opportunity to acquire data that are useful, for instance, for detecting weather fronts in the regions where the receivers are deployed and, more generally, for improving weather forecasts if the information is properly processed in numerical weather-prediction systems. Several regional and global networks of ground GPS receivers are in place today providing data for both geodetic and meteorological applications (see Table 1; not exhaustive). As an example, Figure 2 shows the German SAPOS (SATelliten-POSITIONierungsdienst) network, data from which is used for various precise positioning applications and will soon be used for tropospheric water-vapour determination also.

Satellite navigation systems, such as the US Global Positioning System (GPS) and its Russian counterpart GLONASS, were initially established to provide accurate positioning information. They have, however, also led to a great variety of unforeseen applications, many of which are in fields that at first sight are unrelated to navigation. One of the most successful examples is the development of observation techniques of interest for the Earth sciences.

On going developments, such as the advent of the European navigation system Galileo, will enhance the use of these techniques for ocean and atmosphere remote sensing.

ESA contributes to the International GPS Service (IGS) network with six receivers at various tracking stations, and with the routine determination of precise orbits and geodetic parameters at its European Space Operations Centre (ESOC) in Darmstadt (cf. 'Satellite Navigation Using GPS' in ESA Bulletin No. 90, May 1997, which also provides an overview of GPS).

Additional information is provided by the correction for ionospheric effects realised with the reception of navigation signals at two frequencies (the ionosphere is a dispersive medium and so the propagation paths depend on frequency). The information retrieved is the total content of electrons along the propagation

Table 1

| Network | No. of receivers | Goals |
|---------------------------|------------------|--|
| EUREF, Europe | > 100 | Geodesy, tectonics, meteorology |
| GSI, Japan | > 1000 | Tectonics, meteorology |
| SAPOS, Germany | > 150 | Positioning, surveying, geodesy, meteorology |
| South California Net, USA | > 250 | Tectonics, meteorology |
| CORS + NOAA/FSL, USA | > 100 | Meteorology |
| International GPS Service | > 200 | Geodesy, tectonics, meteorology, ionosphere |
| Suominet | > 100 | Meteorology, ionosphere |

estimates of orbit perturbations of a geophysical nature. The technique will therefore be used in future missions aimed at improving our knowledge of the Earth's gravity field, such as the Gravity and Steady-state Ocean Circulation Explorer (GOCE) selected in October 1999 as the first ESA Core Earth Explorer mission for launch in 2005 (cf. 'Probing the Earth from Space: the Aristoteles Mission', ESA Bulletin No. 72, November 1992, and 'The Gravity and Steady-State Ocean Circulation Explorer', ESA SP-1233 (1)). Several other altimetry and land-topography mapping missions also rely on GPS-based precise orbit determination.

Active atmospheric sounding by radio occultation

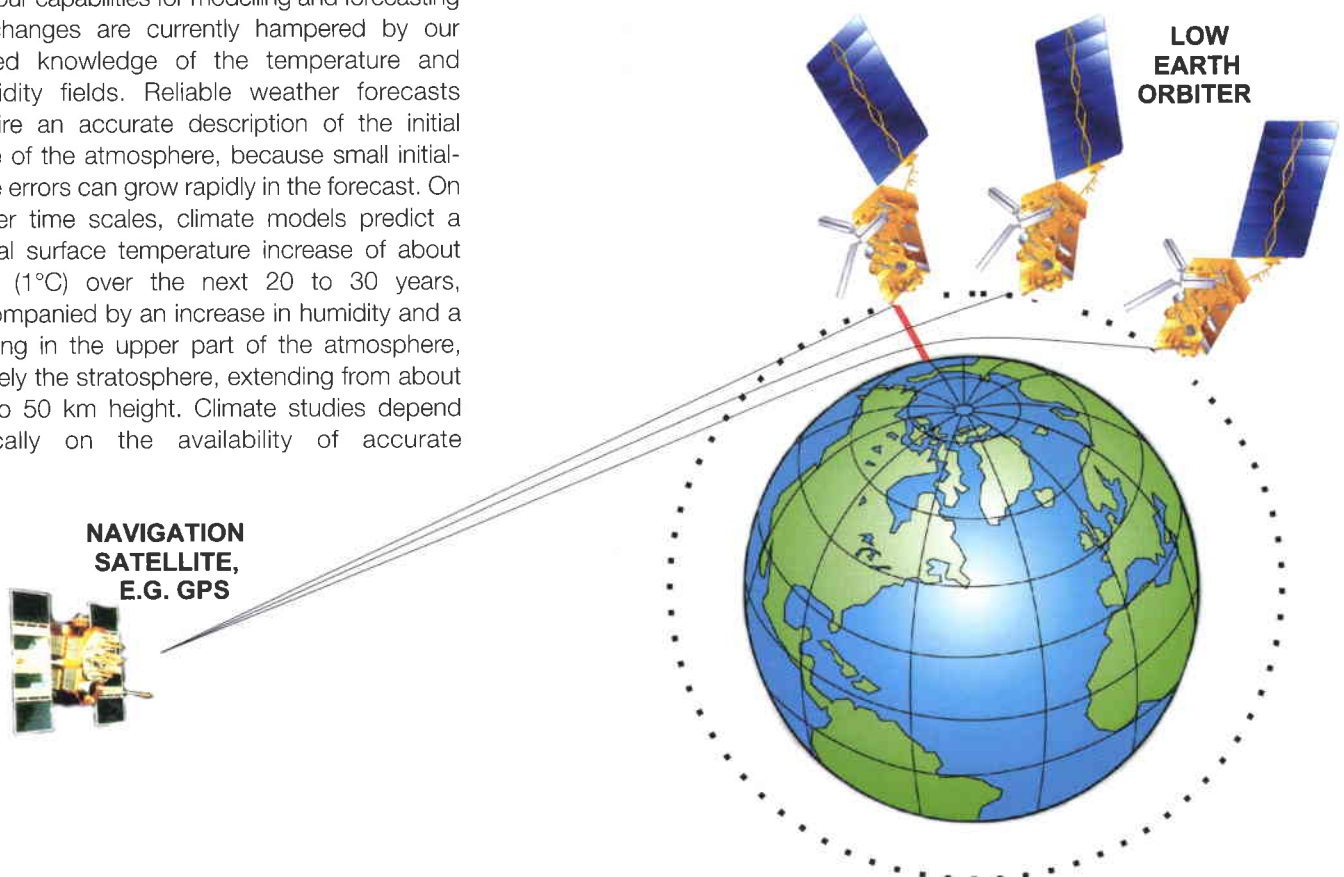
The exploitation of the radio-occultation technique using navigation signals as the transmitters of opportunity probably represents the most important development for the Earth sciences. Well-known in Solar System missions where it has been applied since 1964 with the first observations of Mars' atmosphere, this technique uses radio signals passing through the atmosphere in a so-called 'limb-sounding geometry' to sense atmospheric properties. When applied to the Earth, it can provide data of great value for meteorology and climatology, particularly because of its excellent geographical coverage, accuracy, vertical resolution and all-weather capability.

Our understanding of the Earth's atmosphere and our capabilities for modelling and forecasting its changes are currently hampered by our limited knowledge of the temperature and humidity fields. Reliable weather forecasts require an accurate description of the initial state of the atmosphere, because small initial-state errors can grow rapidly in the forecast. On longer time scales, climate models predict a global surface temperature increase of about 1 K (1°C) over the next 20 to 30 years, accompanied by an increase in humidity and a cooling in the upper part of the atmosphere, namely the stratosphere, extending from about 15 to 50 km height. Climate studies depend critically on the availability of accurate

observations of long-term consistency, which is what the radio-occultation measurements from navigation satellites can provide.

As navigation signals pass through the atmosphere, either through a descending propagation path (so-called 'set event') or an ascending one ('rise event') when observed by an orbiting instrument, they are retarded and refracted (bent) through an angle determined by the gradients of refractivity along the path, as depicted in Figure 3. The main refraction effect is caused by the vertical gradient of refractivity in the lowest atmospheric layer crossed by the path. The effect results in an excess path and in a decrease in the observed signal Doppler shift compared to a path in vacuum. The path can be precisely determined from the phase and amplitude measurements of the received signals and used to determine the refraction-angle profile through a rise or set event. The refractivity gradients depend on the gradients of air density (and ultimately temperature), humidity and electron content. In the region above about 8 km (upper troposphere and stratosphere, up to 40 – 50 km), the humidity is negligible and the refractivity is due mainly to vertical temperature gradients, so that temperature profiles can be retrieved. Below this, the humidity effect dominates and, if a temperature estimate of moderate accuracy is available, the humidity profile can be retrieved. Vertical profiles of electron density in the ionosphere can also be reconstituted.

Figure 3. Principle of radio occultation using navigation signals: the signal is received on a low-Earth orbiting satellite, and the propagation path is observed to bend because of atmospheric refraction



The first proposal to use GPS signals for radio occultation measurements was advanced by Russian scientists in 1987, shortly followed by a US proposal that led to a proof-of-concept with the GPS/MET experiment launched in April 1995 on the MicroLab-1 small satellite. Following extensive GPS/MET data analysis and research into the retrieval process, a significant part of which was conducted in Europe through ESA studies, it is now widely accepted that radio occultation with navigation signals can provide useful profiles of density, pressure and temperature in the middle atmosphere and the colder troposphere, as well as humidity profiles in the tropical and mid-latitude regions of the troposphere. The features that make this technique so interesting for meteorology and climate studies include the global coverage (about 1000 profiles per day can be obtained for each instrument on a polar low Earth orbiter, with 48 navigation satellites), the all-weather capability (no blockage by clouds, unlike classical satellite sounders), the high vertical resolution (varying from some 1.5 km in the stratosphere to some 0.2 km in the troposphere), the retrieved temperature accuracy (about 1 K up to 35 km), and the long-term consistency. This latter quality stems from the fact that the measurements are essentially time-interval observations, which can be referred to fundamental metrological standards (atomic time).

In addition to measuring the precise phase and amplitude of the carrier signal from each navigation satellite occulted by the atmosphere, the instrument also measures other signals that do not cross the atmosphere so as to determine precisely its own velocity and position. These are needed to compute the (large) Doppler shift caused by orbital motion and derive the excess

Doppler caused by the propagation in the atmosphere. The required accuracy, particularly for the along-path velocity component, is high (order 0.1 mm/s), which makes it mandatory to use differential positioning techniques, supported by a global ground network of receivers. The use of differential techniques also allows the correction of transmitter and receiver oscillator errors, which might otherwise be confused with the atmospheric contribution. When the gradients of refractivity in the atmosphere are small over spatial scales of the order of the signal wavelength (0.2 m), the processing can be based on geometric optics, so that the propagation paths can be treated as well-localised rays. The excess-Doppler profile can be transformed into a refraction-angle profile, which in turn enables one to derive a refraction-index profile.

The atmospheric parameters of interest are linked by a simple mathematical relation to the refraction index, which enables one to reconstitute them with the help of the known gas and hydrostatic equilibrium laws. The refraction-angle profiles can also be used directly in numerical weather-prediction models in order to combine them with other atmospheric measurements in an optimal estimation approach, which is routinely done in operational meteorology. These prediction models can provide temperature estimates with good accuracy (2 – 3 K) over the humid regions, where radio-occultation data can therefore be used to retrieve humidity with about a 10 – 20% accuracy.

Figure 4. Typical excess-path and Doppler-shift profiles through a radio-occultation event

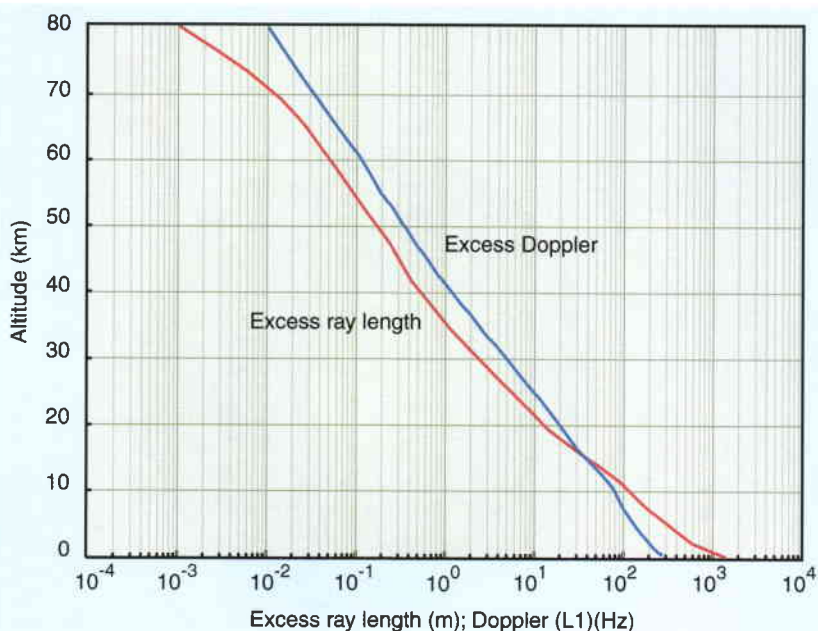


Figure 4 shows a typical profile of the excess path. This is clearly a substantial effect if compared to the millimetric accuracy with which one can measure it. The profile has been generated with a complex software simulator developed under an ESA study in order to analyse the end-to-end performance of the technique, and currently in use at various European institutes and companies. Figure 5 shows an example of temperature and water-vapour pressure retrievals from actual data collected in the GPS-MET experiment and compared to similar retrievals from numerical weather-prediction systems using a large set of conventional measurement systems (radiosondes, satellite radiometers, etc.). The total refraction angle reaches about 1 deg at grazing incidence and can be determined from the data to an accuracy of better than 0.01% of a degree. Because of the limb-sounding geometry, the horizontal resolution of the measurements is between 100 and 300 km, which is sufficient considering the atmosphere's stratified structure and assuming proper data treatment in weather and climate models.

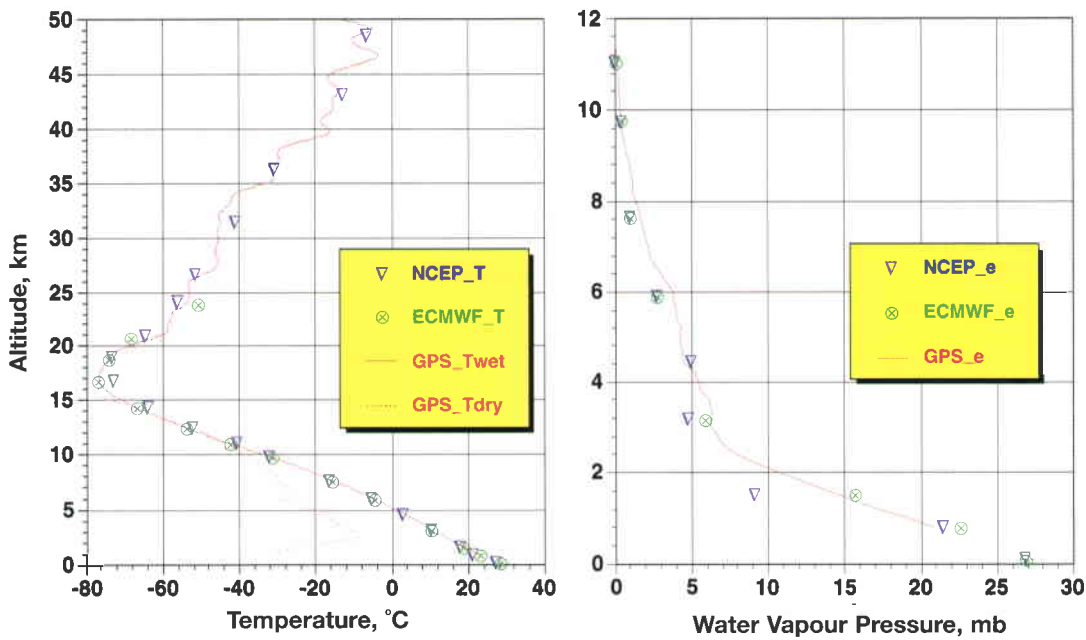


Figure 5. Example of temperature and water-vapour-pressure retrievals from data collected in the GPS-MET experiment, showing the agreement with similar retrievals from numerical weather-prediction systems that use a large set of conventional measurement systems. The GPS_Tdry retrieval neglects the presence of humidity and results in an underestimate of temperature (Data courtesy of the UCAR GPS-MET Project, the National Center for Environmental Prediction (NCEP, USA) and the European Centre for Medium-Range Weather Forecasts (ECMWF, UK))

Often the geometric (ray) optics description is no longer valid in humid regions, because the complex geometry of the humidity field can cause rapid fluctuations in refractivity. Such fluctuations cause multiple propagation paths and significant diffraction effects. In this case, the probed region behaves like a focussing rather than a defocussing lens, and the sensor measures a rapidly varying signal. In terms of rays, it is as if the instrument is measuring the result of the interference of an unknown number of rays (Fig. 6). To handle such effects correctly, the data processing must be based on wave optics (physical optics). A satisfactory method has been elaborated in the course of various studies, based on the concept that the rays can be 'disentangled' by propagating the received signal backwards until it is reconstructed on a virtual surface (auxiliary plane in Fig. 6) where the effects are negligible. Once this is achieved, the retrieval can be carried out as before, starting with the derivation of the excess Doppler shift. The

method requires one to measure also the amplitude of the received signal. An added advantage of the method is that it allows the vertical resolution to be sharpened further and makes it possible to observe vertical features in the atmosphere with sizes below 100 m. All of the retrieval methods have been verified by means of the end-to-end performance simulation software mentioned and will be used in the data processing for forthcoming missions.

Other studies have addressed the accuracy of the GPS/MET retrievals compared with other sensors, e.g. radiosondes providing in-situ measurements of comparable accuracy, and with various weather-prediction models. The results show that temperature errors are below or close to 1 K, although the comparison becomes difficult for regions where the errors of existing sensors and models are above this value. This is the case for a large part of the Southern Hemisphere, where the limitations in the existing data are particularly strong.

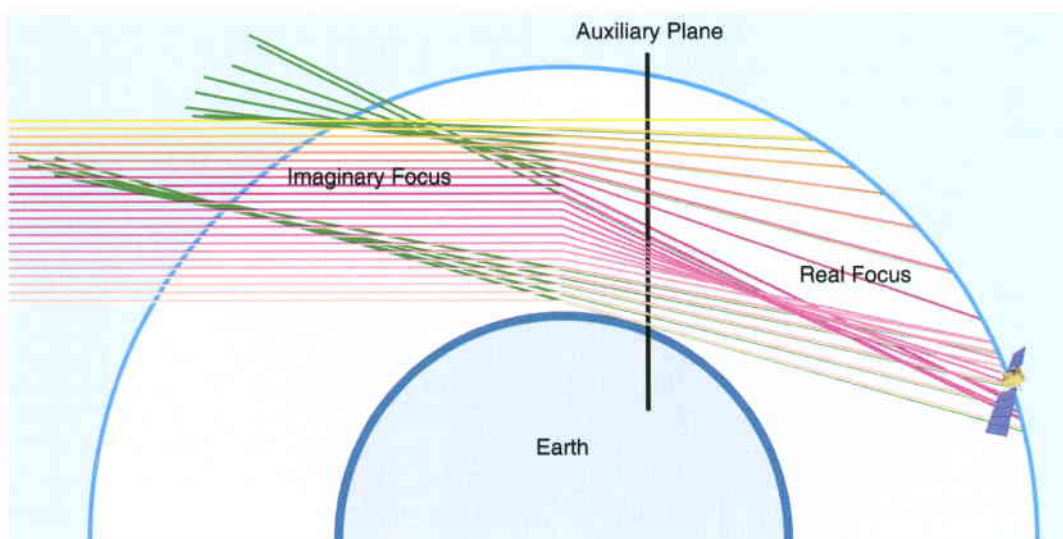


Figure 6. Illustration of multiple propagation effects in radio occultation caused by large atmospheric refractivity gradients. The effects are removed by processing the received data so as to propagate the paths backward up to a (virtual) auxiliary plane

Instrument development

Navigation sensors, even if space-qualified, cannot be used as instruments for the applications described, since substantially higher performances and different modes of operation are needed. For this reason, the development of suitable instruments was initiated in 1994 within ESA's Earth Observation Preparatory Programme. Relevant differences with respect to navigation equipment include: a larger number of receiving channels, since both positioning and sounding must be supported; low-noise measurements at high data rates; an ultra-stable oscillator; high-gain beam-shaped antennas, to compensate for losses incurred in the atmospheric propagation; improved sensitivity to observe the weak signals during a

tropospheric occultation, including a so-called 'open-loop' mode where an on-board atmospheric model aids the instrument operation when closed-loop phase locking of the signal is no longer possible. The GNSS Receiver for Atmospheric Sounding (GRAS) has been developed to provide radio-occultation measurements in an operational way. Initially proposed in 1996 as the instrument for a prospective constellation of micro-satellites (cf. 'The Atmospheric Profiling Mission', ESA SP-1196 (7)), it is now being implemented on the Metop mission

following a request by Eumetsat to include it in its meteorological payload. It is worth mentioning that the experience gained with GRAS has also given European industry the opportunity to win important development contracts for similar sensors in the US market. Recently, additional activities have been started to develop a miniaturised version of GRAS for the Atmospheric Climate Experiment (ACE) mission, selected in 1999 as a potential Earth Explorer Opportunity mission and currently being studied at Phase-A level, as well as for other flight opportunities.

Emerging applications

The Earth-observation applications of navigation systems could soon extend to ocean remote sensing, following various proposals elaborated since the late eighties regarding the exploitation of navigation signals reflected at the sea surface. The goals are mainly observation of the sea state (waves) and surface winds, and ocean altimetry. While some successful proof-

of-concept airborne experiments have been conducted (see ESA Bulletin No. 101, p. 133), studies and further experiments are now underway to assess the feasibility and usefulness of a spaceborne system. If these are confirmed, benefits similar to those of the atmospheric-sounding application could be achieved via this new use of navigation satellites as transmitters of opportunity. These include the reduced implementation effort, because of the receive-only instrumentation, and a substantial data return because of the large number of transmitters. Improved spatial and temporal sampling of both ocean and atmospheric conditions could then be achieved.

Future prospects

The advent of the European navigation system Galileo, and the planned GPS enhancements, represent promising developments for all of the applications described here, mainly because of the anticipated increases in the number of transmitting satellites, in signal power, and in the number of carrier frequencies. Future instrument developments will certainly take advantage of these advances.

On the user side, while the operational meteorology community is already working on the exploitation of ground-based water-vapour and radio-occultation data, climate scientists are becoming increasingly interested in the prospective of a long-term climate observing system based on principles very different from those of the current instruments and able to provide improved long-term data consistency. Proposals such as the ACE mission mentioned above and similar ones in the USA are driven by this vision. Considering how quickly the initial concepts for using navigation satellites for Earth observation have moved from a pure research scenario to one driven by operational applications, we can expect a very healthy future for this young domain of space techniques.

Acknowledgement

The current European leadership in the exploitation of the radio-occultation technique is the result of the work and dedication of many ESA contractors, including the Danish Meteorological Institute, the University of Graz (A), the Max-Planck Institute for Meteorology (D), the Aeronomy Service of CNRS (F), the Catalan Institute for Space Studies (E), the UK Meteorological Office, the University of Leeds (UK), Austrian Aerospace, Saab Ericsson Space (S) and Terma (DK). The support of the ESA Earth Science Division is also gratefully acknowledged.



Figure 7. Anechoic chamber testing of the GRAS antenna breadboard developed within the EOOP and GSTP programmes (courtesy of Saab Ericsson Space)

The European Multi-User Facilities for the Columbus Laboratory

G. Reibaldi, P. Manieri, H. Mundorf, R. Nasca & H. König

Microgravity and Space Station Utilisation Department, ESA Directorate of Manned Spaceflight and Microgravity, ESTEC, Noordwijk, The Netherlands

Introduction

The Columbus laboratory, planned for launch in 2004, will accommodate the following multi-user facilities:

- Biolab
- Fluid Science Laboratory (FSL)
- European Physiology Modules (EPM)
- European Drawer Rack (EDR)
- European Stowage Rack (ESR)
- Materials Science Laboratory (MSL).

In 1995, ESA Member States confirmed their participation in the International Space Station (ISS) Programme. This participation consists of infrastructure elements (e.g. Columbus, Automated Transfer Vehicle, European Robotic Arm) and utilisation elements (e.g. Microgravity Facilities for Columbus, European Drawer Rack, Laboratory Support Equipment).

Once in orbit, Columbus will be outfitted with several multi-user facilities. The experiments will provide a much-needed boost to the European scientific and industrial community. Equally important, they will greatly increase the competitiveness of European industry by fostering innovative research – a major priority for ESA and the European Union. They will also facilitate the start of the commercial utilisation of the Space Station.

Biolab, FSL, EPM and MSL are being developed within the Microgravity Facilities for Columbus (MFC) Programme, while EDR and ESR come within the Utilisation Programme. Columbus will be launched with all the facilities installed (Figure 1) except for MSL, the launch of which is still to be defined. There will also be an allocated stowage volume (e.g. one-quarter of ESR for each facility) to upload a minimum set of maintenance spares and the required experiment hardware (containers, cartridges, etc). Once in orbit, Columbus will accommodate 10 active racks. In the framework of the Space Station Agreements with the USA, ESA is allocated 51% usage of Columbus, the other five racks being allocated to NASA.

Physical and Life Sciences research under microgravity conditions covers a wide range

of activities such as fundamental physics, solidification physics (e.g. crystal growth, metallurgy), physical chemistry, fluid science, biology, biotechnology, human physiology and medicine. These areas cover the largest group of European users of the Space Station. The objective of the ESA Microgravity and Life Sciences Programme is to have materials and fluid sciences, biology and human physiology continuously aboard the Station in order to maximise the return to European scientists. Until 1996, the microgravity effort was funded only via the European Microgravity Research Programmes EMIR-1 and -2. In January 1997, the MFC Programme was initiated, complementing EMIR-2; it covers the development of a set of multi-user microgravity facilities in Columbus and, via Co-operative Agreements with NASA, in the US Laboratory (e.g. MSL).

EDR is a multi-purpose carrier able to support experiments in disciplines such as technology, biology and physical science. ESR is a passive multi-user facility for modular and standardised stowage of Columbus payload support equipment, samples, experiment containers, etc.

Each active multi-user facility has a specific Science Team, of well-known European scientists, that advises the Agency about the scientific requirements. The Team also reviews the facility design to ensure the science requirements are satisfied. The highly demanding scientific and engineering requirements of the facilities, coupled with the low mass budget (e.g. 500 kg for each ESA facility, whereas NASA's is around 800 kg) and reduced financial resources, have necessitated the development of new design solutions, including new technologies that could find application in the commercial market. The strong synergy with ESA technology programmes such as the Technology Research Programme (TRP) and General Support Technology Programme (GSTP) has also played an important role in containing the facilities' development costs.

In order to select experiments for the facilities, International Life Sciences and ESA Physical Science Announcements of Opportunity (AOs) were released in 1998 and in 1999. Following the relevant peer recommendations and endorsement from the Microgravity Programme Board, the first batch of experiments was selected for each facility. New AOs are planned to be issued every 1-2 years.

The development schedule for each facility is shown in Figure 2, and the principal features in Table 1. All facilities will make use of the Japanese International Standard Payload Racks (ISPRs) and the Standard Payload Outfitting Equipment (SPOE, including standard payload computer, smoke sensor and remote power distribution assembly), developed through the Utilisation Programme. A laptop will serve as the primary interface between the flight crew and each facility. It allows full monitoring and control of the facility and the experiment modules. Crew members can view scientific images (digital video and analogue NTSC) from the experiment processes, as well as information on the health and operational status of the facility. Table 1 indicates the technical features common to all facilities. The main features are available on <<http://www.estec.esa.int/spaceflight/inmfc.htm>> to increase awareness of the possibilities offered to the scientific and industrial community.

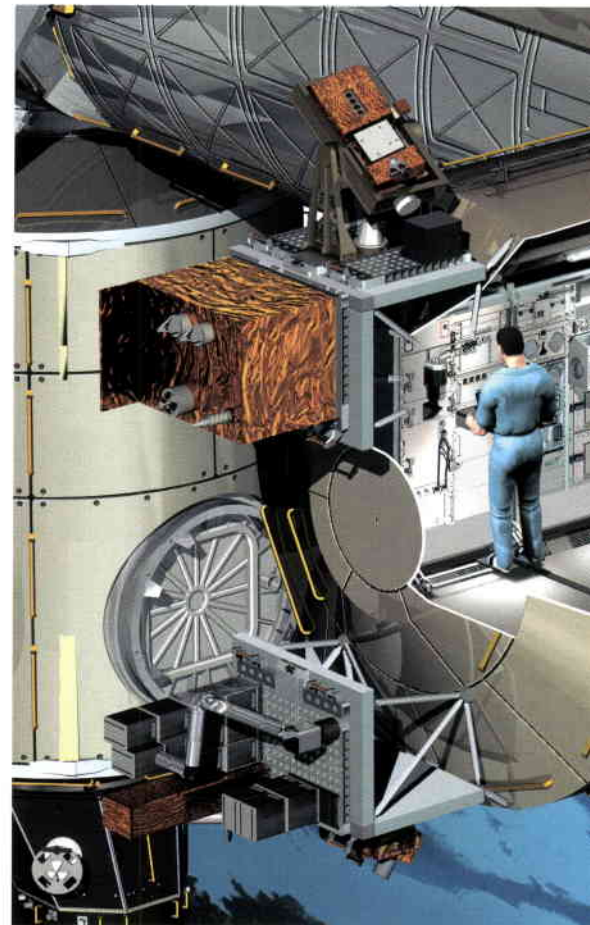
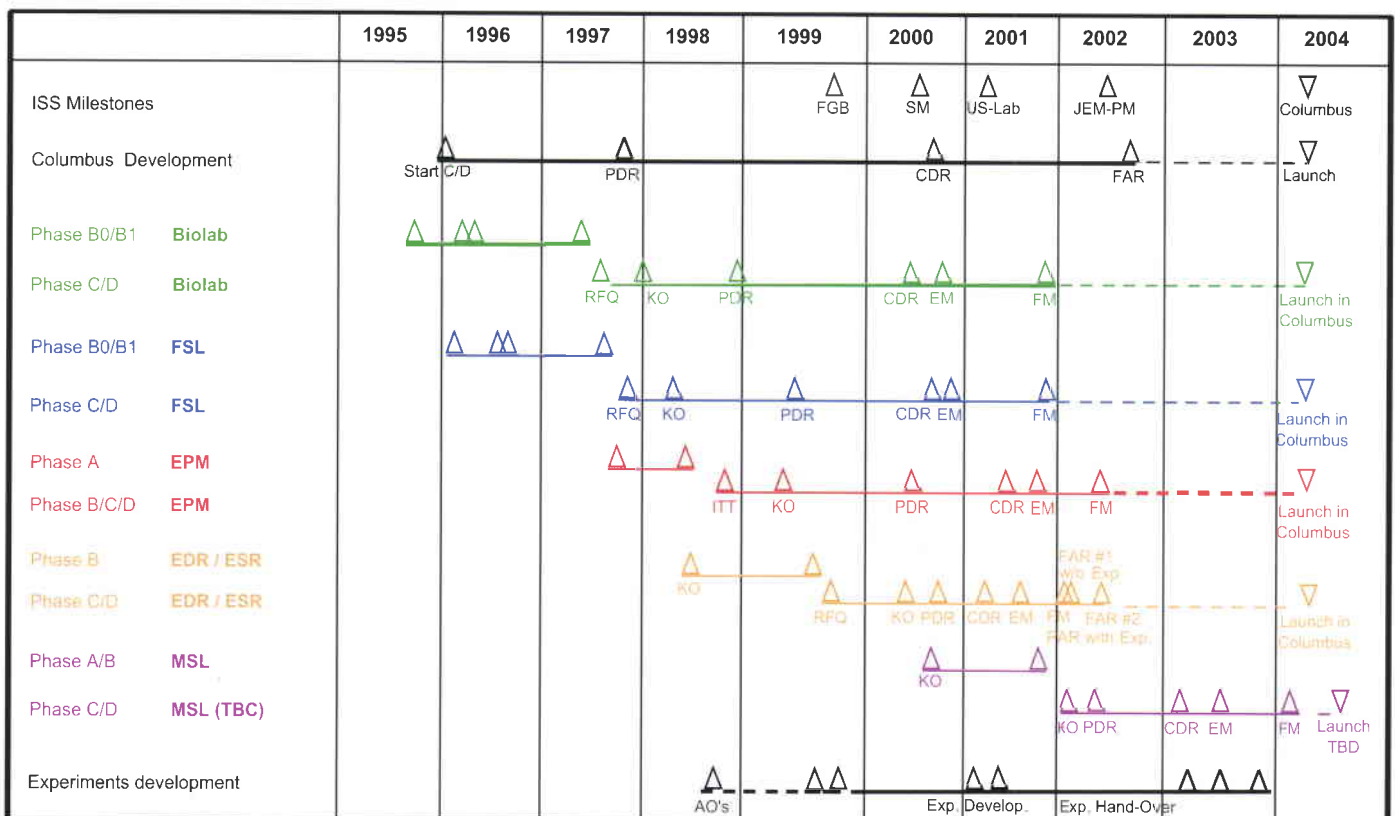


Figure 1. The multi-user facilities inside the Columbus laboratory. (ESA/D. Ducros)

Figure 2. Development schedule of the Columbus multi-user facilities





Biolab

Scientific objectives

Life Sciences experiments in space aim to identify the role that microgravity plays at all levels of life, from the organisation of a single cell to the nature of gravity-resisting and -detecting mechanisms in the more highly developed organisms, including humans. While the effects of microgravity on humans will also be investigated by other facilities (e.g. EPM), it is important to begin the investigation with the smaller elements of the biological structure. At the science community's behest, ESA has always been strongly involved in the investigation of biological samples, e.g. with Biorack and Biobox. The scientific results from these flights can certainly influence our everyday lives, particularly in the areas of immunology, bone demineralisation, cellular signal transduction and cellular repair capabilities. Such results could eventually have a strong bearing on critical products in the medical, pharmacological and biotechnological fields.

- ¹ISIS = International Subrack Interface Specification,
²SED = Standard European Drawer (8-PU size),
³MDL = Middeck Locker,
⁴MPLM = Multi-Purpose Logistics Module,
⁵ATCS = Automatic Temperature Controlled Storage,
⁶ASS = Automatic Ambient Storage
⁷PU = Panel Unit

Table 1. Principal features of the Columbus multi-user facilities

| | Biolab | FSL | EPM | EDR |
|---|--|--|--|---|
| Research Field | <ul style="list-style-type: none"> - Cell culture - Microorganisms - Small plants - Small invertebrates | <ul style="list-style-type: none"> - Bubble formation/growth - Condensation phenomena - Thermophysical parameters - Directional solidification | <ul style="list-style-type: none"> - Metabolic Functions - Cardiovascular - Muscular/Skeleton system - Neuroscience | <ul style="list-style-type: none"> - Platform for up to 8 experiment modules - PCDF is part of first experiment module set |
| Automation | Complete experiment execution including analysis by using handling mechanism | Experiment execution including analysis | When feasible to shorten experiment set-up and teardown times | <ul style="list-style-type: none"> - All experiments can be executed in parallel - Each experiment module will be fully autonomous |
| Telescience | All automatic features can be altered from ground | All automatic features can be altered from ground | All automatic features can be altered from ground | All automatic features can be altered from ground and be replaced by manual crew commands or from ground |
| Advanced Diagnostics | <ul style="list-style-type: none"> - Microscope - Spectrophotometer | <ul style="list-style-type: none"> - Particle image velocimetry - Thermographic mapping - Interferometric observation | <ul style="list-style-type: none"> - Science Modules | <ul style="list-style-type: none"> - N/A - Experiment modules may contain their own diagnostics |
| Modularity/ Serviceability | <ul style="list-style-type: none"> - Modular design of the facility - Experiments in standard container box - Experiments carried out in 0-g and 1-g simultaneously | <ul style="list-style-type: none"> - Modular design of the facility - Experiments in standard container box | <ul style="list-style-type: none"> - Modular design of the facility - Science Modules can be exchanged and operated in other Space Station locations | <ul style="list-style-type: none"> - Each of the 8 experiment modules can be accommodated in ISIS¹ SEDs² or standard ISS MDLs³ - SEDs and MDLs can be frequently up/downloaded in MPLM⁴ |
| Facility Configurability | Experiment Containers, ATCS ⁵ inserts, AAS ⁶ inserts and analysis instruments can be exchanged in orbit | Experiment Containers, reference targets and front-mounted cameras can be exchanged in orbit | All Science Modules can be exchanged in orbit | <ul style="list-style-type: none"> - Experiment Modules can be exchanged in orbit - Control software can be reconfigured from ground |
| Experiments Container Box/Cartridge size/Science Module (WxHxL) | <ul style="list-style-type: none"> - 60x60x100 mm - 170x120x140 mm | 400x270x280 mm | Internal usable volume for Science Modules: 4 PU ⁷ = 400x143x580 mm 8 PU = 400x321x580 mm | Internal usable volume for Science Modules: <ul style="list-style-type: none"> - SED: 387x327x573 mm - MDL: 440x253x566 mm |

The current Biolab concept is that of a multi-user facility for conducting biological experiments on cells, microorganisms, small plants and small invertebrates, as well as research in biotechnology (Figure 3). The design respects the science recommendations, the outcome of the scientific and feasibility studies (e.g. Phase-A/B), the experience gained from facilities flown previously, and the requirements and possibilities offered by the Space Station.

Facility description and operation

Biolab is divided physically and functionally into two sections: the automated section in the left side of the rack, and the manual section, including the BioGlovebox, in the right side. In the automated section, also known as the Core Unit, all activities are performed automatically by the facility after manual sample loading by the crew. By implementing such a high level of

automation, the demand on crew time is drastically reduced. The manual section, in which all activities are performed by the crew themselves, is mainly used for sample storage and specific crew activities. The biological samples are contained in standard Experiment Containers (ECs), which offer standard external interfaces with Biolab, an approach that has been well-proved with Biorack. The internal volume available to experimenters is 60x60x100 mm for the standard container, but the larger Advanced Experiment Container (170x120x140 mm) is also available. Biolab's main features are indicated in Table 1.

The biological samples, with their ancillary items, will be transported from the ground to Biolab either already in the ECs or in small vials if they require temperatures as low as -80°C, taking advantage of the ESA-developed MELFI freezer. Once in orbit, samples already in ECs will be manually inserted into Biolab for processing, while frozen samples need to be thawed in the Experiment Preparation Unit (EPU) installed in the facility's Bioglovebox.

Once the manual loading is completed, the automatic processing of the experiments can start. These experiments will be run in parallel on the two centrifuges, one at 0 g and the other at 1 g for reference. During the experiment, the handling mechanism



Figure 3. The Biolab multi-user facility. (ESA/D. Ducros)



Figure 5. The Biolab Engineering Model under integration. (ESA/MMS-F)

will transport the samples to Biolab's diagnostic instruments. With the aid of teleoperations, the scientists on the ground can participate in this preliminary analysis process. Typical experiment durations can be between a few days and a few months.

Industrial organisation and development status

Biolab's Phase-C/D was initiated in December 1997 with Matra Marconi Space of Toulouse (F) as prime contractor. The consortium is shown in Figure 4. The manufacturing of all Engineering Model (EM) subsystems has been completed and the EM is under integration (Figure 5). Completion of the functional and performance test campaign is planned for the second half of 2000. The Flight Model will be delivered by the end of 2001.

Among the subsystems, one of the first elements to be manufactured was a set of ECs. Great care was taken to ensure that their construction materials are bio-compatible with the widest range of biological samples. In this respect, the industrial consortium benefited from the results of the Experiment Container Standardisation (ECS) study, a GSTP study that identified a set of standard items for use in ECs.

The Centrifuges (Figure 6) were manufactured early in the Biolab development plan, to ensure smooth integration inside the complex Incubator. Each centrifuge is equipped with a central gas slip-ring to supply its six ECs with a controlled atmosphere. Biolab's slip-ring had to fulfil stringent requirements in terms of reduced torque, reduced leakage and material bio-compatibility, combined with a low-pressure

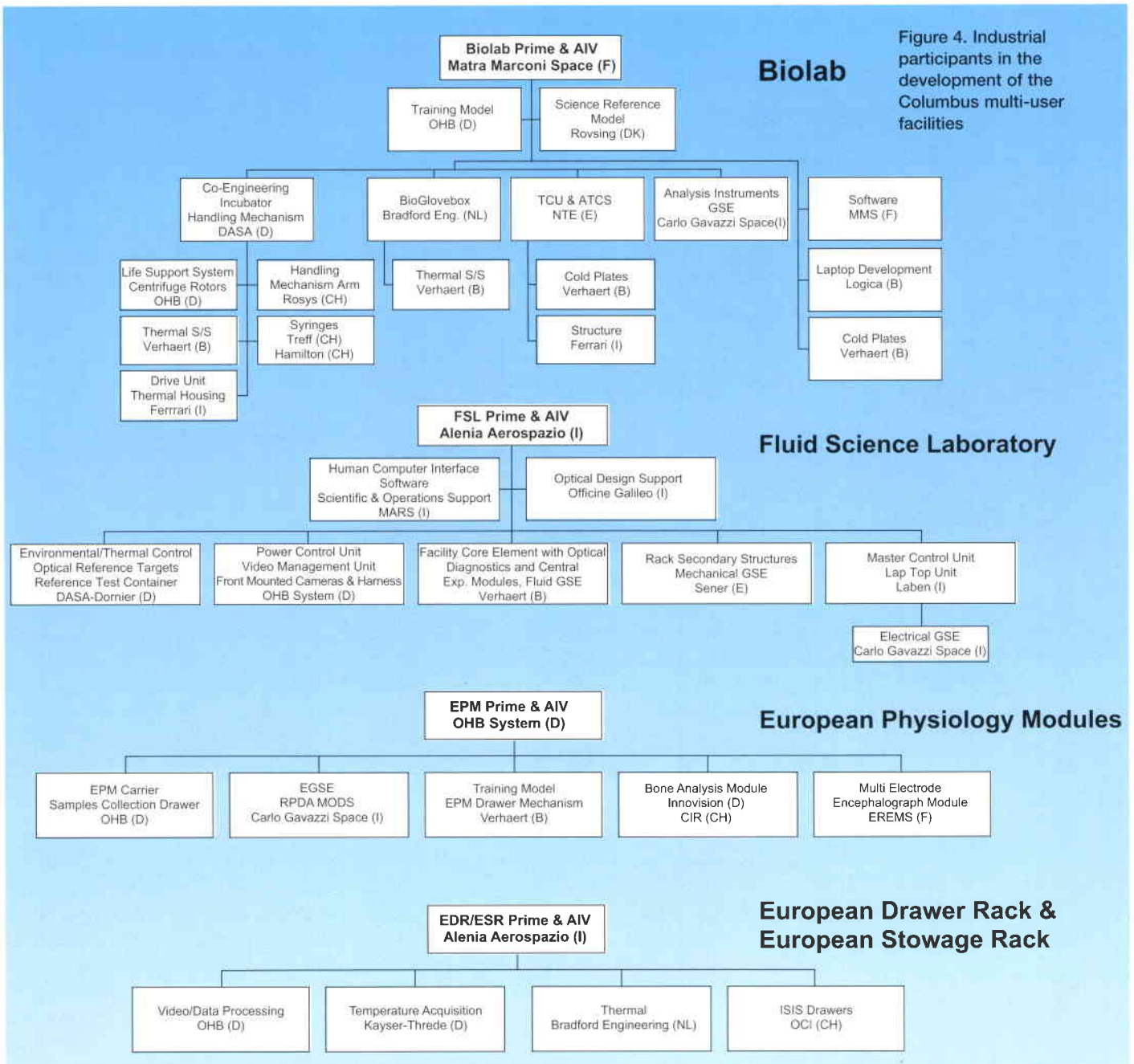


Figure 4. Industrial participants in the development of the Columbus multi-user facilities

supply gas. Since no suitable commercial slip-rings were available on the market, the critical development was supported in Phase-B by a dedicated breadboard, which proved the design's acceptable performance. Biolab's Science Team supported the Industrial Consortium by performing dedicated bio-compatibility tests.

Owing to the nature of Biolab's experiments, the BioGlovebox includes an ozone generator to clean and sterilise some of Biolab's subsystems. The ozone is created by a high-voltage alternating electrical discharge through the air, breaking down molecular oxygen into atomic oxygen. The generator will be used to:

- sterilise Biolab before starting experiments, to avoid contamination from the Station infecting the experiment;
- clean and sterilise a sample spillage, to avoid biological contamination growing uncontrollably within Biolab.

repair processes in mammalian cells in microgravity, after these cells are damaged by known doses of radiation. The results will be important in assessing the risks of spaceflight, since there is a synergistic link between space radiation and microgravity. One set of damaged cells will be studied in space by fluorescence microscopy using telescience, while the second set will be deep-frozen for analysis on the ground.

The second candidate experiment will study the effect of spaceflight on the virulence potential of bacteria that are infectious to humans. This will also be an important contribution to risk-assessment for space travellers, since the space environment may alter the pathogenic potential of the bacteria. This is of particular importance because microgravity negatively affects the human immune system.

Fluid Science Laboratory (FSL)

Scientific objectives

Fluid science experiments in space are designed to study dynamic phenomena in the absence of gravitational forces. Under microgravity conditions, such forces are almost eliminated, including their effects in fluid media such as gravity-driven convection, sedimentation and stratification, and fluid static pressure. This allows the study of fluid dynamic effects that are normally masked by gravity, such as the diffusion-controlled heat and mass transfer in crystallisation processes – the absence of the normally dominant convective flow processes results in reduced defect density.

The absence of gravity-driven convection eliminates the negative effects of density gradients (inhomogeneous mass distribution) that always arise on Earth in processes involving heat treatment, phase transitions, diffusive transport or chemical reactions. Convection in terrestrial processes is a strong perturbing factor, the effects of which are seldom predictable with great accuracy and which dominate heat and mass transfer in fluids.

The ability to control such processes is still limited. Their full understanding requires further fundamental research by conducting well-defined model experiments for the testing and development of related theories under microgravity. This will allow the optimisation of manufacturing processes on Earth and improvement in the quality of high-value products such as semiconductors.

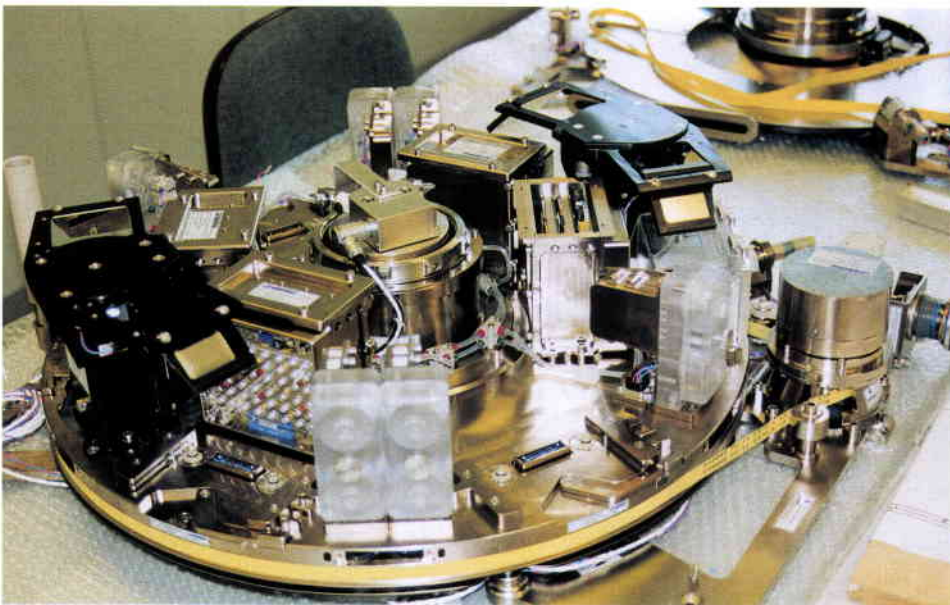


Figure 6. One of the two centrifuges for Biolab. (ESA/OHB)

Developed specifically for Biolab, this ozone generator may find a large commercial market on the ground, where it can quickly and easily sterilise medical tools.

User-support activities and selected experiments

In the frame of the user-support activities, the EPU's Phase-B/C/D began early in 2000 with the prime contract awarded to Verhaert (B). The breadboarding tests will be completed by the second half of 2000.

Following the 1998 International Life Sciences Research Announcement (LSRA), two experiments are in the definition phase, with Biolab as one of the selected possible facilities. The first experiment will provide insight into the

ESA has already been involved in studying fluid science phenomena under microgravity conditions for several years, notably with the Bubble, Drop and Particle Unit (BDPU) facility that produced important results from several Spacelab missions.

Facility description and operation

FSL is illustrated in Figure 7. The kernel of the facility consists of the Optical Diagnostics Module (ODM) and the Central Experiment Modules (CEM), into which the Experiment Containers (ECs) (Figure 8) are sequentially inserted and operated. Together, these modules represent the Facility Core Element (FCE), which is complemented by the functional subsystems for system and experiment control, power distribution, environmental conditioning, and data processing and management.

In order to cope with the experiment observation requirements, a set of optical diagnostics is integrated in FSL, including:

- visual observation in two axes (y, z) with direct registration via electronic imaging and photographic back-up via Front Mounted Cameras (FMCs) providing high speed, high resolution and colour recording;
- background, sheet and volume illumination with white light and monochromatic (laser) light sources;

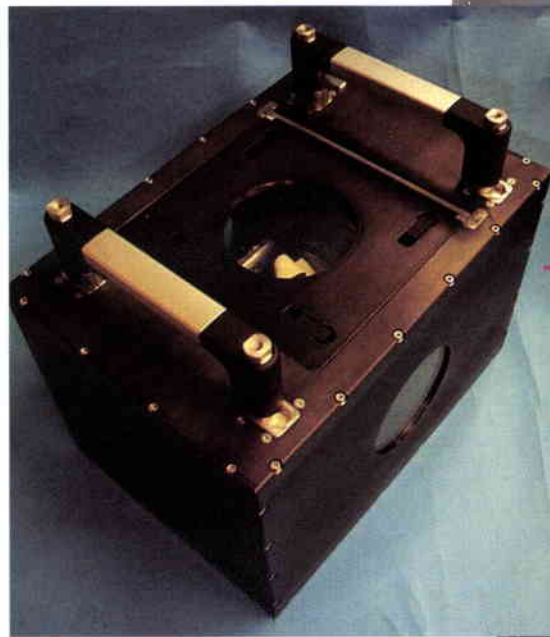
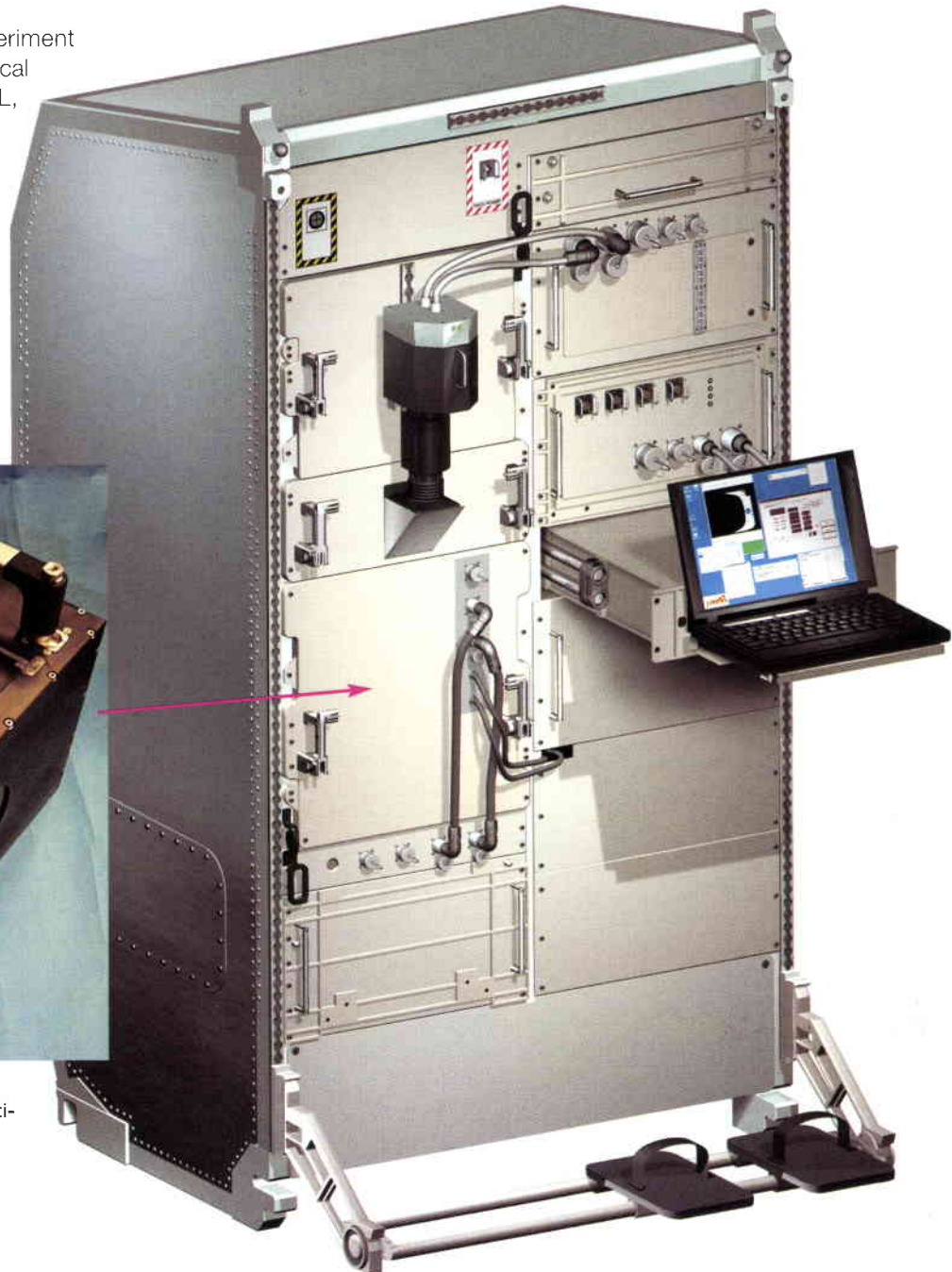


Figure 7. The Fluid Science Laboratory multi-user facility (right). (ESA/D. Ducros)

Figure 8. The Engineering Model of the FSL Experiment Container (above). (ESA/DASA)

- particle image velocimetry, including liquid crystal tracers for simultaneous velocimetry and thermometry;
- thermographic (infrared) mapping of free liquid surfaces (also via FMC);
- interferometric observation in two axes (y, z) by convertible interferometers with active alignment:
 - holographic interferometer;
 - Wollaston/shearing interferometer;
 - Schlieren mode combined with shearing mode;
 - Electronic Speckle Pattern Interferometer (ESPI).

In addition to the integrated system, Flight Support Equipment (FSE) will be available onboard: spare parts, special tools and consumables such as cleaning agents, the



FMCs and the Optical Reference Targets (ORT) for calibration of the experiment and diagnostic equipment before an experiment run.

For each experiment or experiment category, an individually developed EC will be used. Stored in the ESR during non-operational phases, each EC will be inserted by the crew into the CEM drawer, where it will undergo an experiment and diagnostics calibration cycle before any process activation. Each EC, with a typical mass of 30-40 kg and standard dimensions of 400x270x280 mm, provides ample volume for accommodating the fluid cell assembly, including the process stimuli and control electronics. It may also be equipped with dedicated experiment diagnostics to complement the standard diagnostics provided by FSL itself.

The control concept for system and experiment operation provides for alternative modes comprising fully automatic experiment processing, even during certain communication outage phases such as regular Loss Of Signal, semi-automatic processing of defined experiment subroutines, and fully interactive step-by-step command keying. All operating modes can be triggered either by the flight crew or from the ground, thus ensuring the possibility of quasi-real-time tele-operation (telescience).

Industrial organisation and development status

FSL's Phase-C/D contract was signed in April 1998. The industrial consortium, shown in Figure 4, is led by Alenia Aerospazio (I) as prime contractor. The Engineering Models for most of the subsystems have been completed. The system EM programme will be completed by the end of 2000. The Flight Model will be completed by the end of 2001.

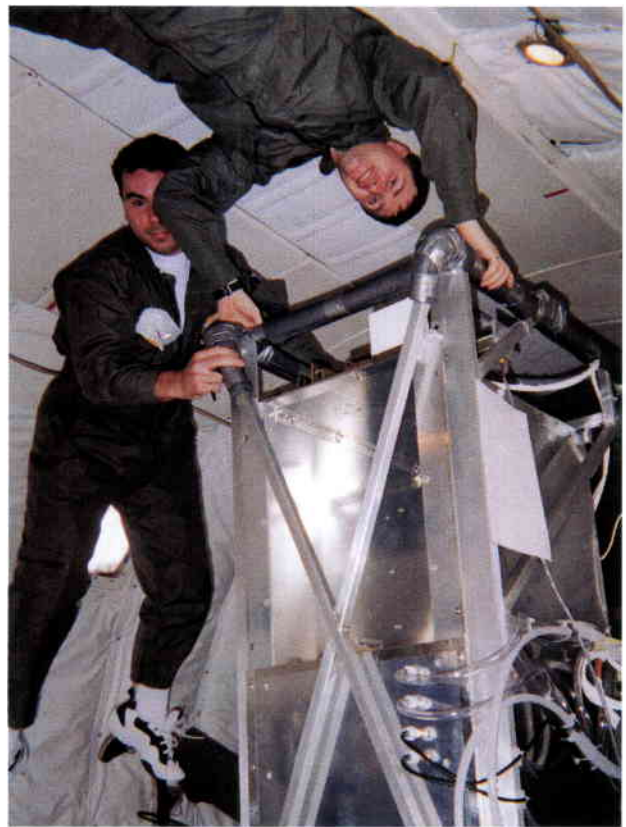
There are particular technical challenges in designing the diagnostics and the scientific data management system. The combination of four different convertible and state-of-the-art interferometers offers very high flexibility for experiment observation and diagnostics but, on the other hand, inevitably increases complexity. It requires not only a very dense and compact layout but also a high end-to-end optimisation effort, in view of the manifold technical and scientific performances required.

Potential upgrades, partly resulting from new technology developments, are under

investigation for a decision in the near future on their implementation:

- the active Microgravity Vibration Isolation Subsystem (MVIS, Figure 9), using magnetic levitation. Each Principle Investigator (PI) can activate the subsystem to isolate his experiment from the *g*-jitter perturbation induced by Space Station dynamics. MVIS is being developed by the Canadian Space Agency;
- diagnostics, replacing the bulky and heavy thermoplastic film camera with the now-mature technology of photorefractive crystals in combination with digital holographic interferometry.

Figure 9. The breadboard of the FSL Microgravity Vibration Isolation Subsystem (MVIS) with the Facility Core Element being tested during a parabolic flight. (CSA)



Experiments selected

Based upon the 1998 Physical Science AO, about 15 peer-recommended experiment proposals, from various scientific and industrial research organisations all over Europe, require FSL. Even in the USA, a growing interest was found in running experiments on FSL. Definition studies of experiment containers will be initiated for the following experiments in view of their maturity:

Development of Advanced Foams and Hydrodynamics of Wet Foams

These experiments will provide knowledge to European industry on the development and production of advanced foams by overcoming the limits imposed by various instabilities experienced in normal gravity.

Several industries including the oil industry are participating.

– *Fundamental and Applied Studies of Emulsion Stability*

These experiments will investigate the physio-chemical aspect of surfaces in support of emulsion science technology of special interest for the food, cosmetic and pharmaceutical industries.

– *Convection and Interfacial Mass Exchange*

These experiments are devoted to the study of mass-transfer processes through interfaces. These phenomena are of the utmost importance for chemical engineering processes. Thirteen European and two US groups are involved. Industrial applications are expected for thermal-control equipment in space industries.

– *Simulation of Geophysical Flows under Microgravity*

These experiments will investigate, on a small scale, large-scale motions in the outer layer of the Earth and in the atmospheres of giant planets. The results will be used to improve models predicting thermal convection in those situations.

All of the other experiment proposals will undergo further definition work.

European Physiology Modules (EPM)

Scientific objectives

Human physiology experiments in microgravity not only increase knowledge of how the human body reacts to long exposure weightlessness, but also contributes to a better understanding of Earth-related problems such as ageing processes, osteoporosis, balance disorders, biomedical research, cancer research and muscle wasting in limb immobilisation (casts) and bed-rest. Investigations have been conducted for many years and ESA has successfully flown facilities, such as Sled and Anthrack on several Spacelab missions.

In order to evaluate the data collected onboard, it is essential that reference (or baseline) data be collected both before the mission and after the crew returns to Earth. For this purpose, EPM will provide a Baseline Data Collection (BDC) system that includes functional copies of the onboard instruments. The BDC will be easily transportable to ensure that the equipment is available at the crew location shortly before launch and immediately after landing.

NASA's Human Research Facility (HRF) will be similar to EPM. The first of two ISPRs will be launched early in the Space Station assembly sequence and the second somewhat later, although still well before Columbus. ESA and NASA plan to collocate EPM and HRF in Columbus, thereby allowing experiments using scientific instruments from both.

Facility description and operation

The multi-user EPM (Figure 10) consists of a complement of Science Modules (SMs) plus the Carrier infrastructure to support their coordinated operation. The Carrier provides data handling, thermal control and mechanical accommodation for the SMs. A maximum of nine active Science Modules can be accommodated at any one time, allowing for different Module sizes.

Figure 10. The European Physiology Modules multi-user facility. (ESA/D. Ducros)



The SMs are accommodated in standard drawers of sizes of 4 PU and 8 PU (1 PU = 4.45 cm). They interface with the rack via a standardised guide system that simplifies the on-orbit exchange and installation of new SMs. All rack-mounted SMs are cooled via a ducted air system provided as part of the Carrier.

EPM's modularity allows a very flexible configuration of SMs. Based on inputs from the Facility Science Team, it has been decided to include the following instruments in the initial configuration:

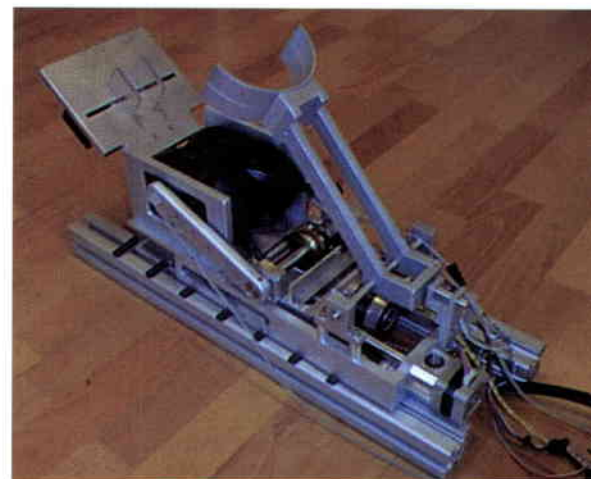
– **Multi-Electrode EEG Measurement Module (MEEMM)**

MEEMM will be used for different types of non-invasive brain function investigations. During experiments, the test subject wears a cap equipped with up to 128 electrodes (Figure 11) connected to sensitive, low-noise electronics to measure the very small signals at very high sampling rates. In order to generate appropriate stimuli, different stressors can be used that are available onboard. Examples are the Virtual Environment Generator and muscle stimulators (associated with NASA's Human Research Facility). Together with EPM's ELITE-S2 module (see below), it will be possible to perform experiments that simultaneously measures brain activity and body movements. MEEMM also contains an ambulatory unit that will allow measurements to be made while the test subject is performing other activities or asleep. The data are recorded on a removable hard disk and later transferred to the EPM Data Management System to be sent to ground.

– **Bone Analysis Module (BAM)**

Bone loss is a severe problem in long-duration space flights. Understanding the related dynamics and developing effective countermeasures are important requirements for flying long missions. BAM will study the efficacy of various countermeasures by evaluating changes in the ultrasound transmission properties of the heel bone (Figure 12). BAM is based on a commercial system, where the foot is placed in an open water tank. This approach is unsuitable for space, so instead water-filled latex bags are placed on each side of the foot. A test campaign using the prototype and other bone densitometers on a large number of subjects will verify the new design.

Figure 12. The breadboard model of EPM's Bone Analysis Module. (ESA/Innovision)



– **Sample Kit Drawer**

This drawer will help the crew to take blood and urine samples. Most samples must be stored onboard in a controlled environment for later download to the ground for analysis. Limited analysis can also be performed onboard.

Apart from the above hardware being developed as part of the EPM contract, National Agencies will contribute the following instruments:

– **Cardiolab**

Cardiolab (CNES and DLR) comprises different equipment supporting cardiovascular research, e.g. electro-cardiogram and blood pressure holter, portable Doppler, air plethysmograph, cardiopres;

– **ELITE-S2**

The 'Elaboratore Immagini Televisive-Space 2nd generation' ELITE-S2 (ASI and CNES) is a facility for the quantitative analysis of human kinematics in weightlessness. Four cameras mounted around the test subject record the movements. Special software detects sensor positions mounted on the

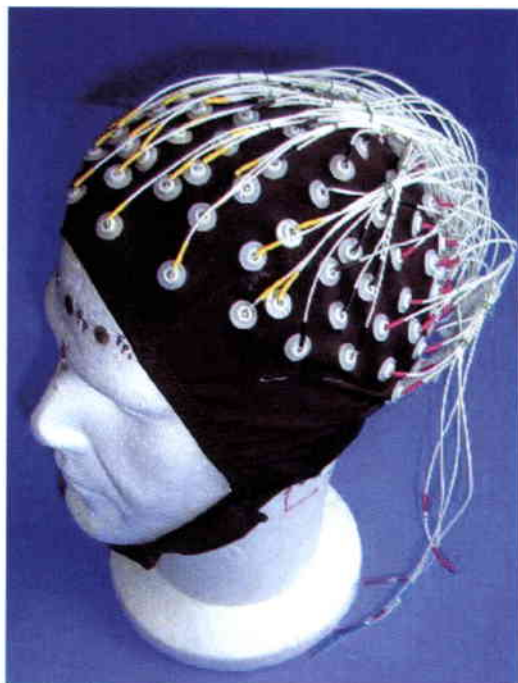


Figure 11. The EPM Multi-Electrode EEG Measurement Module cap. (ESA/EREMS)

subject and from this recreates a 3D model that can be used to analyse the movement patterns in detail.

– *XSMI/PPMI*

The Xenon Skin Blood Flow Measurement Instrument (XSMI) and the Physiological Pressure Measurement Instrument (PPMI) (Danish space agency) are two small ambulatory instruments to measure skin blood flow and physiological pressures such as central venous and oesophageal pressures.

Standard European Drawers (SEDs) and standard Shuttle-type Middeck Lockers (MDLs). It is a flexible experiment carrier since it is not dedicated to a specific discipline. EDR's main design drivers are modularity and standardisation. The use of standard drawers and lockers assure quick turnaround and thereby increased flight opportunities for the microgravity user community. Mission preparation activities are estimated to take 6 months. In particular, SEDs and MDLs can be exchanged in orbit.

The EPM contribution to NASA's Human Research Facility

ESA is developing a number of instruments for contribution to NASA's HRF, thereby allowing their earlier in-orbit deployment than possible aboard Columbus. One is a collaboration with NASA to develop a Pulmonary Function System (PFS). This will consist of four building blocks, two provided by NASA (Gas Analyser System for Metabolic Analysis Physiology; Gas Distribution System) and two by ESA (Photoacoustic Analyser Module, PAM; Pulmonary Function Module). Together, these blocks will make up a highly flexible and sophisticated pulmonary and cardio-vascular research tool. PAM is based on a European niche technology and it will be reduced in volume compared with the earlier version (Figure 13). This development has helped the commercial application of this technology in hospitals.

Industrial organisation and development status

OHB (D) was awarded the prime contract in May 1999 for Phase-B/C/D; the industrial consortium is shown in Figure 4. For the EPM Contribution to the HRF-2, the prime contractor is Innovision (DK). EPM's Preliminary Design Review is planned by mid-2000. Breadboardings of MEEMI and BAM are underway. Delivery of the Flight Model is expected by mid-2002.

Experiments selected

One experiment selected for Definition from the 1998 International LSRA requests the use of PFS. Its objective is to evaluate cardiac fluid volume regulation. The 1999 LSRA is the first to include EPM's capabilities. Of the 43 proposals involving human research, there are 13 that could make use of the EPM and/or PFS instrumentation.

European Drawer Rack (EDR)

EDR is a multi-user facility (Figure 14) providing the infrastructure for accommodating and servicing experiment modules housed within

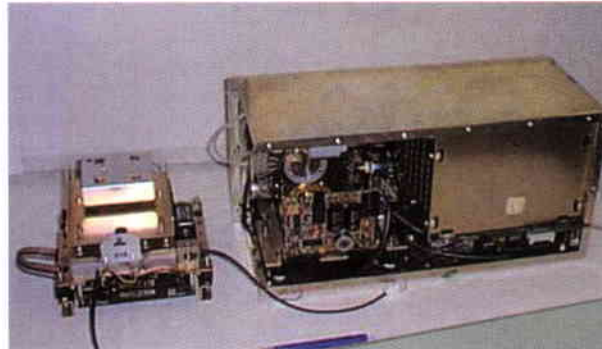


Figure 13. The Photoacoustic Analyser Module (PAM, left) for EPM. The earlier version is at right. (ESA/Innovision)

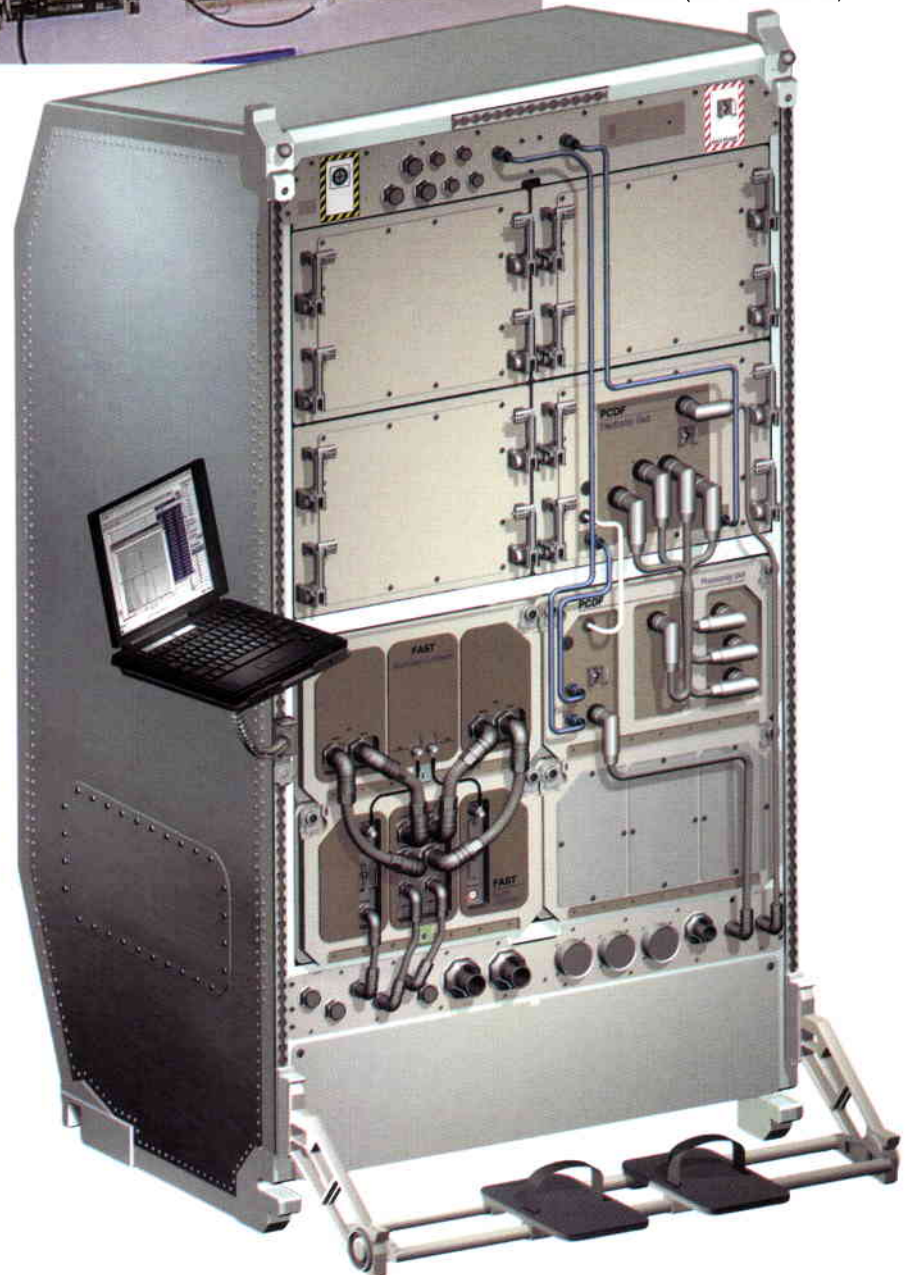


Figure 14. The European Drawer Rack multi-user facility, including the FAST and PCDF experiment modules. (ESA/D. Ducros)

Facility description and operation

EDR provides small and modular experiments in SEDs and MDLs with access to Columbus services. Its main features are shown in Table 1. A fundamental EDR goal is to support the development of smaller sub-rack payloads (Class-II) by providing accommodation resources and rapid-turnaround flight opportunities. EDR's design is oriented to maximise user-friendliness and flexibility of experiment accommodation and operation.

EDR's SED and MDL concept allows experiment module access to the EDR centralised services, ranging from the distribution of system resources (e.g. power, data, venting and cooling) to dynamic resource management (e.g. simultaneous access to system resources by more than one experiment module). EDR includes all the capabilities for monitoring and controlling the facility, its operations and resource usage envelopes, as well as the capability for operating the experiments. Its main subsystem functions are implemented in five units: Power; Thermal; Processing Control and Command; Video Management Units; Laptop. It supports simultaneous control of up to eight different experiments, i.e. one for each drawer and locker within the allowed resource budgets. EDR is reconfigurable in flight to allow the exchange of SED/MDL experiments on-orbit. It is designed to need only minimal crew intervention.

The SEDs are compatible with the International Subrack Interface Standard (ISIS). This ensures mechanical compatibility between the NASA Express Transport Rack (ETR) and EDR and, as such, allows rapid EDR payload turnaround by using ETR for EDR SED up/download. The Standard ISS Lockers (MDLs) are mechanically compatible with the ISS Shuttle Middeck interfaces and ETR. This allows rapid EDR experiment locker turnaround by using either the Shuttle or ETR for EDR MDL up/download.

Industrial organisation and development status

EDR completed Phase-B in July 1999 and Phase-C/D will begin in 2000. Some breadboarding activities were completed during Phase-B. The industrial consortium is led by prime contractor Alenia Aerospazio (I); the industrial consortium is shown in Figure 4.

Experiments

A set of potential experiment modules for EDR accommodation has been identified:

- FAST (Facility for Adsorption and Surface Tension Studies) is an ESA multi-user facility that has already flown on the STS-95/

Spacehab mission (October 1998). It is now undergoing refurbishment for flight on STS-107/Spacehab in March 2001 and is a candidate for reflight in EDR for long-duration experiments in Columbus. FAST is accommodated in two MDLs (Figure 14).

- PCDF (Protein Crystallisation Diagnostics Facility) is an ESA multi-user facility under development to provide in-depth knowledge and understanding of the protein crystal growth process under microgravity. PCDF crystal growth processing may use either batch or dialysis crystallisation. Protein crystal growth takes place in four reactors with the temperatures and temperature gradients of the protein solutions individually controlled. The built-in advanced diagnostics system allows the scientists to operate the experiments in a fully automatic mode (time-line and parameter controlled) or in a semi-automatic mode (telescience from ground).

The PCDF consists of two elements to be accommodated in EDR (Figure 14): the Process Unit (PU) and the Electronic Unit (EU). The PU accommodates the process chamber in which the four reactors are contained. The reactors contain the protein and salt solutions. The PU incorporates two temperature control layers. The EU accommodates the control circuitry for experiment execution and the PCDF diagnostics system, which incorporates a monochrome digital video camera with a wide field of view and microscope optics, the Dynamic Light Scattering (DLS) system and a Mach-Zehnder interferometer. For future applications, the PCDF can be expanded to support osmometry and pH measurement. The PU will be accommodated in the new ISS MDL, and the EU in a SED. For harvesting the protein crystals and reloading the protein and salt solutions on the ground, the complete PU has to be transported from/to Columbus within the Space Shuttle's middeck. This allows power provision to guarantee temperature control during transport, early access to the PU for protein crystal retrieval and late access for the PU installation in the middeck for uploading. This is mandatory, as proteins are sensitive and fast-deteriorating macromolecules.

PCDF is being developed under ESA's Microgravity Programme EMIR-2. The completed breadboarding has confirmed the design. The prime contractor is DASA/Dornier (D) with subcontractors Aerospaziale Matra Lanceurs (AML, F), Laben (I), Chevalier Photonics (B) and ALV (D).

European Stowage Rack (ESR)

ESR is a passive multi-user facility to allow

modular and standardised stowage of European payload support equipment and experiment samples within Columbus (Figure 15). It is based upon an enhanced ISPR structure with a number of inserts (shelves and dividers) that can be adjusted according to specific configuration requirements. These inserts enable optimal accommodation of standardised ISS Cargo Transport Bags (CTBs). During on-orbit operations, the CTBs may be removed from ESR and temporarily attached near to the payload racks where their contents are required. As a standardised ISS capability, CTBs are compatible with the NASA transport capabilities such as the Multi-Purpose Logistics Module (MPLM) Re-Supply Rack (RSR) and the Shuttle middeck provisions.



ESR's industrial organisation and its development status are the same as for EDR.

Materials Science Laboratory (MSL)

MSL is a follow-up to the version intended for the US Laboratory, allowing extensive reuse of hardware. The scientific objective is the study of thermodynamics and kinetics that control the delayed solidification of molten materials, as well as the measurement of physical properties in under-cooled melts.

Figure 15. The European Stowage Rack multi-user facility. (ESA/D. Ducros)

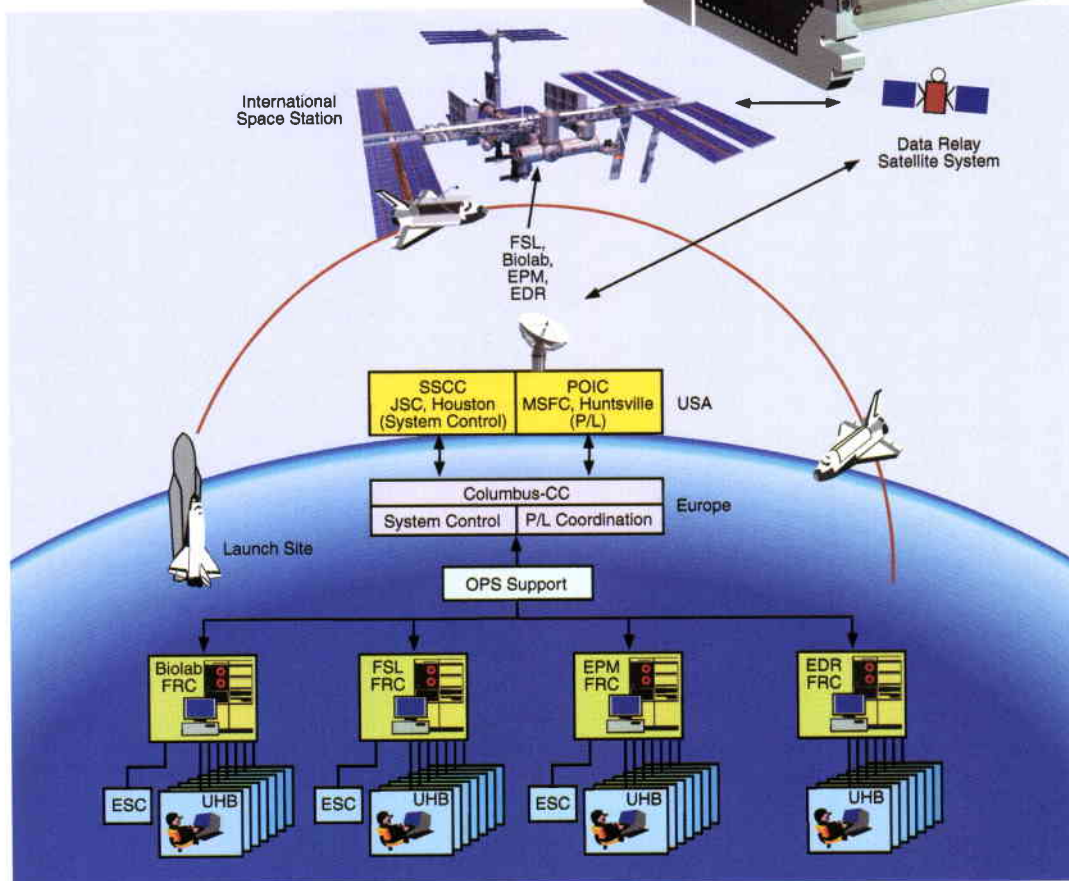
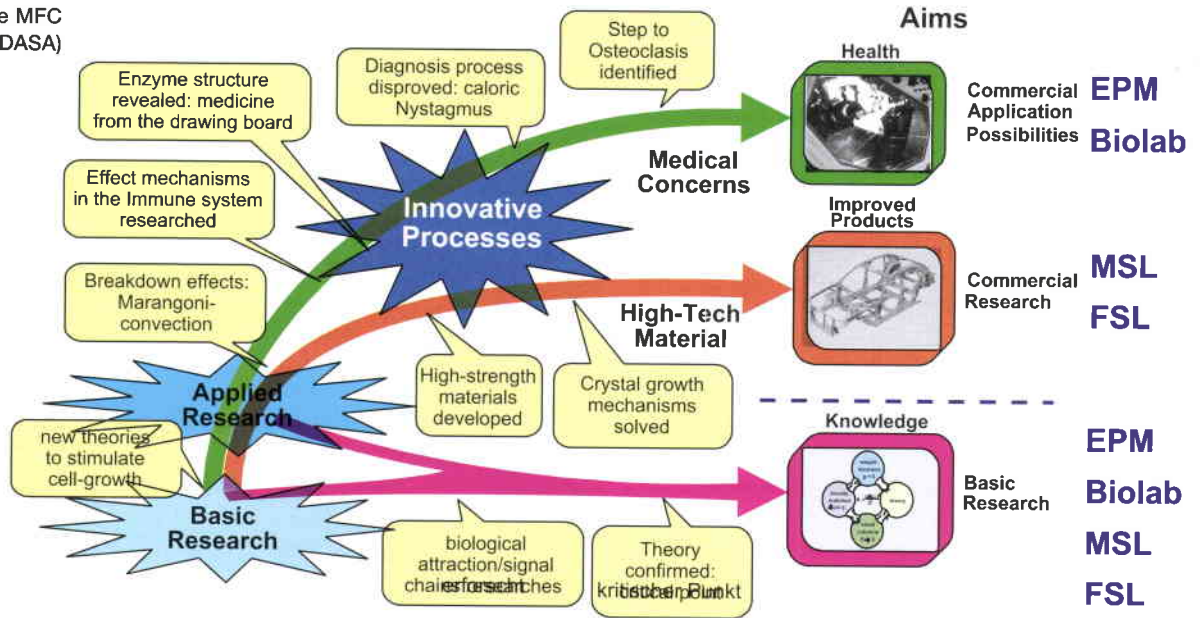


Figure 16. Operation of the Columbus multi-user facilities. CC: control centre. JSC: Johnson Space Center. MSFC: Marshall Space Flight Center. OPS: operations. P/L: payload. POIC: Payload Operation Integration Center. SSCC: Space Station Control Centre. Other acronyms are explained in the text

Figure 17. Possible fields of utilisation for the MFC facilities (ESA/DASA)



An industrial definition Phase-A/B is expected to begin in the second half of 2000. The start of Phase-C/D will be decided at the end of the definition phase.

Operation of the facilities

During development of the facilities, the science teams, user representatives (e.g. Facility Responsible Centres and User Operation Support Centres) and astronauts are helping to optimise the designs. At the end of the FSL, Biolab, EPM and EDR development phases, their final acceptance will take place using the Rack Level Test Facility (RLTF) to simulate the Columbus interfaces. Once Columbus is in orbit, this will be the only means of accepting payloads before uploading them to the Space Station.

Figure 16 shows a scenario for the scientific operation of the multi-user facilities aboard Columbus. Each laboratory will make use of a dedicated Facility Responsible Centre (FRC) that serves as the interface between all of the scientific users and the appropriate payload control centre. These FRCs will also prepare the timing for the experiments and perform the first level of troubleshooting during operations. The prime contractor for each facility will support a second level of troubleshooting and provide sustaining engineering support.

The following FRCs have been selected: MUSC (D) for Biolab, MARS (I) for FSL, CADMOS (F) for EPM and ESTEC (NL) for EDR. For some complex experiments, Experiment Support Centres (ESCs) will provide specific expertise in defined scientific fields. Some have already been identified: ETH (CH) for Biolab, DARIVA (E) for FSL and DAMEC (DK) for EPM.

Experiments may be executed from the User Home Bases (UHBs, primarily universities and research centres), with overall coordination by the FRC and, when required, by the ESCs. This decentralised payload processing is seen as the most efficient approach for implementation of Columbus utilisation.

Each mission increment will last 3-6 months and the selection of successive experiment complements will follow a similar schedule. The equipment required to conduct the experiments will be uploaded by the MPLM aboard the Space Shuttle.

Commercial use of the facilities

In view of the request by the ESA Council at Ministerial Level in 1999 to propose a scheme for commercialising the Space Station, the MFC Programme has completed a preliminary study with a consortium of MMS (F; Biolab), Alenia (I; FSL), DASA-RI/Dornier (D; MSL) and OHB (D; EPM) on defining a strategic plan for attracting commercial users. The goal of the study will be to generate income for ESA from conventional fields (such as R&D centres) and from 'unconventional' fields such as education. Possible fields of utilisation for the facilities are indicated in Figure 17. A follow-up phase will concentrate on some pathfinder projects to prove the effectiveness of the proposed plan with the identification of specific commercial customers.

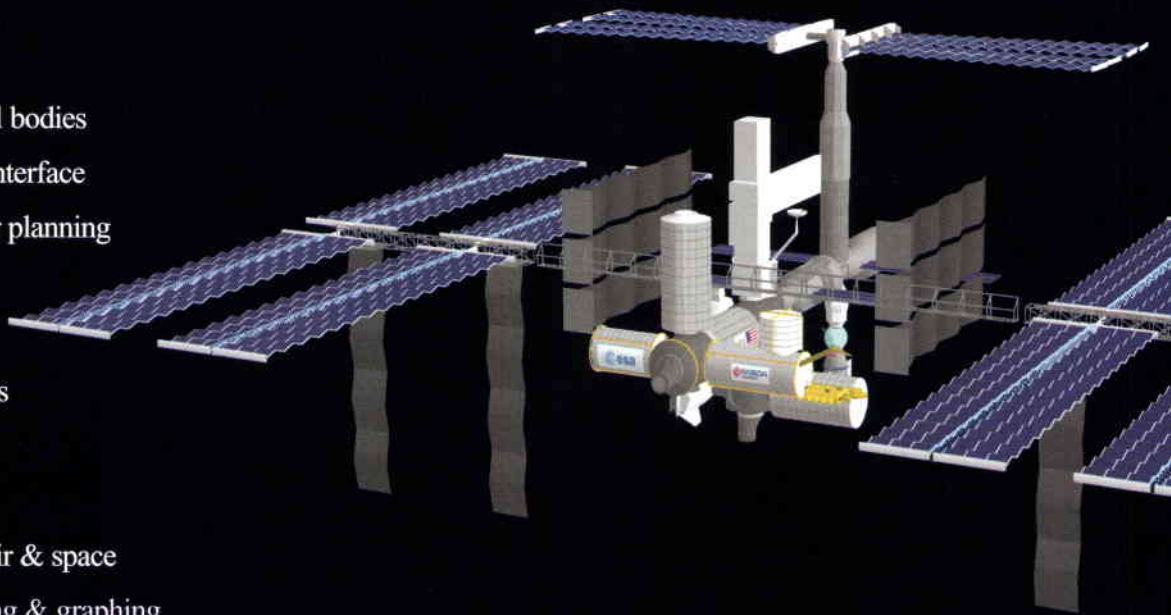
Acknowledgements

The authors wish to thank three members of the ESA/ESTEC Microgravity and Space Station Department: J.C. Ives (EPM contribution to the HRF); V. Pletser (PCDF); and C. Schmidt-Harm (FAST).

Satellite Tool Kit

Better. Faster. Cheaper.

Interplanetary mission design
High-fidelity orbit propagation
3D visualization
Communication link analysis
Navigation and coverage analysis
Orbit determination
Orbit maneuvering
User-definable central bodies
Real-time telemetry interface
Deep space maneuver planning
Collision analysis
Attitude modeling
Planetary ephemerides
Constellation analysis
Formation flying
Integrated land, sea, air & space
Customizable reporting & graphing



Contact +44 1908 551105 or visit www.stk.com for your free copy of STK®.

ANALYTICAL GRAPHICS, INC.
325 Technology Drive • Malvern, PA 19355
info@stk.com • www.stk.com



Software Solutions for the Aerospace Industry



INTAERO

International STK Resellers
Stoke Goldington, Bucks MK 16 8NY, UK
Tel: +44 1908 551105
Email: info@intaero.com

**Advanced System Engineering & Proven Solutions
for Spacecraft AIT & Ground Infrastructure**



A prime Dutch Aerospace System Engineering, Telecommunication, Simulation, Data Processing & EGSE Solution Provider

**Satellite
SERVICES BV**

**Scheepmakerstraat 40
2222 AC Katwijk aan Zee
The Netherlands
Tel: +31-(0)71-402-8120
Fax: +31-(0)71-402-7934**

**www.satserv.nl
info@satserv.nl**

Vulcain-2 Cryogenic Engine Passes First Test with New Nozzle Extension

D. Coulon

Directorate of Launchers, ESA, Paris

The development of the Vulcain-2 cryogenic engine forms part of ESA's Ariane-5 Evolution Programme, which was endorsed by the Ministers of the Agency's Member States in October 1995, at the Ministerial Council in Toulouse. Vulcain-2 is an improved version of the original Vulcain engine powering the main cryogenic stage of the Ariane-5 launcher, which

increases the available thrust from 1145 to 1350 kN.

The first studies associated with the new engine began in early 1991. They covered the engine system, the oxygen and hydrogen turbopumps, the combustion chamber, the nozzle extension and other equipment. Preliminary Design Reviews of each of the new engine's main components were undertaken throughout 1997.

On 17 August 1999, at the P5 test rig in Lampoldshausen, Germany, the new Vulcain-2 engine for Ariane-5 was tested as a complete configuration equipped with a new nozzle extension. Two previous tests had been performed with a short nozzle configuration: the first, on 17 June, lasted 7 sec and allowed the engine to reach stable operation conditions, thereby qualifying the starting sequence; the second, on 25 June lasted a total of 600 sec, as foreseen. By the end of the year, the Vulcain-2 engine had accumulated 1878 sec of running, shared between two engines and 14 tests.

Vulcain-2 is being developed by SNECMA (F), leading a team of manufacturers from 11 European countries. The French national space agency CNES manages the Ariane-5 Programme on ESA's behalf.

The oxygen turbopump developed by Fiat Avio (I) is the subsystem that has undergone the most significant changes. The combustion chamber developed by DaimlerChrysler Aerospace (D) has been adapted to accommodate the new flow rates. The mixture ratio has been raised from 5.3 to 6.1, and the expansion ratio of the nozzle extension, developed by Volvo Aerospace (S), has been increased by 30%, together with the reintroduction of the turbine exhaust gases.

The 20% increase in thrust demanded of the Vulcain-2 engine has called for a 25% increase in the power of the hydrogen turbine, corresponding to an increase of 9% in hydrogen flow through the combustion

Figure 1. Test firing of the M201 engine on the P5 test rig



Figure 2. Vulcain-2 oxygen turbopump assembly

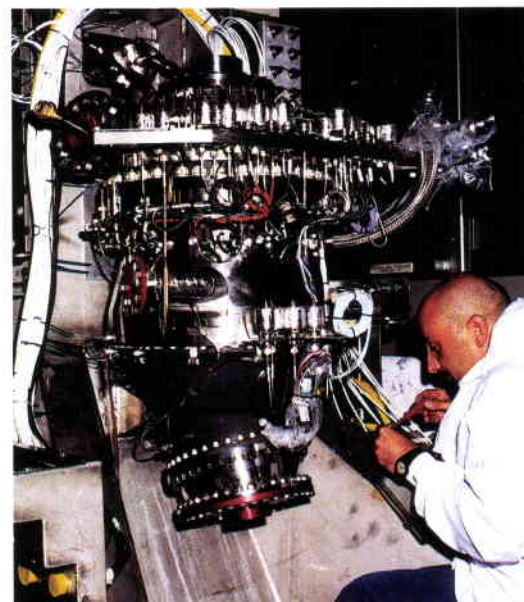




Figure 3. Vulcain and Vulcain-2 nozzle extensions

Figure 4. Vulcain-2 thrust chamber

chamber. This higher flow rate is achieved via a 16% hydrogen inlet pressure increase, driving the pump at 35 680 rotations per minute. The 16% gain in the hydrogen turbine inlet pressure, in turn, is produced through a 22% increase in the hot gas flow coming from the gas generator, which at the same time satisfies the 30% increase needed for the oxygen turbine. The new gas generator has 72 injectors instead of 60; doing away with the high frequency absorber has made room for these 12 additional injectors.

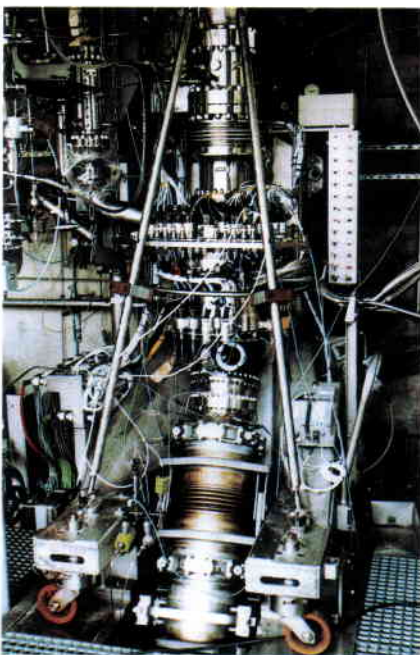


Figure 5. Vulcain-2 oxygen turbopump on the P593 test rig

The test campaigns for the hydrogen turbopump and the gas generator began on 8 September 1997 and lasted until 20 February 1998, at the PF52 SNECMA test rig. These tests demonstrated good turbine and pump behaviour under extreme loads. The latter were characterised by a turbopump speed of 40 700 rpm, developing a power of 21 MW with a hydrogen flow of 52.8 kg/s, compared with the nominal operating point of 35 680 rpm, 14.29 MW and a hydrogen flow of 44.9 kg/s. The gas generator demonstrated both stable behaviour and an important gain in margins.

As far as the oxygen turbopump is concerned, the turbine's elements were tested under both cold and hot conditions. The pump inducer was tested using water rather than liquid oxygen, and the pump itself is currently undergoing cavitation tests. The first complete turbopump was delivered in August 1998 for the liquid-oxygen test campaign, which is still in progress at DaimlerChrysler Aerospace, on the P5.9.3 test rig in Ottobrunn (D).



The Vulcain-2 nozzle extension was delivered in March 1999 for the engine test campaign, following delivery the chamber in the previous November. Preliminary assembly of the Vulcain-2 engine had also begun in November 1998, and it was delivered on 7 April 1999 to the P5 test rig in Lampoldshausen (D), operated by the German Aerospace Centre (DLR). The second PF50 test rig in Vernon (F), operated by SNECMA, received the second engine at the beginning of October 1999.

A further four test engines will be used to qualify the subsystems and the Vulcain-2 engine itself before authorisation of the first flight of the new Ariane-5 Evolution launcher, scheduled for December 2001.



Table 1. Technical characteristics of the Vulcain-2 cryogenic engine

| | |
|-------------------------------|------------|
| Vacuum thrust | 1 350 kN |
| Specific impulse | 433 s |
| Chamber pressure | 115 bar |
| Mixture ratio | 6.10 |
| Section ratio | 58.5 |
| Total propellant flow | 320 kg/s |
| Mass | 1935kg |
| Turbopumps: | |
| Rotation speed | |
| LOX : | 12 600 rpm |
| LH ₂ : | 35 500 rpm |
| Turbine power | |
| LOX : | 5 100 kW |
| LH ₂ : | 14 100 kW |
| Dimensions: | |
| Height | 3.60 m |
| Diameter (nozzle ext. outlet) | 2.15 m |

Distributed Interactive Simulation for Space Projects

L. Argüello & J. Miró

Modelling and Simulation Section, ESA Directorate of Technical and Operational Support, ESTEC, Noordwijk, The Netherlands

What is distributed simulation and what are its benefits?

Distributed Interactive Simulation (DIS) allows geographically separated simulators to work together, interacting in real-time, to provide predictions just like a single integrated simulator. The technology also allows real entities to be included in the simulation loop. Before this approach can be applied to space projects, however, it has to be established whether current simulation and communications technology can effectively support the critical requirements of space scenarios. It also needs to be demonstrated that this approach results in a cost-effective solution compared with the conventional approach of centralised simulators.

Distributed Interactive Simulation is an innovative technology that will dramatically change the way in which simulation is developed and applied in space projects. It will only be effective, however, if based on well-accepted standards, such as the IEEE High-Level Architecture (HLA) standard. A number of studies and experiments have been carried out as part of ESA's R&D effort to evaluate the benefits of distributed simulation for space projects in general, and the International Space Station in particular. These have led to the first ever applications of the HLA standard to the space domain. Promising results have already been obtained with the simulation of the Automated Transfer Vehicle's rendezvous with the Space Station and of satellite payload operations, which can be extrapolated to other space projects and scenarios.

These questions have been addressed in a number of studies at ESA, including early experiments conducted in the framework of a co-operation between ESTEC and the Gagarin Cosmonaut Training Centre (GCTC) in Russia. The distributed interactive simulation paradigm can be implemented in many ways, but in order to become a useful technology it has to be based on a standard defining the interface between two interacting simulators/entities, i.e. defining how two or more simulators/entities have to talk to each other. The co-operation between ESTEC and GCTC has led to the first ever application of this technology in a space context, based on well-accepted standards.

The technical challenge

The technical issues involved in implementing the distributed-simulation paradigm are related to interoperability and to the communications links. Interoperability requires the simulator to respect a certain architecture in order to be able to communicate with the outside world. As far as the communications links are concerned, the main difficulty is in coping with the time-span data requires to travel from the originating simulator to the receiving one (the so-called 'latency'). In a real-time simulation, the distribution of the simulation models at remote sites introduces an error, because the data required by one model from another physically remote model needs a finite time to travel over the network. Assumptions about the current values of the remote model parameters therefore need to be made on the basis of earlier values (extrapolation using 'dead-reckoning algorithms').

The key question to be answered here is whether the error introduced by the distribution of the simulation can be kept within pre-defined, acceptable error bounds. This is evaluated by comparing results obtained from the distributed system with those obtained from the non-distributed system. This will be particularly critical for simulation applications involving closed control loops, such as are encountered in attitude and orbit control systems. For simulations with flight software and hardware in the loop also, the response time expected from the simulator will constitute a critical challenge for this approach. In addition to the latency, the real-time behaviour of the communication link will also be a critical requirement for real-time simulations, and one not always possible to meet with conventional communication protocols.

The network requirement is also an important issue. Setting up a complex communications scheme is often difficult and requires considerable effort. The application of modern DIS technology not only simplifies the distribution of the data and the supporting

network architecture and protocols required, but also reduces the bandwidth needed to a minimum, making the use of affordable ISDN lines and equipment possible.

Applicable standards

The first standard for interactive distributed simulation was IEEE 1278.1, also known as the DIS protocol. This standard, whose generation was sponsored by the US Department of Defence through the Defence Modelling and Simulation Office (DMSO), was applied extensively in defence simulations. It was based on the use of standard formatted packets, designed for the data required by these specific applications. Problems due to the inflexibility and lack of scalability of this approach have eventually led to a completely different approach, the High Level Architecture (HLA), which is in the process of becoming the IEEE 1516 Standard.

The elements of an HLA-compliant distributed simulation are summarised in Figure 1. The various components of the 'federation', the 'federates', are described using the Object Model Template (OMT). During a distributed simulation, the federates must interact in accordance with the HLA interface specification. While HLA is an architecture, the Run Time Infrastructure (RTI) is the software needed to support simulation execution.

Practical experience

To evaluate the distributed simulation approach for space, a number of practical applications (experiments) have been implemented. The first ever application of this technology to the space domain was demonstrated in the framework of the co-operation between ESTEC and GCTC. The results obtained both confirmed the feasibility of the approach and highlighted the

critical issues for its application in the space domain. The resulting demonstration system was deployed to European industry, and facilitated the initiation of several related R&D activities in the frame of the European Union programme for High Performance Computer Networks (HPCN).

Another experiment was performed in parallel using a satellite simulator to validate the use of HLA in the context of distributed payload user centres. The application of distributed simulation in the context of the International Space Station, and more precisely for spacecraft proximity operations, was further investigated in the framework of ESA's Technology Research Programme (TRP).

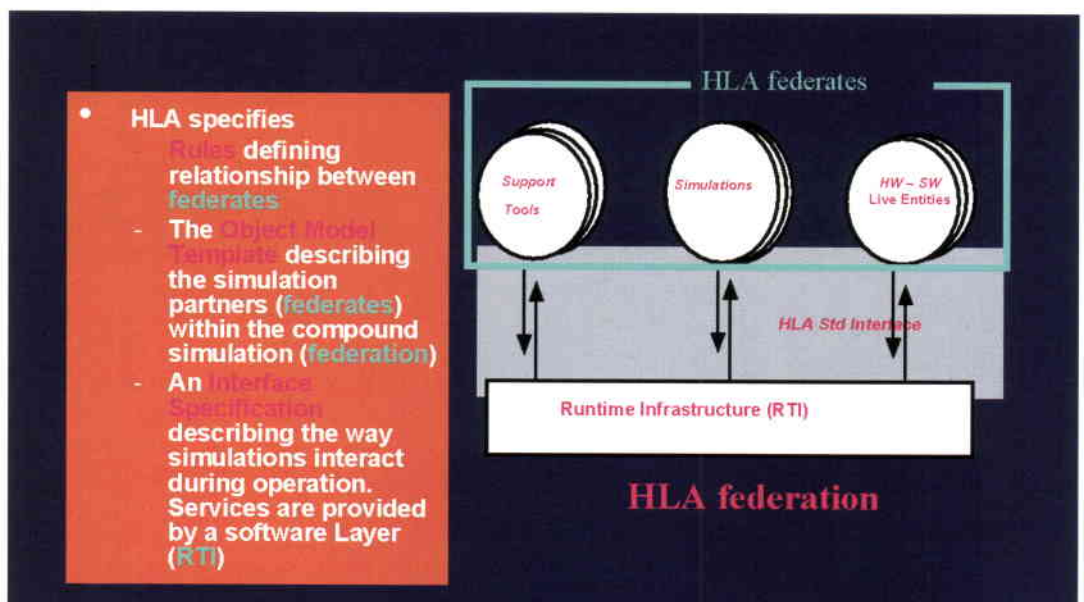
The results of these activities are summarised in the following paragraphs.

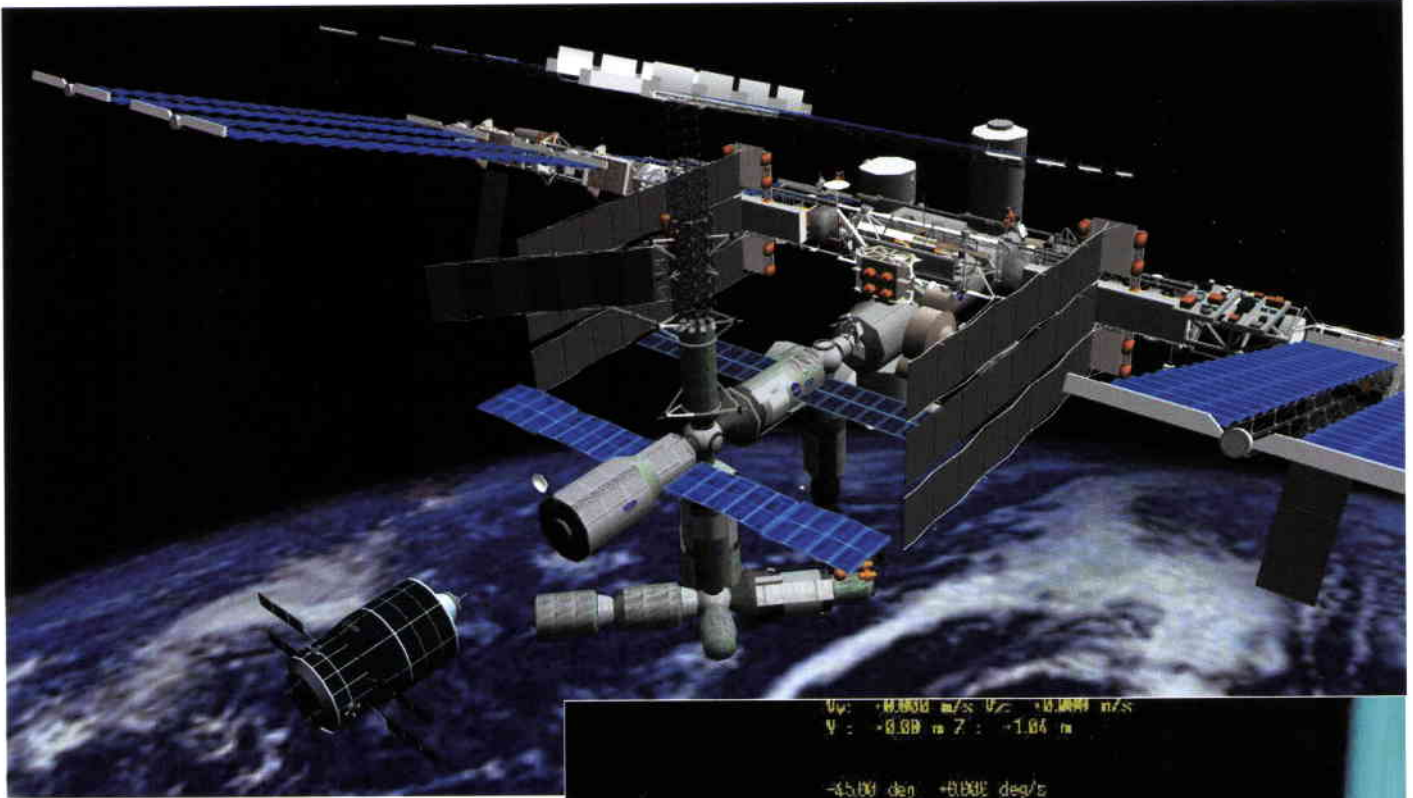
Spacecraft rendezvous

A distributed simulation of the rendezvous and docking (RVD) of the Automated Transfer Vehicle (ATV) with the International Space Station (ISS) has been implemented in order to validate the technology in a challenging space scenario. This scenario is particularly critical due to the very tight coupling of the two spacecraft through the ATV trajectory control loop, and the very small tolerances for the docking in terms of linear and angular displacements. This means that the accuracy requirements for the position and velocity of the interacting spacecraft are very high, and the error introduced by the communication latency has to be kept at least one order of magnitude below the docking tolerances.

Several simulation experiments were carried out with simulation nodes at ESTEC, GCTC, ESOC and several industrial sites in Europe.

Figure 1. Overview of an HLA-compliant distributed simulation





The RTI software infrastructure required to implement an HLA federation was made available by the DMSO. The use of ISDN as the basic communications infrastructure was selected as the most cost-effective and practical solution.

Mission scenario

The simulation scenario was the rendezvous and docking of the ATV to the ISS both in automatic and in manual mode. 3D visualisation was used to monitor the manoeuvres and to assist the manual control, activated in case of contingencies. Figure 2 shows the final approach manoeuvre from above. Figure 3 shows a view through an ISS-mounted camera, used to monitor the final metres of the approach. The overlay parameters provide information on relative position and attitude.

For the purposes of DIS, it was decided to concentrate only on the ATV manoeuvres to be performed near the Station, the beginning of the final translation being selected as the starting point for the simulation scenario.

Context

Three different demonstration scenarios relating to the Rendezvous and Docking (RVD) of the ATV to the ISS were selected, pertinent to different phases in the ATV development life-cycle:

- The collaborative engineering context assumes distributed simulation involving geographically distributed industrial partners responsible for different parts of the ATV. The



Figure 2. Three-dimensional visualisation of the ATV approaching ISS

Figure 3. The ATV viewed through the ISS camera

emphasis here is on the early detection of problems, which can occur long before system integration is attempted. This should also help shorten the development cycle.

- The operational procedure validation context assumes the need to define the procedures and the parameters to be monitored and associated thresholds for nominal and contingency scenarios, involving more than one ISS segment.
- The mission rehearsal and training context assumes the need for multi-segment integrated simulations involving several control centres and the crew. It also covers remote access to high-fidelity simulations for crew members.

Distributed scenario

The entities represented in the simulation ('federation' in HLA terms) are the ATV vehicle (federate called ATV-F), the ISS (ISS-F) and the Mission Control Centre (MCC-F). A federation manager (FM-F) was defined to implement the simulation control functions. Switch over from automatic to ISS crew control is decided by the MCC, which also prescribes the flight plan and monitors the manoeuvre.

The geographical allocation of the above federates is configurable, but for the experiment the configuration selected (Fig. 4) was: ISS simulated at GCTC (Star City, Russia), ATV simulated at ESTEC (Noordwijk, The Netherlands), and the Mission Control Centre federate simulated at ESOC (Darmstadt, Germany). Table 1 shows the functions allocated to the different simulation nodes.

Results

The limits considered allowable based on the simulation requirements were expressed in the form of misalignments of 0.02 m in position and of 0.3 – 0.5 deg in orientation. However, this is not sufficient in order to assess some of the integral performances of a simulation session, e.g. it is conceivable that the differences in state vector components are within the prescribed boundaries, but that the total amount of fuel consumed differs considerably compared to the non-distributed simulation. This would render the simulation inadequate, since it could trigger wrong decisions and unnecessary changes in control strategy.

The simulation results show that the accuracy criteria are met even for an acceleration of the simulation by a factor of 4 with respect to real time. This is equivalent to increasing the latency by the same factor. It was therefore proven that the delay introduced by the distributed approach does not affect the overall validity of the simulation.

Distributed payload user centres

A distributed simulation experiment has been carried out at ESTEC taking a small technology-demonstration satellite mission, Proba, as a basis. The purpose of this experiment was to evaluate the applicability of HLA for familiarising and training satellite payload users.

Table 1. Functions allocated to the different ATV/ISS RVD simulation modes

ATV-F:

- GNC subsystem
- Chaser orbital mechanics (differential equations of motion)
- Computation of Chaser dead-reckoning (DR) parameters
- Reconstruction of the Target (ISS) variables using its DR parameters
- Computation of variables describing relative (ATV-ISS) motion
- Computation of parameters and variables for the GUI
- Process inputs from the remote control post
- Introduction of failures and contingencies onboard ATV

ISS-F:

- Target GNC subsystem
- Target orbital mechanics (differential equations of motion)
- Computation of Target dead-reckoning (DR) parameters
- Reconstruction of the Chaser variables using its DR parameters
- Computation of variables describing relative (ATV-ISS) motion
- Computation of parameters and variables for the GUI
- Remote control post functionality
- Computation of the position of Sun
- Module to initiate CAM

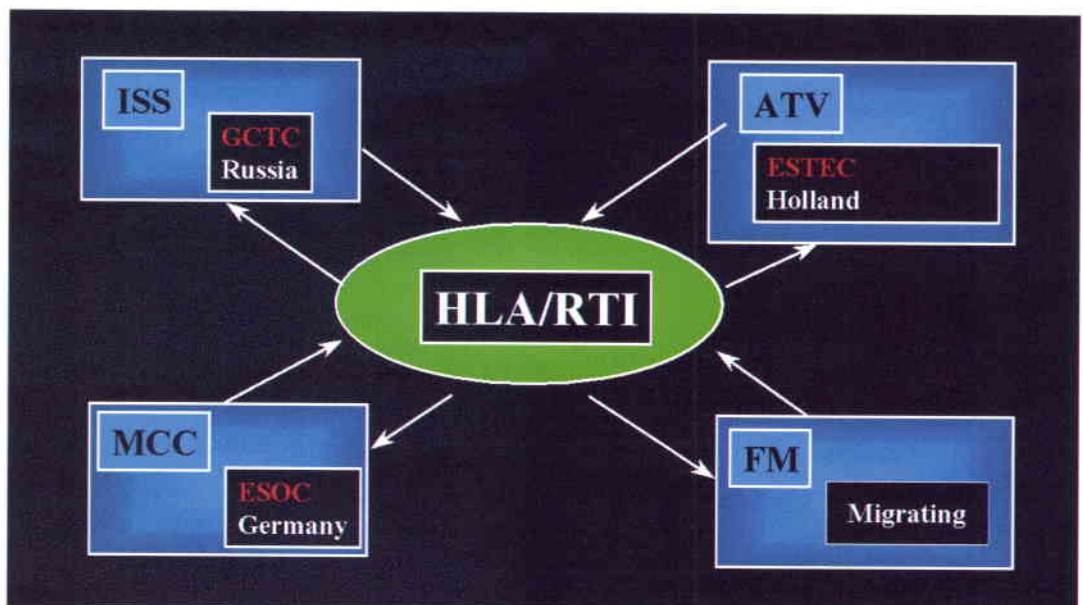
MCC-F:

- Reconstruction of Chaser and Target variables using DR parameters
- Remote control post functionality
- Computation of variables describing relative Chaser and Target motion in various coordinate systems (for 3D and 2D graphics, data logger)
- Algorithms to form and modify the Mission Plan for Chaser

FM-F:

- Federation management (commands like "restart", "resume", "pause")
- Changing of the time-scale factor
- Introduction of failures and contingencies

Figure 4. Geographical configuration of the RVD distributed simulation



Mission scenario

The Proba simulation focussed on one of the payloads, namely an imager. Its users, distributed at different locations, will be able to send observation requests to the satellite (via the Control Centre) and will receive directly the image requested. The mission-simulation part of the Project Test Bed has been re-engineered to work in a distributed configuration. Using the distributed approach allows the parallel transmission of various selections of the telemetry produced by the simulator to several remote monitors in parallel, and the reception of telecommands from a remote user station.

The distributed simulation experiment (Fig. 5) consisted of the mission simulator and the separate control and monitoring tasks (telecommand, telemetry, event table MMIs, Earth track graphical displays and 3D visualisation) running in a distributed manner, both at ESTEC in Noordwijk, representing the mission Control Centre, and at Headway (UK) simulating the remote user centre.

The users located at the remote user centres are able to:

- send observation requests to the Control Centre
- monitor the outcome of spacecraft autonomous operations following user image requests
- display spacecraft position, orbital track and ground-station visibility zones on a 2D map.

The Control Centre at ESTEC is able, in addition to the user operations, to:

- uplink telecommands and downlink house-keeping data when the spacecraft is in contact with the ground station
- monitor an on-board event table containing the housekeeping history from the last ground-station contact
- provide visualisation of a realistic model of the spacecraft overlaid with spacecraft body vectors as well as Sun-, Moon- and Earth-pointing vectors, and real-time visualisation of the pointing manoeuvres required during the mission lifetime (i.e. Earth, ground-station and user-station pointing) on the 3D visualisation (Fig. 6).

In particular, the test executed demonstrated the stability of the distributed system while the distributed federates join and leave the federation. Data updates were not affected by federation management.

Lessons learnt

The advantages of distributed simulation versus the conventional approach are: earlier availability of the simulation (since it can use

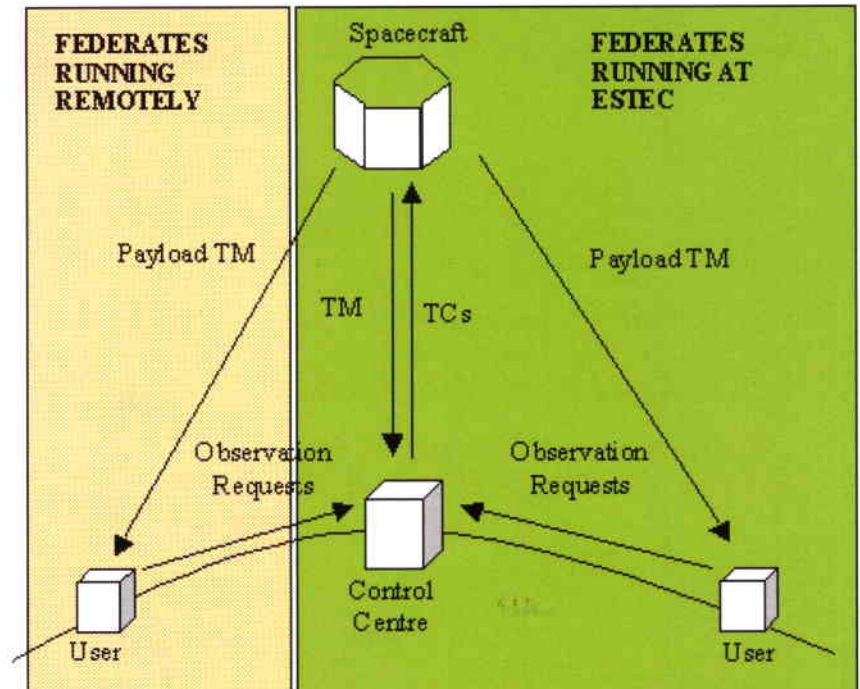


Figure 5. Overview of the Proba project test-bed distributed simulation

pre-release versions), savings in the time and effort needed for installation of simulation products locally, savings in computer hardware, and access to simulations not otherwise available (e.g. access to high-fidelity simulations at industrial sites).

In particular, in the case of the ATV study, productivity gains and a reduction of 20% in development time seem achievable through collaborative engineering during the development phase, depending on the duration and scope of the simulation campaign. Early analysis of coupled effects is an area where distributed simulation becomes an enabling technology.

In the case of the ISS, for example, the potential of distributed simulation to save development effort and time is significant due to the distributed nature of the project, involving numerous geographically separated partners, and to the large number of simulation facilities distributed throughout the world. The use of distributed simulation in support to the multi-segment operations and training involving crew and ground-station personnel within the International Space Station programme is in the process of evaluation.

The HLA standards are in the process of becoming an IEEE standard and show considerable potential for being widely applied in a variety of simulation domains. The real-life experiments carried out by ESA and summarised here highlight the potential to support operations preparation tasks using affordable, commercial ISDN lines. Since the use of this technology only makes sense in a global context, its broad adoption by industry



Figure 6. A typical Proba test-bed simulation

and other space agencies is required before it can be exploited effectively.

Some critical issues associated with this technology also need to be pointed out. The tools needed to build the distributed simulation system according to the HLA standards are only starting now to become available. The software infrastructure needed to conduct distributed simulations has not yet reached the standard of a commercial product. Distributed interactive simulation also conflicts with the implementation of computer-access security measures in that dedicated systems have to be placed outside firewalls or access through firewalls needs to be granted. Last but not least, significant expertise is required to configure the simulation computers to communicate over ISDN lines.

Future work

It is planned to focus the future work on three specific areas:

- Deploying the distributed rendezvous simulation system implemented in the ESA R&D effort for a transatlantic demonstration involving NASA and ESA: this would allow

NASA to evaluate this technology for ISS operations and training.

- Establishing a prototype infrastructure at European level to facilitate the use of this technology by space industry in support of collaborative engineering: the infrastructure should include a space federation model, guidelines for plug-and-play in this federation, and the associated software tools.
- Extending the demonstration to simulation systems including flight hardware in the loop, typically the on-board computer.

Acknowledgements

The authors wish to acknowledge the pioneering work carried out by GCTC in the framework of the co-operation with ESTEC, and its initiative in promoting the distributed simulation technology. The support of DMSO, which provided training courses and software to ESA and European industry in order to facilitate the implementation of the applications presented in this article, also merits special mention. Finally, the authors want to acknowledge the valuable work carried out by the companies D3 (D), AML (F) and Headway (UK).



INTELMOD

– An Intelligent System for Capturing Operations Knowledge and Providing Advanced Operations Support

A. Donati

Special Projects Division, ESA Directorate of Technical and Operational Support, ESOC, Darmstadt, Germany

E. Romani

Dataspazio, Rome, Italy

Introduction

Knowledge-based systems

Artificial Intelligence is a branch of computer science research that, sometimes in the past, has generated expectations in potential future users well beyond the possibilities and results subsequently achieved. The consequent mistrust is somehow influencing today's approach towards the implementation of intelligent applications.

expressed can be represented in the form of algorithms (e.g. operations manuals) to the declarative representation, such as statements stored in the form of symbolic structures accessible by general procedures capable of treating the knowledge thus expressed.

Modelling techniques to represent systems dynamics and decision support systems were researched in early 1990s. Substantial progress has also been achieved in the refinement of expert systems' control strategies and in the definition of methodologies for human-machine systems research. The availability of commercial tools to provide a user-friendly development and implementation environment has facilitated the introduction of intelligent systems in the domains noted above. The enhancement of human capabilities and the automation of specific activities were (and are) the major immediate objectives for such applications, with intelligent systems expected to contribute positively to risk mitigation and cost reduction.

This article provides an overview of the implementation of a knowledge-based intelligent system to support flight operations personnel in their mission execution tasks, by means of a decision support system for fault management. After a brief snapshot of expert-system techniques, the inherent complexity of flight-operations knowledge is reviewed, before addressing the concept, architectural definition and implementation of the INTELLigent MODeller (INTELMOD). The customisation of INTELMOD for the Cluster-II mission, and potential future applications, are also described.

In the meantime, the applied research has made progress and commercial applications of intelligent systems are now available and being used quietly and successfully in several application fields, including manufacturing, communications, and operations management, and in business areas like marketing, logistic and finance.

The evolution in this domain has stepped through the rule-based behavioural system to the knowledge-based system, making use of object-oriented modelling, up to the inclusion of fuzzy logic and neural-network techniques, within the inference engine. A major area for further improvement is still the knowledge representation and the knowledge transfer between human 'experts' and the 'assistant' systems. Examples range from the classical procedural representation, where the knowledge

Expert systems in mission-control domains

The demand for ever greater satellite performances has resulted in a continuous increase in the complexity of spacecraft platforms and payloads in recent years. Progressive use of on-board software, implementation of automatic or autonomous functions, increased complexity of on-board data-handling system and fault management are just some examples. The payloads themselves make increased demands on mission control systems, in terms of higher payload duty cycles, more payload modes, and shorter mission planning cycles.

At the same time, the pressure for savings has been reflected in the role of the operators, who are sometimes overloaded with tasks and

responsibilities previously assigned to more than one expert. There is therefore an implicit necessity to provide additional support, in particular during critical mission phases, to the flight operations staff in order to make their work safer, more efficient and more competitive.

Expert systems could provide an answer in specific and well-defined domains: monitoring, failure management, trend analysis, planning and resource management are just a few examples among many. However, effective benefits from expert systems can only be experienced after thorough iterative refinement and validation of the stored knowledge.

In the area of supervision and fault detection and diagnosis, for instance, knowledge-based systems can provide a performance enhancement for the traditional monitoring activity. The current limit-value-based supervision method is simple and reliable: it provides an alarm only after a sudden fault or a gradual trend. However, the alarm is generated at individual parameter level, but does not represent a synthesis of the overall situation; moreover an in-depth fault diagnosis is usually not possible. Advanced methods for supervision and fault diagnosis would provide an answer to early detection of small developing faults, to diagnosis at unit or subsystem or system level, and to supervision of processes in transient states.

Lessons learnt from past science and applications space missions show that the majority of on-board failures occur in the attitude- and orbit-control systems and in the data-handling systems, which are known for being highly complex and software-driven. In addition, experience shows that the occurrence of simultaneous multiple failures within the same area is not as rare as is often claimed. Such results merely serve to confirm the urgency to identify additional supervisory and diagnostic tools for the operations staff.

ESA's European Space Operations Centre (ESOC), as a centre of excellence in the research and delivery of flight-operations services to the spacecraft user community, continuously strives for improvement in its own processes, methods and tools in order to maintain its outstanding record of successful mission operations and to make them available to other flight operations centres within Member States. In this context, INTELMOD represents a pioneering activity in understanding and exploiting, at prototype level, the potential benefits offered by presently available knowledge-based system technology when applied to flight-operations processes.

Previous studies in the mission-control field
Past research at ESOC associated with artificial intelligence has covered such topics as automated procedure selection and execution, timeline planning, spacecraft dynamic modelling versus real-time telemetry and diagnosis, architecture concepts for operations automation, and the applicability of advanced technology (ATOS-4).

The INTELMOD activity was preceded by an initial prototyping exercise using the same development platform, with the aim of exploiting the basic capabilities of an object-oriented rule-based system and support system-level monitoring, fault management and resource-consumption evaluation. The software was, at that time, hard coded and took the Automated Transfer Vehicle (ATV) as the reference mission. A simple ATV telemetry and failure-injection simulator was included within the application. The results, both in terms of demonstrated capabilities and potential applications to adjacent areas such as support to flight operations training and procedures definition, were satisfactory and paved the way for the INTELMOD concept.

Operations knowledge

How a spacecraft is operated

The recipe for flying a mission requires, as ingredients, a mixture of trained human resources, pre-programmed computers and pre-validated procedures. The nature of the tasks to be executed varies with the phase of the mission, but they can be grouped into two families: executional tasks and supervisory tasks. The first are usually automated, on board, and used for the implementation of the mission. They require progressive uplinking of pre-programmed automated command sequences. Critical executional tasks, such as GO/NO-GO decisions, are usually performed manually by the flight controllers.

The supervisory tasks include the recognition that all executional tasks are progressing as expected and the verification that all measurements are within the agreed fields of tolerance. The required supervision of the execution of complex, parallel tasks and the monitoring of hundreds or even thousands of parameters gives the flavour of the complexity and the responsibility assigned to the flight controllers, equivalent to those of a crew in an aircraft cockpit.

The mission follows a Flight Operations Plan. It consists of temporally sequenced, pre-validated procedures giving the spacecraft flight controller instructions on the monitoring of telemetry parameters, and on controlling the

evolution of the mission by means of pre-configured and validated telecommands. The real trajectory is monitored against the planned one and manoeuvres are prepared and executed according to the plan.

Vigilant supervision implies the capability to quickly recognise anomalies and to react, with the prime objective of continuing the mission, via the implementation of specific contingency recovery procedures (e.g. activation of a redundancy unit). The diagnostic activities are then carried out by the experts, to understand the cause of the failure and to identify the necessary corrective and preventive measures to be implemented.

All of the spacecraft platform and payload subsystems, although loosely coupled, when properly engineered, have anyway a certain degree of interactivity and mutual dependency. This makes matters more complicated if a specific subsystem unit stops working correctly. A deep knowledge of the on-board architecture, functions and interdependencies is mandatory for the flight controller sitting at the console, and makes 'flying a space mission' an activity that can only be learned by experience.

The knowledge repository

The fundamental knowledge required to fly a mission is initially based on the information provided by the manufacturer in the Spacecraft User Manual and on the mission-analysis results. It is then complemented with the Mission Database, providing the definition and validity of all telemetry and telecommand parameters, and the Flight Operations Plan, written by the 'pilots' of the spacecraft, consisting of detailed timelines and associated operational procedures for nominal and contingency cases. Most important of all is the knowledge that the 'spacecraft pilots' have acquired during the mission-preparation phase, in specialised training sessions, while writing and validating operational procedures and participating in simulation sessions.

INTELMOD

The primary objective of the INTELIgent MODeller is to demonstrate in practice whether new technologies could be beneficially applied as new tools for supporting human judgement of complex process anomalies and of related decision making. As such, it has to provide the flight-operations experts with an experimental test bed to probe the capabilities and limits of intelligent systems as a sophisticated advisory tool in support of complex and time-constrained operations tasks, using data from real missions.

The 'toolkit' was initially developed by knowledge engineers, providing all the necessary features to save and exploit available knowledge, and is then directly 'programmed', or customised, and further exploited by the flight-operations expert staff. It is connected to the existing Mission Control System (MCS) and, for cost-efficiency reasons, is based on a commercially available object-oriented software development and utilisation environment for intelligent applications, with already existing high-level functional blocks (e.g. for diagnostics) and interface blocks.

Conceived as an evolutionary toolkit, INTELMOd will provide a sufficiently user-friendly man/machine interface for the user who is knowledgeable about the spacecraft functions and mission plan, but not necessarily expert in low-level programming. The system is open, modular and expandable. Its library allows progressive growth and re-usability of modelled objects. The toolkit is now available for testing in its prototype version, after which the software knowledge engineers will implement/correct further features based on user feedback.

The operational concept

The flight operations staff can use the INTELMOd toolkit during both the mission-preparation and mission-execution phases. In the first phase, the spacecraft operations domain experts implement and organise the knowledge of the spacecraft system, mission phases, and diagnostic rules into the INTELMOd knowledge database. The INTELMOd toolkit provides a user-friendly modelling environment. During mission operations, the stored 'know-how' is driven by telemetry and telecommand data and provides advice to operations staff when, and possibly just before, an anomaly occurs. As is usual for such pioneering systems, it will initially be used to support very specific spacecraft units. It will be interfaced to the existing Mission Control System with the objective of optimising and expanding the current MCS-supported functions.

The users

To support the different stages of model development and implementation, three different INTELMOd user profiles have been identified:

- Spacecraft Component Developer (SCD), responsible for the creation of spacecraft components (modules, subsystems and units), which are then inserted into a Component Library to be used later during a model-definition phase. Component

Developers are expected to have a high level of knowledge concerning typical spacecraft 'building blocks'.

- Spacecraft Model Developer (SMD), creates a mission-specific model representation by selecting and configuring items created by the SCD. Models are progressively assembled and configured to provide a physical, functional and mission-related representation of the spacecraft in question.
- Spacecraft Operator (SO), interacts with the models created by the SMD during mission operations / training scenarios.

The toolkit has been conceived to be used in two modes, for two distinct phases of the spacecraft operations lifecycle (Fig. 1):

- *INTELMOD customisation during mission preparation*
The users will access the toolkit as SCD, to create, modify or augment the models of the 'terminal' elements of the hierarchical representation of generic spacecraft, to be then stored in a library. In the very same phase, the user will access also as SMD to model selected subsystems, down to the end item, the related mission modes, the diagnostic and failure propagation rules, the contingency procedures and the trend analysis rules belonging to a specific spacecraft and mission.

- *INTELMOD exploitation during the flight execution phase*
INTELMOD will be connected to the existing MCS, to receive telemetry (and a copy of telecommands). This time the toolkit will provide the INTELMOD SO, as part of the flight-control team, with an operational advisory service throughout the mission-execution phases.

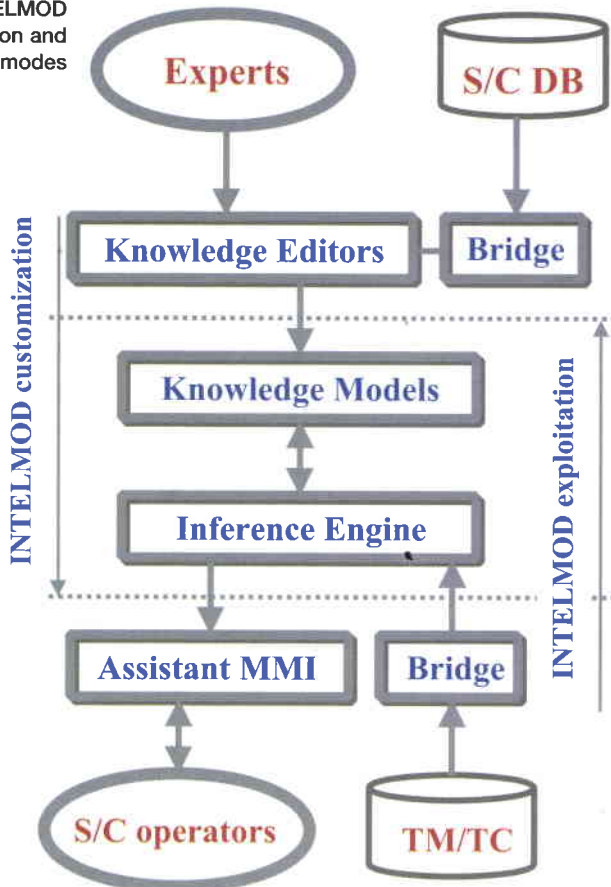
The spacecraft operator can be supported by INTELMOD for:

- enhanced visual monitoring, at system level (synthesised monitoring) and alarm alerts
- diagnostic support, including failure detection and anticipation, failure isolation, diagnosis and recovery, and failure propagation analysis
- resource evaluation and assessment.

The toolkit has been developed taking into account the following requirements:

- support multi-mission environment
- user-friendliness of the interface for the operations and spacecraft experts during both modelling and flight-operations phases
- minimal software customisation effort when applying the toolkit to a specific mission limited to interface adaptation
- hardware-platform-independent application
- open interface, easily adapted to the existing Mission Control System environment.

Figure 1. INTELMOD customisation and exploitation modes



The toolkit architecture

Knowledge representation techniques are still in an evolutionary phase and the INTELMOD developers have therefore designed the toolkit using structured knowledge domains specifically adapted to contain, respectively, spacecraft knowledge, mission knowledge and functional knowledge, by means of objects, procedures and rules. A set of editors for each knowledge-representation domain has been specifically developed: they represent the meta-knowledge domain of INTELMOD. A logical decomposition of the INTELMOD knowledge architecture is represented Figure 2, which is a high-level object-oriented diagram showing the logical editors' behaviour and user relationships.

The editors implemented are suitable for supporting the acquisition of knowledge represented in the spacecraft model, in the mission model and in the behavioural model, as shown in Figure 3 and described below.

The spacecraft model

This model provides a hierarchical representation of the spacecraft, its subsystems and individual components. For example, a spacecraft may be partially represented in terms of power, thermal and AOCMS subsystems. The power subsystem in turn may be composed of a

power distribution unit, batteries, etc. This knowledge is entered using a breakdown editor to interactively gather and structure knowledge related to the physical organisation of the spacecraft. The breakdown editor configures itself according to the user currently interacting with the system (SCD, SMD or SO).

The mission model

The Mission Model provides a hierarchical representation of the mission in terms of the various activities performed within various phases and modes, together with the expected configuration (e.g. status and resource consumption profile) for all the physical components defined in the physical spacecraft model. As with the physical model, a breakdown editor allows the SMD to gather and structure this knowledge.

The functional model

The functional model uses a graphical rule-based language to define knowledge related to the functions to be performed during the course of a mission. This knowledge falls into the following areas:

- Spacecraft behavioural knowledge: includes knowledge describing the behaviour of the spacecraft systems with respect to the interaction between the various components and subsystems. This knowledge enables the model to perform basic diagnostic functions including failure isolation and recovery.
- Mission behavioural knowledge: describes the spacecraft behaviour exhibited during the execution of different mission phases and the activities performed during those phases. This model also uses the Flight Operations Plan (FOP) to enable INTELMOD to perform resource evaluation.
- Spacecraft/mission relationship knowledge: captures the heuristics used by the operations, spacecraft and payload engineers to identify and rectify problems that occur over the lifetime of the spacecraft. Once defined, the spacecraft/mission relationship knowledge enables INTELMOD to perform trend analysis, failure detection, diagnosis and prevention
- Spacecraft/mission propagation effect knowledge: cause and effect knowledge, available from the Flight Operations Plan and mission specialists, which relates sections of the spacecraft and mission models. A causal network allows the flight controllers to perform an analysis of process and hardware failures and predict the consequences of failure if no corrective action is taken. It also allows the controller to assess the impact on the mission in terms of unavailable hardware and lost functionality.

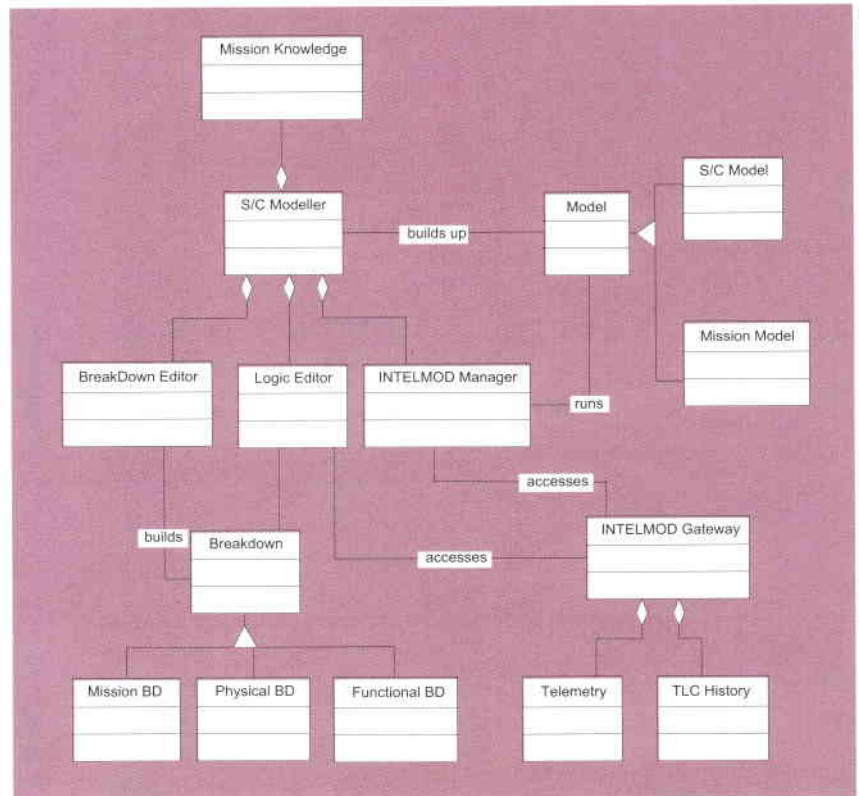


Figure 2. The INTELMOD knowledge architecture

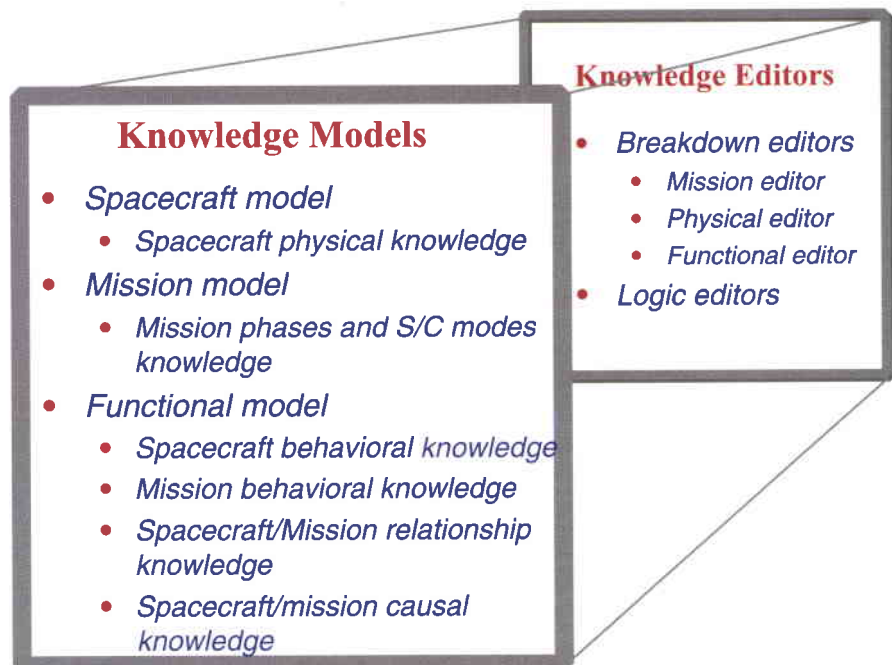
The INTELMOD knowledge models and associated supported functions are summarised in Figure 4.

The Cluster-II test case

The modelling

The INTELMOD toolkit was initially tested, from a functional point of view, by simulating support for the AOCMS and power subsystems of Cluster-II. Taking the power subsystem as an example, this has been decomposed using INTELMOD's breakdown editors into the

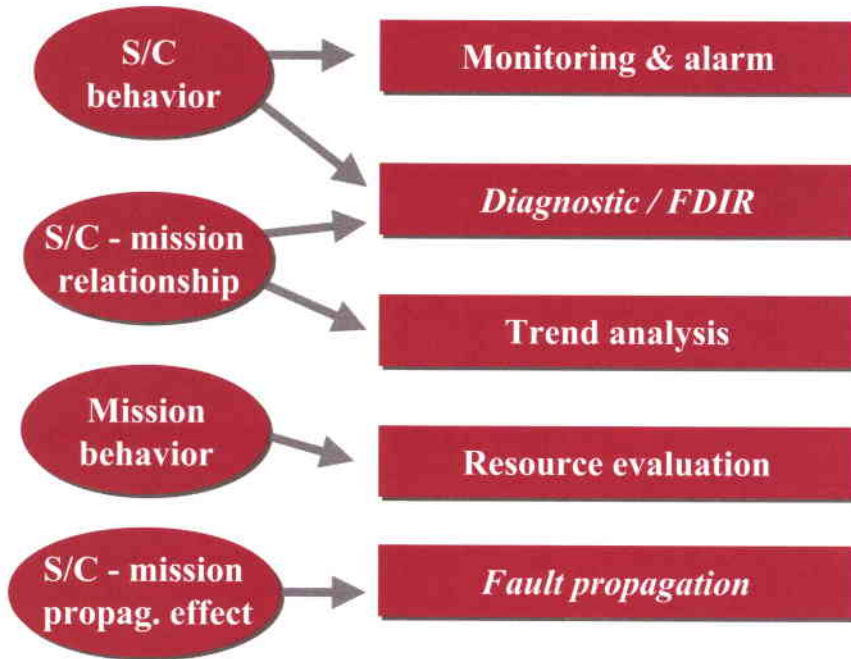
Figure 3. INTELMOD knowledge editors and knowledge models



- following units:
- * power control
 - * power distribution
 - * internal power dumpers
 - * external power dumpers
 - * battery regulation
 - * batteries, and
 - * pyro-electronics.

Figure 4. INTELMOD knowledge models and supported functions

Knowledge Models Supported Functions



Once these breakdown components have been identified, attributes can be added, again using a dedicated editor; e.g. a battery would typically be described using properties such as voltage, temperature, charge current and discharge current (Fig. 5).

Having linked the INTELMOD breakdown components with their external counterparts (i.e. telemetry parameters or groups of telemetry) by interactively querying the spacecraft database, it is then possible to construct the monitoring and diagnostic 'rules'. Monitoring rules allow mapping of the status of breakdown leaves (as derived from the incoming telemetry) with synthesis information: whenever the status changes, the colour of the related component displayed in the breakdown mimics changes according to the following table:

- 1 - green: OK
- 2 - red: fault
- 3 - yellow: off-line
- 4 - blue: stand-by
- 5 - orange: redundancy lost.

This information travels upwards in the hierarchy. Once colours have been computed for all the components belonging to a specific level (e.g. units), the same colours are logically combined to derive the colour representing the 'assembling' component at the upper level (e.g. subsystem). Colour propagation and telemetry association logic is entered within

INTELMOD Implementation

The INTELMOD toolkit has been developed using a RAD-style (Rapid Application Development) approach, based upon the Dynamic System Development Method (DSDM), which is a non-proprietary method developed in the UK and currently used worldwide. This approach was partially adopted in this project to help ensure that the system could be developed in a much shorter time scale, and that the final system would more closely match ESA's real needs.

DSDM employs an iterative approach to development with heavy emphasis on end-user involvement and a project-management philosophy focusing on products rather than on the activities needed to achieve them. Time-boxes were used to control the development process, allocating a fixed amount of time to complete a given area of functionality.

INTELMOD has also made extensive use of commercial off-the-shelf (COTS) software products, including: G2, GDA, G2-Weblink, ODBC Bridge and Space UniT. The G2 (Gensym Corporation) software platform provides an object-oriented environment for building and deploying mission-critical, intelligent applications. It is typically used to represent knowledge captured from operations experts performing complex tasks in real-time situations. GDA (G2 Diagnostic Assistant) is a layered application product for G2, which provides an integrated visual development and execution environment for modelling application logic/diagnostics. Its intuitive graphical user interface allows faster development of the complex system models required for INTELMOD. G2-Weblink allows the distribution of intelligent decision-support information to intra/internet users throughout the organisation. Gensym also provides bridges for ODBC-compliant databases, in our test case a Microsoft Access copy of the Cluster-II database. Space UniT (Universal Intelligent Toolkit, from Science Systems Space Ltd.) has been developed in a partnership programme for ESA to provide a component-based suite of graphical products for procedure execution, schedule execution, monitoring and event handling. It enables INTELMOD to automatically prompt (and execute) contingency procedures following the detection of anomalies by the functional model.

These COTS products were used in order to provide rapid delivery of high-level functionality required. In addition, the industrial-partnership approach with Dataspazio and SSSL allowed the project to remain within the allocated budget.

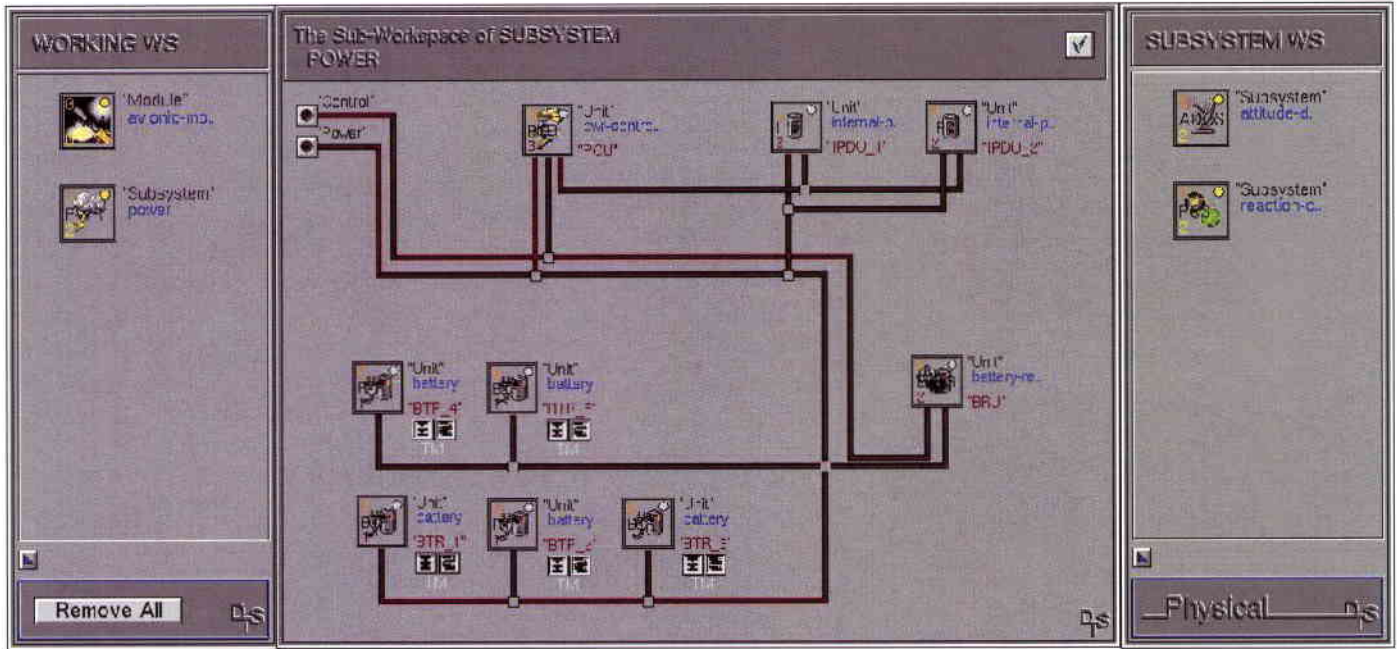


Figure 5. Screenshot of breakdown components

INTELMOD via dedicated parsers, which allow this logic to be defined in a 'natural language' way.

Figure 6 shows, as an example, a simple INTELMOD GDA-based diagnostic (spacecraft behavioural) model. The blocks on the left of the diagram are 'entry points', usually corresponding to a telemetry value that can be automatically created from the breakdown components. Signals are fed through various GDA logic blocks in an attempt to diagnose the cause of operational problems - in this case an internal power subsystem failure arising from a battery over-discharge. If all the logic paths entering the 'AND' block on the left of the diagram are true, then a diagnosis can be made. A message will be sent to one of INTELMOD's message areas, alerting operators to the cause of the problem. It should also be noted that the outputs/conclusions of one GDA diagram could pass information to other diagrams and other INTELMOD model types. Customised GDA blocks are available to link diagnostic models with fault propagation models.

pull-down menus and palettes to select the building blocks that are required. These are placed on a workspace, configured with any necessary information, then connected together. Such models are then immediately ready for use, allowing the developer to concentrate on the expression of expert domain knowledge rather than writing conventional programs.

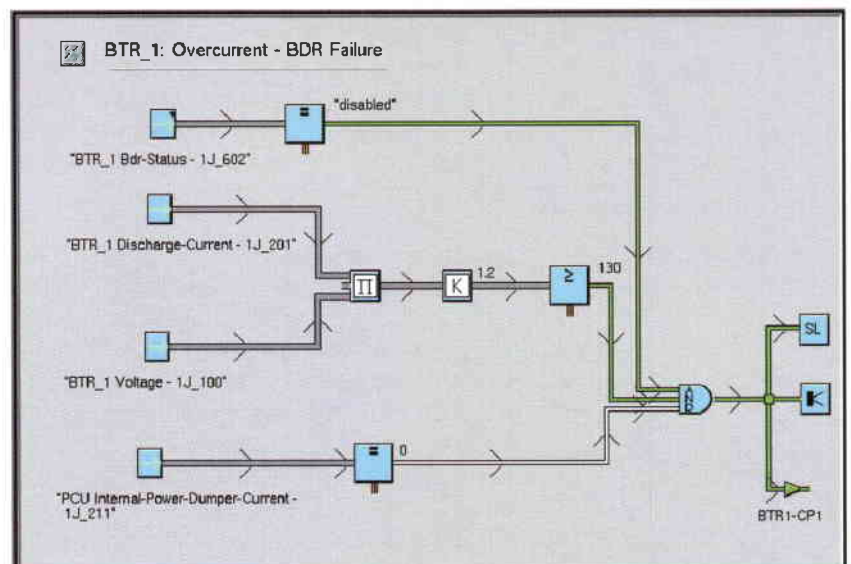
The external interfaces

In order to demonstrate that INTELMOD could operate in a realistic manner and could provide the expected support to flight controllers during mission execution, the system had to be provided with a high degree of connectivity. This was achieved using three separate interfaces (Fig. 7): a telemetry/telecommand bridge, a spacecraft database bridge, and an Intranet bridge (for message broadcasting).

Figure 6. GDA-based diagnostic model

In this way, operators are not only alerted to system failures and their potential causes, they can also be supported in assessing the likely knock-on effects, when these are expected to occur, and the impact on mission operations. In the example shown, the GDA model also incorporates a link to a UNIT procedure (shown by the block labelled 'SL'). Consequently, when the diagnosis is made, a contingency procedure can be automatically invoked to provide failure recovery.

All of INTELMOD's model types share a common mode of use. Model Developers use



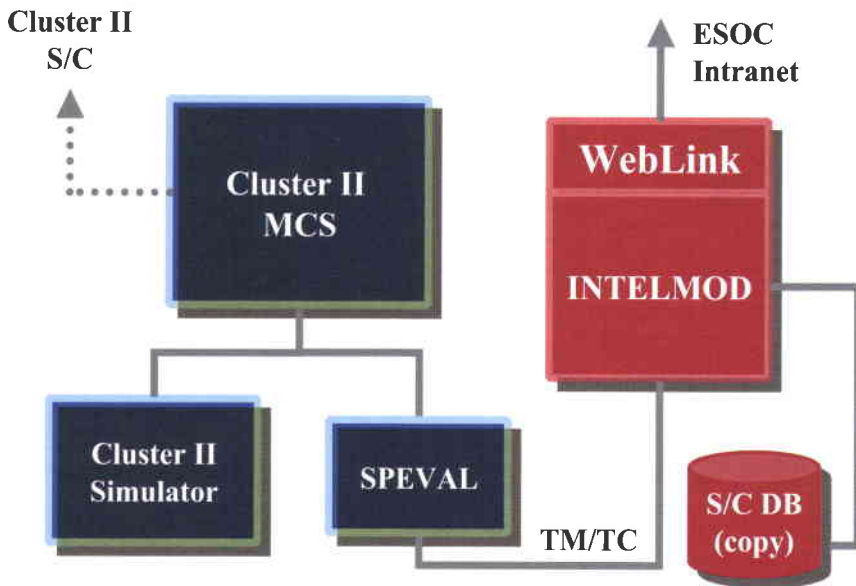


Figure 7. INTELMOD interfaces for Cluster-II implementation

The telemetry and telecommand bridge provides INTELMOD with the information required to perform its analysis. In a 'live' implementation, this information would be supplied directly from the Mission Control System (MCS) software. However, in the time frame of the current study, data files were provided using a client server application (SPEVAL) developed during a previous ESOC study. SPEVAL maintains its own archive of data from the Cluster-II MCS, can be read by INTELMOD using a dedicated bridge.

The purpose of the database bridge is to connect the INTELMOD modelling environment to a satellite database containing information regarding the various parameters, command definitions and scaling/limit data specific to the particular spacecraft under study.

To provide a means for the distribution of alarms, warning messages and general information, G2 Weblink has been incorporated into INTELMOD. Whilst it would have been possible to provide a dedicated bridge to send, for example e-mail messages within ESOC, the use of Weblink enables information to be accessed from the widest possible range of platforms by means of web browsers.

Simulations and evaluation

All of the functions implemented within INTELMOD have been successfully tested through simulation sessions using Cluster-II telemetry history files. The next step will be the operational validation in a real environment with the spacecraft operator using it in open loop during a mission to supervise a target critical area of a spacecraft. This will allow INTELMOD's performance to be judged in the real operational environment.

Conclusion

INTELMOD is a generic satellite-modelling toolkit that has been developed to offer faster, incremental development of spacecraft models. Thanks to its user-friendly man/machine interface, the system requires no formal programming expertise.

The use of AI techniques within INTELMOD has provided a significant enhancement in supporting such operational tasks as system monitoring, anomaly detection and anticipation, failure detection, isolation, diagnosis and recovery, failure propagation analysis and resource management. The toolkit could also be exploited in the training of new operations staff during simulated test-case sessions, making use of the previously captured expertise. Moreover, it could potentially assist engineers during trade-off analysis, specifically to investigate alternative design solutions, alternative operational strategies and contingency recovery procedures.

To be justified, the investment required in the modelling process has to have an economic return. From initial estimates, the toolkit should provide substantial cost savings in the flight-operations budget, especially if applied to long-duration missions (e.g. interplanetary missions) or recurrent/ repetitive missions (e.g. satellite constellations, meteorological satellites, etc.). In the first case a common repository of deep knowledge of spacecraft behaviours is guaranteed, facilitating the turn-over in flight control teams over the years. In the second case, the multi-mission operation supervisory tasks are eased, mitigating risk and/or facilitating the assignment of operations responsibilities. In both cases the 'modelling' investment is either redistributed across several years of operations or across several parallel missions.

The results achieved with INTELMOD to date indicate that it can pave the way for an innovative operations concept in which AI-based tools, integrated into an existing mission control system, will provide more effective and efficient support to the flight controllers during both safety-critical and routine operations. 

The authors would welcome feedback from others working on similar projects. They can be contacted by e-mail at: adonati@esoc.esa.de and enrico.romani@dataspazio.it.

The Tether System Experiment

– Preparing for ESA's First Tether Mission

J. Gavira Izquierdo

Mechanical Engineering Department,
ESA Directorate of Technical and Operational Support,
ESTEC, Noordwijk, The Netherlands

H. Rozemeijer

Atos, Leiden, The Netherlands

S. Müncheberg

Kayser-Threde GmbH, Munich, Germany

Introduction

The advantages and benefits of applying conducting and non-conducting tethers in space have been known for many years. Possible applications range from orbit and re-entry manoeuvres, to attitude stabilisation, power generation and scientific experiments. Early space tether experiments in the 1960s focussed on artificial gravity (Gemini XI and XII, 1966), and in the 1970s Giuseppe Colombo

proposed using electrodynamic tethers as continuous thrusters for spacecraft. In the 1980s and 1990s, both Canada and Japan deployed conductive tethers many hundreds of metres long from sounding rockets. The longest tethers ever deployed in space were those of SEDS-1 (1993) and SEDS-2 (1994), which used 20-km wires to demonstrate momentum transfer and coordinated orbit change for the first time. In 1996, the TSS experiment, a USA-Italy cooperative venture, deployed a 19.5 km tether from the Space Shuttle.

The Tether System Experiment (TSE) has been identified by the European space community as an important initiative for demonstrating the application of tethers in space. An international project team has studied the feasibility of this tethered-capsule re-entry mission, which could be launched as early as 2002 on a Russian Progress vehicle. It will prove the feasibility of tether-assisted sample return from the International Space Station (ISS) and could ultimately lead to many other practical applications of tethers in space.

ESA has a lot of tether knowhow. The electrodynamic tether and more recently the bare-tape tether are both European inventions. The new concepts promise a much higher efficiency and could make ISS station-keeping feasible with a tether just a few kilometres long.

Several tether deployer concepts have already been developed in Europe: the TMM&M deployer (Alenia Spazio) is a spool-reel combination with torque control, which has been extensively tested; and the RAPUNZEL (Kayser-Threde/TU München) is a low-friction spool-based deployer that uses technology from the textile industry to control the deployment. A fully reel-based deployer has also been developed (FIESTA, RST Rostock) and several momentum-transfer demonstration missions have been studied (TARGET, 1995; SESDE, 1996-1998).

Tether basics

In space, the absence of matter and the small forces in vacuum make it possible to deploy extremely long wires, or 'tethers', with diameters of only a few millimetres. The polyethylene tether for the TSE application, for example, has a diameter of 0.5 mm and is 35 km long, but



Figure 1. Tether deployment on Gemini XII

weighs just 7 kg. A distinction is made between mechanical and electrodynamic tethers:

- A mechanical tether is a link between satellites that forces them to maintain a constant separation, thus offering possibilities for multi-point atmospheric research, artificial gravity generation, momentum transfer, etc. The principle of momentum transfer is crucial for many applications, including TSE: if two satellites in circular orbit are connected by a vertical wire, both are forced to orbit with the velocity of their combined centre of mass. The upper mass will then orbit at a velocity higher than the local circular velocity, while the lower mass is actually too slow for its orbit. The gain of tethered momentum transfer is achieved by cutting the tether: the lower mass is then released into an elliptic orbit with decreased perigee (which will be about seven times the tether length lower than the original orbit), whereas the upper mass raises its apogee. The total momentum is preserved, but two satellites have had their orbits changed for the cost of only a few kilograms of tether mass.

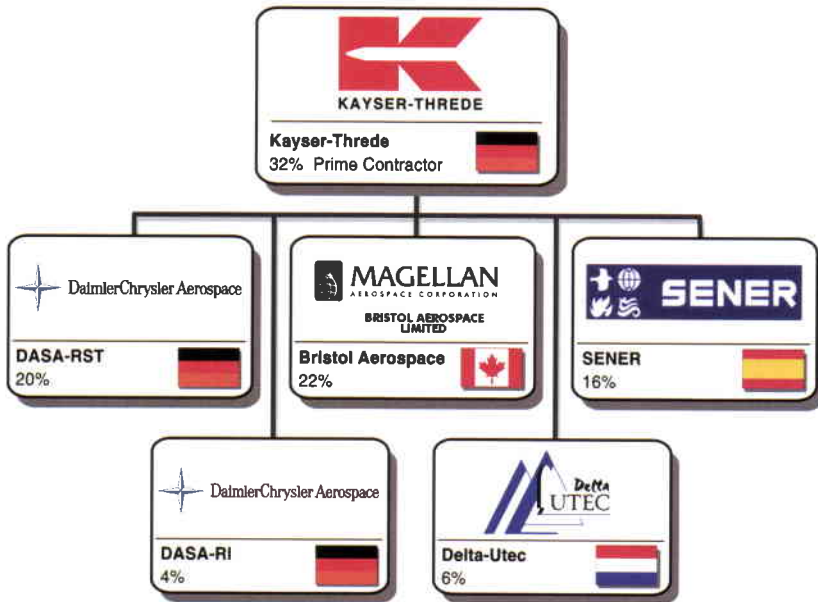


Figure 2. The TSE project team

- Electrodynamic tethers are conductive wires that interact with the ionospheric plasma when speeding at orbital velocity through the Earth's magnetosphere. If there is sufficient contact with the plasma, electrons can be collected on one side of the tether (or even by the surface of a bare tether itself), while being emitted back into the plasma on the other side. The current created will subject the tether (and its end masses) inside the Earth's magnetic field to a Lorentz-force that can be used to either raise or lower a satellite's orbit. Multi-wire or tape-like tethers can provide the meteoroid resistance required for long-duration missions relying on such tethers.

The TSE mission

In 1986, ESA's Space Mail study indicated the need for a frequent Earth sample-return capability from the International Space Station in order to stimulate the production and dissemination of in-orbit research results. In 1994, a Round Table on Tethers held at ESTEC identified such a sample-return and waste-disposal capability as the primary applications for tethers in the near future. Supported by many companies, institutes and universities, this initiative resulted in many developments in the fields of re-entry capsules and strategies, tether dynamics and tether mechanisms. Following up these developments, in 1997 the TSE study (Phase-A/B) was initiated as part of ESA's General Support Technology Programme GSTP-2.

The TSE study is being carried out by an international project team led by Kayser-Threde (D). All of the team members (Fig. 2) have participated in previous tether projects and therefore provide a broad knowledge base. The current Phase-B began with the selection of the mission's mother spacecraft and continued with the preliminary design of the complete system. The target launch date for the demonstration mission is 2002 (Fig. 3).

Mission objectives

The objectives for the TSE demonstration mission are to:

- demonstrate the operation of a tether-deployment mechanism that is suitable for ISS sample return and able to operate properly within the ISS environment
- demonstrate a robust tether-deployment control strategy for initiation of the re-entry, proving that the precision required for the accurate landing of future sample-return capsules can be achieved
- demonstrate the critical technologies associated with the re-entry capsule of an ISS tethered sample-return system
- collect experimental data on system dynamics to support the validation of models used for tether-deployment simulations, including the measuring of tether oscillations and librations.

Mission scenario

The TSE hardware will be installed on a Russian Progress cargo vehicle. The Progress will first conduct its supply mission to the ISS, before being transferred to the selected orbit to eject the sub-satellite and start the tether deployment.

In order to achieve a higher accuracy, the tether-deployment strategy involves two phases (Fig. 4). During the first phase, the tether will be deployed to 3 km vertically below Progress to stabilise the capsule and reduce sensitivity to

ejection errors and other system variations. After synchronisation with the target landing site, the second phase leading to the full 35 km tether deployment will begin. At the end of the deployment, the brake will stop the movement of the tether so that it will swing back towards the local vertical. On reaching the local vertical and at a predefined optimum moment, the tether will be pyrotechnically cut by the deployer system (Fig. 5). The resulting momentum exchange will send the sub-satellite on a re-entry trajectory, dragging the tether behind it as a passive orientation device.

Thirty minutes later, the sub-satellite will hit the Earth's upper atmosphere and decay above the Pacific Ocean. From activation until burn-up, the sub-satellite will collect such experiment data as position and velocity (from GPS), angular rates and accelerations (from IMU) and temperatures. It will transmit them to the Tether Deployer System on board Progress, where the data will be stored. The sub-satellite's telemetry and similar data collected by the Tether Deployer System itself will be transmitted to a ground station in Germany after the experiment has been completed. TSE will then be deactivated and Progress will re-enter the Earth's atmosphere and decay. Post-flight analysis of the experiment data will validate whether the required accuracy for the re-entry trajectory has been achieved.

Design as a low-cost system

TSE is strictly designed as a low-cost mission and uses existing hardware (Fig. 6) wherever possible to minimise development time, cost and risk. The data-handling, power-supply and communications subsystems will be assembled mainly from existing components available from European space hardware suppliers. The sub-satellite also relies also on a large number of existing components and data is available from earlier projects to support its aerodynamic shape.

The new developments are mainly the deployer structure with the sub-satellite separation system, and a new active sub-satellite guidance system using a moving mass. The latter moves the centre of mass relative to the centre of pressure of the sub-satellite and will improve the achievable landing accuracy.

The preliminary design for the system, the tether deployer, the sub-satellite and the electrical subsystems, is now established. The control algorithms have been developed and tested in end-to-end 2D and 3D simulations and the accommodation on the mother

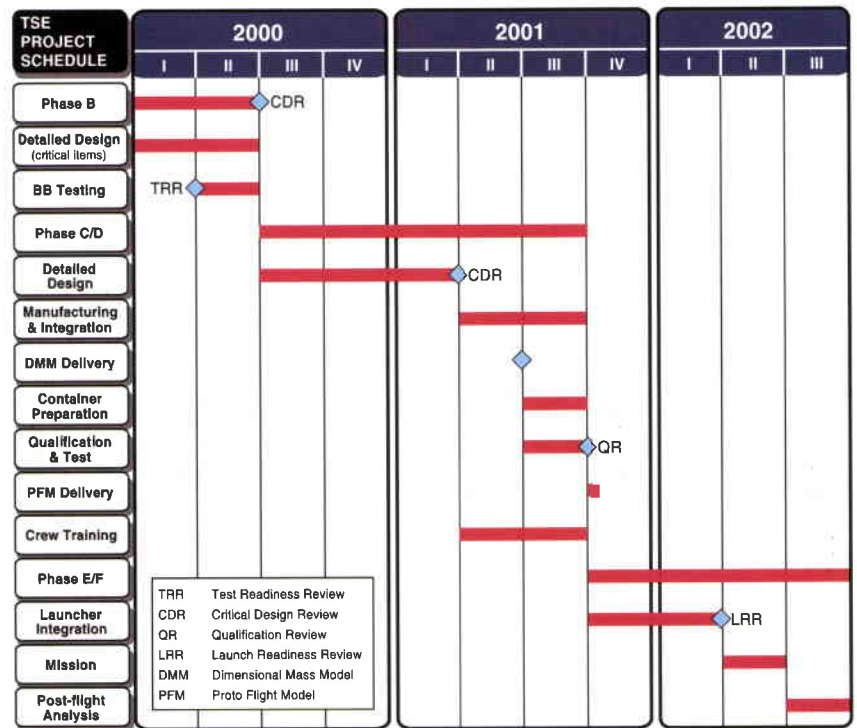


Figure 3. Project schedule

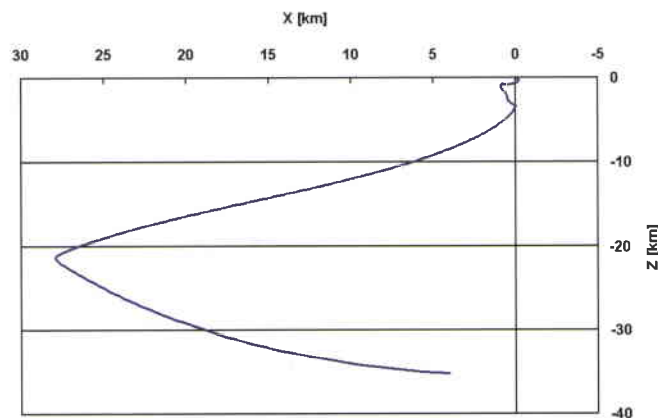


Figure 4. Tether deployment

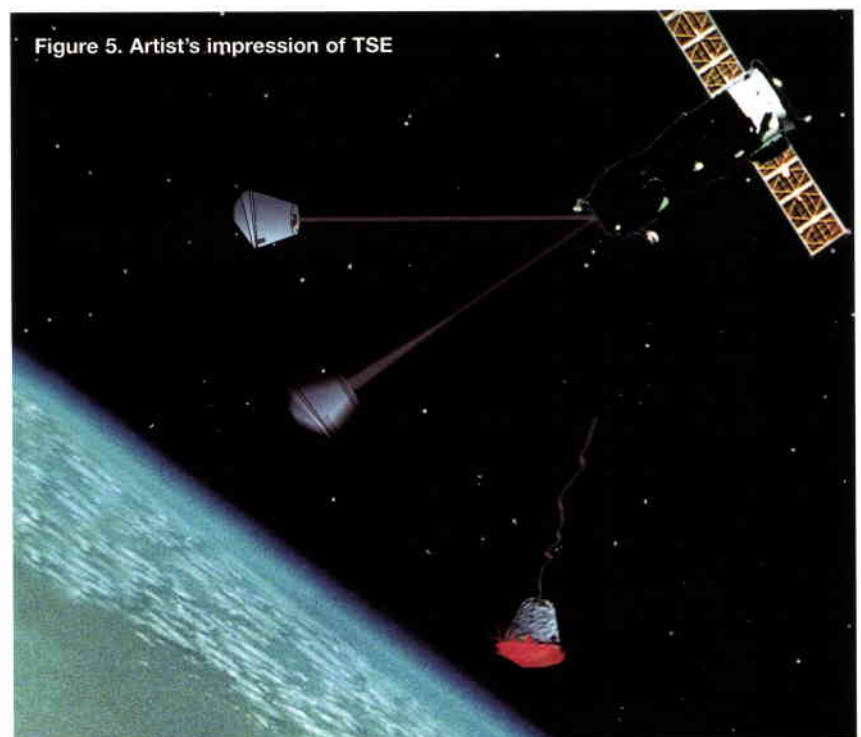
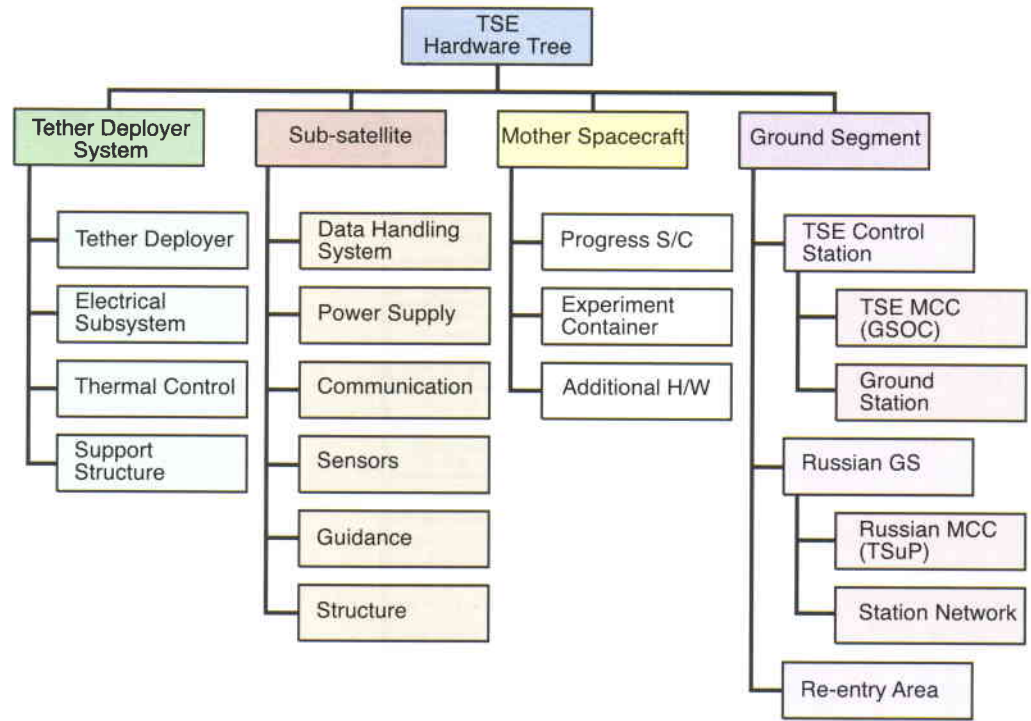


Figure 5. Artist's impression of TSE

Figure 6. The TSE hardware tree



spacecraft Progress has been discussed and agreed with RSC-Energia (Fig. 7).

The tether deployer

The success of TSE depends heavily on the design of the Tether Deployer System (TDS), as the deployment of the sub-satellite is a very sensitive operation. The Tether Deployer is designed to fulfil the following functional requirements:

- storage of the tether during transportation, launch and pre-experiment phases
- ejection / acceleration of the sub-satellite at the beginning of the TSE experiment
- guidance of the tether during the experiment to prevent tether damage
- monitoring of tether system behaviour
- control of tether deployment by tether tension and tether velocity
- cutting of the tether in nominal and off-nominal modes
- providing status signals to the data-handling system.

During all pre-experiment phases and at the start of the experiment, the whole tether is stowed on a core, which is protected against mechanical damage by the canister of the tether storage device. The 35520 m long tether passes out of the canister into a guidance system, brake, tensiometer and finally a cutter.

The brake is able to provide accurate braking forces of up to 100 N if deceleration of the tether or sub-satellite is required. The tensiometer is designed to measure tether forces and tensions in two different ranges, for TSE post-flight evaluation. The guidance system ensures a sufficient tether deployment angle to avoid contact between the tether and the edge of the experiment canister. Cutters are arranged in the tether path to sever the tether at the end of the swing-back phase or if something unforeseen occurs.

Critical technology development, manufacture and testing

In the course of the studies, several critical components and technologies, which are

Table 1. TSE technical data

| | |
|---|--------------------------------------|
| System mass | 143 kg |
| - Tether deployer & electrical subsystems | 60 kg |
| - Sub-satellite | 42 kg |
| - Experiment container | 41 kg |
| TSE dimensions (w/o container) | 1267 mm x 588 mm x 588 mm |
| Power consumption | 88 W during tether deployment |
| Tether type | Dyneema 4 x 400 denier, diam. 0.5 mm |
| Tether length | 35 km |

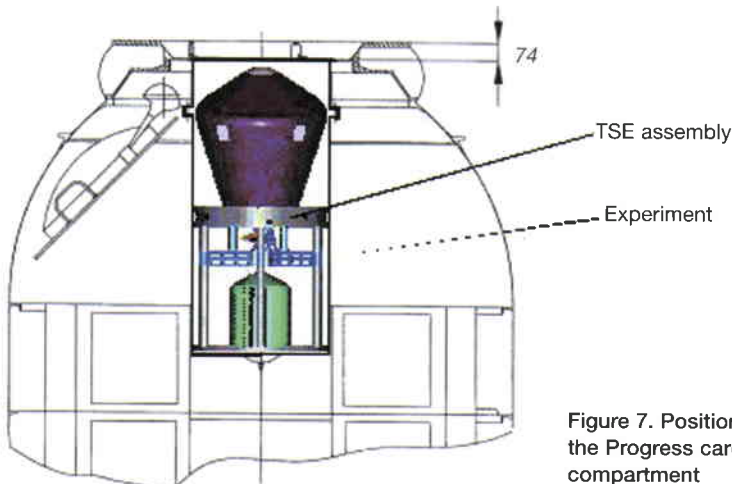


Figure 7. Position of TSE in the Progress cargo compartment

therefore included in the breadboard test programme, have been identified:

- Tether Motion Device/Brake: required to control tether deployment, this is the most critical component of the deployer. The ability to properly control the deployment process and the final braking determine the accuracy of delta-v that can be achieved in the swinging release of the tether. It is therefore essential to acquire sufficient knowledge and experience with the brake in order to achieve the TSE mission objectives.
- Tether: its properties (stiffness and friction) affect the deployment process as well as collision risk, and mission safety.
- Tether Motion Sensor: used to measure the deployed tether length, and to derive the deployment velocity. These optical turn counters have been tested, qualified and already flown, but are classified as critical because the deployment algorithms rely on proper functioning of these sensors.
- Tether Guidance/Tether Cutter: minimisation of the internal friction during early deployment phase is a prerequisite for successful sub-satellite deployment. The friction generated by the deployer components will therefore be evaluated in the breadboard test campaign.
- Control Algorithms: ensure that the tether deploys along the pre-defined reference profile.

The main objectives of the breadboard tests are:

- familiarisation with the tether hardware
- measurement of deployer characteristics to support analytical simulations (canister + brake + cutters/tensiometer)
- measurement of system friction at various

deployment stages and velocities

- testing of the algorithms and feedback
- demonstration of controllability of the hardware assembly.

The test campaign covers component testing as well as functional system testing. During component testing the tether modulus of elasticity, breaking strength and component/brake friction will be determined. In the functional system test, a tether deployment will be executed in real-time with a controller and tether simulator in the loop. The controller responds to measurements of the deployed length, while the space dynamic simulator responds to a tension measurement and drives the deployment via a motor. The functional system tests will re-use a test set-up originally manufactured for the TMM&M project by Alenia Aerospazio.

This test campaign will complete the Phase-B activities, and will provide key inputs for the TSE Critical Design Review.

Conclusion

Over the past 18 months, the feasibility of tether-assisted sample return has been proven and the TSE project team have prepared a solid, cost-efficient design for the ESA tether mission. In addition to providing European industry with an efficient near-term technology solution to meet many challenges in space, this demonstration mission will provide valuable flight experience that will put European industry in a competitive position for the development of an operational system for International Space Station users.



SPACE IS OUR CORE BUSINESS!

WHAT'S YOURS?

KEC has contributed to various international, governmental and commercial space programmes. Whether you are looking for new opportunities or have already established a steady space business, KEC can offer you attractive services in the field of:

Management: Interim Management, Project Management, PA&S Management, Industrial Organisation, Trouble Shooting, Consultancy

Systems Engineering: Methodology, AOCS, OBDH, Data Storage, Electrical Power Systems, Mechatronics, Mechanical Engineering, Using COTS in harsh environments, Consultancy

Business Development: Strategic Alliances, Opportunities, Market Development, Business Plans, Technology Transfer, Investments, Feasibility Studies, Consultancy



KEC
Van Kampen Engineering & Consultancy

P.O. Box 2226, 5001 CE Tilburg, The Netherlands, Tel.: (+31) 13 4 55 00 44 - Fax: (+31) 13 4 55 04 50
E-mail: kec@planet.nl - Internet: <http://www.kec-home.nl>

KEC
Van Kampen Engineering & Consultancy

Intra-European Co-ordination in the UN Committee on Peaceful Uses of Outer Space

K. Bergquist

International Relations Office, Directorate of Strategy and Technical Assessment, ESA, Paris

Introduction

Despite the Committee on Peaceful Uses of Outer Space and its two Subcommittees initially proving something of a verbal battleground between East and West, it took less than ten years for COPUOS to produce a treaty of global importance, namely the treaty on 'Principles Governing the Activities of States in the Exploration and Uses of Outer Space including the Moon and other Celestial Bodies',

One of the International Relations Committee's main roles is to provide an opportunity for Member States to prepare and co-ordinate their positions vis-a-vis the meetings of COPUOS and its two Subcommittees. Over the years, this co-ordination has involved items in both the Legal Subcommittee and the Scientific and Technical Subcommittee, when key issues have been raised that Member States felt they needed to discuss within the European framework.

Two years after the Soviet Union successfully launched the first Sputnik into space, the General Assembly of the United Nations created the ad-hoc Committee on Peaceful Uses of Outer Space in 1959. This Committee was set up because Member States of the United Nations were worried by the spectre of an arms race in outer space. It later became known as COPUOS, the 'ad-hoc' being removed. In order to carry out its functions, COPUOS in turn set up a Legal and a Scientific and Technical Subcommittee. A Secretariat, Outer Space Affairs Division, was created within the United Nations. This Secretariat is now known as the Office for Outer Space Affairs (OOSA).

COPUOS and its various Subcommittees and activities provide a unique opportunity for Europe's space-faring States to present themselves and their programmes and negotiate in a unified manner on a global stage.

Pre-UNISPACE III

This co-ordination process was reinforced lately in view of a debate in COPUOS on whether to hold a Third United Nations Conference on the Exploration and Peaceful Uses of Outer Space, UNISPACE III. The two previous conferences were held in 1968 and in 1982, respectively. Given the mixed results of UNISPACE II, ESA Member States were very active in COPUOS in debating the reasons for and against holding this event and how it should be structured.

now commonly referred to as the 'Outer Space Treaty'. This treaty constitutes the legal framework for conducting space activities. Since then, several other treaties dealing with specific aspects of space research and or use have been concluded, such as the Agreement on the Rescue and Return of Astronauts and the Registration Convention.

In 1973, ESRO and ELDO were both granted Observer status in COPUOS and its two Subcommittees. In order to co-ordinate the positions at the UN of their respective Member States, they set up the International Relations Advisory Group (IRAG). This Group and the Observer status were subsequently taken over by ESA. As international relations developed, so did the agenda of IRAG, which has since been re-designated the 'International Relations Committee (IRC)'.

In order to facilitate discussions at the United Nations, the ESA Member States proposed at the IRC meeting in November 1996 that the Executive should prepare a joint position document based on their contributions, which would be supported by all ESA countries and express the European views and positions on the proposed UNISPACE III event. This working document was presented at the 34th Session of the Scientific and Technical Subcommittee meeting by the UK Delegation, in the name of all ESA Member States. Prior to introducing the document, Delegations asked the Executive to consult with those European countries having signed co-operative agreements with the Agency (the Czech Republic, Greece, Hungary, Poland, Portugal and Romania) as to whether they would be prepared to co-sign the document. The European document, finally co-signed by 20 European countries, had a great impact on the work of the 34th Session and proved a model for future European co-ordination.

This first success led to a series of other documents being prepared jointly by the ESA Executive and Member States and co-signed by the above-mentioned European States in view of the UNISPACE III event. This active European preparation and co-ordination included participation in the Preparatory Regional Meetings that were held in Malaysia, Morocco, Chile and Romania. The co-ordination was not limited only to UNISPACE III matters, but included general items relevant to the Scientific and Technical Subcommittee and the Legal Subcommittee.

All of these active preparations by Europe led to a coherent presence at the Conference and strong European participation at the Exhibition (the Conference took place on 19 – 30 July 1999 in Vienna). Given this transparency and co-ordination, the ESA delegations were aware of what the others were going to say and could act accordingly.

It was felt by many delegations that UNISPACE III represented a landmark and that it was a timely opportunity to improve some of the guidelines and actions for the future work of the UN-COPUOS, notably to improve the agenda structure of its Subcommittee meetings.

Post-UNISPACE III

In order to maintain and keep this co-ordination tool effective, the German Delegation proposed to host an Informal IRC Meeting at the DLR Centre in Oberpfaffenhofen on 28/29 November 1999, inviting not only ESA Member States, but also those European countries having signed a co-operative agreement with the Agency (same as above). These countries had often co-signed the European position documents without having had the opportunity to participate in the debates. The first day of the meeting was dedicated to intra-European co-ordination in the light of the COPUOS meetings, as well as European expectations concerning the work of the UN Office for Outer Space Affairs. The newly appointed Director of OOSA and the United Nations Expert for Space Applications had been invited to participate in the second day in order to present their views on the future work of COPUOS and the Office, as well as the future guidelines for the Programme on Space Applications. As regards the Programme itself, three items were of particular interest:

- *The United Nations Regional Centres for Basic Science and Technology Education.* These Centres are located in different parts of the world: India, Morocco, Nigeria, and Brazil alternating with Mexico. Soon, Jordan will set up a centre for the Middle Eastern countries. A Dedicated Network of Space Science and Technology Education and Research Institutions has been set up in

Central-, Eastern- and South-Eastern Europe.

- *The training activities of the UN Programme of Space Applications.* Since UNISPACE I in 1969, the Office has had a mandate to promote training activities in order to spread knowledge and support the introduction of space applications in developing countries. This programme is based on the financial contributions of Member States to the United Nations. ESA is its biggest financial contributor.
- *The special fund.* At UNISPACE III, there was a long debate on the pros and cons of the United Nations creating a special fund to support the recommendations of the Conference, many Member States being against the proliferation of funds within the UN system. The compromise solution was to replace the existing fund with a new fund and to transfer the resources to the new fund. It was also suggested that the Secretary General send a letter each year to the UN Member States requesting them to provide voluntary contributions.



Figure 1. Participants in the COPUOS Intra-European Coordination Meeting at DLR in Oberpfaffenhofen (D), on 28/29 November 1999

Another issue that was discussed at the meeting was the future work of COPUOS. As noted above, COPUOS has agreed on a new agenda structure for the Legal Subcommittee and the Scientific and Technical Subcommittee. In Oberpfaffenhofen, delegations discussed what subjects the two Subcommittees should address in the near future.

The UN Programme on Space Applications: Conclusions

Following the first day's discussions, it was decided to continue the ESA contribution to the UN Programme on Space Applications, according to a proposal discussed with the Member States and the representatives from the Office of Outer Space Affairs, i.e. to continue support for the realisation of three or four training activities in developing countries. However, the courses should be accompanied by follow-up

measures. The objective of the Programme should be to stress continuity to enable the training-course participants to be able to apply their knowledge when they go back to their own institutions, through work on pilot projects.

Similarly for the fellowship programme, to stress continuity and increase efficiency, the fellows will be selected not only on the basis of their curriculum vitae, but also of on a project proposal. The idea is that they start working on the project, and when they come to the ESA establishment their training will be specifically related to that project. The duration of their stays will also be reduced to 6 months, from the present 12. This scheme is limited to those fellowships related to Earth-observation applications.

As regards the other training activities that the Office organises, the participants supported the Basic Space Science Course, the ninth of which will be held in Toulouse in June 2000. The importance of the UN/Sweden International Training Course on Remote-Sensing Education for Educators was also reaffirmed.

The above-mentioned activities have been decided upon and will take place in the year 2000. In addition, some other proposals were discussed for future activities to be included in the programme. The Czech delegation proposed to host, together with the OOSA, a workshop in 2001 on remote sensing for environmental monitoring, to which ESA will also contribute.

Disaster Management was discussed at great length at the UNISPACE III Conference and many thought that the OOSA should play a role in the dissemination of space-technology knowledge for the better management of natural disasters. ESA will explore in what ways the ESA/CNES Charter on the provision of data in cases of Natural Disasters that was announced at UNISPACE III could play a role in this work.

Another topic raised in order to ensure continuity in the actions that the Office undertakes in developing countries is to involve the donor organisations. ESA, together with the interested Member States and the UN, will organise a one-day presentation for the regional development banks to inform them of the usefulness of space technology for achieving sustainable development.

COPUOS's future work

Discussions concentrated on the new agendas for the two Subcommittees. Europe having pushed for this change, the question addressed in Oberpfaffenhofen was what new subjects should Europe try to promote. Previously, the Agendas of these meetings

were very rigid and it was difficult to get a new subject included and very difficult to stop considering old ones. The idea with the new structure is to avoid this and to introduce greater flexibility into the system.

In Oberpfaffenhofen, the participants suggested several new items for possible future consideration by the Scientific and Technical Subcommittee. One was funding sources. With UNISPACE III having stressed the importance of space applications in developing countries, the question arises of what possibilities exist to attract donor agencies to finance these applications. Another topic proposed was that of Energy Sources and the Use of Solar Panels.

Since strengthening of Inter-Agency co-ordination within the United Nations has always been a priority, it was suggested to propose that the issue be addressed under a three-year work plan. This issue has often been stressed in that the Office must seek to inform other specialised agencies of the United Nations of the potential of space applications to make their work more efficient.

Similarly, topics for the Legal Subcommittee were also addressed. The French delegation presented a working paper at the last session of COPUOS aimed at introducing the space debris issue for Legal Subcommittee consideration. This proposal was based on the fact that the Scientific and Technical Subcommittee had adopted its report on the consideration of space debris. At the time, two major delegations blocked the initiative, but now it seems that only one is still against the proposal. The French delegation, on behalf of several other European and non-European members, will reintroduce the document at the Scientific and Technical Subcommittee's next session, asking it to request that the Legal Subcommittee analyse some legal aspects of space debris in the present treaties.

It was also agreed that the item 'Launching State' as defined by the present treaties needs to be addressed, given the new launch ventures that are emerging. The item will be discussed according to a work plan in the Legal Subcommittee. The first year will include special presentations on new launch systems and ventures. In the second year, there will be a "Review of the Concept of the Launching State as contained in the Liability Convention and the Registration Convention as applied by States and International Organisations". During the third year, the Subcommittee will review measures to increase adherence to these Conventions and to promote their full application.

Programmes under Development and Operations

Programmes en cours de réalisation et d'exploitation

(status end-March 2000)

In Orbit / En orbite

| PROJECT | 1998 | | 1999 | | 2000 | | 2001 | | 2002 | | 2003 | | 2004 | | COMMENTS | | | | | | | | | | | |
|------------------------|--------------------|---|------|---|------|---|------|---|------|---|------|---|------|---|----------|---|---|---|---|---|---|---|---|-----------------------|------------------------|------------------------|
| | J | F | M | A | M | J | J | A | S | O | N | D | J | F | | M | A | M | J | J | A | S | O | N | D | |
| SCIENCE PROGRAMME | SPACE TELESCOPE | ■ | | | | | | | | | | | | | | | | | | | | | | | | LAUNCHED APRIL 1990 |
| | ULYSSES | ■ | | | | | | | | | | | | | | | | | | | | | | | | LAUNCHED OCTOBER 1990 |
| | SOHO | ■ | | | | | | | | | | | | | | | | | | | | | | | | LAUNCHED DECEMBER 1995 |
| | HUYGENS | ■ | | | | | | | | | | | | | | | | | | | | | | | | LAUNCHED OCTOBER 1997 |
| | XMM-NEWTON | ■ | | | | | | | | | | | | ▲ | ■ | | | | | | | | | | LAUNCHED DECEMBER 1999 | |
| APPLICATIONS PROGRAMME | MARECS-B2 | ■ | | | | | | | | | | | | | | | | | | | | | | | | POSSIBLE NEW LEASE |
| | METEOSAT-5 (MOP-2) | ■ | | | | | | | | | | | | | | | | | | | | | | | | OPERATED BY EUMETSAT |
| | METEOSAT-6 (MOP-3) | ■ | | | | | | | | | | | | ■ | ■ | | | | | | | | | | OPERATED BY EUMETSAT | |
| | METEOSAT-7 (MTP) | ■ | | | | | | | | | | | | ■ | ■ | | | | | | | | | | OPERATED BY EUMETSAT | |
| | ERS - 1 | ■ | | | | | | | | | | | | | | | | | | | | | | | | BACKUP TO ERS-2 |
| | ERS - 2 | ■ | | | | | | | | | | | | | | | | | | | | | | | | LAUNCHED APRIL 1995 |
| | ECS - 4 | ■ | | | | | | | | | | | | ■ | ■ | | | | | | | | | | OPERATED FOR EUTELSAT | |
| ECS - 5 | ■ | | | | | | | | | | | | ■ | ■ | | | | | | | | | | OPERATED FOR EUTELSAT | | |

Under Development / En cours de réalisation

| PROJECT | 1998 | | 1999 | | 2000 | | 2001 | | 2002 | | 2003 | | 2004 | | COMMENTS | | | | | | | | | | | | | |
|---------------------------------------|------------------------------|---|------|---|------|---|------|---|------|---|------|---|------|---|----------|---|---------------------|---|---|---|---|---|---|---|---|---------------------------|---|-----------------------------|
| | J | F | M | A | M | J | J | A | S | O | N | D | J | F | | M | A | M | J | J | A | S | O | N | D | | | |
| SCIENTIFIC PROGRAMME | CLUSTER-II | ■ | | | | | | | | | | | | ▲ | ■ | | RE-LAUNCH MID 2000 | | | | | | | | | | | |
| | INTEGRAL | ■ | | | | | | | | | | | | ▲ | ■ | | LAUNCH APRIL 2002 | | | | | | | | | | | |
| | ROSETTA | ■ | | | | | | | | | | | | ▲ | ■ | | LAUNCH JANUARY 2003 | | | | | | | | | | | |
| | MARS EXPRESS | ■ | | | | | | | | | | | | ▲ | ■ | | LAUNCH JUNE 2003 | | | | | | | | | | | |
| | SMART-1 | ■ | | | | | | | | | | | | ▲ | ■ | | LAUNCH LATE 2002 | | | | | | | | | | | |
| COMMS./ NAV. PROG. | ARTEMIS | ■ | | | | | | | | | | | | | | | | | | | | | | | | LAUNCH DATE TBC | | |
| | GNSS-1/EGNOS | ■ | | | | | | | | | | | | | | | | | | | | | | | | INITIAL OPS. END 2003 | | |
| | GALILEOSAT | ■ | | | | | | | | | | | | ▲ | ■ | | | | | | | | | | FIRST LAUNCH 2003 | | | |
| EARTH OBSERV. PROGRAMME | EOPP | ■ | | | | | | | | | | | | | | | | | | | | | | | | | | |
| | EOEP | ■ | | | | | | | | | | | | | | | | | | | | | | | | INCL. CRYOSAT, SMOS, GOCE | | |
| | ENVISAT 1/ POLAR PLATFORM | ■ | | | | | | | | | | | | ▲ | ■ | | | | | | | | | | LAUNCH JUNE 2001 | | | |
| | METOP-1 | ■ | | | | | | | | | | | | ▲ | ■ | | | | | | | | | | LAUNCH MID-2003 | | | |
| | MSG-1 | ■ | | | | | | | | | | | | ▲ | ■ | | | | | | | | | | LAUNCH OCTOBER 2000 | | | |
| MANNED SPACE & MICROGRAVITY PROGRAMME | COLUMBUS | ■ | | | | | | | | | | | | | | | | | | | | | | | | ▲ | ■ | LAUNCH OCTOBER 2004 |
| | ATV | ■ | | | | | | | | | | | | ▲ | ■ | | | | | | | | | | LAUNCH DECEMBER 2003 | | | |
| | X-38 | ■ | | | | | | | | | | | | | | | | | | | | | | | | ▲ | | V201 TEST FLIGHT MARCH 2002 |
| | CRV | ■ | | | | | | | | | | | | | | | | | | | | | | | | | | OPERATIONAL 2005 |
| | NODE-2 & -3 | ■ | | | | | | | | | | | | ▲ | ■ | | | | | | | | | | LAUNCHES FEBRUARY 2003 & SEPTEMBER 2004 | | | |
| | CUPOLA | ■ | | | | | | | | | | | | ▲ | ■ | | | | | | | | | | LAUNCH MAY 2004 | | | |
| | ERA | ■ | | | | | | | | | | | | ▲ | ■ | | | | | | | | | | LAUNCH JUNE 2002 | | | |
| | DMS (R) | ■ | | | | | | | | | | | | ▲ | ■ | | | | | | | | | | LAUNCH JULY 2000 | | | |
| | FREEZER | ■ | | | | | | | | | | | | ▲ | ■ | | | | | | | | | | LAUNCH AUGUST 2001 | | | |
| | GLOVEBOX | ■ | | | | | | | | | | | | ▲ | ■ | | | | | | | | | | LAUNCH AUGUST 2001 | | | |
| | HEXAPOD | ■ | | | | | | | | | | | | ▲ | ■ | | | | | | | | | | LAUNCH OCTOBER 2003 | | | |
| | EMIR | ■ | | | | | | | | | | | | | | | | | | | | | | | | ▲ | ■ | BIO, FSL, EPM in COLUMBUS |
| | MFC | ■ | | | | | | | | | | | | | | | | | | | | | | | | ▲ | ■ | |
| LAUNCHER PROGRAMME | ARIANE-5 DEVELOP | ■ | | | | | | | | | | | | ▲ | ■ | | | | | | | | | | V504 LAUNCHED DECEMBER 1999 | | | |
| | ARIANE-5 PLUS | ■ | | | | | | | | | | | | ▲ | ■ | | | | | | | | | | FIRST LAUNCH APRIL 2002 | | | |
| | FESTIP | ■ | | | | | | | | | | | | | | | | | | | | | | | | | | REUSABLE LAUNCHER DEFIN. |
| | FTLP | ■ | | | | | | | | | | | | | | | | | | | | | | | | | | TECHNOLOGY DEVELOPMENT |

■ DEFINITION PHASE

■ MAIN DEVELOPMENT PHASE

▲ LAUNCH/READY FOR LAUNCH

■ OPERATIONS

■ ADDITIONAL LIFE POSSIBLE

▼ RETRIEVAL

■ STORAGE

Cluster-II

All testing and refurbishment activities on all four spacecraft have been successfully completed. The first two spacecraft to be launched (FM6 and FM7) are ready for shipment at Dornier's premises in Friedrichshafen (D), whilst the second pair (FM5 and FM8) are ready to be shipped from IABG in Munich.

The Flight Acceptance Review, which included co-location of the review team at Dornier during 20-24 March, culminated with the Review Board meeting in Paris on 28 March. The Review Board expressed full satisfaction with the status of the four Cluster-II spacecraft and endorsed the review team's positive findings. The Board also shared the Project's concerns over a general problem with the type of spacecraft propulsion system used, which is currently affecting several programmes, both in-orbit and about to be launched. The course of action proposed by the Project, and fully endorsed by the Board, will lead to a final decision concerning the suitability of the system for the Cluster mission. It was decided to delay shipment of the four spacecraft to the Baikonur Cosmodrome until investigations are completed.

The Ground-Segment Readiness Review (GSRR) was successfully held on 15 March. The flight simulation programme was started at ESOC and several simulations were performed in March with Project and Industry participation. The programme will be resumed at the end of April after a short interruption due to the delay in shipment of the spacecraft.

The science data system functional testing has been completed and has proved the

system ability to support experiments through remote commanding by Principal Investigators and data distribution via the Data Centres. A successful Science Data System Readiness Review on 14 March confirmed system readiness.

Two successful qualification launches of the new Fregat upper stage for the Soyuz launch vehicle took place on 9 February and 20 March. The very good accuracy achieved in all orbital parameters confirmed the ability of the launch vehicle and upper stage to launch the Cluster mission successfully.

The Baikonur Launch Facilities Acceptance took place on 15-18 March. The fuel for the four spacecraft arrived in Baikonur on 19 March after sea transport from the UK to St. Petersburg and subsequent shipment by train to its final destination. It is currently stored in the hazardous-goods storage facility.

The launch dates of June and July are presently affected by the delay in the shipment of the spacecraft to Baikonur. The exact impact is currently being assessed, but a postponement of the two launch dates by at least three weeks can be envisaged.

Integral

The spacecraft, launcher and ground-segment activities have continued to follow the recommendations from the Critical Design Review held in December 1999.

The first part of the System Validation Test (SVT) was successfully completed in March. The SVT demonstrates the ability

of the Mission Operations Centre (MOC) to control and monitor the spacecraft. It also confirms the basic functionality of the spacecraft Service Module.

For this first SVT phase, the emphasis was on validation of the functions needed to handle the telemetry and telecommand data for the Service Module. The next phase will also include the execution of real operational scenarios, such as the Launch and Early Orbit Phase (LEOP), to validate the relevant flight procedures. At a later stage, when the payload has been integrated, similar tests will be conducted to ensure that the MOC will also be able to control the instruments on board Integral correctly.

The status of the four scientific instruments making up the Integral payload was reviewed in April. A revised completion schedule leading to launch in April 2002 has now been agreed.

Rosetta

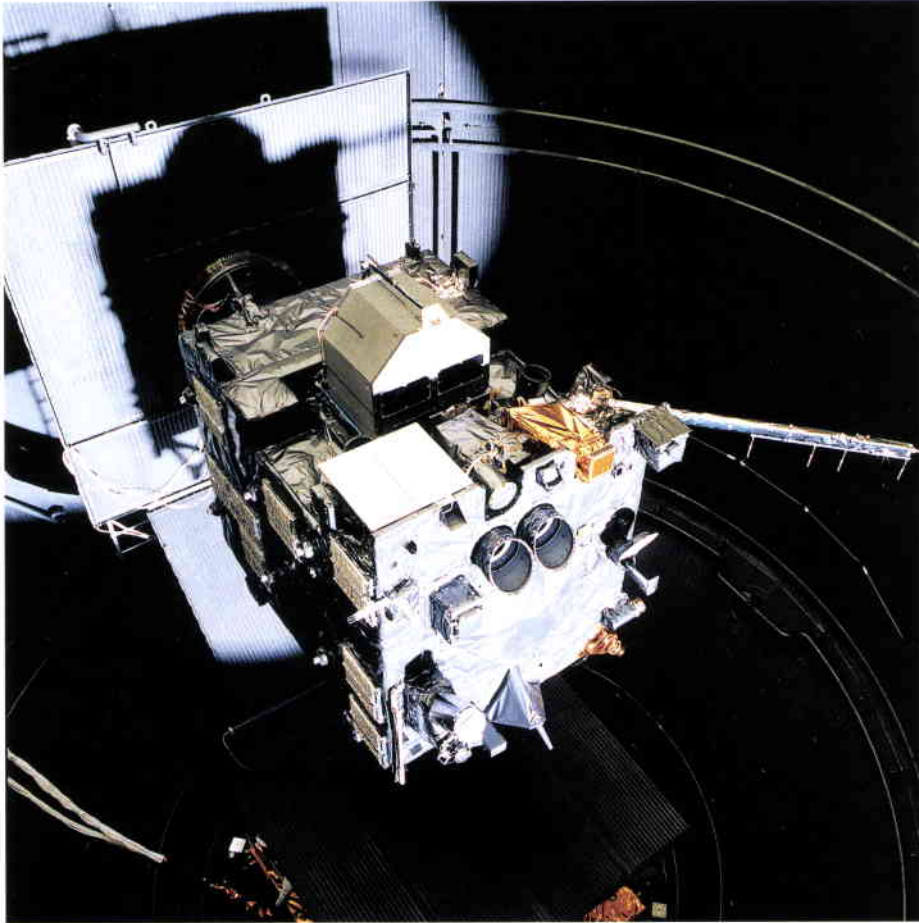
The Rosetta Structural and Thermal Model (STM) testing has been completed, which is consistent with the planned schedule. The structural tests were completed in February and it was demonstrated that the primary structure can withstand the expected launch loads. In addition, the expected environment for all subsystem and payload units was below the specifications to which they have been designed.

The thermal-balance testing was also very successful. It demonstrated that the spacecraft can withstand the extreme thermal conditions that it will encounter during its long voyage, at distances from the Sun of between one and more than five times the distance from the Earth to the Sun. This is one of the most challenging features of the Rosetta mission and this successful demonstration is therefore a major milestone in the programme.

The Electrical Qualification Model (EQM) programme has also started in mid-April. Although this was one month behind schedule, contingency planning has ensured that it can still be completed by



The Integral System Validation Test (SVT) in progress at ESOC



The Rosetta Structural and Thermal Model (STM), under test at ESTEC (NL)

mid-March 2001, before the flight model starts its integration. During this time, full functional testing of all spacecraft and payload units will take place, ending with the electromagnetic compatibility (EMC) test. The subsystem units have started to be delivered and integrated, as well as the first version of the onboard software, which will be incrementally updated according to the functional requirements of the tests to be performed.

The Hardware Design Review (EMR) held in November 1999 had identified various areas of the system design that were still insufficiently defined. These areas have been actively addressed with the prime contractor and the major subcontractors, resulting in positive closure of most of the resulting actions.

Development of the scientific payload is also proceeding according to plan, with delivery of all the EQM units expected before the end of June, in time for integration on the spacecraft EQM. Pre-shipment reviews have been held at all of the participating institutes. For the Rosetta lander, a major effort has been made to consolidate the system design, resulting in solutions being found for most critical areas.

Work is progressing satisfactorily in all areas of the ground-segment development. In particular, the foundation stone has been laid for the new ESA 35 m Deep Space Antenna at New Norcia in Western Australia, and construction is planned to be completed by the end of 2001.

Mars Express

The implementation of the Mars Express mission has continued to progress at a rapid pace. The final meeting of the Preliminary System Design Review Board took place on 11 January. The Board, co-chaired by ESA Directors R.M. Bonnet and J-J. Dordain, heard presentations on all aspects of the missions, including a detailed technical assessment of the spacecraft design compiled by an independent Science and Engineering Review Team. The Board concluded that the current spacecraft design allows the formal starting of Phase-C/D, i.e. the building of the spacecraft. The Board also issued eight recommendations that the Project has accepted and already incorporated into the spacecraft design. The International Mars Exploration

Working Group, coordinating the international aspects of all Mars missions, met on 26 and 27 January in London. The Working Group was debriefed on the then available facts relating to the NASA investigations into the loss of the Climate Orbiter and Polar Lander missions. These results are of high interest for ESA, as every effort will be made to take NASA's 'lesson learnt' into account for Mars Express.

The new Fregat upper stage of the Soyuz launcher has been successfully test-flown twice. Its performance was outstanding and it should therefore be able to inject Mars Express onto a very precise cruise trajectory to the planet.

The Prime Contractor Matra Marconi Space (F) has organised a meeting of all of their subcontractors. During this industrial day, the companies also exchanged views on ESA's new approach to the procurement of the spacecraft. The new management approach seems well appreciated, as it allows, inter alia, quicker decision making and faster financial payments.

Preparation of the ground segment at ESOC is in full swing and the team is being expanded as planned to cope with the increasing workload.

EOEP

The Earth Observation Envelope Programme (EOEP) was formally initiated on 1 January although, as previously reported, considerable effort had already been devoted to ensuring a smooth start-up. The programme covers the two types of Earth Explorer mission, 'Core' and 'Opportunity'. The first mission of each type has already been initiated into Phase-B, namely GOCE and CRYOSAT, respectively. In addition, a second mission of each type is currently under preparation, namely ADM/AEOLUS, for which instrument pre-development has started, and SMOS, which is entering Phase-A.

As well as these new satellite missions, the programme is funding the continuity of

the ERS-2 mission and a new Market Development activity, aimed at the development of new information products derived from existing satellite data. It is also planned to utilise EOEP resources in the future for the preparation of Earth Watch programmes.

EOPP

Following the agreed selection and initiation of the first two Earth Explorer Core missions, the Executive, with advice from the Earth Observation Science Advisory Committee (ESAC), is preparing for the next candidate mission selections. The first step will be an open invitation to the science community in the programme's Participating States to propose new missions. This invitation should be issued in June.

With the agreed implementation of the first two Opportunity missions, CRYOSAT and SMOS, and the continued support to ACE as a 'hot standby' in the event of problems, the Executive has been investigating opportunities to implement other recommended missions by proposing them to NASDA and NASA as payloads on GCOM and NPP, respectively. NASDA has selected three – SWIFT, COALA and GRAS – for further study.

EOPP is also continuing various activities aimed at supporting the establishment of an Earth Watch strategy.

Meteosat Second Generation

One of the final tests on the engineering model has been the end-to-end spin test, in which the satellite was spun at its actual in-orbit rate of 100 rpm. In this test, a target was imaged and the data transmitted successfully via the spacecraft's electronically despun antenna.

The MSG-1 flight-model satellite has successfully undergone mechanical and

thermal environmental testing and is currently in the indoor Compact Test Range for antenna verification and electromagnetic compatibility testing, soon to be followed by optical vacuum tests to test the optical performance of the cold channels of the SEVIRI instrument.

The MSG-2 flight-model satellite's integration has started and most of the equipment for the MSG-3 flight model, and spares, have been delivered to the prime contractor Alcatel Space in Cannes (F).

The Qualification Results Review is still in progress due to the late availability of engineering-model test results and reports. It is now scheduled to be completed in May.

The Flight Acceptance Review (FAR) is confirmed for August as planned, which

means that the predicted launch date for MSG-1 could remain October 2000, although Eumetsat, the satellite system operator, is presently contemplating a launch delay in consultation with its delegate bodies.

The recent successful Ariane-505 launch (in March) will provide important data for solving the Ariane-5-related shock problem and will hence help in the final selection of the launcher for MSG-1, i.e. Ariane-4 or Ariane-5.

Metop

Following completion of the technical and contractual baseline for the GOME-2 contract, the contract signature took place at a ceremony on 3 March in the Palazzo



The MSG engineering model undergoing spin testing at Alcatel Space, Cannes (F)

Vecchio in Florence (I), attended by ESA's Director of Application Programmes, Mr C. Mastracci, the Director of Eumetsat, Dr T. Mohr, and the Head of Alenia Difesa's Avionics System and Equipment Division, Mr G. Grasso. The signing coincided with a round-table press event on the topic 'Ozone, A Problem for Europe?'

Meanwhile, the satellite design and development activities are proceeding nominally. Initial integration of the instruments provided by NOAA/NASA with the Interface Unit on the Payload Module (PLM) engineering model has been completed. Despite one or two interface problems being identified by this test campaign, the results still represent a very positive achievement and allow the PLM engineering-model integration to be started with good confidence. The major interface problem identified, namely with the synchronisation of the US HIRS instrument, which does not operate correctly with the agreed interface definition, is under investigation.

The overall schedule and integration logic of the PLM and satellite programmes has been examined in depth together with the prime contractor, Matra Marconi Space (F), to take into account the realities of the Customer Furnished Instrument delivery schedules. These efforts are aimed at optimising the resulting revised approach.

Envisat/Polar Platform

Envisat system

The system activities have focused on the following key activities:

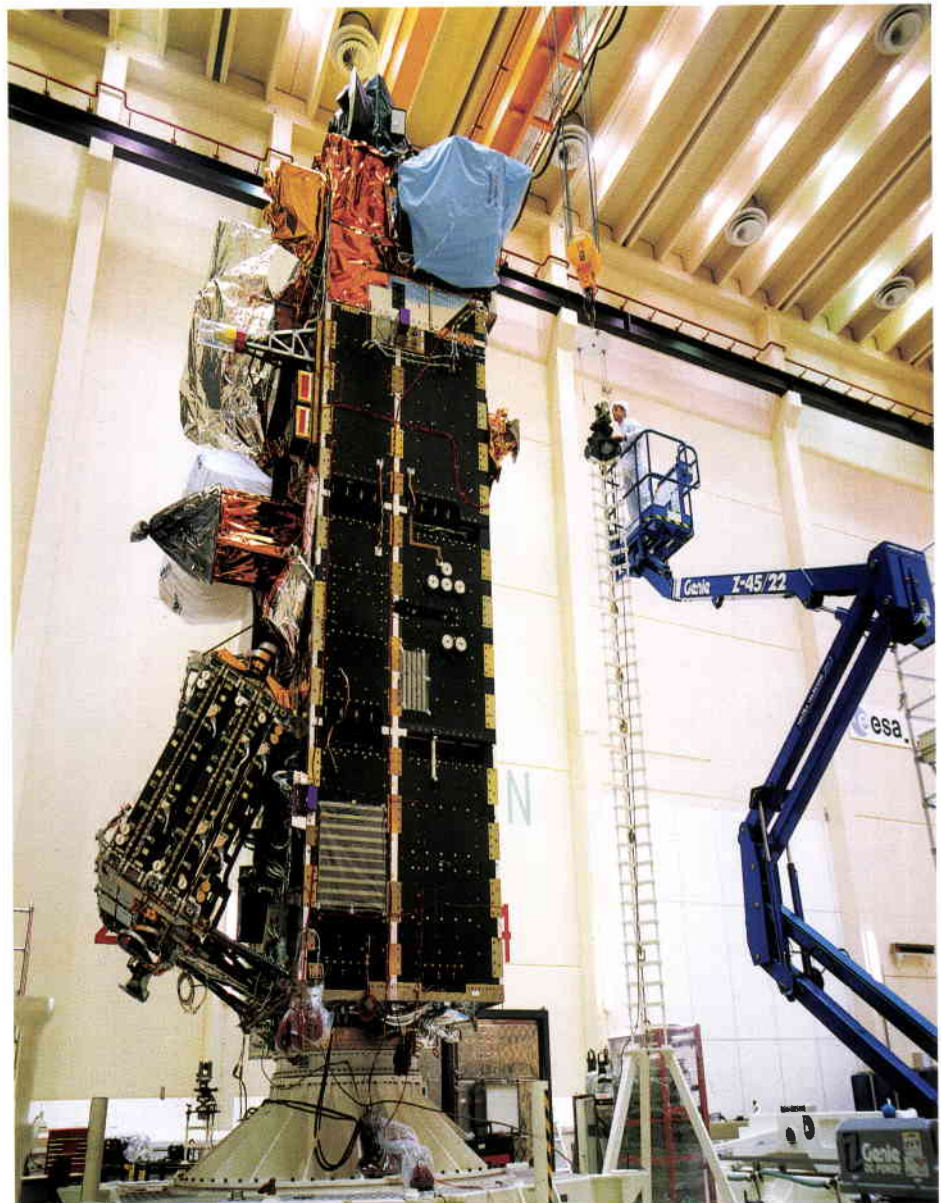
- preparation for the satellite system tests
- preparation for the Ground Segment Overall Verification (GSOV) and initialisation of some of the corresponding compatibility tests between the satellite and the ground segment (PDS and FOS)
- preparation for the in-orbit commissioning, in particular the setting up of payload calibration/validation teams and the definition of corresponding activities.

Envisat satellite and payload

With the delivery of SCIAMACHY, the return of the ASAR central electronics



Signature of the Metop GOME-2 contract. From left to right: Mr G. Grasso (Alenia), Mr C. Mastracci (ESA) and Dr T. Mohr (Eumetsat)



Envisat flight-model spacecraft in the ESTEC test facilities

(CESA), and delivery of the ASAR antenna, the flight-model payload is now completely integrated on the flight-model Payload Module.

The flight-model Service Module has been submitted to the shock tests simulating the Ariane-5 launch (shock generator and clamp-band release). The post-test analysis has confirmed that the Service Module and all of its critical subsystems successfully passed this test.

The Service Module and Payload Module are now being re-mated together in preparation for the satellite system tests planned for the second quarter of 2000.

The satellite assembly, integration and test (AIT) schedule is being regularly scrutinised and optimised to ensure compatibility with the target launch date of end-June 2001.

Envisat ground segment

The Flight Operations Segment (FOS) is being prepared for the Satellite Verification Tests (SVT-2) to be executed as part of the satellite system testing. SVT-2 will be a key test in the demonstration of compatibility between the satellite and the Flight Operation Control System and Satellite Operation Planning implemented at ESOC.

The acceptance of the Payload Data Segment (PDS) Version 2 has been completed. The PDS version V3 Critical Design Review has been conducted and the go-ahead given for implementation of the time-critical upgrades. PDS V3 will cope with the improved mission-management strategy provided by the use of the two on-board solid-state recorders, modifications identified in the flight-model payload-telemetry data streams, and improvements in some data-processing algorithms for level-1B and level-2 products.

The Processing and Archiving Centre (PAC) implementation activities are in progress. Iterations are ongoing between ESA and the PAC providers to ensure compatibility between their PDS Generic Element procurements and the ESA PDS V3 evolution.

The commercial distributors' offers in response to the ESA Invitation to Tender (ITT) are currently being evaluated.

International Space Station

European participation in the ISS Exploitation Programme

A High-Level Commitment was signed by Industry on 3 March. The target price for the complete Exploitation Phase Operations Contract amounts to 2.6 BEuro and the Firm Fixed Price commitment for Early Activities and ceiling price offer for Phase-1 are both within ESA targets. On 22 March, the ESA Council approved the proposed approach to industrialisation and commercialisation and also approved entrusting the Operations Preparation and Early Activities to the same industrial group. A procurement proposal for the entire operations contract and preparatory activities is being prepared.

ISS Overall Assembly Sequence

Following the Proton launch failures in 1999 and their impact on the Service Module launch date, NASA decided to launch a Shuttle logistics mission to the ISS in March. The aim was to carry out a number of necessary maintenance actions on Zarya's systems, and to exchange a number of limited-life hardware items in order to re-certify Zarya's service life to end-2000.

A General Designers' Review (GDR) was held in Moscow on 11 February, at which the proposed planning for returning Proton to flight, and the status and future planning for the preparation of the Service Module for launch, were discussed. This resulted in the endorsement of the proposed planning for Proton and a launch window of 8–14 July for the Service Module.

In March, an interim update to Revision E of the ISS Assembly Sequence was approved, but is limited to assembly flights up to and including UF1. All subsequent assembly flights remain under review, but delays of approximately 8 months can be expected, leading to a Columbus launch date around October 2004. The next Assembly Sequence update is expected in June/July.

Columbus laboratory

Revised project planning taking into account the significant overall ISS assembly delays has now been completed, and project activities are being realigned accordingly. A full-scale mock-up of Columbus, with all external features incorporated, has been tested in the

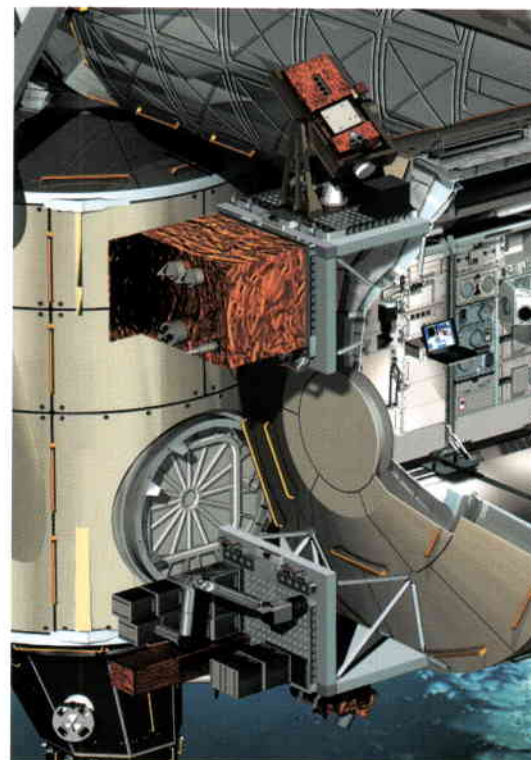
NASA/JSC Neutral Buoyancy Facility, and astronauts have verified that all planned and contingency EVA activities can be carried out. The system Electrical Test Model phase-2 testing preparation is complete, and the Data Management subsystem software integration has been performed. All low-level Critical Design Reviews (CDRs) have been completed, except for the video equipment, the high-rate multiplexer and the DMS subsystem. The system CDR will now be conducted in the fourth quarter of 2000. Manufacture of the flight-unit primary structure is complete and the first phase of proof pressure testing has been successfully performed.

Columbus Launch Barter

Nodes-2 and -3

Discussions have been held with ASI (to whom management of the Nodes-2/3 project is delegated by ESA) and NASA, to address the impact of the multiplicity of design changes, which have affected the Nodes design quite fundamentally and which were introduced in response to NASA requirements changes. The impact of these changes significantly alters the industrial cost of the Nodes and therefore also the balance of the Columbus Launch Barter, and the discussions have been aimed at redressing this balance.

Meanwhile, the Node-2 flight-unit primary structure welding has been completed and that of the Structural Test Article is well advanced. Updating of the Node-3



design baseline is underway in preparation for a System Review in Summer 2000.

Cryogenic Freezer Racks

The negotiation of NASA's requirements is still ongoing. However, following an end-March agreement on guidelines to solve the residual conflicts, it is hoped that the final specification can soon be agreed and the project started.

Cupola

The Design Consolidation Review has been successfully completed. Forgings for the primary structure of the Structural Test Article (STA) have been delivered and are being machined to final dimensions. Manufacturing-tool design activities have been completed, Mechanical Ground Support Equipment (MGSE) manufacturing release has been granted, and procurement of the STA and flight-unit window frames has been initiated.

Automated Transfer Vehicle (ATV)

Technical agreement has been reached to use the Ariane-5 Versatile configuration with a restartable upper stage for ATV launches. An agreement on the total price and associated payment conditions for a batch order of nine ATV launches with this Ariane-5 configuration was concluded on 31 March.

The ATV/Russian Segment Integration Preliminary Design Review (PDR) has been completed.

Negotiations with RSC-Energia on the procurement of Russian hardware for the ATV are well advanced, but with some important issues still to be resolved. Agreement has been reached on the baseline to be used for relative GPS navigation.

The System PDR was kicked-off on 14 March and should be completed by mid-June.

X-38/CRV and Applied Re-entry Technology (ART)

Flight-hardware manufacture and delivery is continuing on schedule. Flight rudders were delivered to Johnson Space Center in December, and manufacturing of all critical components of the CMC leading edges has been completed, as has the manufacturing of the landing-gear system. The nose primary structure is in final manufacturing, and qualification of the TPS thermal blankets has started.

The first test of V132 was performed successfully on 30 March.

Selected critical CRV Phase-1 tasks were initiated with European industry in December under the running X-38 contract.

Ground-segment development and operations preparation

The Columbus Control Centre Phase-B2 studies have been extended to allow more time for the detailed definition of the system architecture. The ATV Control Centre system-definition studies are continuing in line with agreed planning. Phase-C/D kick-off for the Control Centres will now take place in the first quarter of 2001.

The Phase-A study for the ATV Trainer has been completed, and the Phase-C/D for the Columbus Functional Crew Trainer has been initiated.

Utilisation

Promotion

At its January meeting, the Industrial Policy Committee (IPC) endorsed a first group of Microgravity Application Projects (MAP). The individual contracts were negotiated in February and March. New

life-science MAPs were approved by the Microgravity Programme Board in March.

Due to the delays in the Space Station Programme, the Organising Committee of the Global Utilisation Symposium initially planned for June 2000 in Berlin, has decided to postpone the Symposium by one year, to 5 – 7 June 2001.

Preparation for commercial utilisation

The European Utilisation Board (EUB), meeting in February, discussed the commercialisation of ISS utilisation and the issue of the variable cost-contribution scheme. The Executive continued to refine its ideas regarding the composition and terms of reference of the Space Station User Panel (SSUP) with a view to finalising them by mid-2000, and with an emphasis on ISS utilisation by industry.

The Industry Space Station Advisory Committee (ISSAC) met in March and also discussed commercialisation issues.

The Executive has further developed its approach to utilisation commercialisation and was aided in this task by the delivery of final reports of parallel studies by consultants Battelle/Cranfield/AccessMatrix on ISS commercialisation. The studies conclude that industry is not yet prepared to pay the full ISS utilisation costs for research and development, but R&D sponsorship has been identified as a possible source of income.

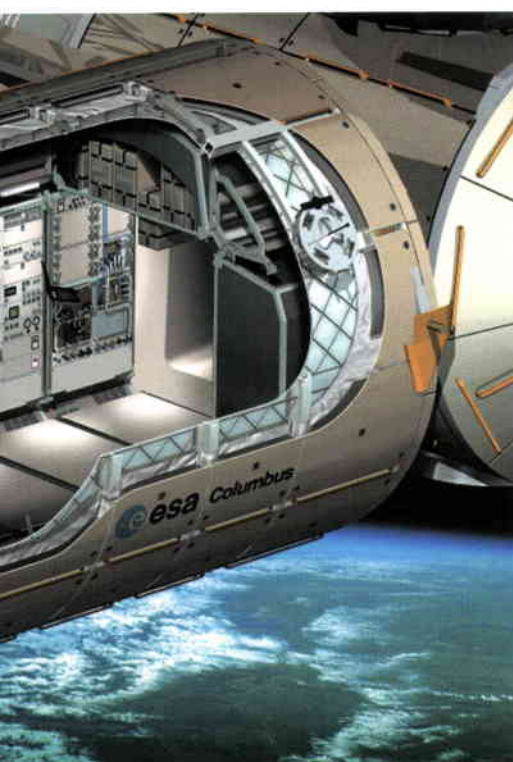
The course of further action proposed by the Executive was endorsed by the Manned Space Programme Board (PB-MS), reported to the IPC and approved by the Council in March. A definitive approach is to be finalised by end-2000.

A Call for Interest to undertake ISS commercialisation will be sent out in mid-June to industrial/commercial entities.

Accommodation hardware development

The conversion proposal from industry covering Phase-C/D of each the European Drawer Rack (EDR) and the European Stowage Rack (ESR) was received on 4 April and is under evaluation. Extensive negotiations are anticipated due to a significant overrun on the ceiling price. It is planned to negotiate the proposal with a kick-off of Phase-C/D in September.

The final report on the ACES Express Pallet Phase-B2 was delivered in February



ESA's general-purpose Columbus laboratory is scheduled for launch in about October 2004. (ESA/D. Ducros)

and is currently under review. A dedicated Special Atomic Clock Ensemble in Space (ACES) session was held during the European Frequency & Time Forum (EFTF). ESA's and CNES's ACES activities will be synchronised by the autumn, enabling instrument Interface Control Documents (ICD) to be agreed prior to the start of Phase-C/D.

Columbus payload integration and operation

The Columbus Payload Integration (CPI) has been implemented in the form of a Contract Change Notice (CCN) to the Phase-C/D contract for the Columbus laboratory. The starting of initial tasks was authorised in January. Negotiation of the full CCN is planned to start once the changes in the Columbus schedule have been approved.

Astronaut activities

F. De Winne joined the European Astronaut Corps on 1 January as its 16th member. He is currently supporting the X-38/CRV Project at ESTEC.

G. Thiele participated as a Mission Specialist in the Shuttle Radar Topography Mission STS-99, which achieved three-dimensional mapping of most of the Earth's land surface.

As part of their basic training, three NASDA astronaut candidates, together with their ESA colleagues A. Kuipers and F. De Winne, attended a course at EAC on ESA and its programmes.

The Manned Space Programme Board has unanimously endorsed the principles of co-operation for the EAC operations, and in particular the build-up of an EAC Team under full ESA responsibility. This team will be composed of ESA staff and personnel seconded from national entities (DLR, CNES, ASI). The ESA/DLR Arrangement started on 1 April with 23 DLR staff seconded as training-infrastructure and medical support to EAC, and will run until end 2003, with the intention for further continuation.

Early deliveries

Data Management System for the Russian Service Module (DMS-R)

Integrated testing of DMS-R with Service Module avionics systems has been completed at Baikonur as an integral part of Service Module launch preparations. The latter are on schedule for an 8-14 July launch slot.

All initial flight spares have been delivered to RSC-Energia, and manufacture of the first operational spares is in progress.

European Robotic Arm (ERA)

Testing of the Engineering/Qualification Model of ERA on the Fokker Space Flat Floor Facility is in progress and electrical-bench testing on the ERA flight-model joints has been completed.

The Mission Preparation and Training Equipment (MPTE) is being integrated in readiness for delivery to ESTEC in June 2000.

Assembly of the ERA system flight model is held up pending delivery of the end-effector flight units. ERA flight-model delivery has now moved to the second quarter of 2001. However, this delivery remains non-critical as the Science Power Platform Flight has also been postponed to September 2002 at the earliest, due primarily to budget shortfalls.

Laboratory Support Equipment (LSE)

The MELFI (Minus 80°C Freezer Laboratory) Training Unit will be delivered to NASA in May. All major subsystems have been manufactured and are undergoing qualification testing. The electrical subsystem has been qualified and system-level testing is planned to start in June.

The manufacture of critical flight-unit parts for the Material Science Glovebox has started and integration of the engineering unit is in progress.

The dedicated Safety Review caused by the modified re-entry configuration of the Hexapod Pointing System took place from 14 to 18 February. Following the indications of the Safety Panel Structural Working Group, the linear actuators were modified to include locking systems for landing. The High-Fidelity Mechanical Interface Simulator was delivered to NASA in March. Preparation of the data package for the Critical Design Review (CDR) is in full swing and expected to be completed in May.

Microgravity

EMIR programmes

In a common approach with CNES and DLR, the conditions for a Foton-13 flight in

the second half of 2002 were negotiated with Rosaviakosmos at ESA Headquarters in Paris, on 2 March. The results were reported at the Programme Board meeting on 29-30 March and led to the approval of the Foton-13 mission with 355 kg of CNES, DLR and ESA payload. The CNES (IBIS) and DLR (AGAT) elements still need to be confirmed, as national approval procedures will only be completed in June.

The Texus-37 sounding-rocket flight carrying one ESA-funded experiment, the capillary flow experiment of Dr. Dreyer, was successfully launched and retrieved on 27 March, after a 4-day delay due to strong winds. Texus-38 with a 100% ESA-funded payload was successfully launched on 2 April. All three experiments performed well and sent back interesting scientific results, telemetry and video data. Unfortunately, Texus-38's main parachute did not deploy and the payload itself was badly damaged on landing. This was the first such Texus recovery-system failure in approximately 45 missions.

The proposal for the main development (Phase-C/D) of Matroshka was received on 29 February from DLR and its evaluation has started.

For the running projects, a number of Preliminary and Critical Design Reviews (PDRs and CDRs) and Safety Reviews are in progress or about to be initiated, for the Materials Science Laboratory (MSL), the Fluid Science Laboratory (FSL), the Biolab and the Protein Crystallisation Diagnostics Facility (PCDF).

Microgravity Facilities for Columbus (MFC)

The engineering models for Biolab, FSL and MSL in the US Laboratory are well advanced and the subsystem Critical Design Reviews (CDRs) have been initiated. Engineering-model integration has started for Biolab. Breadboarding activities for some of the European Physiology Modules have been initiated.

The MFC Commercialisation Study – Phase 1 final presentation has taken place, with the MFC prime contractors explaining the role that they can play in ISS commercialisation.

FIRST INTERNATIONAL SYMPOSIUM ON

MICROGRAVITY RESEARCH & APPLICATIONS IN PHYSICAL SCIENCES & BIOTECHNOLOGY

10-15 September 2000 Sorrento, Italy

Co-sponsored by
ASI, CNES, CSA, DLR, ESA, NASA and NASDA

Aims and Scope

The Symposium intends to provide a forum for scientists from academia and industry to present and discuss recent advances in their research on gravity-dependent phenomena in Physical Sciences and Biotechnology. Results originating from theoretical work, numerical modelling, ground-based and flight investigations are solicited. The major topics include Fundamental Physics, Fluid Physics, Heat and Mass Transport Phenomena, Physical Chemistry, Fluid Thermodynamics, Thermophysical Properties of Fluids, Combustion, Solidification Physics and the Crystallisation of Inorganic Materials and Biological Macromolecules. Topics in Biology and Bioengineering, which are expected to benefit from cross-fertilisation and synergy with physicists, such as multi-phase flows and surface physical chemistry, including structured deposition of macromolecules, will also be addressed.

International Scientific Committee Chairman

Prof. Ilya Prigogine, Nobel Laureate in Chemistry
ULB Brussels, Belgium
University of Texas at Austin, USA

Symposium Chairman

Prof. Antonio Viviani
Seconda Università di Napoli
Aversa, Italy

Conference Secretariat

ESTEC Conference Bureau
P.O.Box 299
2200 AG Noordwijk
The Netherlands
Tel.: +31-(0)71-5655005
e-mail: confburo@estec.esa.nl

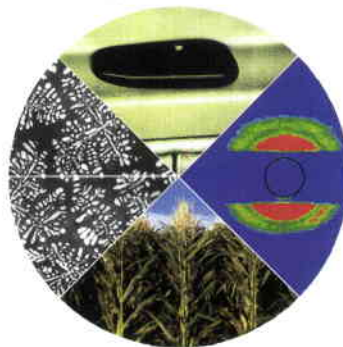
<http://www.estec.esa.int/CONFANNOUN/>

Co-Chairman

Prof. Francesco Gaeta
Microgravity Advanced Research
and Support Centre, Naples, Italy

ESA Coordinator

Dr. Olivier Minster
ESA/ESTEC
Noordwijk, The Netherlands



In Brief

3rd Space Station Element to be Launched

NASA and the Russian Aviation and Space Agency (Rosaviakosmos) plan that the next component of the International Space Station (ISS) – the Zvezda service module – will be launched on 12 July from the Baikonur Cosmodrome in Kazakhstan.

Following a Joint Programme Review and a General Designers' Review in Moscow, it was agreed that Zvezda (Russian for 'star') will be launched by a Proton rocket with the second and third stage engines modified to increase engine reliability.

Zvezda will provide the early living quarters for ISS crew, together with the life support, electrical power distribution, data management, flight control, and propulsion systems for the ISS.

ESA, together with a European industrial consortium headed by DaimlerChrysler (D) and including Belgian, Dutch and French partners, was responsible for the design, development and delivery of the core data management system, which provides Zvezda's main computer.

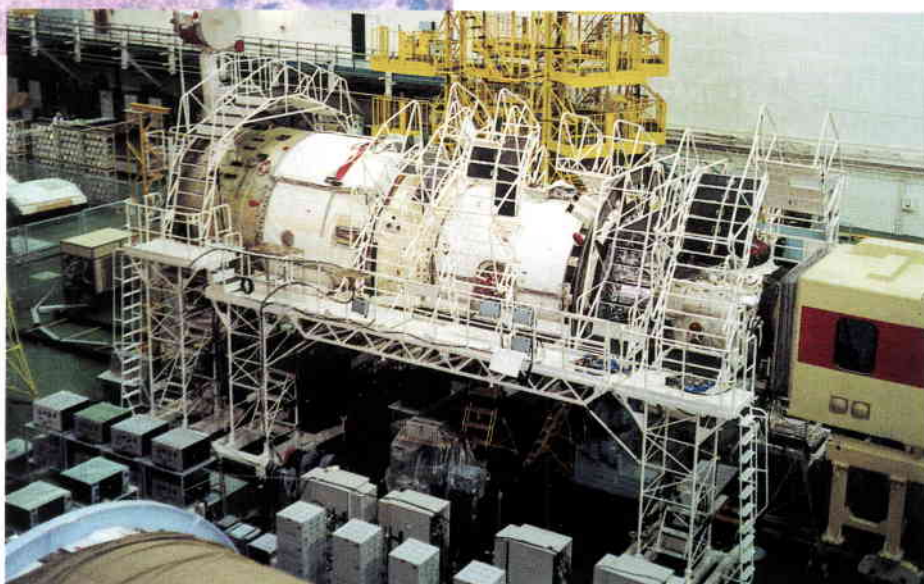
ESA also has a contract with Rosaviakosmos and RSC-Energia for performing system and interface integration tasks required for docking with Zvezda by ESA's Automated Transfer Vehicle (ATV), which will be used for ISS re-boost and logistics support missions from 2003 onwards. Through its ATV industrial consortium led by Aerospatiale Matra Lanceurs (F), ESA is also procuring some Russian hardware and software for use with the ATV.

On the scientific side, ESA has concluded contracts with Rosaviakosmos and RSC-Energia for the conduct of scientific experiments on Zvezda, including the Global Timing System (GTS) and a radiobiology experiment (called Matroshka) to monitor and analyse radiation doses in ISS crew. Cooperation on further scientific experiments to be conducted on the Russian segment of the ISS is continuing with Rosaviakosmos and Russia's IBMP (Institute for Biomedical Research). 



Zvezda (left-most module) is the third infrastructure element of the International Space Station (ESA/D. Ducros)

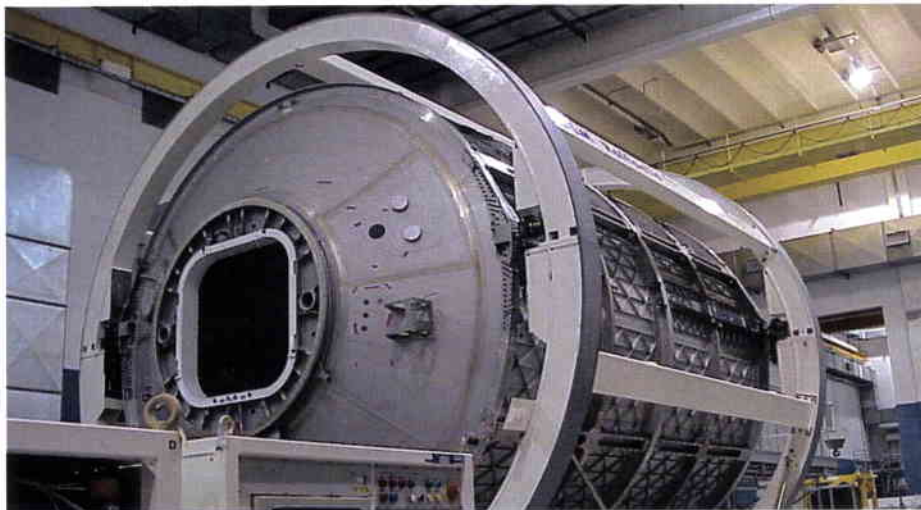
Zvezda integration at the Baikonur Cosmodrome



Synergies and Cooperation Save on European Contribution to the ISS

At a ceremony held on 14 April at Alenia Spazio in Turin, Italy, the Columbus flight structure was handed over to ESA by ASI (Italian Space Agency). On the same occasion, the Environmental Control and Life Support Subsystem (ECLSS) ownership transfer from ESA to ASI was formalised.

Columbus, the cornerstone of ESA's contribution to the International Space Station, is a scientific laboratory scheduled for launch in 2004. Astronauts from Europe and elsewhere will be able to use the laboratory to conduct material sciences, medicine, biology and technology experiments, many eventually leading to benefits in commercial processes or everyday life on Earth.



The ECLSS, composed of fans, heat exchangers, sensors and motorised and pneumatic valves, all operated and monitored via the onboard computer, provides comfortable working conditions inside the space laboratories. In particular, the system controls temperature, humidity and ventilation, regulates atmospheric pressure, detects fire and monitors contamination of the living environment.

Prior to the ESA Council meeting at ministerial level in Toulouse in November 1995, it had seemed that approval of European participation in the ISS would be impossible to obtain, owing to the excessive price of the proposed programme. In mid-1994, ESA had embarked on a serious 'design-to-cost' exercise to revive the

programme. The main thrust of this effort was to make Columbus a four-rack module, similar in length to the ASI Multi-Purpose Logistics Module (MPLM), in order to radically reduce the programme's design and operational costs.

In the second half of 1994, and into 1995, ESA and ASI reached an agreement whereby they would cooperate both generally on the development of pressurised modules and specifically on two particular cases. The essence of this agreement was that:

- ESA would design and verify an Environmental Control and Life Support Subsystem which would satisfy the requirements of both the MPLM and the Columbus laboratory, and would deliver to ASI engineering models, three sets of flight hardware, some spares and the ground support equipment for the MPLM. ESA would then use this equipment for its Columbus module.

- ASI, which was already developing the MPLM, would supply ESA with a flight unit primary structure for Columbus based on that of the MPLM, and would provide the MPLM qualification data to enable ESA to qualify Columbus on the basis of commonality, thereby avoiding the need for a separate qualification test model.

Thanks to this agreement, both Agencies would avoid duplicating high development costs and would help save roughly € 70 million of taxpayers' money. Further reductions arising from the downsizing of the Columbus laboratory enabled the Columbus part of the ESA ISS development programme to be literally halved in price, down to approximately

€ 700 million. On that basis, the ministers responsible for space gathered in Toulouse in November 1995 were able to approve the overall ISS programme.

Alenia Spazio, as the MPLM prime contractor, manufactured the structure and performed ECLSS integration for the Multi-Purpose Logistics Module under ASI contract; DASA-Dornier, as the ECLSS subcontractor for Columbus, was entrusted with ECLSS development and verification under a contract with ESA. The industrial activities were jointly controlled by ESA and ASI.

In addition to these specific joint developments, further synergies were found. Alenia Spazio became the prime contractor for ISS Nodes-2 and -3, a contract managed by ASI on behalf of ESA, the price of which is being used to offset the launch costs of the Columbus laboratory by NASA's Space Shuttle. European industry is thus developing hardware for the Station using ESA funds, rather than ESA paying NASA in dollars for the launch of Columbus.

Alenia Spazio is also the contractor for the pressurised Carrier part of the Automated Transfer Vehicle (ATV) which, launched atop Ariane-5, will be used as a 'ferry' vehicle for payload, propellant, fresh food and general provisions.

This agreement has also fostered an increasing use of common subcontractors (and hence common design principles) for the Columbus and Node harnesses and Mechanical Ground Support Equipment (OHB, Germany) and Thermal Control Subsystems (Microtecnica, Italy), further improving the cost-efficiency of European human spaceflight projects. These synergies will continue into the operational phase, in terms of integration, payload operation and logistics activities.

The final ECLSS equipment and the Columbus primary structure were delivered in March/April. Much of the ECLSS hardware is already at NASA/Kennedy Space Center awaiting the first launch of the MPLM Leonardo, currently planned for February 2001, but several tonnes of ECLSS and structure equipment can still be viewed in Turin, together with other elements of ASI and Alenia Spazio's contribution to the development of the International Space Station.

Physics on Stage

Physics is everywhere. The laws of physics govern the Universe, the Sun, the Earth and even our own lives. In today's rapidly developing society, we are becoming increasingly dependent on high technology – computers, transport and communication are just some of the key areas that are the result of discoveries by scientists working in physics.

But how much does the average person really know about physics? There is now a unique opportunity to learn more about this elusive subject! Three major European research establishments have organised a unique Europe-wide programme to raise public awareness of physics and related sciences.

'Physics on Stage' was launched in February by ESA, CERN (European Laboratory for Particle Physics) and ESO (European Southern Observatory) with support from the European Union. Other partners include the European Physical Society (EPS) and the European Association for Astronomy Education (EAAE). This exciting programme is part of the European Week for Science and Technology and will culminate in a Science Festival, on 6-11 November, at CERN (Geneva).

The primary goal of 'Physics on Stage' is to heighten interest in and knowledge of physics in Europe by means of a series of high-profile, physics-related activities. It will bring together leading scientists and educators, government bodies and the media, to confront the diminishing attraction and knowledge of physics in young people and to develop strategies to reverse this trend. The objective in the short term is to infuse excitement and to provide new educational materials. In the longer term, it will generate new developments by enabling experts throughout Europe to meet, exchange and innovate.

During the first phase of the programme (until October), the National Steering Committees (NSC) will survey their own country's* respective situation and collaborate with national media to identify new and exciting educational approaches to physics. These may involve demonstrations, interactive experiments, video and CD-Rom presentations, web applications, virtual reality, theatre performances, etc. Nationally-run

competitions will select some of the best and most convincing new ideas for presentations and educational materials which will receive development support from the programme.

The project will culminate in November 2000, with approximately 400 delegates converging at CERN for the 'Physics on Stage' conference. The conference will enable the national competition winners, science teachers, science communicators, publishers, top scientists and high-level representatives of the ministries and European organisations to brainstorm solutions to bolster the popularity of physics. The conference will also include spectacular demonstrations of educational tools, the best of which will be disseminated over national TV networks and other media to the European public.

Statements by the Directors General of ESA, CERN, and ESO

Antonio Rodotà (ESA): *"Space has become an integral part of every day life. The immense technological development that has led to this achievement has taken place and might be taken for granted. But now is the time to follow up and form the future on this basis, a future that has to be made by the youth and has to give its benefits to the youth. The European Space Agency is dedicated to support the youth in its development to become a space generation. Many activities have been done and are taking place, and many more are planned for the future. Teachers and educational institutions and organisations form a key role in this development. ESA is enthusiastic about cooperating with ESO, CERN and the European Union to create an opportunity to receive ideas from the educational society and will perform a dedicated effort in finding ways to support the realisation of those ideas."*

Luciano Maiani (CERN): *"Science is a critical resource for mankind and, among natural sciences, physics will continue to play a crucial role, well into the next century. The young people of Europe deserve the best possible physics teaching. An enormous resource of first class teachers, teaching materials and innovative thinking exists in our countries. The 'Physics on Stage' project will bring these together to generate a new interest in physics education which will be to the long-term benefit of children all over*

Europe. CERN is delighted to take part in this collaboration between the European Community and the continent's three leading physics research organisations."

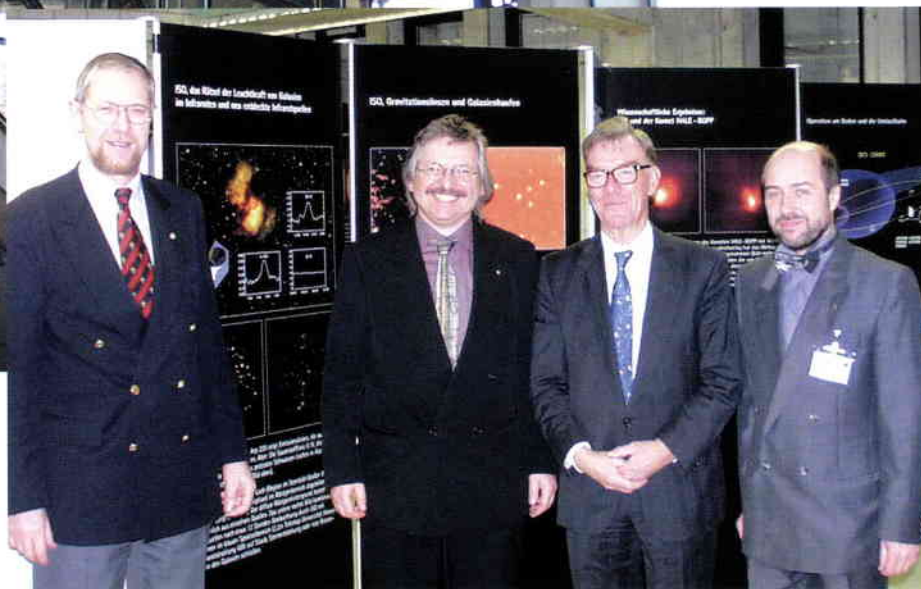
Catherine Cesarsky (ESO): *"Astronomy and astrophysics are at the very heart of modern physics. As vibrant research disciplines they use the most advanced technology available to humanity to explore the cosmos. It is also a science of extreme conditions – the largest distances, the longest periods of time, the highest temperatures, the strongest electrical and magnetic fields, the highest and lowest densities and the most extreme energies. The cosmos is indeed the greatest physics laboratory. For years, ESO - Europe's Astronomy Organisation - has been engaged in communicating the outcome of the exciting research programmes carried out at the ESO observatories to a wide audience and in particular to Europe's youth. I warmly welcome the broad international collaboration within 'Physics on Stage'. I am confident that working together with the European Union and our sister organisations ESA and CERN, as well as teachers' organisations and dedicated individuals in all member countries, this innovative education programme will make a most important contribution towards raising the interest in fundamental research in Europe."*

* 'Physics on Stage' is being initiated in 22 European countries which are members of at least one of the participating organisations or the EU: Austria, Belgium, Bulgaria, the Czech Republic, Denmark, Finland, France, Germany, Greece, Hungary, Ireland, Italy, Luxembourg, the Netherlands, Norway, Poland, Portugal, the Slovak Republic, Spain, Sweden, Switzerland, United Kingdom. More information can be found via the 'Physics on Stage' website: <http://www.estec.esa.nl/outreach/pos>.



The XMM-Newton model welcomes visitors in the exhibition entrance hall (photo courtesy E. Popow)

At the exhibition (left to right): Dr G. Hartmann (DLR, Bonn), Prof G. Hasinger (Director AIP), Prof R. Lüst (MPI for Meteorology) and Dr F. Jansen (author of ESA 2000). (photo courtesy E. Popow)



ESA 2000 Space Science Exhibition

The ESA 2000 Space Science Exhibition (13 March - 25 May) was opened by Prof. R. Lüst (ESA's Director General from 1984 to 1990) during the inauguration of the new Schwarzschild-building of the Astrophysical Institute Potsdam in Germany. A scientific talk was also given by Prof. R. Giacconi (Associated Universities Inc., Washington).

The exhibition consisted of 8 scale models and more than 70 information panels which informed the public about ESA in general and its science missions in particular. In addition, guided tours, videos, and the ESA brochures 'ESA 2000

The scientific programme of the European Space Agency' and 'Success Story: 30 discoveries from ESA's science missions in space' provided further insight. 



ERS-1: Nine-year Success Story Comes to an End

Having given excellent service for nine years,

over three times its planned lifetime, the ERS-1 mission was ended on Friday 10 March by a failure in the onboard attitude control system. Since its launch on 17 July 1991, ESA's first sun-synchronous polar-orbiting mission, has made 45 000 orbits, acquiring more than 1.5 million individual Synthetic Aperture Radar (SAR) scenes. ERS-1 SAR images,

together with the data from other instruments on board, were delivered to a worldwide community of some 4000 users in science and applications. Surface winds derived from the scatterometer and altimeter have been supplied to meteorological services worldwide since 1991. The duration of the mission has also meant that scientists have already observed several El Niño phenomena through combined observations of surface currents, topography, temperatures and winds. The measurements of sea surface temperatures, critical to the understanding of climate change, made by the ERS-1 Along-Track Scanning Radiometer, are the most accurate ever from space. All these critical measurements are being continued and enhanced by the current ERS-2 mission.

The most exciting results from the ERS-1 mission have been in the field of SAR interferometry, where for the first time precise topographic information could be routinely produced from space data. The ERS-1 and ERS-2 tandem operations demonstrated this technique for various applications and paved the way for the definition of new dedicated SAR interferometry missions. ERS-2 (launched in 1995) took over the operational services of ERS-1 in 1996. It too has now exceeded its nominal lifetime and remains in excellent condition. Next year Envisat will be launched to continue this series of Earth Observation missions. 

Long-Term Ozone Measurements from Space Assured

The continued monitoring of ozone is assured well towards the end of the next decade through a € 38.3 million contract signed on 3 March in Florence, Italy for three new Global Ozone Monitoring Experiment (GOME-2) instruments.

GOME-2 is an enhancement of the ESA GOME-1 instrument flown on ERS-2, the Earth Observation satellite which continues to provide a wealth of scientific data from orbit. Within the EUMETSAT Polar System, consisting of a space segment comprised of three METOP satellites and their payloads, and a ground segment for command, control and data processing, GOME-2 is the operational instrument specifically devoted to measuring the ozone content in the atmosphere. GOME-2 measurements will allow the daily global retrieval of total ozone and vertical ozone profile in the atmosphere and, in addition, the measurement of atmospheric trace gases.

The EUMETSAT Polar System and the ESA METOP-1 Programme together form a cooperative venture between the two organisations, and lead to the launch of the first METOP satellite in mid-2003. The system provides operational meteorological data from polar-orbiting satellites,



The contract on the procurement of three flight models of the GOME-2 instrument was signed by (left to right) Dr. Giancarlo Grasso, Deputy Head, Defence Sector of Finmeccanica for Alenia Difesa/Officine Galileo BU Spazio, Dr. Claudio Mastracci, ESA Director of Applications Programmes, and Dr. Tillmann Mohr, EUMETSAT Director

to complement and complete an international system of polar satellites operated together with the US.

The variations of atmospheric ozone are of vital importance for many reasons, and its distribution in the atmosphere needs to be mapped continuously. The enhanced GOME-2 instrument on METOP will continue the series of ESA measurements started by GOME-1 on ERS-2 and to be provided by the SCIAMACHY instrument on ESA's environmental satellite Envisat due to be launched in 2001.

In addition, to innovative data for Numerical Weather Prediction, one of the most important contributions of GOME-2 will be the continuation and improvement of the climate record of ozone. Monthly and seasonal maps of ozone distribution throughout the atmosphere will provide a record of its variation with time and will help detect long-term trends of major importance for the health of the planet and its population.



ISU Summer Session

The International Space University is a non-profit organisation, founded in 1987, with the aim of educating professionals in the field of space and its peaceful applications. Its programs are designed to meet the needs of a rapidly expanding sector where international and cross-disciplinary understanding and cooperation are fundamental to the success of future development. Specialised educational opportunities and training are offered by international experts in all space-related disciplines from a global perspective. Programmes include: Master of Space Studies, Professional Development Programs, tailor-made Forum Activities and the ISU Summer Session.

ISU Summer Session Program (SSP)

This intensive summer program covers the

principal space-related fields, both technical and non-technical. These include space and society, space business and management, space policy and law, space system architecture and mission design, space engineering, space resources, robotics and manufacturing, satellite applications, space physical sciences, space life sciences and an informatics lecture series.

The interdisciplinary curriculum with its emphasis on international cooperation gives students broad new perspectives on the world's space activities, perspectives otherwise reserved for those with years of professional experience.

The SSP has proved to be an excellent forum where students and faculty alike can network with leaders in space research and development from around

the globe. The interactive, international environment provides participants with numerous opportunities to forge new professional relationships. SSP alumni, numbering over 1200 to date, faculty members, visiting lecturers and members of the host community have all contributed to creating a professional network facilitating access to information and exchanges.

Summer Session 2000

This year's summer session will take place from 1 July - 2 September and is hosted by the Universidad Tecnica Federico Santa Maria in Valparaiso, Chile.

For more information visit the ISU SSP site at:

<<http://www.isunet.edu/Programs/SSP/SSP.html>>.



SOHO Top Comet Finder

Calculations confirm that a comet spotted by a Lithuanian astronomer on 4 February is a previously unknown object, making it the 100th comet discovered with the SOHO spacecraft.

Launched four years ago as a project of international cooperation between ESA and NASA, the Solar and Heliospheric Observatory has revolutionised the science of the Sun.

Although this latest comet, SOHO-100, is an 'ordinary' comet, SOHO has also revealed an amazing number of kamikaze comets plunging into the solar atmosphere, which help to make SOHO the most prolific comet finder in the history of astronomy.

Like nearly all of SOHO's discoveries, the 100th comet showed up in images from the LASCO instrument. This is a set of coronagraphs that view the space around the Sun out to 20 million kilometres, while blotting out the bright solar disk with masks. Developed for SOHO by a multinational team led by the US Naval Research Laboratory, LASCO watches for mass ejections from the Sun that threaten to disturb the Earth's space environment. The comet discoveries are a big bonus.

SOHO's experts spot many of the comets as soon as the images come in. But still pictures and movies from LASCO are freely available on the Internet to astronomers around the world, who can discover less obvious comets without leaving their desks. This was the case when Kazimieras Cernis of the Institute of Theoretical Physics and Astronomy in Vilnius, Lithuania, found SOHO-100.

"On 4 February I saw the comet as a small speck of light in the previous day's LASCO images," Cernis explained. "It had no visible tail, but it was too fuzzy to be an asteroid. By the time I had seen the object moving steadily across the sky in six successive images, I was convinced it was a comet and I sent the details to the SOHO scientists for verification."

The competition to find SOHO's 100th comet was keen. An amateur astronomer, Maik Meyer of Frauenstein, Germany, discovered SOHO-98 and -99. On 5 February, less than 24 hours after Cernis reported the candidate SOHO-100, Meyer

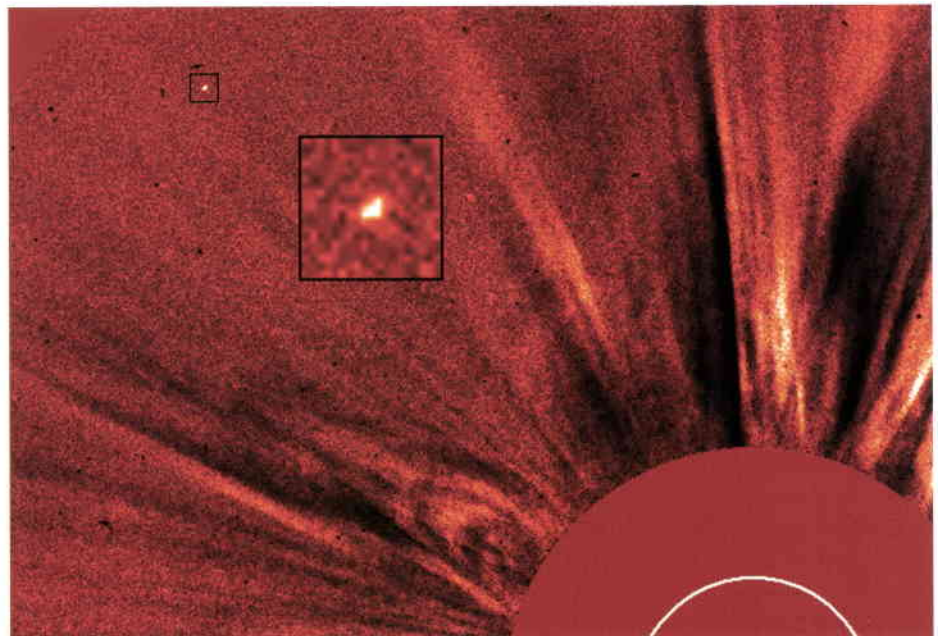
found the candidate SOHO-101. On the same day and in the same LASCO images, Douglas Biesecker, a member of the SOHO science team, spotted the candidate SOHO-102 travelling ahead of 101. Computations have now validated the orbits for all three candidates, and shown them to be bona fide comet discoveries.

Other amateur astronomers have used the LASCO images to find comets. In the summer of 1999, Terry Lovejoy in Australia found five and, since September 1999, an amateur in England, Jonathan Shanklin, has spotted three more.

Snowballs in hell

Of the first 100 SOHO comets, 92 vaporised in the solar atmosphere. Isaac Newton suggested 300 years ago that infalling comets might supply the Sun with fuel, but no one has ever tracked a comet that definitely hit the bright surface. Near misses are well known, and 100 years ago Heinrich Kreutz in Kiel, Germany, realised that several comets seen buzzing the Sun seemed to have a common origin, because they came from the same direction among the stars.

These comets are now called the Kreutz sungrazers, and the 92 vanishing SOHO



In this coronagraph image, the shaded red disk is a mask in the LASCO instrument that bolts out direct sunlight. The white circle added within the disk shows the size and position of the visible Sun. The square black outline (upper left) shows the position of SOHO-100 and the larger black outline is a zoomed-in view

"SOHO is a special chance for comet hunters," said Shanklin, Director of the British Astronomical Association's comet section. "It allows amateurs to discover some of the smallest comets ever seen. Yet they link us to sightings of great comets going back more than 2000 years."

Nine of the comets found with LASCO, including SOHO-100, 101 and 102, passed the Sun at a safe distance. SOHO-49, which showed up in LASCO images in May 1998 and was designated as Comet 1998 J1, became visible to the naked eye in the Southern Hemisphere. But the great majority of SOHO's comets failed to survive very close encounters with the Sun.

comets belong to that class. They were not unexpected. Between 1979 and 1989 the P78-1 and SMM solar satellites spotted 16 comets closing with the Sun.

Life is perilous for a sungrazer. The mixture of ice and dust that makes up a comet's nucleus is heated like the proverbial snowball in hell, and can survive its visit to the Sun only if it is quite large. What's more, the very strong tidal effect of the Sun's gravity can tear the loosely glued nucleus apart. The disruption that created the many SOHO sungrazers was similar to the fate of Comet Shoemaker-Levy 9, which went too close to Jupiter and broke up into many pieces that eventually fell into the massive planet in 1994.

"SOHO is seeing fragments from the gradual breakup of a great comet, perhaps the one that the Greek astronomer Ephorus saw in 372 BC," commented Brian Marsden of the Center for Astrophysics in Cambridge, Massachusetts. "Ephorus reported that the comet split in two. This fits with my calculation that two comets on similar orbits revisited the Sun around AD 1100. They split again and again, producing the sungrazer family, all still coming from the same direction."

The sungrazing comets slant in from the south, at 35° to the plane where the Earth and the other planets orbit. As SOHO moves around the Sun, in step with the Earth, it sees the comets approaching the Sun from the east (left) in February and from the west (right) in August. In June and November the sungrazers seem to head straight up towards the Sun.

"The rate at which we've discovered comets with LASCO is beyond anything we ever expected," said Douglas Biesecker, the SOHO scientist personally responsible for the greatest number of discoveries, 45. "We've increased the number of known sungrazing comets by a factor of four. This implies that there could be as many as 20 000 fragments."

Their ancestor must have been enormous by cometary standards. Although SOHO's sungrazers are all too small to survive, other members of the family are still large enough to reappear, depleted but intact, after their close encounters with the Sun. Among them were the Great September Comet (1882) and Comet Ikeya-Seki (1965).

The history of splitting gives clues to the strength of comets, which will be of practical importance if ever a comet seems likely to hit the Earth. And the fragments seen as SOHO comets reveal the internal composition of comets, freshly exposed, in contrast to the much-altered surfaces of objects like Halley's Comet that have visited the Sun many times. LASCO reveals how much visible dust each comet releases. Gas produced by evaporating ice is detected by another instrument on SOHO, the Ultraviolet Coronagraph Spectrometer or UVCS, and enables scientists to measure the speed of the solar wind as it emerges from the Sun.

A comet spotted by its gas cloud

The count of SOHO's comet discoveries would be one fewer without a recent bonus from SWAN. This instrument's name unpacks into Solar Wind Anisotropies, and it was provided by the French Service d'Aéronomie and the Finnish Meteorological Institute. SWAN looks away from the Sun to survey atomic hydrogen in the Solar System, which glows with ultraviolet light and is altered by the solar wind. The instrument also sees large clouds of hydrogen surrounding comets, produced by the breakup of water molecules evaporating from the comets' ice.

In December 1999, the International Astronomical Union retrospectively credited SWAN and SOHO with finding Comet 1997 K2 in SWAN full-sky images from May to July 1997. It made number 93 on the SOHO scorecard. This comet remained outside the orbit of the Earth even at its closest approach to the Sun. Although it was presumably a small, faint comet, the gas cloud grew to a width of more than 4 million kilometres.

"The discovery was a surprise," said Teemu Mäkinen, a Finnish member of the SWAN group. "Our normal procedure is to observe hydrogen clouds of comets detected by other people. In that respect, SWAN on SOHO is the most important instrument now available for routinely measuring the release of water vapour from comets."

When Comet Wirtanen, the target for ESA's Rosetta mission (2003), made its most recent periodic visit to the Sun, it pumped out water vapour at a rate of 20 000 tons a day, according to the SWAN data. For the great Comet Hale-Bopp the rate reached 20 million tons a day and SWAN watched its hydrogen cloud grow to 70 million kilometres – by far the largest object ever seen in the Solar System.

For further information on SOHO, pictures and movies visit the ESA science web pages at

<<http://sci.esa.int/soho>> and
<<http://sohowww.estec.esa.nl>>.



Farewell to a Legendary Mission

ESA hands the IUE archive over to the global scientific community

The IUE (ESA/NASA/UK) spacecraft launched in January 1978 became the first space observatory facility available to the entire astronomical community. It marked the beginning of UV astronomy, a field for which space telescopes are essential since UV light does not reach the Earth's surface. By the time IUE was switched off, in September 1996 – 14 years later than originally planned – IUE had changed the view astronomers had of the Universe. Among many other findings, IUE discovered the auroras in Jupiter; detected for the first time the halo in our galaxy and measured the size of a black hole in the core of an active galaxy.

The IUE archive, storing two decades of ultraviolet astronomy, has become a historical reference. It contains more than 110 000 spectra from observations that in most cases cannot be repeated, and is an excellent source for studying variable phenomena. The long time-lapse covered and the stability of the instrument have enabled astronomers to witness events they never thought they would. The archive was the first of its kind accessible online – already in 1985, when the World Wide Web did not yet exist – and has been a key catalyst for science. To date, it has triggered the publication of some 3600 articles in refereed journals and a whole generation of astrophysicists has used IUE data at some stage.

Now, the IUE archive will belong to the global scientific community. ESA has just released the new IUE archive, INES (IUE Newly Extracted Spectra) as the first astronomical database distributed to national data centres all over the world for faster and easier access. "This is the best farewell from ESA to a historic mission. Thanks to the new distributed system the IUE archive will become both a mine of discoveries and a powerful educational aid for future astronomers. It is a legacy worthy of the IUE project", says Willem Wamsteker, ESA astronomer and ESA IUE Project Scientist.

"The INES system and its data guarantee that future generations of astronomers will be able to use IUE data as much as they want, regardless of whether they know

about the technicalities of the mission or whether there is an improvement in archive technology. And the distributed structure is better adapted to changes in user needs than a single archive centre", says Antonio Talavera from the Laboratory for Space Astrophysics and Theoretical Physics (LAEFF), based at Villafranca. "ESA has created INES using a minimalist engineering approach for the world scientific community, and has made it to last. INES is easy to use and easy to upgrade, and LAEFF in Spain is proud to serve as the hub for the whole world".

The INES Principal Centre is at the LAEFF, owned by INTA, the Spanish National Institute for Aerospace Technology. This centre, with a data mirror at the CADC in Victoria (Canada), holds the complete database and provides information not available from national hosts. So far 17 national hosts have come online. Together they form with the Principal Centre an efficient and highly reliable distribution system for the community. The whole process of data retrieval is fully automated and totally transparent to the end user. This distributed structure avoids localised connectivity problems and guarantees availability of data.



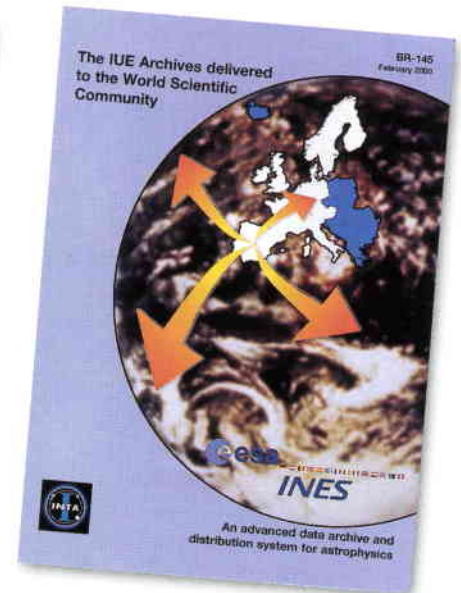
Envisat, the Largest Environmental Satellite Takes Shape at ESA's Test Centre

ESA's Envisat satellite is currently undergoing integration and tests at the European Space research and Technology Centre (ESTEC) in the Netherlands.

Last August, the Envisat Payload and Service Modules were submitted to thermal and space environment tests in ESTEC's Large Space Simulator (LSS).

While the flight model instruments were progressively integrated on board the Payload Module, the Service Module verification was proceeding in parallel, including the recent demonstration of compatibility to the Ariane-5 in-flight shocks and separation tests.

Mating of these two modules of Europe's largest-ever environmental satellite took place at ESTEC's test facilities in mid-April. Envisat stands over 10 metres tall and the two elements combined weigh over 8



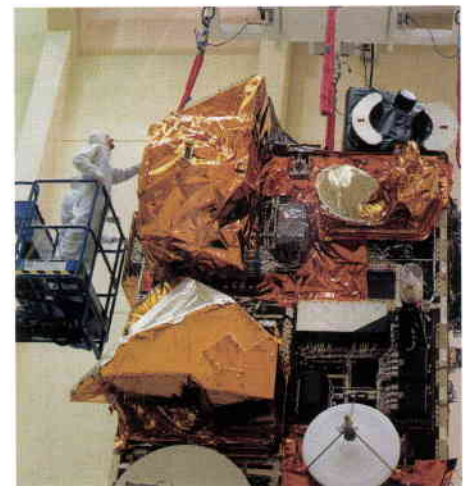
The INES Newsletter and Brochure are available from ESA Publications <<http://esapub.esa.int>>

tons. Even the engineers who have worked on it for years are still impressed by the size of the satellite.

Designed for at least 5 years of in orbit operation, Envisat with its ten highly advanced instruments on board will help European scientists advance our understanding of global warming, climate change, ozone depletion, and changes in the oceans, ice sheets, vegetation and atmospheric composition. Thanks in particular to its advanced imaging radar, Envisat will produce – all weather day and night – high-quality images of the oceans, coastal zones, polar ice and land regions.

The solar array will be integrated early summer. After a solar array deployment test, Envisat will be submitted to acoustic tests in the Large European Acoustic Facility (LEAF). The HYDRA hydraulic shaker will then be used to check the satellite's ability to cope with the vibrations it will experience during the launch phase. With its eight actuators delivering a force of 60 000 newtons each, the HYDRA is one of the largest test facilities of its kind.

With the Envisat flight model test programme, ESTEC demonstrates its capabilities as one of the most complete test centres in the world. Over 100 highly skilled specialists from ESA and European companies, led by the prime contractors Matra-Marconi Space (UK) for the satellite platform and DaimlerChrysler-Dornier Satellitensysteme (D) for the payload, are currently involved in the testing of Envisat. In March next year the spacecraft will



finally be prepared for shipment to Kourou.

Scheduled for launch on an Ariane-5 in June 2001, Envisat will fly on a Sun-synchronous orbit at about 800 km altitude with an orbit repeat cycle of 35 days, identical to the ERS-2 ground track. ESA's European Space Operations Centre (ESOC) in Darmstadt, Germany, will handle the command and control of Envisat. The Agency's Earth Observation application team, located at ESRIN, Frascati, Italy, will coordinate the payload data exploitation from instrument data recovery to delivery of products to the scientific and application user communities.

Once in orbit, Envisat will provide remote sensing data of unprecedented quality, helping Europe to meet the environmental challenges of the 21st Century.



ESA's First Biomedical Application Research Contract for the ISS

ESA and researchers from academia and industry signed the contract on 3 May for a health research project that will develop a space bioreactor for research aboard the International Space Station into biomedical applications. At the ceremony, held in the Erasmus User Centre at ESTEC, Mr Jörg Feustel-Büechl, ESA's Director of Manned Spaceflight and Microgravity, pointed out that *"This is the first in a series of almost 50 contracts for application-oriented research projects that involve the International Space Station."*

A bioreactor is used for growing bacteria, yeast or animal cells and, more recently, for tissue. The new bioreactor will be designed specifically for cultivating medically-relevant mammalian cells, tissues and organ-like structures, with particular emphasis on vessels and cartilage.

Millions of people every year suffer organ and tissue loss from diseases and accidents. Transplanting tissues and organs from other human bodies is severely limited by the availability of donors. Taking tissue samples from healthy areas of the patient's own body, growing them *in vitro*, outside the patient's body, to a size and structure which then allow their reimplantation into the damaged parts is a promising alternative. Reimplantation also avoids the fundamental problem of rejection of foreign tissues and organs. Growing tissue samples *in vitro* – in a bioreactor – is currently one of the major goals of medical research. It is expected that such techniques will revolutionise biomedical and surgical procedures in the near future. Space research may be instrumental for the breakthrough in tissue engineering – the microgravity environment may provide much better conditions for obtaining proper 3D cell structures.

A potential application is the mass cultivation on Earth of biological implants to regenerate the meniscus and articular cartilage of the knee, using techniques resulting from the space experiments. Cartilage regeneration is urgently needed for 20 to 50 year-old patients, many of them suffering from sports accidents. The demand for such implants in Europe alone is estimated to be 100 000 per year.



Mr Jörg Feustel-Büechl (left) and Prof Augusto Cogoli sign the contract for the first in a series of almost 50 new projects in ESA's Microgravity Applications Promotion Programme

The modular space bioreactor for medically-relevant organ-like structures was proposed by a European scientific and industrial research team under the coordination of Prof. Augusto Cogoli from the Swiss Federal Polytechnical University (ETH) Zurich. It will be essential in clarifying the cellular and molecular mechanisms responsible for cell aggregation and differentiation control mechanisms, and in obtaining better pseudo-organs for possible clinical uses.

Prof. Cogoli's team comprises participants from Switzerland, Italy and Germany: Dr. Isabelle Walther from ETH, Dr. Werner Müller from the Sulzer Medica company in Winterthur (CH), Prof. Saverio Ambesi-Impombato from the University of Udine (I), Dr. Augustinus Bader from the Medical University of Hannover (D), Prof. Peter Bruckner from the University of Münster (D) and Dr. Ralf Pörtner from the Technical University of Hamburg-Harburg (D).

The modular space bioreactor project is one of more than 50 microgravity application projects for the Space Station that ESA expects to initiate in the near future. They will use the Station to obtain application-oriented data that provide deeper insights into Earth-based industrial processes or be used in numerical simulations. The availability of the Space Station means that examining specific applied-research questions in that unique environment may be, in the long term, rewarding for industry.

The modular space bioreactor project is sponsored by ESA's Microgravity Applications Promotion Programme and is funded jointly with the participating

scientific research institutes and industry. A major aspect of this MAP Programme is the setting up of Europe-wide teams and networks involving partners from academia and industry to work together on industrially-relevant research. The aim is to initiate concrete industrial projects in which terrestrial research with industrial objectives and commercial funding, together with the participation of researchers from scientific institutes, are supported by ESA, including the sponsoring of space flight opportunities and associated ground-based activities.

Prof. Cogoli and his scientific-industrial team proposed the space bioreactor project in response to ESA's first Announcement of Opportunity (AO) for Physical Sciences and Biotechnology. This 1998 AO for Space Station research proposals produced 145 responses, substantially exceeding expectations. After a review by independent peers, 6 proposals were rated as 'outstanding', 26 as 'highly recommended' and 30 as 'recommended'. Of these, 31 dealt with application-oriented research, including thermophysical properties of liquid metals, advanced foams, biological tissue culturing, osteoporosis and combustion processes.

The peer review panel summarised its evaluation of the proposal made by Prof. Cogoli and his team as *"The proposal for producing cartilage ... is an outstanding and innovative approach. ... this may be the only way for in vitro production of a functional cartilage analogue. This approach cannot be done except under microgravity conditions."*

Historic WA Town to Host Deep Space Ground Station

The start of construction of a Deep Space Ground Station, just outside the historic monastic town of New Norcia, Western Australia, has been marked with a Foundation Stone Laying Ceremony by ESA on Thursday, 2 March 2000.

Mr David Dale, ESA Director of Technical and Operational Support, and the Western Australian Minister for Planning, Graham Kierath, officially buried a time capsule and laid the first foundation stone.

Part of ESA's global network, the Ground Station features a 35-metre high antenna which will be built 8 km south of New Norcia.

The \$40 million antenna will transfer data to and from ESA's deep space missions. The first large mission, the Rosetta satellite, will leave in 2003 on a 10-year mission to study the Wirtanen Comet. Rosetta will send a Lander to the surface of the comet to analyse its structure and composition.

The antenna will also communicate with ESA's first mission to Mars, The Mars Express will also be launched in 2003 as part of an international flotilla of spacecraft sent to study the planet.

Construction of the antenna tower commenced in April. Components for the antenna will be shipped from Europe and assembled on site. The expected completion date is Spring 2001.

Mr Dale said New Norcia was chosen over a number of sites in the Southern Hemisphere. *"This site has excellent weather conditions, sits on the perfect latitude for the launch operations and is sufficiently distant from urban areas so that no other transmission devices disturb the satellite's operations."* *"Western Australia also has high quality telecommunications infrastructure and we are working closely with Telstra because of its experience in the maintenance and operation of tracking stations."*

Bovis Lend Lease will oversee the construction under the leadership of the Canadian company, SED, which will head the International Antenna Consortium



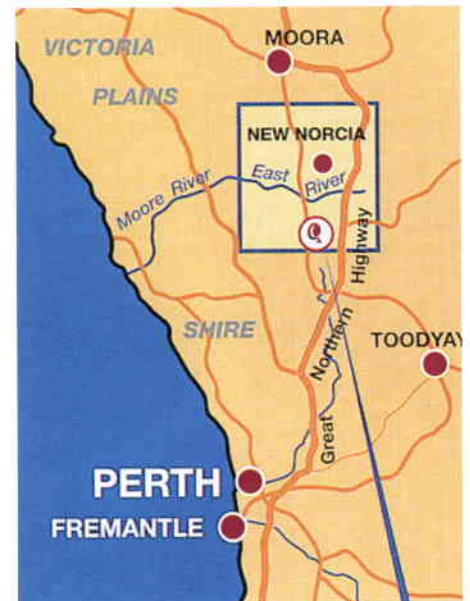
Site of the new Deep Space Ground Station outside New Norcia, Western Australia

formed to manage the project. Telstra has been contracted to maintain the Ground Station on ESA's behalf.

Further information is available from ESOC Public Relations (Robert-Bosch-Str. 5, 64293 Darmstadt, Germany).



Mr David Dale (right), ESA Director of Technical and Operational Support, and Mr Graham Kierath, Western Australian Minister for Planning, during the stone laying ceremony



ESA Astronaut Brings Back New Views of Earth

German astronaut Gerhard Thiele landed back on Earth on 22 February with his five international colleagues after a ground-breaking Space Shuttle mission that will change the way we look at the Earth.

The Space Shuttle Endeavour glided to an early evening landing at the Kennedy Space Center, touching down on the runway after a mission of over 11 days.

Elated scientists from all over the world gave the international SRTM team a standing ovation and heralded the mission as a huge success.

ESA astronaut Gerhard Thiele, completing his first space flight, described the mission as a 'fantastic experience'. *"We have mapped regions that are home to 95% of the world's population and this data will*

be used to produce unrivalled three-dimensional images of the world," he said.

Orbiting at 233 km above the Earth, with two radar antennas mounted in the Shuttle payload bay and two extended on a 60-metre mast, the imaging system has measured the undulations of landscapes that have been sculpted through the millennia.

NASA extended mapping operations for nine hours, allowing Endeavour's astronauts to continue collecting data until a day before returning to Earth and, therefore, achieving almost 100 percent of the planned coverage. The mission's target mapping area included about 123 million square kilometres and more than 65% of this – nearly 80 million square kilometres – was mapped with two or more passes.

The Shuttle Radar Topography Mission (SRTM), consisting of a specially modified

radar system, was designed to demonstrate the technology for obtaining high-resolution digital topographic maps of the Earth. The radar has imaged mountains and deep valleys carved by glaciers and rivers – like those in the Andes, the Rocky Mountains and the Himalayas of Asia – vast expanses of deserts and coastal plains around the world, as well as cold regions and forests of the northern latitudes.

In the future, any project that requires accurate knowledge of the shape and height of the land – such as flood control, soil conservation, reforestation or volcano monitoring – will benefit.

After a series of delayed launch attempts, the mission got off to a perfect start on 11 February with Thiele reporting successful deployment of the 60 metre radar mast – the longest structure to be flown in space from the Shuttle – and activation of the complex radar instruments going more smoothly than expected. *"We'd expected that there would be more teething problems but the intensive training and preparations paid off,"* he said.

STRM is a joint project between NASA, the United States National Imagery and Mapping Agency (NIMA), the German Aerospace Centre (DLR) and the Italian Space Agency (ASI). NASA's Jet Propulsion Laboratory (JPL) developed the C-band Spaceborne Imaging Radar and DLR developed the X-band Synthetic Aperture radar (X-SAR). Dornier Satellitensysteme GmbH, a corporate unit of Daimler-Chrysler Aerospace (Dasa), is the prime contractor for the X-SAR system.

Although the first images have already been released, the gathering of the radar data from orbit marks only the end of the first phase. Scientists will spend another 18 months processing the huge volume of SRTM data.

For further information, see the following web pages:

ESA:

<<http://www.estec.esa.int/spaceflight/operations/sts99.htm>>

DLR:

<<http://www.dlr.de/srtm>>

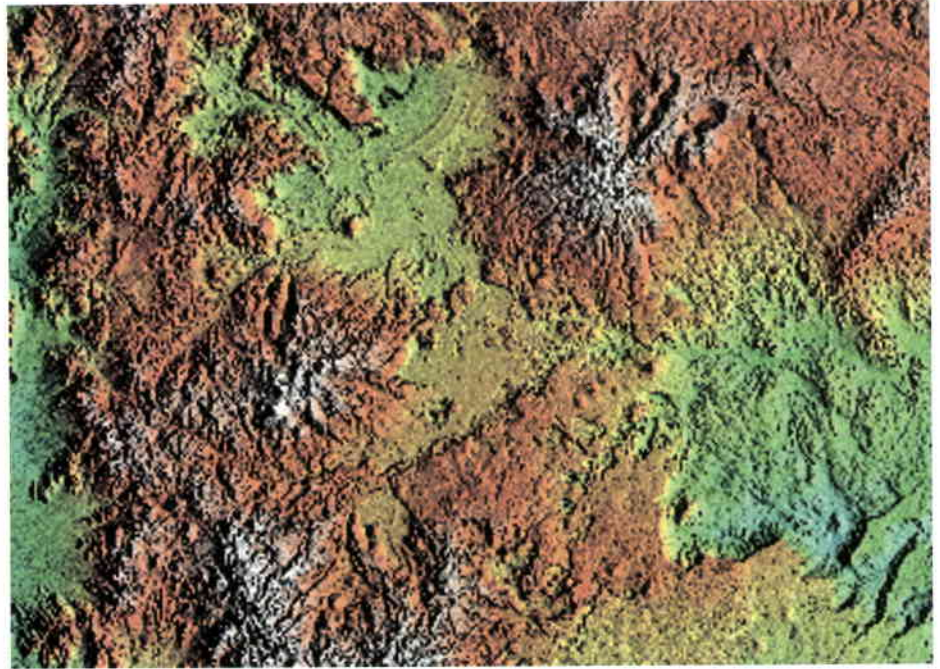
NASA:

<<http://spaceflight.nasa.gov/shuttle>>



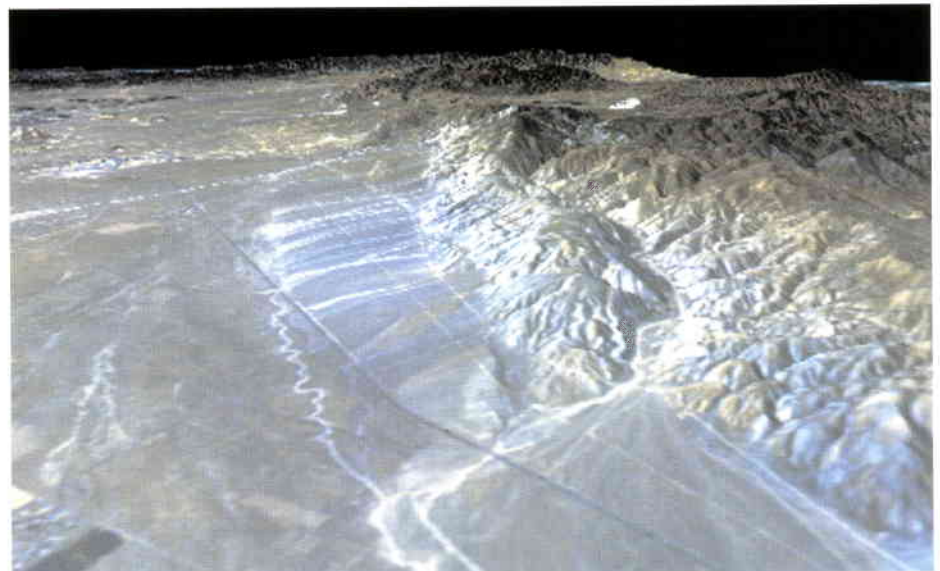
The STS-99 crew poses at the entrance to the orbiter Endeavour. From left are Mission Specialists Janet Lynn Kavandi (NASA), Gerhard Thiele (ESA), Janice Voss (NASA) and Mamoru Mohri (NASDA), Commander Kevin Kregel (standing) and Pilot Dominic Gorie (kneeling)

This topographic image of Patagonia, Argentina, shows a spectacular landscape formed by volcanoes, rivers, and wind. The area is located just east of the narrow range of the Andes Mountains, about 100 km east of the border with Chile. Interesting features include basalt-capped mesas with sink holes (lower centre), arcuate ridges of windblown beach sands downwind from a salty desert lake (upper centre), young volcanic cones (right). A computer-generated artificial light source illuminates the elevation data to produce a pattern of light and shadows. Colours show the elevation as measured by SRTM, ranging from blue at the lowest, to white at the highest elevations. White speckles on the face of some of the mountains are holes in the data caused by steep terrain and will be filled using coverage from an intersecting pass. Geologists will use SRTM topographic data to study the interaction of volcanic, climatic and erosion processes



Honolulu, on the island of Oahu, is a large and growing urban area with limited space and water resources. This perspective view, combining a Landsat image with STRM topography, shows how the topography controls the urban growth pattern, causes cloud formation, and directs the rainfall runoff pattern. Features of interest in this scene include downtown Honolulu (right), Honolulu harbour (right), Pearl Harbor (centre), and offshore reef patterns (foreground). The Koolau mountain range runs through the centre of the image. Clouds commonly hang above ridges and peaks of the Hawaiian Islands, and in this rendition appear draped directly on the mountains. The clouds are actually about 1000 metres above sea level. This type of display adds the important dimension of elevation to the study of land use and environmental processes as observed in satellite images, allowing ecologists and planners to assess the effects of urban development on the sensitive ecosystems in tropical regions

California's Garlock Fault, marking the northwestern boundary of the Mojave Desert, lies at the foot of the mountains, running from the lower right to the top centre of this image. These mountains are the southern end of the Sierra Nevada and the prominent canyon emerging at the lower right is Lone Tree Canyon. In the distance, the San Gabriel Mountains cut across from the left side of the image. At their base lies the San Andreas Fault, which meets the Garlock Fault near the left edge at Tejon Pass. The dark linear feature running from lower right to upper left is State Highway 14 leading from the town of Mojave in the distance to Inyokern and the Owens Valley in the north. The lighter parallel lines are dirt roads related to power lines and the Los Angeles Aqueduct which run along the base of the mountains. The data will be used by geologists studying fault dynamics and landforms resulting from active tectonics



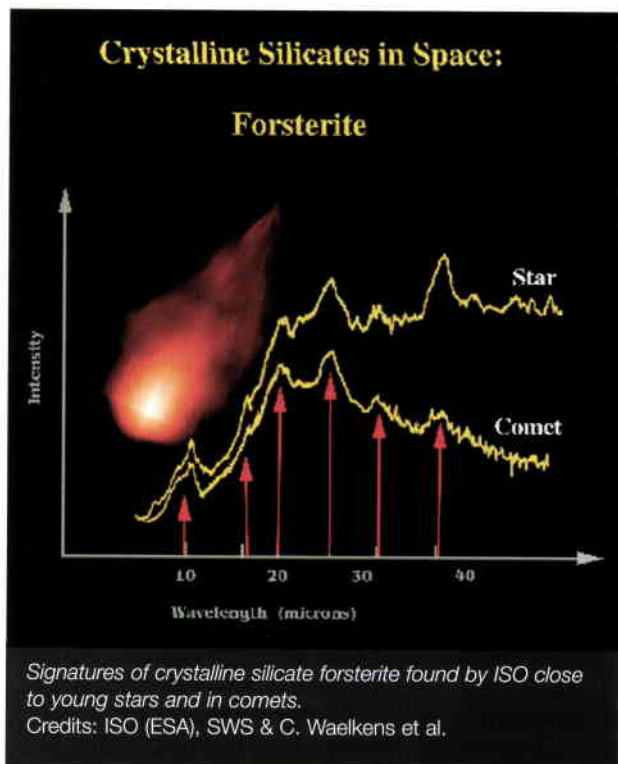
'Beyond the Peaks'

On 2-4 February 2000, the 'ISO beyond the Peaks' workshop was held in Villafranca del Castillo, Madrid, Spain. This workshop was the second in a series initiated with the successful 'First ISO Workshop on Analytical Spectroscopy', held in October 1997, in which 100 astronomers gathered in Villafranca to discuss ESA's Infrared Space Telescope ISO observations and associated scientific interpretation, 2 years into the ongoing mission. This second workshop took place with all ISO data having entered the public domain. 140 astronomers, more than expected, attended the workshop, discussing in 38 talks and 50 posters, aspects of the detailed ISO spectroscopic heritage including, among other topics, the cosmic cycle of water and the derivation of an inventory of cosmic ices. Many results lead to the development of more sophisticated models, such as dynamical models for AGB stars, or upper layers of warm molecular gas in the atmospheres of Mira stars. Representatives of upcoming IR missions such as SIRTf, SOFIA and ASTRO-F were also present.

The Crystalline Revolution ISO's Finding Opens a New Research Field, 'Astro-Mineralogy'

Silicate crystals, the most abundant minerals on Earth, are also found in great quantities around old stars and in protoplanetary discs – the discs where planets form. This finding, presented at a press conference on the last day of the 'Beyond the Peaks' workshop, is considered by experts in space chemistry as one of the main results of ESA's infrared space telescope, ISO. Silicate minerals were known to be a main component of dust in space, but detecting them in a crystallised state has been a surprise. It allows the identification of precise silicates in astronomical objects, which will open a totally new field in astronomy: 'astro-mineralogy'. "This is the crystalline revolution", said the author, Dutch astronomer Rens Waters of Amsterdam University.

"It's really fantastic, this possibility of identifying the silicates. Before ISO everybody thought that all silicates in space were amorphous, without a well-



ordered internal structure; that means you cannot differentiate among the many different silicates existing. Now we can try to identify them and track their presence in different regions. A whole new research field is starting", said Waters, who brought to the press conference samples of several terrestrial crystalline silicates: olivine and pyroxene, the most common silicates on Earth.

Crystals give key clues about the physical conditions and evolutionary history of crystal-bearing objects. The precise mechanisms for crystal-making are now being actively researched in laboratories, although some working-hypotheses are already being used. For instance, crystals can be made by heating the material to temperatures above 1300°C and then slowly cooling it down. Those found so far by ISO are at -170°C, both in stellar envelopes and in protoplanetary discs.

In the case of the old stars – red giant stars, where crystals are found to account for as much as 20% of all the surrounding dust – astronomers think that the high temperatures near the star triggered the crystallisation of the silicates. In the protoplanetary discs some experts postulate that electric shocks – like lightning flashes – heated the dust, which cooled afterwards.

"The crystals detected by ISO in these discs have a size of about a thousandth of

a millimetre. They collide with each other, forming bigger and bigger bodies. Models predict that in about ten to one hundred million years they will make planets", Waters says. "In fact, crystalline silicates are very common in our own Solar System. You also have them in the comet Hale Bopp!".

The reason why crystalline silicates had not previously been detected in stars has to do with their low temperatures. Cold material emits mostly infrared light, which means an infrared space telescope like ESA's ISO was needed. The two high-resolution spectrometers onboard the satellite, able to detect the 'chemical fingerprint' of the crystals, did the rest.

Astronomers are sure about the discovery because those chemical fingerprints, the spectra, can be compared in laboratories with spectra from crystalline silicates found on Earth. This method has demonstrated the crystalline structure and has even already allowed the identification of some of the crystals, such as forsterite and enstatite. However, crystalline silicates are a large family and their chemical signatures can be very similar; to enlarge the list of precise crystals more work will be needed, say experts in space chemistry.

"Crystalline silicates are synthesised around the stars; then that dust goes into the interstellar space, and enriches the raw material out of which more stars and planets will form. So you would expect crystals also to be in the interstellar medium! Crystals will certainly make us learn a lot...", according to Waters.

"This finding shows that ISO is really unveiling the chemistry of the Universe", says ESA astronomer Alberto Salama, chairman of the workshop about ISO results in spectroscopy held this week at ESA's Villafranca station in Madrid where the results were presented to the scientific community. "This is becoming more and more a 'hot field' of research. Initially we intended to organise a modest workshop, but we have had 140 astronomers coming from all over the world!".

AP2000 Millennium Conference Summary

The AP2000 Millennium Conference on Antennas and Propagation was held from 9-14 April in Davos, Switzerland. Some 1100 delegates, one third from overseas, attended the conference, presenting over 900 papers in 65 specialised oral and poster sessions. Several short courses were also offered to delegates by eminent scientists. Equipment, software and books were displayed by industry in some 20 exhibitions. AP2000 is the largest conference ever organised in this field in Europe.

Current work in Antennas and Radio-wave Propagation is driven by new requirements for expanding wireless communication and remote sensing applications.

For mobile communications, multibeam reflector and planar or conformal arrays with active or semi-active feeding and smart beam forming, are being developed for satellites and for cellular base stations. Channel modelling in complex communication environments, building penetration and avoidance of interference are key topics in mobile propagation. Interactions of microwave with biological tissues is also an area of extensive research activity. Concurrent engineering involving antenna, propagation and signal processing disciplines is becoming the key to mobile communication system design.

For wideband multimedia communications, the trend is to use higher frequencies up



into the millimetre-wave range. This requires new propagation models, new impairment restoration techniques to overcome fading and scintillation at higher frequencies. Here also, closer cooperation between propagation modelling and antenna design is required to develop active fade compensation techniques for satellite and terrestrial systems, where antenna gain and power are continuously adapted to propagation conditions. At millimetre wave frequencies, integrating active components and radiating elements on the same substrates, some of them with frequency sensitive (Photonic Band Gap), or for multifrequency capability (fractal antennas) is the object of sustained research activities.

The new concept of stratospheric communication relay, and perhaps observation platforms, also introduces new challenges to propagation and antenna engineers, which are currently being investigated.

In the field of remote sensing, challenging perspectives have been discussed both for passive and active instruments. In particular, the SMOS sensor, accepted by ESA in the framework of the Earth

Explorer Opportunity Missions, will monitor from space soil moisture, salinity, vegetation biomass and surface temperature using microwave interferometry at L-band. Such a new instrument, with its large two-dimensional array poses challenging antenna engineering and retrieval problems. Atmospheric remote sensing for communication and radar applications is also an expanding field.

Multifrequency synthetic aperture radar requires new low-cost printed antenna technologies, much discussed at the conference. Spaceborne repeat and single-pass SAR interferometry opens new perspectives and challenges for digital elevation mapping, cartography and seismology

Finally, ground penetration radars, involving both antennas and complex propagation issues, have been extensively discussed at AP2000, mostly for the detection of buried objects. They are also being considered for planetary observation missions.

This successful conference has provided ESA with precious inputs for its future R&D in the key areas of antennas, wave propagation and microwave remote sensing. It has also enhanced the image of ESA's technical excellence in the antenna and propagation communities world-wide, as well as in the associated engineering societies.

For technical information on the AP2000 conference, please consult the AP2000 website:

<<http://www.estec.esa.nl/AP2000/>>

or contact:

Dr Antoine G. Roederer

AP2000 Chairman

ESTEC,

2200 AG Noordwijk

The Netherlands

E-mail: aroedere@estec.esa.nl

The Proceedings of the conference are available on CD-ROM from the ESA Publications website

<<http://esapub.esa.int>> (ESA Publications Bookshop) or fax +31-71-565-5433. 



Photos of the AP2000 Opening Session

ESA and Hubble: Changing our Vision

In light of the Hubble Space Telescope's 10th anniversary on 27 April, ESA held a press conference at the Space Telescope-European Coordinating Facility (ST-ECF) in Munich in which the new and fully European outreach initiative, the 'European Space Agency Hubble Information Centre' was presented and launched.

With the astronauts who took part in the most recent Servicing Mission (SM3A) in attendance, ESA presented a complete overview of Europe's major contribution to the HST mission, and reviewed the first ten years of operations and the outstanding results that have 'changed our vision' of the cosmos.

With this initiative, ESA shows its commitment to public outreach and to the communication of science.

With an expected life time of 20 years, Hubble is now at the midpoint of its life. It has so far been one of the most successful scientific space missions, and the continuous maintenance and upgrading of the observatory through the Servicing Missions makes Hubble's next ten years appear even more promising.



ESA Brochure-157 '10 Years that Changed our Vision' covers the background and science information of the Hubble Telescope Project. It is available from the ESA Publications Bookshop at <http://esapub.esa.int>

Visit the new 'European Space Agency Hubble Information Centre' at <http://hubble.esa.int>

ERS – ENVISAT SYMPOSIUM

'Looking Down to Earth in the New Millennium'

Organised by: *ESA and the Chalmers University of Technology*

16-20 October 2000 – Gothenburg, Sweden
<http://www.esa.int/sympo2000>

Contacts:

- for Website aspects, registration, information:

Barbara Scarda, ESRIN
tel. +39-06-94180941
fax +39-06-94180942
E-mail: bscarda@esrin.esa.it

- for Symposium contents:

Gianna Calabresi, ESRIN
tel. +39-06-94180625
fax +39-06-94180552
E-mail: gianna.calabresi@esrin.esa.it



- for Local Support:
Britt-Marie Boisen
Chalmers University of Technology,
Gothenburg, Sweden
tel. +46-31-7721840
fax +46-31-164513
E-mail: boisen@rss.chalmers.se

ESA Newsletters

**PREPARING FOR THE FUTURE
(MARCH 2000)**
VOLUME 10, NO. 1
BRISSON P. (ED. M. PERRY)
NO CHARGE

ON STATION (MARCH 2000)
NEWSLETTER OF THE DIRECTORATE OF
MANNED SPACEFLIGHT AND MICROGRAVITY
WILSON A. & KALDEICH B. (EDS.)
NO CHARGE

**EARTH OBSERVATION QUARTERLY NO. 65
- ATSR SPECIAL ISSUE**
INCL. RECORD OF IMAGES (MARCH 2000)
DANESY D. (ED.)
NO CHARGE

**REACHING FOR THE SKIES, NO. 21
(MAY 2000)**
WILLEKENS P. (ED. B. SCHÜRMANN)
NO CHARGE

ECSL NEWS
NUMBER 21 (APRIL 2000)
ELLOUZE S. & BATTRICK B. (EDS.)
NO CHARGE

ESA Special Publications

**SPACECRAFT GUIDANCE, NAVIGATION
AND CONTROL SYSTEMS (FEB. 2000)**
**PROCEEDINGS OF THE 4TH ESA
INTERNATIONAL CONFERENCE, ESTEC,
NOORDWIJK, THE NETHERLANDS,
18 - 21 OCTOBER 1999**
SCHÜRMANN B. (ED.)
ESA SP-425 // 612 PAGES
PRICE: 130 DFL / 60 €



Publications

The documents listed here have been issued since the last publications announcement in the ESA Bulletin. Requests for copies should be made in accordance with the Table and Order Form inside the back cover

**AP 2000 – ANTENNAS AND PROPAGATION
(APRIL 2000)**

**PROCEEDINGS OF THE MILLENNIUM
CONFERENCE, DAVOS, SWITZERLAND,
9 - 14 APRIL 2000**

DANESY D. & SAWAYA H. (EDS.)
ESA SP-444 // CD-ROM
PRICE: 60 DFL / 25 €

**MULTISCALE/MULTIPOINT PLASMA
MEASUREMENTS (FEBRUARY 2000)**

**PROCEEDINGS OF THE CLUSTER-II
WORKSHOP, IMPERIAL COLLEGE,
LONDON, UK, 22 - 24 SEPTEMBER 1999**

BALOGH A., ESCOUBET C.P. &
HARRIS R.A. (EDS.)
ESA SP-449 // 421 PAGES
PRICE: 90 DFL / 40 €

**SAR CALIBRATION AND VALIDATION
(MARCH 2000)**

**PROCEEDINGS OF THE CEOS WORKING-
GROUP WORKSHOP, TOULOUSE, FRANCE,
26 - 29 OCTOBER 1999**

HARRIS R.A. & OUWEHAND L. (EDS.)
ESA SP-450 // 729 PAGES
PRICE: 90 DFL / 40 €

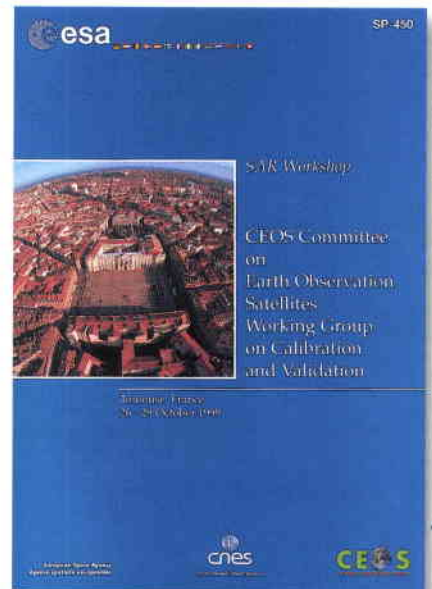
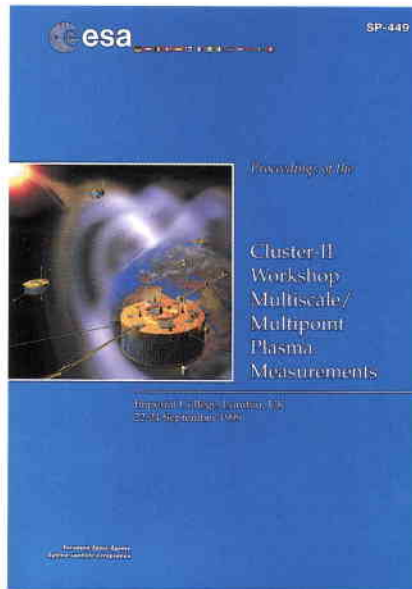
**DARWIN AND ASTRONOMY – THE
INFRARED SPACE INTERFEROMETER
(MAY 2000)**

**PROCEEDINGS OF AN INTERNATIONAL
SYMPOSIUM, STOCKHOLM, SWEDEN,
17 - 19 NOVEMBER 1999**

FRIDLUND M., LISEAU R. &
SCHÜRMANN B. (EDS.)
ESA SP-451 // 244 PAGES
PRICE: 90 DFL / 40 €

**ENVISAT – MIPAS: AN INSTRUMENT FOR
ATMOSPHERIC CHEMISTRY AND CLIMATE
RESEARCH (MARCH 2000)**

READINGS C. (ED. R.A. HARRIS)
ESA SP-1229 // 124 PAGES
PRICE: 70 DFL / 30 €

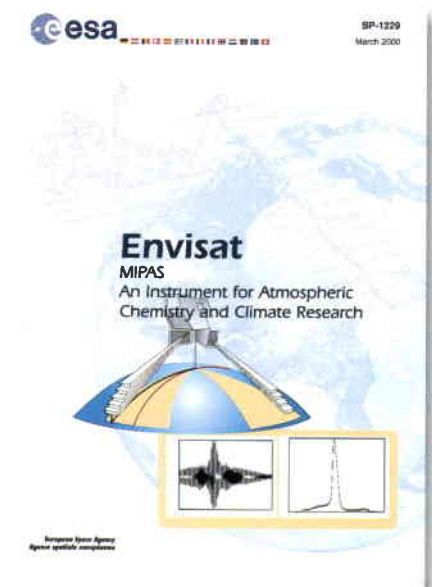
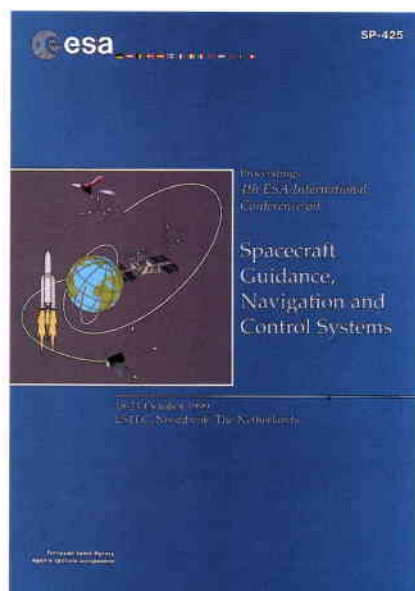
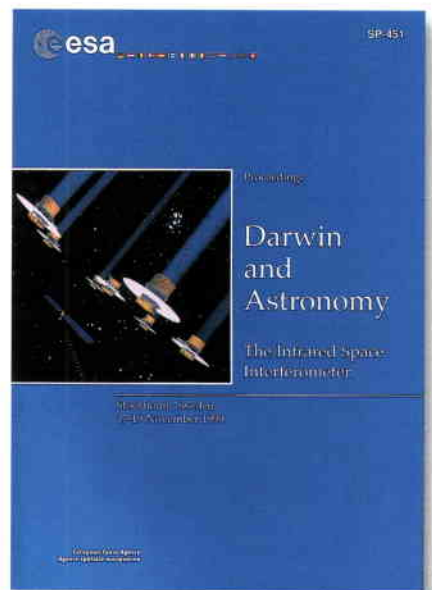


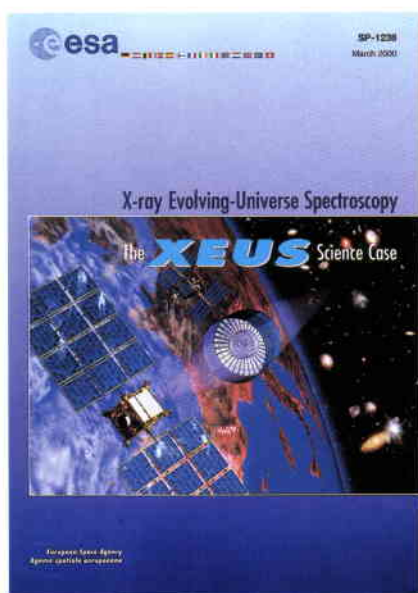
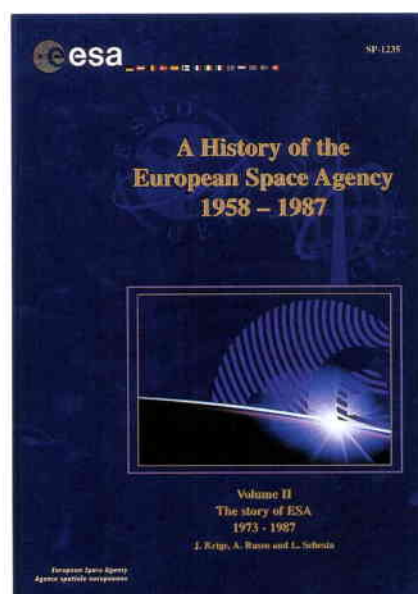
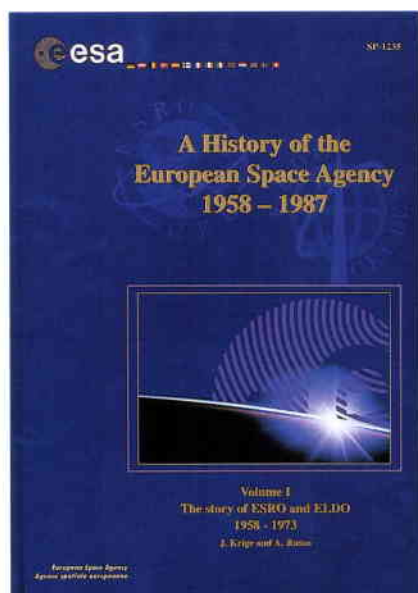
**A HISTORY OF THE EUROPEAN SPACE
AGENCY 1957 – 1987 (APRIL 2000)
VOLUME 1 – THE STORY OF ESRO AND
ELDO 1958-1973
VOLUME 2 – THE STORY OF ESA,
1973-1987**

KRIGE J., RUSSO A. & SEBESTA L.
(ED. R.A. HARRIS)
ESA SP-1235 // 462 AND 703 PAGES
PRICE: 160 DFL / 75 € (2 VOLS.)

**X-RAY EVOLVING-UNIVERSE
SPECTROSCOPY – THE XEUS SCIENCE
CASE (MARCH 2000)**

XEUS ASTROPHYSICS WORKING GROUP
(EDS. A. PARMAR & B. BATTRICK)
ESA SP-1238 // 30 PAGES
PRICE: 25 DFL / 10 €





ESA Contractor Reports

SEPARATION SYSTEM TECHNOLOGY PROGRAMME, PHASE B - FINAL REPORT (SEPTEMBER 1999)

SAAB ERICSSON SPACE, SWEDEN
ESA CR(P)-4271 // 121 PAGES
PRICE: 70 DFL / 30 €

ROBOT CALIBRATION TECHNOLOGIES (ROBCAT) - EXECUTIVE SUMMARY (SEPTEMBER 1999)

TRASYS SPACE, DENMARK
ESA CR(P)-4272 // 47 PAGES
PRICE: 25 DFL / 10 €

NON-DESTRUCTIVE INSPECTION OF CERAMIC/COMPOSITE MATERIALS USING NON-CLASSICAL X-RAY TECHNIQUES - FINAL REPORT AND EXECUTIVE SUMMARY, VOL. 2 AND 3 (JULY 1999)

BAM, GERMANY
ESA CR(P)-4273 // 48, 25 AND 31 PAGES
PRICE: 75 DFL / 30 €

DEVELOPMENT OF TRIAXIAL AND TWINAXIAL CONTACTS - FINAL REPORT (JUNE 1999)

FCI, FRANCE
ESA CR(P)-4275 // 112 PAGES
PRICE: 70 DFL / 30 €

DISCRETE EVENT SIMULATION: SIMULATION OF ROAD-TRAFFIC MONITORING VIA SATELLITE -

FINAL REPORT (JULY 1999)
UNIVERSITY OF ABERDEEN, UK
ESA CR(P)-4276 // 18 PAGES
PRICE: 25 DFL / 10 €

PERFORMANCE OPTIMISATION OF INTERNET PROTOCOLS VIA SATELLITE - EXECUTIVE SUMMARY AND FINAL REPORT (JULY 1999)

UNIVERSITY OF ABERDEEN, UK
ESA CR(P)-4277 // 7 AND 62 PAGES
PRICE: 75 DFL / 30 €

COOPERATIVE DEBRIS TRACKING AND DEVELOPMENT OF ALGORITHMS FOR MID-SIZE DEBRIS DETECTION WITH RADAR - FINAL REPORT AND EXECUTIVE SUMMARY (OCTOBER 1999)

FGAN, GERMANY
ESA CR(P)-4278 // 192 AND 44 PAGES
PRICE: 70 DFL / 30 € AND 25 DFL / 10 €

VIABLE : VISION AND INTERACTIVE AUTONOMY BI-LATERAL EXPERIMENTS - EXECUTIVE SUMMARY (NOVEMBER 1999)

TRASYS, BELGIUM
ESA CR(P)-4279 // 40 PAGES
PRICE: 25 DFL / 10 €

SOFTWARE SYSTEM DEVELOPMENT FOR SPACECRAFT HANDLING AND CONTROL - FINAL REPORT (NOVEMBER 1999)

TERMA ELEKTRONIK, DENMARK
ESA CR(P)-4280 // 20 PAGES
PRICE: 25 DFL / 10 €

Credit Card Payments for ESA Publications

It is possible to purchase the Agency's publications from the ESA Publications Division 'Bookshop' using your corporate or your personal credit card (Eurocard/Mastercard, Visa or American Express).

You can telephone or telefax your orders to the numbers given below, quoting your card's number and its expiry date.

The Bookshop (attn. Mr Frits de Zwaan)
ESA Publications Division
ESTEC
Keplerlaan 1
2200 AG Noordwijk
The Netherlands

Telephone: (31) 71 5653405
Telefax: (31) 71 5655433

Other methods of payment are also accepted. Please call or fax for details.

A list of the latest publications can be accessed via the ESA Publications Division's Home Page at the following Internet/WWW address:

<http://esapub.esrin.esa.it/>

AEROCHEMISTRY IN HYPERSONIC FLOWS – FINAL REPORT (SEPTEMBER 1998)
VOL. 1: INTRODUCTION AND LITERATURE SURVEY
VOL. 2: CODE CHOICES AND INITIAL DATABASES
VOL. 3: DATABASE EXTENSION – TRANSPORT PROPERTIES AND EXPERIMENTAL PROGRAMME
VOL. 4: CODE UPDATES AND FINAL COMPUTATIONS
FLUID GRAVITY ENGINEERING, UK
ESA CR(P)-4281 // 184, 94, 549 AND 195 PAGES
PRICE: 290 DFL / 140 €

GNSS-2 COMPARATIVE SYSTEM STUDIES – 5 VOLUMES FINAL REPORT AND 1 VOLUME EXECUTIVE SUMMARY (JANUARY 2000)
ALCATEL, FRANCE
ESA CR(P)-4282 // 264, 1024, 755, 914, 527 AND 42 PAGES
PRICE: 615 DFL / 280 €

INTEGRATED VISION AND NAVIGATION FOR PLANETARY EXPLORATION – FINAL REPORT (AUGUST 1999)
AEROSPATIALE, FRANCE
ESA CR(P)-4283 // 180 PAGES
PRICE: 70 DFL / 30 €

MULTICOM – FINAL REPORT (DECEMBER 1999)
ESYS, UK
ESA CR(P)-4284 // 19 PAGES
PRICE: 25 DFL / 10 €

NETLANDER 2005: LANDER NETWORK TO MARS – FINAL REPORT (DECEMBER 1999)
FMI, FINLAND
ESA CR(P)- 4285 // 157 PAGES
PRICE: 70 DFL / 30 €

USE OF GPS FOR RENDEZVOUS OPERATIONS (NOVEMBER 1999)
GMV, SPAIN
ESA CR(P)-4286 // 374 PAGES
PRICE: 70 DFL / 30 €

Contractor Reports

There are two types of Contractor Reports: CR(P) and CR(X) reports.

ESA CR(P) documents are available on microfiche from either of the following addresses:

British Library - Doc. Supply Centre
Customer Service
Boston Spa
Wetherby, West Yorkshire
LS23 7BQ
England

Universitaetsbibliothek und TIB
Welfengarten 1B
D-30167 Hannover
Phone: (+49) 511/762-2268
Fax: (+49) 511/715936

ESA CR(X) documents have restricted distribution and are not available on microfiche. Printed copies can be requested via ESA Publications Division



JOB OPPORTUNITIES IN SPACE

Serco is the largest technical services contractor to ESA. We have been supporting the Agency's programmes for over 25 years and regularly have job opportunities based at ESTEC (Netherlands), ESRIN (Italy), ESOC (Germany), ESA/HQ (France) and Kourou Spaceport (French Guiana)

Typical activities within the space field encompass:

- AIV Engineering
- Component Testing and Failure Analysis
- Antenna Engineering
- Earth Observation
- Ground Segment Engineering
- PC Support
- Unix System Administration
- Software Development
- Database Development and Management
- IBM MVS System Ops and Programming
- Web Development
- Project Management
- Product/Quality Assurance
- Technical Authoring

If you would like to be considered for future job opportunities with Serco please send your full curriculum vitae to:

Jane Marcham, Serco Europe Ltd.
5th Floor, Kempton Point
68 Staines Road West, Sunbury-on-Thames
Middlesex TW16 7AX, U.K.
Tel: +44 1932 733 000

Serco is an Equal Opportunities Employer

Publications Available from ESA Publications Division

| Publication | Number of issues per year | Scope/Contents | Price | Source |
|--|---------------------------|--|----------------|--|
| Periodicals | | | | |
| ESA Bulletin | 4 | ESA's primary magazine | Free of charge | ESA Publications Division, c/o ESTEC, 2200 AG Noordwijk, The Netherlands |
| Earth Observation Quarterly | 4 | Remote-sensing news | " | " |
| ECSL News | 4 | News from the European Centre for Space Law (under the auspices of ESA) | " | " |
| Reaching for the Skies | 4 | ESA's Space Transportation Systems news | " | " |
| Microgravity News | 3 | Microgravity Programme news | " | " |
| Preparing for the Future | 4 | Technology Programme news | " | " |
| Monographs | | | | |
| | Code | | | |
| Conference Proceedings | (SP-xxx) | Collection of papers presented at an ESA conference | Prices vary | ESA Publications Division, c/o ESTEC, 2200 AG Noordwijk, The Netherlands |
| Special Publications | (SP-xxxx) | Detailed monographs on post-graduate level subjects | " | " |
| Brochures | (BR-xxx) | Concise summaries on specific subjects | " | " |
| Scientific & Technical Reports | (STR-xxx) | Graduate level — reflecting ESA's position on a given subject | " | " |
| Scientific & Technical Memoranda | (STM-xxx) | Graduate level — latest but not finalised thinking on a given subject | " | " |
| Procedures, Standards & Specifications | (PSS-xxx) | Definitive requirements in support of contracts | " | " |
| Training Manuals | (TM-xxx) | Series for education of users or potential users of ESA programmes, services or facilities | " | " |
| Public-relations material | | General literature, posters, photographs, films, etc. | | ESA Public Relations Service 8-10 rue Mario-Nikis 75738 Paris 15, France |

All periodicals are also available via the Internet at:

<http://esapub.esrin.esa.it/>

Selected public-relations material and other ESA information is available at:

<http://www.esrin.esa.it>

Order Form for ESA Publications

Without receipt of payment no publications are sent. All payments in Dutch Guilders (Dfl). Within Europe, mailing is free of charge. Outside Europe, airmail is free of charge for orders over Dfl. 100; smaller orders are sent sea mail.

| No. of copies | ESA reference | Title | Price per copy Dfl. | Total Dfl. |
|--|---------------|-------|---------------------|------------|
| | | | | |
| | | | | |
| | | | | |
| | | | | |
| | | | | |
| | | | | |
| Order Subtotal: | | | | |
| Discount for orders over Dfl. 100: less 10% of subtotal: | | | | |
| Total amount: | | | | |

MAILING ADDRESS *(please print carefully):*

Name

Function Organisation

Address

Town & Postal Code Country

Date Signature

PAYMENT *please tick one box:*

Cheque enclosed (made payable to ESA Publications Division)
return order form with cheque to: ESTEC - Finance Division (EFA/P)
 P.O.Box 299 - 2200AG Noordwijk - The Netherlands

Items ordered are all free of charge *Credit Card:* Eurocard/Mastercard Visa AmEx

Card No. expires:

Name Card Holder

return form to: The Bookshop (attn. Mr. Frits de Zwaan) - ESA Publications Division - ESTEC
 P.O.Box 299 - 2200AG Noordwijk - The Netherlands; FAX: +31 - (0)71 565 5433

Telephone orders (and further information) : +31 (0)71 565 3405

Information via e-mail: FDEZWAAN@ESTEC.ESA.NL

Internet - list of the latest publications: <http://esapub.esrin.esa.it/esapub.html>

Printed annual catalogues of ESA publications are available free of charge from the bookshop.

ADVERTISE YOUR SPACE-RELATED PRODUCTS/SERVICES IN

esa bulletin

Mechanical Requirements - Copy dates

Printing material: 1 positive offset film (right reading, emulsion side down)

Usable Material: Negative, artwork ready for reproduction.
All production charges are invoiced separately.

Copy date: Ready for printing: 30 days before publication
(in Noordwijk) Any difficulty in observing these deadlines after reservation should be notified immediately.

fax: (+31) (0)71-565-5433
tel: (+31) (0)71-565-3794

Type area: 1/1 page 185/265 mm high
1/2 page 185/131 mm high
1/4 page 185/65 mm high

Screen: 60/cm - 150/inch

Page size: 297 mm x 210 mm

Bleed amount: 3 mm

Issue dates:

ESA Bulletin: February, May, August and November

Rates in Euros

| | 1x | 4x | 8x |
|----------|-----------|---------|---------|
| 1/1 page | € 1.000.- | € 800.- | € 600.- |
| 1/2 page | € 600.- | € 500.- | € 400.- |
| 1/4 page | € 400.- | € 350.- | € 300.- |

Extra charge for 4 colour processing € 750.-

Loose inserts (by application only): one A4 sheet € 1500.- plus the binder's handling charge of (currently) € 75.- per thousand.

Circulation

| | | |
|--|----------------------|------------------------|
| Albania | Germany | Philippines |
| Algeria | Gibraltar | Poland |
| Andorra | Greece | Portugal |
| Argentina | Guatemala | Puerto Rico |
| Australia | Honduras | Qatar |
| Austria | Hong Kong | Romania |
| Bahrain | Hungary | Rwanda |
| Bangladesh | Iceland | Sao Tome & Principe |
| Barbados | India | Saudi Arabia |
| Belgium | Indonesia | Senegal |
| Belize | Iran | Serbia |
| Benin | Iraq | Singapore |
| Bhutan | Ireland | Slovakia |
| Bolivia | Israel | Slovenia |
| Bosnia and Herzegovina | Italy | South Africa |
| Botswana | Ivory Coast | Spain |
| Brazil | Jamaica | Sri Lanka |
| Bulgaria | Japan | Sudan |
| Burkina Faso (Upper Volta) | Jordan | Surinam |
| Burma | Kenya | Swaziland |
| Burundi | Korea | Sweden |
| Cameroon | Kuwait | Switzerland |
| Canada | Latvia | Syria |
| Chile | Lebanon | Tahiti |
| China | Liechtenstein | Taiwan |
| Colombia | Libya | Tanzania |
| Commonwealth of Independent States | Lithuania | Thailand |
| Congo | Luxembourg | Togo |
| Costa Rica | Macedonia | Trinidad and Tobago |
| Croatia | Madagascar | Tunisia |
| Cuba | Mali | Turkey |
| Cyprus | Malta | Uganda |
| Czech Republic | Mauritania | UAE |
| Denmark | Mauritius | United Kingdom |
| Dominican Republic | Mexico | Uruguay |
| Dubai | Monaco | USA |
| Ecuador | Mongolia | Venezuela |
| Egypt | Montenegro | Vietnam |
| El Salvador | Morocco | Yemen |
| Estonia | Mozambique | Zaire |
| Ethiopia | Nepal | Zambia |
| Faroe Islands | Netherlands | Zimbabwe |
| Fiji | Netherlands Antilles | |
| Finland | New Caledonia | |
| France | New Zealand | |
| French Guiana | Nicaragua | |
| Gabon | Niger | |
| Gambia | Nigeria | |
| | Norway | |
| | Pakistan | |
| | Papua New Guinea | |
| | Peru | |

Advertising Management:

Brigitte Kaldeich-Schürmann
ESA Publications Division, DG-CP
ESTEC
Keplerlaan 1
2201 AZ Noordwijk
The Netherlands
Tel.: (+31) (0)71-565-3794
Fax: (+31) (0)71-565-5433
e-mail: bkaldeic@estec.esa.nl

Member States

Austria
Belgium
Denmark
Finland
France
Germany
Ireland
Italy
Netherlands
Norway
Spain
Sweden
Switzerland
United Kingdom

Etats membres

Allemagne
Autriche
Belgique
Danemark
Espagne
Finlande
France
Irlande
Italie
Norvège
Pays-Bas
Royaume-Uni
Suède
Suisse

European Space Agency
Agence spatiale européenne

Contact: ESA Publications Division

c/o ESTEC, PO Box 299, 2200 AG Noordwijk, The Netherlands

Tel (31) 71 565 3400 - Fax (31) 71 565 5433

Visit ESA Publications at: <http://www.esa.int>